Fixational and pursuit eye movements in infantile nystagmus: oculomotor control and perception

Lee McIlreavy

A thesis submitted in fulfilment of the
requirements for the degree of

Doctor of Philosophy (Vision Sciences)
Cardiff University
March 2016

Supervisors:
Professor Jonathan T. Erichsen
Professor Tom C.A. Freeman

Advisor:
Professor Tom H. Margrain

Abstract

Infantile nystagmus (IN) is a pathological condition of continuous, horizontal eye oscillations. Despite ongoing eye movements, those with IN do not experience oscillopsia, i.e. the illusory perception that the environment is moving to-and fro. The correct use of neural compensation for their eye movements, just as in typical individuals, is hypothesised to account for this lack of oscillopsia. This neural mechanism requires that an estimate of eye velocity ('extra-retinal signal') be compared to an estimate of the motion of the retinal image ('retinal signal'), and any difference due to object motion. Despite this hypothesis, there have been no previous investigations on how accurately those with IN can estimate object motion.

Even in typical adults, eye movement compensation is not perfect, which underlies a number of pursuit-based illusions. One such illusion, the Filehne illusion can be used to investigate the relative mismatch between the extra-retinal and retinal signals as individuals judge their perception of stationarity while attempting to follow a moving target. This illusion was used to investigate, through comparison with typical individuals, whether those with IN correctly recover object motion.

Experiments were conducted to characterise the ability of those with IN to fixate as well as follow targets, using a novel two-dimensional eye movement measure. Under repeated testing, the fixation gaze angle at which the IN oscillation is minimum (a null zone) was not consistent. Moreover, those with IN were unable to accurately or precisely follow targets using their slow phase. Results from a comparison of fixation and pursuit performance in those with IN suggested no difference in either the accuracy or precision. Importantly, the psychophysical judgements of those with IN pursuit eye movements are prone to similar compensation errors as typical controls. However, the mechanisms by which this is achieved will require further exploration.

Acknowledgements

My thanks go to my supervisors, Jonathan Erichsen and Tom Freeman, for their guidance and perseverance. Thank you to the Biotechnology and Biological Sciences Research Council, Fight for Sight and the Nystagmus Network UK for funding these studies.

Thanks to all of my participants, without your eyes and your time, this work would not have happened.

I thank my many previous mentors, without their support and teaching, I would never have been in the position to pursue this PhD.

A special thank you to Stacy Littlechild for making the highs and the lows of the PhD journey equally memorable.

I thank John Sanders, Cass Rogers, Fergal Ennis and Tony Redmond for taking the time to listen to my ideas, no matter how ill-conceived some inevitably were.

Whether I viewed the glass half-full or half-empty, I am grateful to Rob Young and Lorna Sumption for ensuring there was always a liquid to ponder.

Table of Contents

List of figures

List of tables

1 General introduction

1.1 Infantile nystagmus

Nystagmus is not a clinical condition per se, but a physical sign describing any repetitive involuntary oscillation of the eyes (Harris, 1997). Nystagmus indicates a disorder, ranging from benign to life threatening, of the eye or brain (Harris, 1997; Buncic, 2004; Lueck, 2005). Much of the terminology relating to nystagmus has evolved over a number of decades, which can be confusing to those not familiar with the literature. In an effort to provide a standardised classification system for use in clinical research, a multi-disciplinary Classification of Eye Movement Abnormalities and Strabismus (CEMAS) working group detailed the nomenclature, description, major criteria for diagnosis and common findings for ocular motor disorders (CEMAS, 2001). The CEMAS report classifies infantile nystagmus (IN) as a pathological nystagmus (CEMAS, 2001), and replaces older terminology of ‘congenital’, ‘motor’ and ‘sensory’ previously used to describe this condition. IN is reported to occur within the first six months of life (van Vliet, 1982; Abadi and Bjerre, 2002) and is frequently associated with and without a plethora of afferent sensory defects including albinism, aniridia, cataract, and achromatopsia (Harris, 1997). The prevalence and incidence of IN in the UK was recently estimated to be 1.4 per 1000 of the population (Sarvananthan et al., 2009), however this result is likely to be an overestimation as other pathological nystagmus (fusion mal-development nystagmus syndrome and spasmus nutans) was included. There is currently no known cause for IN, however a number of treatment options aim to minimise the oscillation, including drugs (McLean et al., 2007) or surgery (Dell'Osso and Flynn, 1979). Different theoretical models have been put forward to explain IN, however the most recent model suggests that there is a conflict between the smooth pursuit and subcortical optokinetic pathways in response to delayed foveal development (Brodsky and Dell'Osso, 2014).

The IN oscillation is characterised by a constant, conjugate oscillation of the eyes (Abadi and Bjerre, 2002). The oscillation is predominantly horizontal, however a vertical or torsional component may exist (Hertle and Dell'Osso, 1999; Averbuch-Heller et al., 2002). The term ‘waveform’ refers to that pattern obtained from eye movement recordings when the horizontal eye position is plotted against time (Figure 1.1).

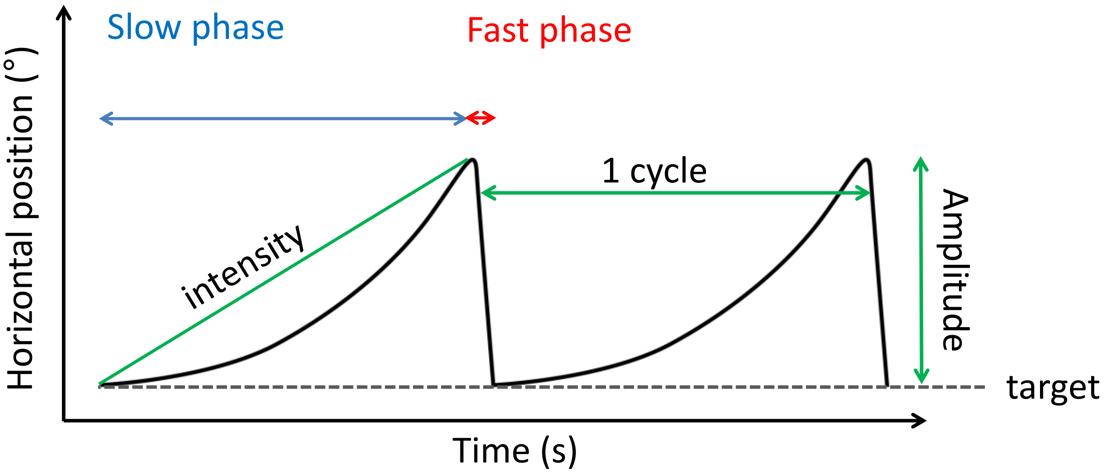

Figure 1.1 Schematic example of an IN jerk waveform. The slow phase moves the eye horizontally away from the intended target, whereas the fast phase redirects the eye onto the target.

Twelve distinct IN waveforms have been identified (Dell'Osso, 1985). Each cycle of the waveform has two basic phases: a slow phase that moves the eye away from the intended target, followed by either another slow phase (giving a pendular waveform) or a fast phase (giving a jerk waveform) that redirects the eye onto the target. In Figure 1.1, two cycles of a jerk waveform are depicted. The slow phase (indicated by the blue line) moves the eye away from the target position (indicated by the grey dashed line). A fast phase (indicated by the red line) redirects the eye onto the target location. A defining characteristic of IN is that the slow phase responsible for moving the eye off target is accelerating (CEMAS, 2001). For example, in Figure 1.1, the eyes are accelerating away from the intended target position. The foveation period is that early portion of the slow phase when the eyes are within ±0.5° (Dell'Osso et al., 1997; Cesarelli et al., 2000; Dell'Osso et al., 1992a; Bifulco et al., 2003) or ±2° (Jones et al., 2013; Wiggins et al., 2007)) of the target and eye speed is less than 4°/s. The IN waveform can be quantified by a number of parameters, including amplitude (the peak-to-peak excursion of the eye), frequency (the number of cycles of IN per second) and intensity (the product of amplitude and frequency) (Figure 1.1). Each of these parameters varies not only between, but also within, individuals with IN (Abadi and Dickinson, 1986).

As horizontal gaze angle is varied, the magnitude of IN is also reported to vary (Abadi and Whittle, 1991; Dell'Osso and Flynn, 1979; Dell'Osso et al., 1974; Kurzan and Buttner, 1989). The gaze angle with the minimum IN oscillation is known as the ‘null zone’ (Abadi and Bjerre, 2002), which is considered a defining feature of IN (CEMAS, 2001). The idea of a null zone has presumably arisen from the early finding that individuals with IN can adopt an abnormal head turn or posture (Cogan, 1967). In the majority of individuals, the null zone is located close to the straight ahead position gaze (Abadi and Bjerre, 2002). However, when the null zone is far from the straight ahead position (e.g. 20° to the right), a face turn may be adopted (e.g. 20° to the left) so that the eyes are placed in the null zone, but gaze is directed straight ahead with respect to the body (Abadi and Bjerre, 2002; van Vliet, 1982). Interestingly, the direction of the slow phase is governed by the horizontal position of gaze relative to the null zone. To the right of the null zone, the slow phase moves to the left, whereas to the left of the null zone, the slow phase moves to the right (Kurzan and Buttner, 1989).

Despite their ongoing eye oscillations, those with IN do not frequently report any perception of the world moving to-and-fro. This illusory perception that the visual environment is moving is known as oscillopsia (Brickner, 1936; Grunfeld et al., 2000; Wist et al., 1983). This is reported to be in contrast to those with acquired pathological nystagmus (Brickner, 1936; Ehrt, 2012; Tilikete and Vighetto, 2011). It would seem, therefore, that those with IN have mechanisms to perceptually compensate for their ongoing eye movements. For this reason, IN presents an invaluable opportunity to test whether those mechanisms thought to generate a stable percept of the world in typical individuals during *normal* eye movements also extends to those with *pathological* eye movements. Through applying current theoretical models of perceptual compensation for eye movements to this research population, it is anticipated that the results may help improve our understanding of oculomotor function in those with IN. I will now consider the mechanisms that achieve perceptual compensation of eye movements.

1.2 Compensating for pursuit eye movements using extra-retinal signals

Sensory receptor stimulation can arise not only from changes in the environment, but can also be self-induced. For example, Figure 1.2 indicates how identical patterns of retinal image motion (R) can arise from an object (H) moving in the environment while the eye are stationary, or from pursuit eye movements (P) when viewing a stationary object. In addition, identical patterns of retinal input can be created by different combinations of eye and object motion.

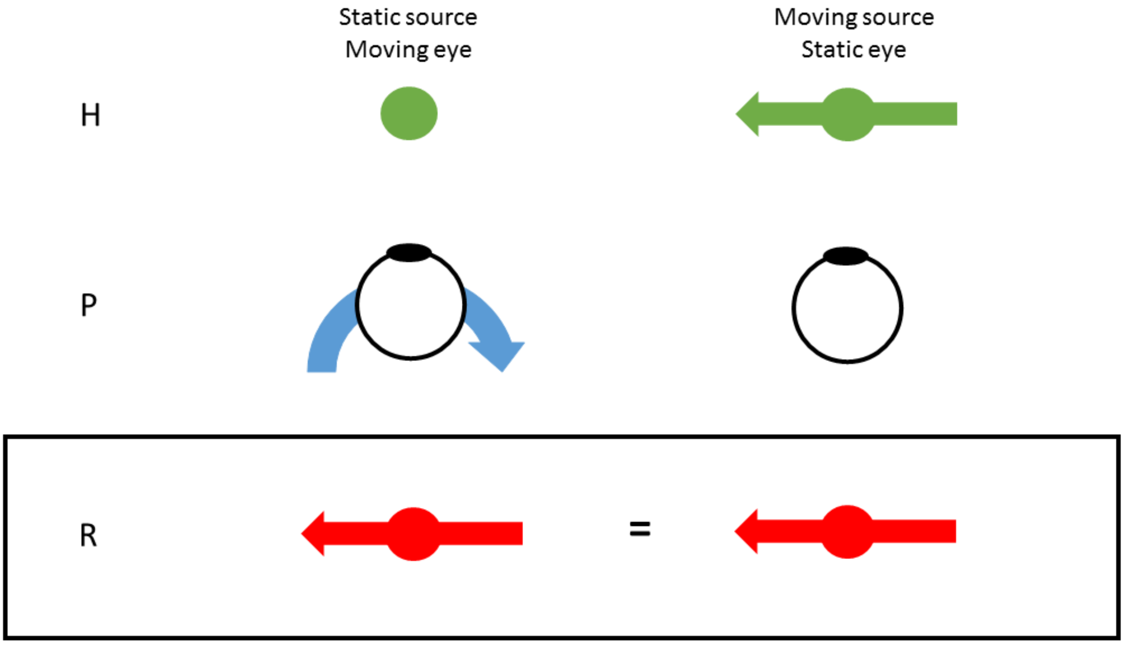

Figure 1.2. The retinal image is ambiguous. The same configuration of retinal image motion (R) may arise for different combinations of object (H) and eye movement (P). In this example, either the eye or the source is static. In reality, there are an infinite number of combinations between these two extremes that would give rise to an exactly identical retinal image.

However, as the retina is indifferent to the source of the retinal image motion, this presents a problem for the visual system. If it were to rely on only the retinal input, a meaningful representation of real-world motion would not be possible. Therefore, in order to solve the ambiguity of the retinal input and to determine whether object motion, pursuit eye movements, or a combination of both are responsible for the pattern of retinal image motion, some mechanism for compensating for the retinal shift produced by the pursuit eye movements is required. Potentially, there are different solutions to this problem. However, one such solution is to use a non-retinal estimate of the eye velocity (known as the 'extra-retinal signal'). In the visual system, it is thought that the extra-retinal signal is either a copy of the motor commands sent to the extra-ocular muscles (Wurtz, 2008) or proprioceptive feedback from the extra-ocular muscles as to eye position (Donaldson, 2000). Of the two potential mechanisms however, a current review of the evidence suggests that the contribution from proprioception is unlikely to be significant in perceptual compensation of eye movements (Wurtz, 2008).

Retinal images will move in the *opposite* direction to an eye movement. Therefore if the eye velocity is sampled (or transduced) so as to yield an extra-retinal signal, and retinal image motion is transduced so as to yield a retinal signal, the sum of the two signals should allow the recovery of head centric motion. More generally, the perceived velocity (H') of an object is the result of summing estimates of retinal image velocity (carried by a retinal signal, R') and eye velocity (carried by an extra-retinal signal, P') (Freeman and Banks, 1998; Souman et al., 2006).

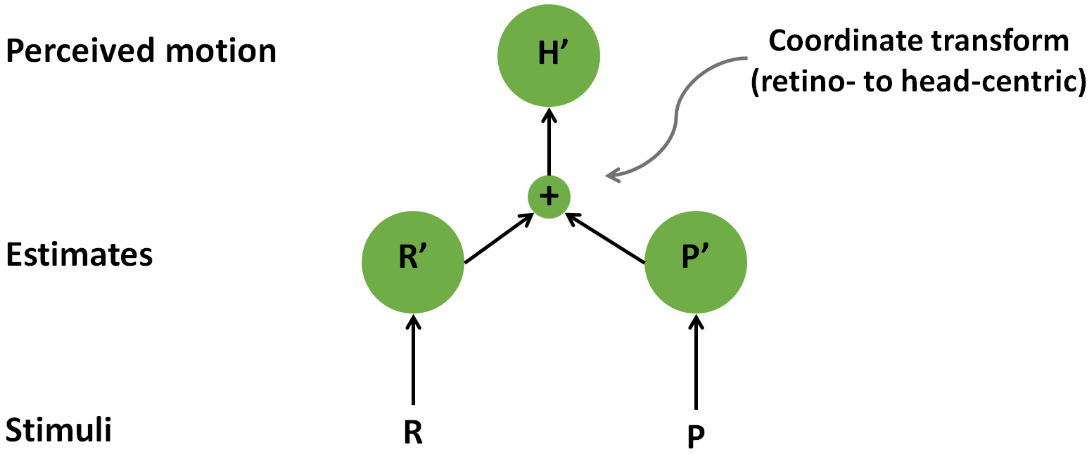

Figure 1.3. The linear transducer model of eye movement compensation to recover perceived object motion. In this model the retinal signal (R') and the extra-retinal signal (P') are estimates of the real retinal image and eye motion, respectively. R' is the actual retinal image velocity multiplied by a gain of r, and P' is the actual eye velocity multiplied by a gain of p. These estimates are summed, together with a co-ordinate transform, yielding the perceived motion (H'). If the gains, r and p, are equal, then head-centric speed would be perfectly recovered

Freeman and Banks (1998) have proposed a linear transducer model (Figure 1.3), such that the transduction of eye velocity and retinal image velocity is not perfect. The errors in transduction can be represented gains, with r representing the retinal gain and e representing the extra-retinal gain. The retinal and extra-retinal signals can be represented as:

$$R' = rR$$

$$P' = eP$$

More recently, an alternative solution to account for an underestimation of eye velocity relative to image velocity during pursuit has been proposed by Freeman et al. (2010). This alternative solution is a Bayesian model with two measurement stages: one for the target (T), and one for relative motion (R). Each measurement stage follows that depicted in (Figure 1.4). The visual system has certain expectations (i.e. ‘prior’, black dashed line) about target and relative motion. Because most objects are at rest the target prior is 0°/s. Similarly, since the target is at rest there should be no relative motion, and so the relative motion prior is also 0°/s. Both target motion and relative motion must be sampled by the visual system (i.e. ‘likelihood’, green or blue unfilled distribution). Respective priors and likelihoods are combined to obtain estimates of target motion (T’) and relative motion (R’) (i.e. ‘posteriors’, green or blue filled distribution). However, in the event that there is uncertainty in either of the two samples, the posterior shifts towards the prior (compare green filled distribution with the blue). Combining the estimates of target (T’) and relative motion (R’) will then yield an estimate of head-centric object speed. The model assumes that precision during pursuit is less than fixation. While both the Bayesian and the linear models predict that eye speed is underestimated relative to retinal image speed resulting in stationary object being perceived to move, the linear model, unlike the Bayesian model, is much better documented in the literature. Since the compensation of pursuit eye movements has not yet been investigated in those with IN, it is important to emphasise that, in this thesis, I will be restricting the interpretation of the perceptual data in relation to the simple linear transducer model proposed by Freeman and Banks (1998). It will remain for future work to extend the less well studied Bayesian model.

1.2.1 Efference copy in IN

Only a small body of work has been carried out on extra-retinal signals in those with IN. In one study, it was found that those with IN could use extra-retinal signals to determine the location of a brief (2ms) laser flash (Bedell and Currie, 1993).

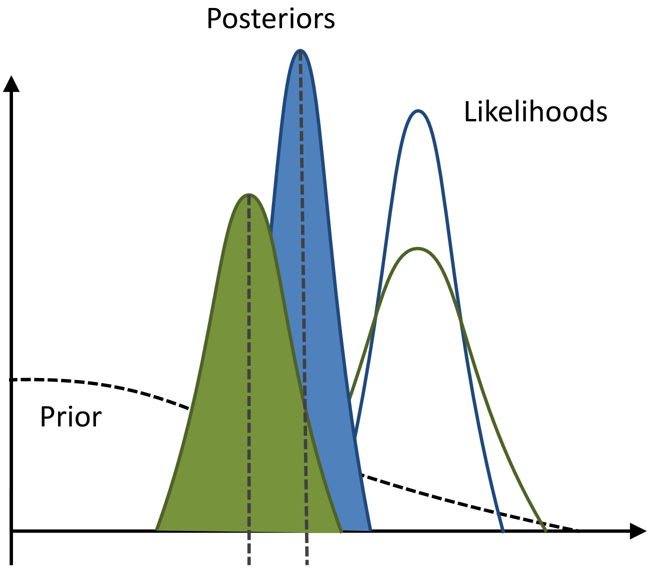

Figure 1.4 Schematic to depict the Bayesian model of head centric motion perception during smooth pursuit proposed by Freeman et al. (2010). The prior expectation of the visual system (the 'prior') is centred on 0°/s, because most objects in the environment are at rest. The sensory evidence (the 'likelihoods') can vary in their precision but are combined with the prior to obtain the perceived speed of objects (the 'posteriors').

For example, if the target was flashed on the retina, and if extra-retinal signals were not available, then it would not have been possible to point to the exact real-world location where the flash took place because multiple real-world locations would have been imaged at the same retinal location throughout the IN oscillation. In a similar study with a brief (2ms) laser flash, it was also found that those with IN were able to localise the location of the target (Goldstein et al., 1992). Interestingly, each of these two studies presented targets at different portions of the slow phase (i.e. early portions with low eye velocity right up to later portions with high eve velocity). Therefore, such results would suggest that those with IN have access to extra-retinal signals for the complete duration of the slow phase.

These studies have investigated the use of extra-retinal signals to localise stationary targets during the IN oscillation. Few studies have investigated extra-retinal signals and motion perception during the IN oscillation. One such study found in some individuals with IN (the study used 4 participants) that oscillopsia was experienced when using various methods of image stabilisation (e.g. retinal after-images) (Leigh et al., 1988). Under this arrangement, the extra-retinal signal from the ongoing IN oscillation should be subtracted from the observed retinal image motion. But, because the image is stabilised with respect to the retina, there is no image motion and so oscillopsia should be perceived. It is not clear why only some of the participants experienced oscillopsia while others did not. Nonetheless, when a deliberate mismatch in the magnitudes of the retinal and extra-retinal signals is introduced, the results strongly suggest that extra-retinal signals are implicated in the perception of oscillopsia. However, to date the extent to which the extra-retinal signal compensates for the retinal image motion during the IN oscillation has not been investigated.

1.2.2 The Filehne illusion

Despite evidence for the use of extra-retinal signals for compensation, the unambiguous perception of real world motion during eye movements is not perfect, even for normally sighted observers, who consistently report that stationary backgrounds appear to move during pursuit eye movements (Freeman and Banks, 1998; Haarmeier and Thier, 1996; Mack and Herman, 1973; Freeman et al., 2000b; Freeman, 1999; Dash et al., 2009; Dicke et al., 2008; Freeman et al., 2002). This illusory motion of stationary objects during a smooth pursuit eye movement is known as the Filehne illusion, named after Wilhelm Filehne who is credited with first reporting it (Filehne, 1922). It is generally accepted that this illusion results from an error in the extra-retinal compensation of retinal image motion; the magnitude of the velocity estimate carried by the retinal signal exceeds that of the extra-retinal signal. Under these circumstances, an object will be perceived to move in a direction opposite to the eye movement. Under controlled conditions, an observer can adjust the velocity of the object in the same direction as the eye movement until a perception of stationarity is achieved. Such a velocity nulling procedure is often used experimentally to estimate the magnitude and direction of the Filehne illusion. Given such a consistent, yet predictable underestimation of eye velocity relative to retinal image velocity during pursuit eye movements, it is not immediately clear why some means of re-calibration of the extra-retinal signal does not occur. In a recent study by Waddington and Harris

(2015), it was concluded that the error associated with the extra-retinal signal was necessary, offering a trade-off between the variability OKN parameters (e.g. slow phase and quick phase duration, amplitude etc.) while still permitting the recovery of head-centric speed.

1.2.3 A comparison of oscillopsia and the Filehne illusion

In this section, an important distinction between oscillopsia and the Filehne illusion will be made. One obvious difference is that typical individuals do not report oscillopsia, which most often only accompanies serious eye and or brain pathology (Brickner, 1936). Therefore, oscillopsia does not represent “normal” oculomotor control. Because of its association with pathology, the magnitude of the oscillopsia may vary with the underlying condition, and while some individuals show partial adaptation to the oscillation it is typically permanent (Buchele et al., 1983). On the other hand, the Filehne illusion is transient, being only present during pursuit. Oscillopsia is also continuously present while an individual attempts to fixate a target (i.e. in the absence of any deliberate eye movement) and so may reflect failure to compensate for small (involuntary) fixational eye movements. In contrast, the Filehne illusion is present in typical individuals, and so can be considered a “normal” manifestation of oculomotor control. Unlike oscillopsia associated with pathology, the Filehne illusion is transient, only being present during a large (voluntary) smooth pursuit eye movement. Oscillopsia is the failure to maintain a percept of stationarity in the absence of deliberate eye movements, whereas the Filehne illusion is the failure to maintain a percept of stationary during a deliberate eye movement. While oscillopsia is typically an ever present symptom that is reported by individuals as they interact with the real world, the Filehne illusion is not normally present in the real world as pursuit eye movements are made, under carefully controlled conditions (i.e. complete darkness removing references for motion so that the participants are forced to utilise extra-retinal signals for motion perception).

The perceptual origins of both oscillopsia and the Filehne illusion have been hypothesised to be identical. That is, the magnitude of the retinal signal is greater than the extra-retinal signal (Abadi et al., 1999; Leigh et al., 1988). In those who experience oscillopsia under normal circumstances, it is not apparent to what extent the gains of the retinal and extra-retinal signals differ, or the extent to which eye movements are perceptual compensated for. That said, by comparison, the published ratios of the gains of the extra-retinal and retinal signals for pursuit based illusions has been collated and summarised by Freeman et al. (2010), and are presented in Figure 1.5. From this figure, it can be appreciated that there is considerable variation, but typically the ratio is around 0.7.

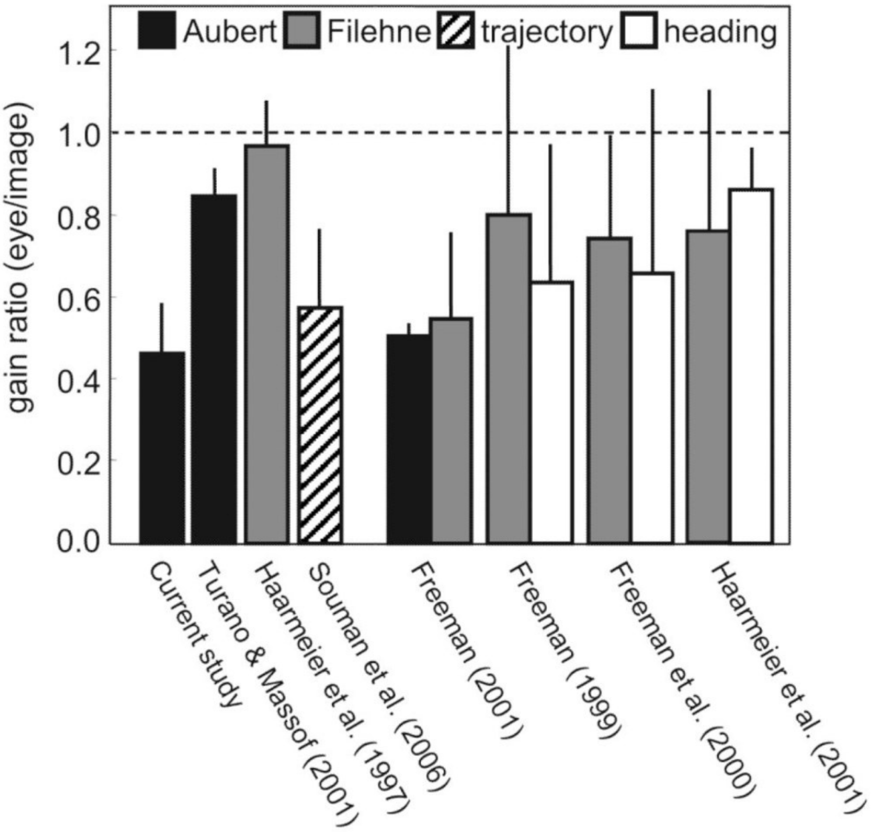

Figure 1.5 A summary of the ratio of the gains for those signals encoding eye velocity and retinal image velocity from Freeman et al. (2010).

Previous studies report that those with IN do not typically perceive oscillopsia while fixating, despite their ongoing eye movements (Leigh et al., 1988; Abadi et al., 1999; Bedell, 2000), in contrast to other clinical populations with nystagmus (Brickner, 1936; Straube et al., 2012). As mentioned before, this lack of oscillopsia is believed to reflect the fact the magnitude of the retinal signal is equal to, but opposite, the extra-retinal signal (Goldstein et al., 1992; Abadi et al., 1999). However, it is well documented that typical individuals experience pursuit-based illusions. Therefore one of the main motivations for this thesis has been to explore the perceptual compensation for pursuit eye movements in those with IN.

1.2.4 Section summary

Oscillopsia is the illusory perception that the world is oscillating to-and fro as an individual views the world (i.e. attempts to fixate). As discussed, those with IN do not typically experience oscillopsia as they view the world, presumably because of the correct use of either an extra-retinal signal that completely cancel the resulting retinal image motion (the 'extra-retinal' account of recovered head-centric motion). In this thesis, I intend to characterise, for those with IN, the perceptual compensation for pursuit eye movements to recover of estimates of head-centric motion. More specifically I will be investigating the recovery of a perception of stationary during the Filehne illusion. While this utilises the same mechanisms as per fixation (i.e. preventing oscillopsia), there has not been any investigation into the perception of stationarity during pursuit eye movements in those with IN. While those with IN behave perceptually similar to typical individuals, (i.e. do not report oscillopsia) when fixating, the extent of perceptual compensation during for pursuit eye movements has never been investigated before. Consequently the extent to which a veridical percept of stationarity while fixating can be extended to pursuit eye movements is unclear. Because the Filehne illusion is a pursuit-based illusion, the current literature surrounding the ability of those with IN to follow a moving target will now be reviewed.

1.3 Smooth pursuit

Smooth pursuit denotes a specific type of eye movement in humans (Carpenter, 1988) the purpose of which is to smoothly and continuously image a moving target either on, or suitably close to, the fovea (Leigh and Zee, 1999). One of the most ubiquitous measures of smooth pursuit performance is smooth pursuit gain, the ratio of eye velocity to target velocity. This presumably relates to the findings of Rashbass (1961) that indicates smooth pursuit is driven by velocity error rather than position error. A smooth pursuit gain of 1.0 would indicate perfect velocity matching between eye and target, whereas a smooth pursuit gain of more or less than 1.0 would indicate that the eye was moving faster than or slower than the target, respectively.

1.3.1 Smooth pursuit in IN

The use of the term “smooth pursuit”, or simply “pursuit”, in the IN literature has long been a source of confusion. It is used interchangeably not just to denote the *act of following a target* as well as a *type of eye movement*. Unfortunately, many previous studies of IN do not provide an explicit operational definition of “pursuit”. In other words, two separate research questions have been conflated:

1. *How well do those with IN follow a target?*
2. *Do those with IN have a normal smooth pursuit system?*

Nonetheless, a problem faced by either research question is how either can be answered given an underlying continuous eye oscillation. In this section, I will consider each of these research questions in turn.

1.3.1.1 How well do those with IN follow a target?

Early quantitative studies made use of the entire velocity distribution of the slow phase when calculating gain (Yee et al., 1980; Yamazaki, 1978). These studies found a reduced gain in those with IN compared to typical individuals when tracking horizontal optokinetic nystagmus (OKN) targets (Yee et al., 1980; Yamazaki, 1978) and horizontal smooth pursuit targets (Yamazaki, 1978) when compared to expected results from typical individuals, suggesting a smooth pursuit impairment in those with IN.

The entire IN slow phase is not an eye movement that occurs in direct response to the target motion, as it persists even if an individual fixates a stationary target. It has been argued before that the entire slow phase should not be included in the calculation of gain (Dell'Osso, 1986). However, if the intention of the authors was to demonstrate how well those with IN perform the act of following a pursuit target or rotating OKN drum, then the use of the entire slow phase seems completely justified.

The study by Yee et al. (1980), had the following motivation:

“*In this study we attempt to determine if OKN differs between patients with associated ocular lesions and those without such lesions*” (Yee et al., 1980)

The operational definition of OKN was given as:

"*Optokinetic nystagmus (OKN) is a jerk nystagmus that is usually induced by movement in a large area of the visual surround during clinical examination of eye movements*" (Yee et al., 1980)

Therefore, this study was seeking to determine whether or not those with IN use the same jerk pattern of linear slow phases and fast phases to follow an OKN target (i.e. how well do those with IN follow a target?). Under these circumstances, it is entirely appropriate to utilise the entire slow phase velocity distribution to calculate gain. However, on this basis, the OKN responses were then used to make inappropriate inferences about the integrity of the neural substrate that governs OKN eye movements (i.e. do those with IN have a normal OKN system?).

The study by Yamazaki (1978) had this motivation:

"*In congenital jerk nystagmus, a defect in the motor fixation system (smooth pursuit system) has been postulated as the primary cause, but quantitative analysis of smooth pursuit has not been reported… This study quantifies smooth pursuit and vestibular function in patients with congenital jerk nystagmus*" (Yamazaki, 1978)

While no operational definition of smooth pursuit was provided, it is clear that, in this study, the eye movements of those with IN were again being used to make inferences about the neural substrate that governs the smooth pursuit (and OKN) system. Therefore, as before, it would have been inappropriate to use the entire slow phase velocity distribution.

Later, Dell'Osso (1986) has argued that gain can only be measured during the foveation period when the contribution from the IN oscillation is zero. In other words, the motivation for the investigation here is not to determine how well the target was followed by the eyes, but rather to establish the integrity of the system governing the smooth pursuit eye movements. Dell'Osso argued that a normal underlying smooth pursuit velocity signal exists in those with IN, but 'superimposed' or added to this normal pursuit velocity signal is noise in the form of the IN slow phase velocity. Using this argument, restrictions could be placed on the eye movement analysis to ensure only the foveation period was used and not the entire slow phase. This would ensure that the contribution from noise (i.e. the IN oscillation) is minimised, unmasking the underlying pursuit signal. This argument will be referred to as the 'superposition-gain' argument in this thesis. An example of the superposition gain calculated from the eye movements of an individual with IN is shown in Figure 1.6. Having first determined the foveation positions, a linear dashed line has been fitted through them.

This image has been removed by the author for copyright reasons

Figure 1.6 An example of applying the method of superposition gain to derive the velocity of the smooth pursuit system (Dell'Osso, 1986). A straight line is fitted through foveation positions. The slopes of the target and the fitted line can be compared to measure pursuit performance.

The slope of this fitted line can then be used to quantify the underlying pursuit velocity signal. This technique of fitting a line through consecutive foveation periods indicates that the underling pursuit signal closely matches that of the target, suggesting that smooth pursuit gains of those with IN are normal (Dell'Osso, 1986).

As discussed in previous sections, the foveation period is that early portion of the slow phase when the eye is directed at the intended target and the eye velocity is sufficiently low. There are specific criteria that more formally define the foveation period: eye velocity should be less than 4°/s (Dell'Osso et al., 1992a; Dell'Osso et al., 1997; Bifulco et al., 2003) and eye position should be within 0.5° (Dell'Osso et al., 1997; Cesarelli et al., 2000; Dell'Osso et al., 1992a; Bifulco et al., 2003) or 2° (Jones et al., 2013; Wiggins et al., 2007) of the target. There are two fundamental problems with the superposition-gain argument that arise from the use of a velocity criterion and a position criterion.

The necessary details concerning criteria used to define a foveation in that study advocating superposition gain have been completely omitted by Dell'Osso (1986). Therefore, we cannot know for certain whether both a velocity criterion and a position criterion were applied, or whether it was one criterion but not the other. Nonetheless, the my criticism will be discussed assuming a velocity and a position criterion were applied

First, I will consider the use of the velocity criterion. The superposition-gain argument argues that eye velocity, v_{eye}, during attempted pursuit in an individual with IN is the sum of the pursuit velocity signal, $v_{pursuit}$, and noise from the IN slow phase velocity, v_{IN}. This can be best represented by the following formula:

$$v_{eye} = v_{pursuit} + v_{IN}$$

However, the pursuit velocity signal can only be estimated when the contribution from the IN is zero:

$$v_{eye} = v_{pursuit} + 0$$

The IN component is zero during the foveation period, which is in turn defined using eye velocity (i.e. v_{eye}). Therefore when the IN component, v_{in}, is zero, then the eye velocity, v_{eye}, must also be zero

$$0 = v_{pursuit} + 0$$

Consequently, the pursuit velocity signal, $v_{pursuit}$, must also be zero:

$$v_{pursuit} = 0$$

On this basis, it cannot be argued that the smooth pursuit system is ‘active’ while those individuals with IN follow moving targets.

In practice, however, foveation periods are not defined by a strict 0°/s eye velocity criterion (i.e. $v_{eye} = 0$) but, as previously mentioned, by a more liberal 4°/s eye velocity criterion (Dell'Osso et al., 1992a; Dell'Osso et al., 1997; Bifulco et al., 2003). While it may be impossible to determine the relative contribution of pursuit velocity and IN velocity, clearly for the purposes of the superposition argument, any velocity criterion should be a stringent as possible, so as to ensure that the contribution IN slow phase velocity is kept to a minimum.

The second problem with superposition-gain is the use of a foveation position criterion. Consider the line traced on a position-time plot by a target moving with constant velocity (Figure 1.7). Each data point on the target trajectory line can be denoted by x_i, and the slope of this line (i.e velocity) will be called v_{target}. The foveation period position criterion will be denoted in this case by the variable p, such that foveation periods are those eye movements within the interval of $x_i \pm p$, assuming the velocity criterion has been met.

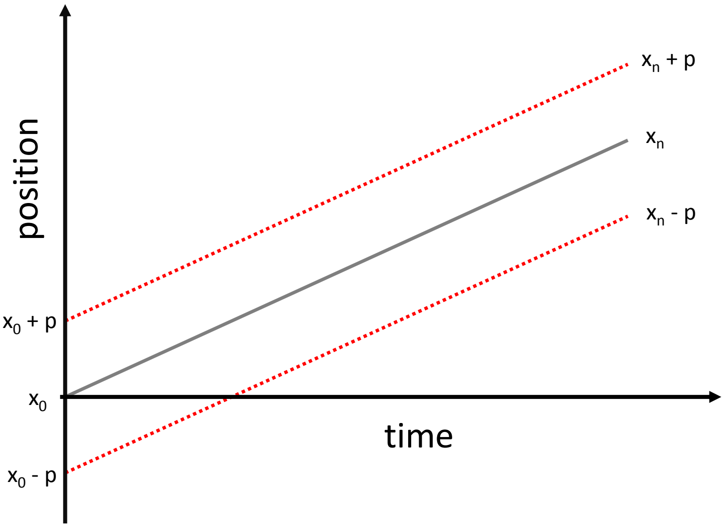

Figure 1.7 A position time plot for a hypothetical target (black line) moving with constant velocity. The foveation position criterion, p (red dashed line) is shown to straddle the target trajectory.

Under these constraints, the maximum and minimum fitted lines of eye velocity that could be included in the calculation of superposition-gain are shown in Figure 1.1 by the steeper and shallower dashed black lines, respectively.

More formally:

$$v_{max} = \left(\frac{(x_n + p) - (x_0 - p)}{t}\right)$$

$$v_{max} = \left(\frac{(x_n - x_0 + 2p)}{t}\right)$$

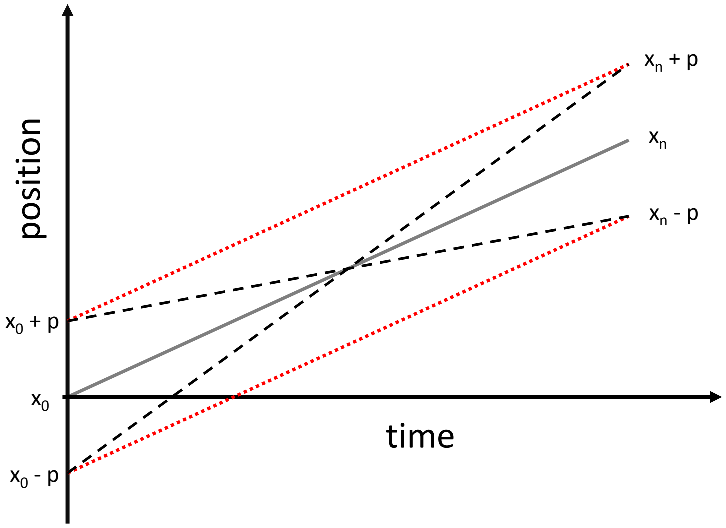

Figure 1.8 The range of possible slopes (i.e. velocities) for lines fitted through foveations during attempted pursuit

and:

$$v_{min} = \left(\frac{(x_n - p) - (x_0 + p)}{t}\right)$$

$$v_{min} = \left(\frac{(x_n - x_0 - 2p)}{t}\right)$$

Hence the range of pursuit velocities, v_{range}, about V_{target} can be calculated as follows:

$$v_{range} = v_{max} - v_{min}$$

$$v_{range} = \left(\frac{(x_n - x_0 + 2p)}{t}\right) - \left(\frac{(x_n - x_0 - 2p)}{t}\right)$$

$$v_{range} = \left(\frac{4p}{t}\right)$$

It therefore follows that the range of possible pursuit gains, g_{range}, about 1 is given by:

$$g_{range} = \left(\frac{4p}{t \times v_{target}}\right)$$

Hence, superposition-gain could be "improved" (i.e. made to approach 1.0 by making g_{range} approach 0) either by reducing the foveation position criterion (compare blue and magenta lines in Figure 1.9), extending the duration of the attempted pursuit (compare blue and magenta lines in Figure 1.10) or by increasing the target velocity (compare both Figure 1.9 and Figure 1.10). In any case, provided that there are two foveation periods so that a line can be constructed, the gain will be constrained to approximately 1.0 (Figure 1.9 and Figure 1.10). Therefore, by virtue of restricting the analysis to foveation periods, a conclusion of normal IN pursuit gain is ensured.

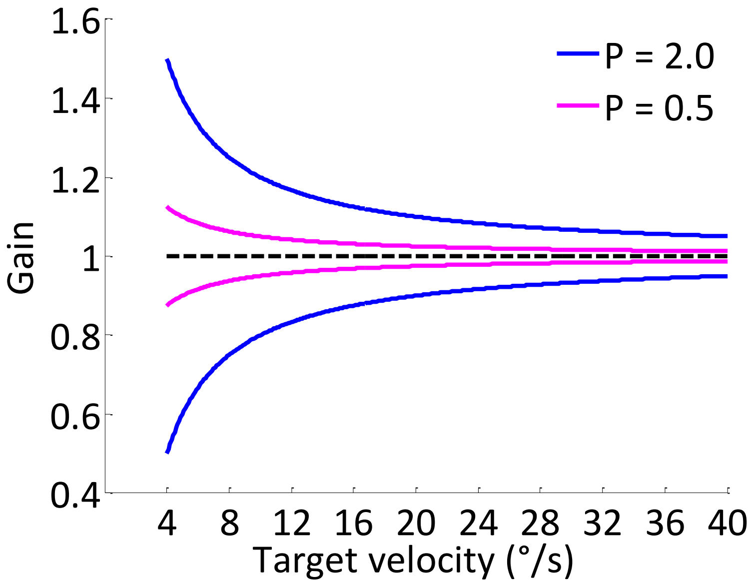

Figure 1.9 Superposition gain when plotted against target velocity, for t = 4s, converges toward a gain of 1.0. For any given target velocity, a more stringent foveation position criterion, p, results in a gain closer to 1.0 than a more liberal foveation position criterion.

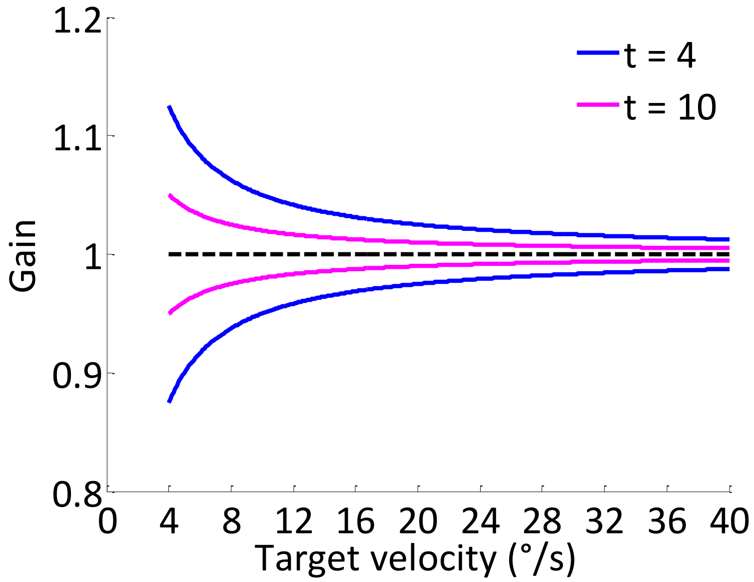

Figure 1.10 Superposition gain when plotted against target velocity, for P = ±0.5°, converges toward a gain of 1.0. For any given target velocity, a longer pursuit duration results in a gain closer to 1.0 than a shorter pursuit duration.

Despite these problems with the superposition-gain argument, other studies have supported the use of only foveation periods when calculating gain. Again, the motivation for this has been to make inferences about the neural substrate responsible for generating smooth pursuit eye movements.

This image has been removed by the author for copyright reasons

Figure 1.11 Smooth pursuit gain measured during the foveation period for rightwards and leftwards pursuit Even for velocities up to 110°/s (6600 minarc/s), the gain is approximately 1.0, indicating normal pursuit. Figure taken from (Dell'Osso et al., 1992b).

By restricting the analysis to within individual foveation periods, it was subsequently found that eye velocity closely matched that of the target (i.e. gain during the foveation period was normal) for target speeds up to 110°/s (Dell'Osso et al., 1992b). Data from this study are presented in Figure 1.11.

However, I have two major concerns about the conclusions of this study. First, it has been demonstrated in typical individuals that, beyond a velocity of approximately 30°/s, catch up saccades begin to be recruited to assist smooth pursuit eye movements (Westheimer, 1954). Therefore, the *normal* smooth pursuit system and the eye movements it generates would seem incapable of sustaining high gain pursuit much beyond 30°/s. In fact, it has been demonstrated that eye velocity saturates at approximately 87°/s during smooth pursuit (Meyer et al., 1985), although in this particular study, eye velocity was only sampled for a few milliseconds as the target passed the straight ahead position rather than for the full duration of the stimulus movement. Nonetheless, 87°/s would represent the upper limits of human smooth pursuit eye movement performance, still considerably less than the 110°/s indicated by the mean for those with IN (Dell'Osso et al., 1992b). Second, as with earlier studies before, there are once again no foveation criteria specified in this study (Dell'Osso et al., 1992b). The only means by which high-gain pursuit for a target moving at 110°/s can be achieved during a foveation period is if the eyes were also moving close to 110°/s. Consequently, the upper limit of the foveation period velocity criterion cannot be 4°/s. Yet, since it is not clear how the foveation periods were selected, it is impossible to properly assess these findings. For example, one cannot know if gain was only calculated once eye velocity was within the position criterion, the velocity criterion, or both. In any event, it could equally be argued that the contribution was not from the pursuit system but merely a consequence of the IN.

1.3.1.2 Do those with IN have normal smooth pursuit eye movements?

The current consensus of the literature is that those with IN have a normal smooth pursuit system. For example, past and present models of IN rely upon this finding:

"*These responses are driven by the (still intact) cortical pursuit system.*" (Brodsky and Dell'Osso, 2014)

"*The smooth pursuit gain is normal in CN*" (Jacobs and Dell'Osso, 2004)

The origin of this acceptance stems from the superposition-gain argument demonstrating that those with IN follow a target normally:

"*…infantile nystagmus is inherent to the pursuit system, yet pursuit gain remains normal.*" (Brodsky and Dell'Osso, 2014)

However, one of the difficulties in accepting the superposition argument is that it is entirely based up on the *assumption* of normal smooth pursuit eye movements, not on actual evidence (Dell'Osso, 1986). Consequently, only by circular reasoning can it be concluded that smooth pursuit eye movements in IN are normal. Despite arguing for a normal smooth pursuit system, the superposition gain argument presents a further difficulty. It would seem to be demonstrating, albeit indirectly, that the act of following a target is not performed by smooth pursuit eye movements, but by an entirely different type of eye movement: saccades (i.e. fast phases). Superposition-gain argues that the line interpolating between foveation periods will reveal the velocity of the motor command that has been generated for the smooth pursuit eye movements. Foveation periods are immediately preceded by a fast phase. In any event, foveation periods are extremely brief, being reported to be approximately 57ms (Dell'Osso et al., 1992a). However, if we take the extreme viewpoint as suggested in the superposition gain argument and consider only those instances when the IN is zero (i.e. when the eye velocity is zero), what we are actually denoting is the end point of the fast phase. Any temporal relationship across successive foveation periods is would therefore estimate the inter-beat accuracy of the fast phases, not the underlying pursuit signal.

As an example, consider the simulated position-time plot for smooth pursuit in Figure 1.12. These simulated IN data were designed to be similar to a jerk waveform: a ‘slow phase’ of 200ms followed by a ‘fast-phase’ of 50ms.

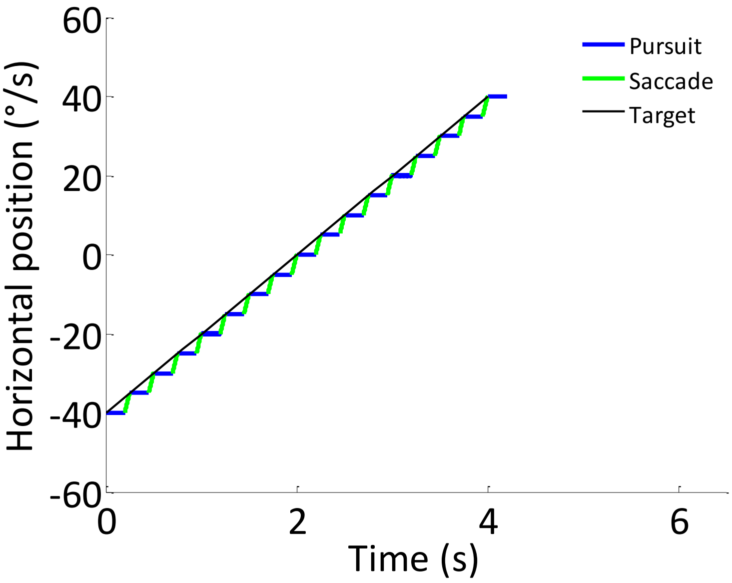

Figure 1.12 Simulated absence of pursuit. Following each epoch of stationary eye position (200ms duration), the target was “re-foveated” by means of a “saccade” (50ms duration).

Each ‘slow phase’ was designed so that it had a constant position (i.e. zero velocity). Added to the position data was Gaussian noise, so as to make the slow phase data representative of real oculomotor data (Figure 1.13).

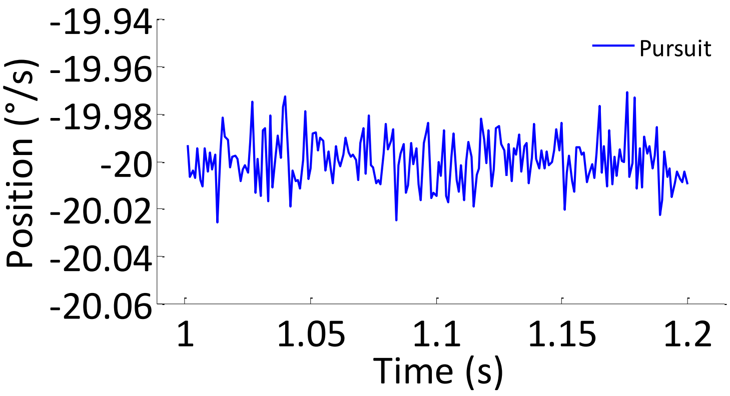

Figure 1.13 A single epoch of during which the eye was stationary. Gaussian noise was added to each epoch of constant eye position to simulate real oculomotor and/or eye tracker noise. In this example the mean position of the epoch was 19.99° (± 0.0103), while mean velocity was -0.0796°/s (± 0.601).

In this scenario, the act of following the target is achieved only by ‘fast phases’ (see the green lines in Figure 1.12). Over 4 seconds duration, the target changes position by 80° (black line in Figure 1.12). If the hypothetical target were pursued perfectly, a ‘smooth pursuit’ velocity of 20°/s would be required. If the ‘fast phases’ are removed and replaced with ‘NaN’s, and the remaining ‘slow phases’ linearly regressed, the slope of the line yields 19.96°/s (Figure 1.14). Such a “smooth pursuit velocity” indicates a near perfect gain of 0.998, despite net change in horizontal position having taken place during any ‘slow phases’.

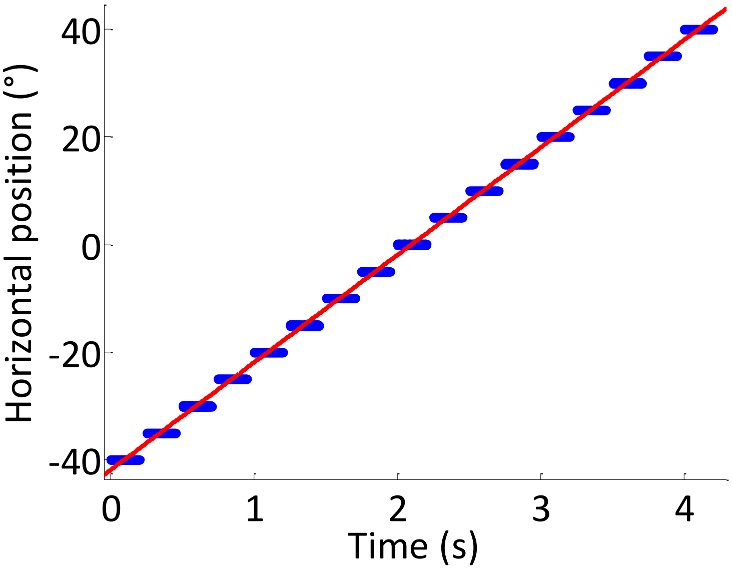

Figure 1.14 Linear regression of simulated epochs where the eye is stationary, using a least-squares linear fitting procedure in MATLAB®. The resulting line yielded a slope of 19.96°/s, which would result in a near perfect gain of 0.998. It could be concluded that the smooth pursuit gain in this simulated scenario was functioning normally.

Therefore, IN would appear to be analogous to the situation where typical individuals can no longer follow targets by smooth pursuit eye movements and employ catch-up saccades to re-image the moving target on the fovea.

It could be argued that changes in how well an individual can follow a moving target could reflect whether or not smooth pursuit eye movements are normal. For example, in typical individuals, each of the following might demonstrate that smooth pursuit is present:

1. Subtract the distribution of eye velocities during fixation (i.e. 0°/s) from those during pursuit of a target of known velocity (e.g. 8°/s), with the difference (i.e. 8°/s) being attributed to the pursuit system.
2. Subtract the distribution of eye velocities when pursing a target of low speed (i.e. 8°/s) from those of a target of high speed (i.e. 16°/s), with the difference (i.e. 8°/s) being attributed to an increased output from the pursuit system in order to follow a faster moving target.

Although seemingly intuitive, using either of these methods is potentially confounded in those with IN by the properties of the null zone when pursuit of a moving target is attempted.

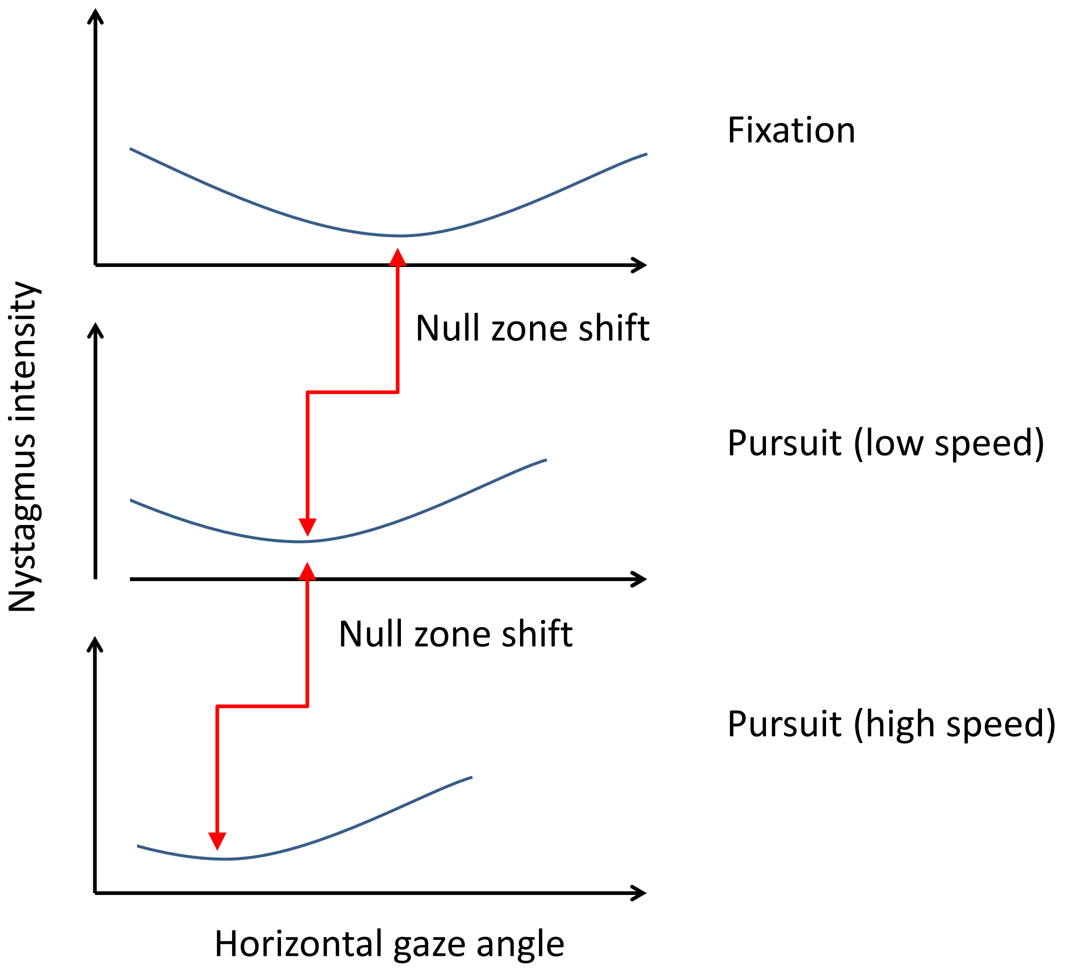

Figure 1.15 Schematic depicting a shift in the null zone location between fixation and pursuit, and between pursuit of a target with a low speed and a target of high speed.

On attempting smooth pursuit, it has been claimed that the location of the IN null zone shifts in a direction opposite to that of the attempted smooth pursuit (Dell'Osso et al., 1972; Dell'Osso et al., 1974; Kurzan and Buttner, 1989) (Figure 1.15). Therefore, the gaze angle at which the null zone is located when attempting pursuit will be different to when attempting fixation. By simply subtracting the eye movements obtained under fixation conditions from those during pursuit conditions would not demonstrate smooth pursuit. The null zone shift on attempted pursuit is also reported to depend on velocity, with greater shifts when attempting to follow faster targets (Dell'Osso, 1986; Kurzan and Buttner, 1989). Again, by subtracting eye movements for a lower pursuit speed from those for a higher pursuit speed would also not demonstrate pursuit. This is because again, any differences would be because the null zones would be located at different gaze angles. It might be conceived that if eye movements are recorded, whether under fixation or pursuit, it would be matter of first re-aligning the null zones to counteract any shift in the null zone, and then performing a simple subtraction. But, although the null zone shifts, the eye movements at equal gaze angles from the null zone are reported to be fundamentally different in their parameters (although these parameters are not specifically discussed) for different velocities (Kurzan and Buttner, 1989).

1.3.2 Section summary

In this section, although the entire slow phase can be used to characterise how well an individual follows a target, these data cannot be used to assess the integrity of the smooth pursuit system. Conversely, although the slow phase can be restricted to just the foveation period, it has been demonstrated that this constrains the resulting gains to nearly 1.0. Previous studies restricted their eye movement analyses to the foveation period in an attempt to demonstrate that the smooth pursuit system was normal during individual foveations. However, insufficient detail was provided about how the foveation period was defined. Finally, the use of the foveation period indirectly suggests that other eye movement systems may be the actual mechanism by which the act of following a target is achieved in IN, i.e. saccades.

The debate about whether those with IN have normal smooth pursuit eye movements is likely to continue. For the purposes of this thesis, it is not essential to establish if the smooth pursuit system is genuinely present and normal, since the present study is concerned with the perceptual compensation for eye movements in IN as a target is “followed”, irrespective of whether or not there is a contribution from the smooth pursuit system. In fact, I decided to explore this perceptual compensation for the whole eye movement (i.e. the entire slow phase), irrespective of any contributions made by the smooth pursuit system. Note that it is not necessary for any portion of the slow phase to be the output from the smooth pursuit system for there to be compensation. In order to fully understand the perceptual compensation, the act of following a target in the presence of a continuing eye oscillation must first be characterised. Therefore, the operational definition of “pursuit” in this thesis will be that act of *following a target*.

When characterising pursuit performance in this thesis, individuals with IN will be moving their eyes through a range of horizontal gaze angles. As discussed previously, the majority of null zones are located within 10° of the straight ahead position and should be within the trackable range of most eye trackers. Additionally, it has been discussed that the null zone undergoes a lateral shift on attempted pursuit. The lateral shift is in a direction opposite to the intended pursuit, and the magnitude of this shift increases with attempted pursuit speed. The lateral shift in the null zone has been reported to be as much as 25° even for the relatively low pursuit velocity of 15°/s (Kurzan and Buttner, 1989). Therefore, for those null zones already located at an eccentric gaze angle (e.g. 10° leftward or rightward), the null zone shift could move beyond the trackable range of the equipment (e.g. 35° leftward or rightward). Nonetheless, null zones will be determined during fixation in an attempt to determine the impact of pursuit on the gaze angle of the null zone. Therefore, it will be necessary to characterise the relationship of the IN oscillation and gaze angle through the study of fixation at different gaze angles.

1.4 Fixation

Unlike smooth pursuit, fixation is not an eye movement per se, but rather a state of very little to no movement of the eyes, the purpose of which is to continuously image the intended target on, or suitably close to, the fovea (Leigh and Zee, 1999). However, when fixating a stationary target, the eye is not truly static (Carpenter, 1988; Martinez-Conde et al., 2004; Skavenski and Steinman, 1970). For example, the eyes make three distinct eye movements during fixation. A small drift carries the eye away from the intended target which is followed by a micro-saccade to redirect the eye back onto the target. Superimposed on the drift is a high frequency, low amplitude tremor (Carpenter, 1988; Pritchard, 1961; Yarbus, 1967). The net effect of all three movements in normal subjects is an ever present, albeit minute, shifting of the retinal image during fixation.

1.4.1 Fixation in IN

Those with IN do not share the same fixation behaviour as typical individuals. The fast-phase redirects the eyes onto the intended target, and immediately after, the slow phase begins to carry the eyes away from the target. Studies of fixation in IN have been have generally been motivated by determining either:

1) Those properties of the slow phase that may constrain threshold visual acuity (e.g. foveation period duration (Abadi and Worfolk, 1989), foveation velocity criteria (Chung and Bedell, 1996))
2) The relationship between the magnitude and frequency of the IN oscillation and gaze angle (i.e. locating the null zone)

Those studies concerned with the impact of IN on acuity are not relevant to this thesis. However, locating the null zone by examining fixation at different angles of gaze is of particular importance in this thesis and has been discussed in the previous section. A number of papers have investigated how fixation varies as a function of horizontal gaze, with the aim of characterising the null zone (Dell'Osso et al., 1974; Kurzan and Buttner, 1989; Abadi and Bjerre, 2002; Abadi and Whittle, 1991; Dell'Osso, 1973a; Dell'Osso and Flynn, 1979). The experimental set up in all of these studies was similar. The participants' head was restrained in a rest while they viewed targets presented at different horizontal eccentricities as their eye movements were recorded.

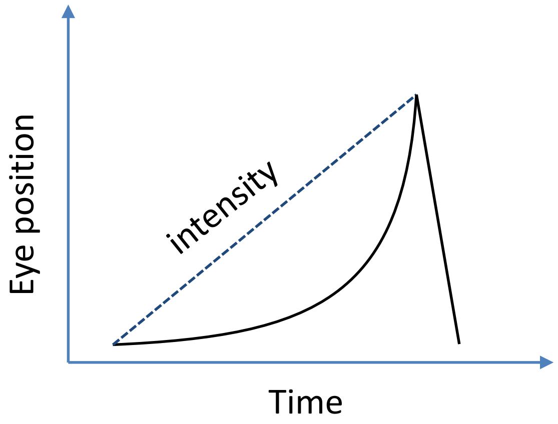

Figure 1.16 Intensity is the approximate mean velocity of the slow phase, and assumes a constant velocity.

The majority of studies investigating the null zone have utilised "intensity" as the metric with which to measure the magnitude of the IN oscillation (Dell'Osso and Flynn, 1979; Dell'Osso et al., 1974; Abadi and Whittle, 1991).

As a reminder, intensity is the amplitude of the oscillation multiplied by the frequency of the oscillation. However, other than providing a basic definition of what intensity is, there are no explicit details provided as to how any intensity values were actually derived in any of these studies. For example, intensity could be calculated on a cycle-by-cycle basis or as the mean amplitude multiplied by the mean frequency. Examples of the descriptions given are:

"*Intensity was calculated by determining the product of the nystagmus amplitude and frequency at each gaze angle. These functions were plotted and used to quantify the required therapeutic gaze angle shifts that were provided by version prisms*" (Dell'Osso et al., 1974)

"*All patients has a static neutral zone while fixating horizontally placed light spots*" (Kurzan and Buttner, 1989)

"*Amplitude of the nystagmus was defined as the peak-to-peak slow-phase displacement, frequency as the number of oscillations per second, and intensity as amplitude x frequency*" (Abadi and Whittle, 1991)

One of the largest studies of IN null zones completely omitted all detail on how the null zones were determined, including the metric used to determine the null:

"*In all, 195 of the 224 subjects had the position and extent of their null zones investigated*" (Abadi and Bjerre, 2002)

In another study, regions of the eye movement recording were cherry picked for use in their analysis, without further discussion on how they were selected:

"*Sections of the data that represented the typical waveform of each of the patients were also selected for slow-phase analysis*" (Abadi and Whittle, 1991)

(a)

This image has been removed by the author for copyright reasons

(b)

This image has been removed by the author for copyright reasons

Figure 1.17 Plot of intensity as a function of gaze angle for a single individual taken from (Dell'Osso et al., 1974). A coarse measurement of the intensity-gaze angle relationship is shown in (a) while a finer measurement is shown in (b).

This image has been removed by the author for copyright reasons

Figure 1.18 Example data showing large variability in the amplitude of the IN oscillation as the participant viewed a target at a fixed location. The colour of the plotted dots indicates the direction of the slow phase as the target was being fixated: blue for left, black for right. Error bars indicate 1 standard deviation. Image taken from (Abadi and Whittle, 1991).

Few studies have ever published images of the relationship between the magnitude of IN and gaze angle to demonstrate a reduction at one particular gaze angle (i.e. the null zone) (Dell'Osso et al., 1974; Dell'Osso and Flynn, 1979; Abadi and Whittle, 1991). Example images demonstrating a null zone are presented by Dell’Osso et al. (1974) (Figure 1.17 (a) and (b)). In Figure 1.17 (a), a coarse sampling of the intensity-gaze angle relationship has been made which follows a “U” shape.

Beginning at the extreme left at a gaze angle of -30°, intensity rapid declines as the participant moves their gaze rightward, with minimum intensity occurring just to the right of the straight-ahead position at approximately +5° to +10°, before intensity rapidly increases at +30°. In Figure 1.17 (b), the same null zone has been determined with more detail. However, it is not clear whether sampling at intervals (1°) that are smaller than the amplitude of the nystagmus (2°) yields any benefit in determining the precise location of the null (sub-sampling). From Figure 1.17 (a), it is evident that only a single value was used to summarize the intensity of the IN oscillations at any given gaze angle, which presumably represents the mean intensity, although this is never explicitly stated. To the best of my knowledge, only one study has documented the variability of the IN oscillation using amplitude as the metric (i.e. this study included error bars on graphs of mean amplitude).

However, the variability was only documented at a few gaze angles (-10°, -20°, 0°, 40°, and 45°), rather than for the entire range of gaze angles (Abadi and Whittle, 1991). Examples of the variability of the IN oscillation are presented in Figure 1.18. Other studies reporting measures of IN magnitude do not document the variability at different gaze angles (Dell'Osso and Flynn, 1979), presumably relating to the operational definition of the null as the minimum intensity, as adjacent values would seem irrelevant, irrespective of their mean value or variability. However, I would argue that knowing the variability in the measurement is useful, as it can aid in determining the width of the null zone, or if the null zone is likely to vary on repeated measurement. For example, the location of the minimum intensity may be due to chance if both the mean and standard deviation of adjacent points are not taken into consideration. In other words, in any set of measurements, one value will inevitably be the minimum, but the important question becomes whether this minimum is a significantly meaningful minimum i.e. can its position vary?

1.5 Eye movement performance measures

In general, measures conventionally used to quantify eye movements are identical for typical individuals and those with IN. For example, gain is used to quantify the pursuit in both those with and without IN, while the main sequence can be used to quantify voluntary saccades in typical individuals or fast phases in those with IN. The only major difference occurs when assessing fixation performance, where one dimensional methods (e.g. intensity) prevail for IN, whereas modern, sophisticated two-dimensional measures are used in typical individuals (Cherici et al., 2012) and those with foveal pathology (Castet and Crossland, 2012; Collewijn et al., 1985; Crossland et al., 2005; Crossland et al., 2004a; Crossland et al., 2009; Crossland and Rubin, 2002; Crossland et al., 2004b). Despite advances in eye tracking technology, there has been little advance on how IN has been quantified. I would argue that the continued use of current eye movement measures in IN should be reconsidered for two reasons. First, they are one one-dimensional rather than two, and second, they can measure either accuracy or precision, but not both. I will now consider each of these issues in turn.

1.5.1 One-dimensional and two-dimensional measures

Historically, eye movement recordings and/or analyses from those with IN were restricted to only the horizontal axis, irrespective of whether targets were stationary (Abadi and Dickinson, 1986; Abadi et al., 1989; Abadi and Whittle, 1991; Abadi et al., 1999; Bedell et al., 1987; Bedell and Currie, 1993; Bedell et al., 1989; Cham et al., 2008; Dell'Osso, 1973a; Dell'Osso, 1973b; Dell'Osso, 1985; Dell'Osso et al., 1983; Dell'Osso and Flynn, 1979; Dell'Osso et al., 1974; Felius et al., 2011; Gresty et al., 1984; Jones et al., 2013; Tkalcevic and Abel, 2003; Ukwade and Bedell, 1992) or moving (Dell'Osso, 1986; Dell'Osso et al., 1972; Dell'Osso et al., 1992b; Gresty et al., 1984; Kommerell, 1986; Kurzan and Buttner, 1989; Wang and Dell'Osso, 2009; Wang et al., 2012; Yamazaki, 1978; Yee et al., 1980). This may have been because the IN oscillation is predominantly horizontal, or because the limitations of eye tracking technology were such that only one component (i.e. horizontal or vertical) could be measured at any one time (e.g. Skalar IRIS), in which case the horizontal would have been the more important as that is the axis containing the majority of the IN oscillation. There have been some notable exceptions that have considered vertical eye movements (Abadi and Dickinson, 1985), but few studies have presented *simultaneous* horizontal and vertical eye movements (Collewijn et al., 1985; Dell'Osso et al., 1997; Thomas et al., 2011; Bedell et al., 1989). If it was the case that the equipment used provided one dimensional measures, then the analyses could only ever be one dimensional. However, both the horizontal and vertical components of eye movements are readily available on modern eye tracking technology (e.g. EyeLink 1000 and Tobii TX300). Despite this, even recent analyses are still restricted to one dimension (Jones et al., 2013; Wiggins et al., 2007). However, this constraint may lead to inappropriate conclusions because the ability to image a target on the fovea is not simultaneously determined. For example, consider a horizontally moving target being pursued by an individual with IN. We cannot calculate the gain in the vertical direction for a horizontally moving target, as this would require dividing vertical eye velocity by zero. Therefore, we are forced to assume that the target was perfectly imaged on the fovea at all times in the vertical axis. This might not seem a major problem since the IN oscillation is predominantly horizontal, and it might be reasonable to assume that eye movements in the vertical axis are no different to those without IN. However, now consider a vertically moving target being pursued by the same individual. In this case, we are unable to calculate the gain in the horizontal direction. Yet, however good the pursuit might be in the vertical direction, given the underlying oscillation it is highly unlikely that the target will be perfectly imaged on the fovea at all times along the horizontal direction. By restricting the analysis to one dimension the IN oscillation has not been fully characterised. Yet, the functional goal of smooth pursuit is to continuously image the intended target on the fovea, in *both directions*.

1.5.2 Accuracy and precision

Success at either pursuit or fixation can be defined in terms of *accuracy* and *precision*. Accuracy describes the proximity of measured values to a reference value, whereas precision describes the variability of the measured values. These concepts are depicted as a schematic in Figure 1.19. To aid understanding, smooth pursuit gain will be used as an example. The reference value, shown as a black line indicates that eye speed necessary to exactly equal the target speed. The measured values are the entire distribution of eye speeds measured in response to the target motion. Performance can therefore be quantified in terms of accuracy, by expressing the proximity of the mean eye speed to that of the reference eye speed. In the case of gain, this accuracy is usually in the form of a ratio (mean measured eye speed divided by the reference eye speed). In this example the gain would be greater than 1.0, since the mean eye speed is greater than (i.e. lies to the right of) the reference eye speed.

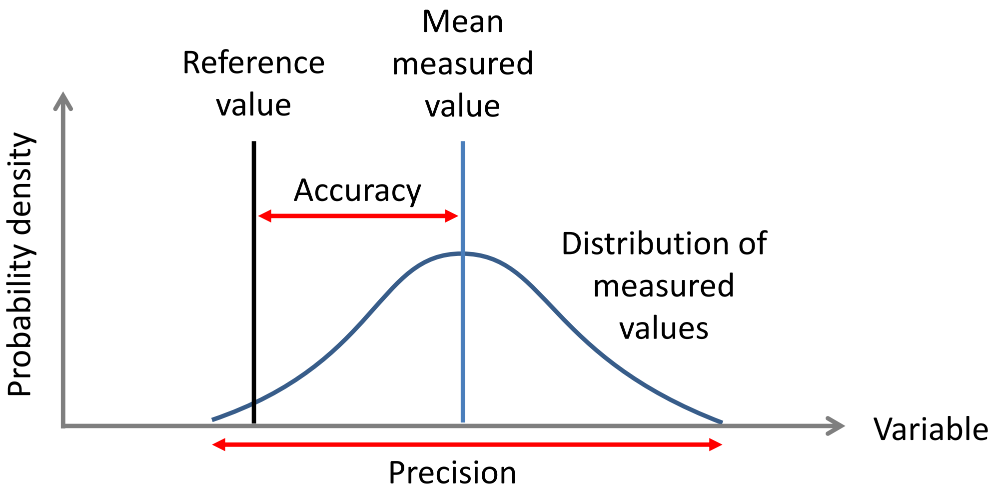

Figure 1.19 Schematic depicting of the concept of accuracy and precision. Accuracy is the proximity of the mean of the measured value (blue line) to the reference value (black line), whereas precision is the variability in the measured data (blue curve).

Performance can also be quantified in terms of precision, by expressing the variability of the measured eye speeds (i.e. standard deviation). In the case of smooth pursuit gain, the variability is also expressed as a ratio of the target speed (i.e. standard deviation gain divided by the reference speed). In all types of eye movement, it is possible to be accurate but not precise (and vice versa). For example, consider a gain of 1.0. From the previous discussion, we know that for the gain to be 1.0, the mean eye velocity was equal to the target speed. However, without a measure of precision it cannot be concluded that at all times the target was imaged perfectly on the fovea.

1.5.3 Section summary

In this section, it became clear that, to adequately characterise eye movements, there needs to be a significant paradigm shift in how they are quantified, especially if comparisons are to be made along differing target directions. This thesis will inevitably require the formulation of a generalised two-dimensional measure, capable of measuring both the accuracy and the precision of pursuit and fixation eye movements in both those with IN and typical individuals

1.6 Thesis outline

In the preceding sections, the characteristics of IN were outlined and a discussion of how those with IN do not report the world as oscillating. This provides an invaluable opportunity to probe whether the mechanisms that are hypothesised to perceptually compensate for eye movements can be generalised to a cohort with pathological eye movements. One possible mechanism for compensating for retinal image motion arising from eye movements has been outlined, and requires the subtraction of the retinal image motion induced by eye movements from the overall retinal image motion. It has been discussed how this mechanism is prone to error, even in typical individuals, giving rise to the Filehne illusion. The lack of information about the process of perceptual compensation of IN eye movements to recover object motion has been the principal motivation for this thesis. To lay the methodological basis for analysing the results of eye movement experiments, I will first describe in *Chapter 3* a generalised two-dimensional measure of accuracy and precision for use in both fixation and pursuit. In *Chapter 4,* I will first attempt to characterise the location of null zone locations during fixation in IN. However, in order to interpret the results of the Filehne illusion, I must first characterise how those with IN follow a moving target in the presence of an ongoing eye oscillation. These experiments will be presented in *Chapter 5*. Differences in the oculomotor performance of fixation and pursuit will be determined in *Chapter 6*. Experiments determining whether those with IN can perceptually compensate for their eye movements will be presented in *Chapter 7*. The conclusions of this work, along with general implications and findings, are discussed in *Chapter 8.*

.

2 General methods

2.1 Introduction

In this chapter, the research population and experimental apparatus will be discussed. In addition, those methods used for the processing of eye movement data and their experimental verification are discussed.

2.2 Participants

In this thesis, the research population was defined as those individuals with IN, whether idiopathic or with an associated condition. They were drawn from across the UK. The research sample was not limited in any way other than aged 18 years or older and with no previous extra-ocular muscle surgery or drug therapy, as these interventions would alter the IN waveform. Participants with IN were recruited through an existing database held by Research Unit for Nystagmus in the School of Optometry and Vision Sciences, and via Nystagmus Network (NN), a UK charity. It was planned that a minimum of 10 participants with IN would complete each experiment, consistent with previous studies that had a cohort of 9 (Dunn et al., 2014) or 11 (Wiggins et al., 2007). Control participants were recruited in two ways: either as volunteers from the community, or using a Participant Panel coordinated by the School of Psychology. The former were paid reimbursement for their time, while the latter consisted of undergraduate students who participated for course credit. All participants gave their informed consent to take part in the study

2.2.1 Pre-screening

All participants underwent an optometric and orthoptic pre-screening using their habitual spectacle correction, if worn. Pre-screening included logMAR acuity (Precision Vision; Illinois, USA) at 2m, Pelli-Robson contrast sensitivity (Precision Vision; Illinois, USA) at 1m, and cover testing for distance (6m) and near (33cm) fixation to determine the presence or absence of any heterotropia. If any participant wore spectacle correction, the prescription was measured using manual focimetry (LM-6, Topcon; Tokyo, Japan). Clinical details for each IN participant can be found in Appendix 1.

2.3 Eye movement recording

Currently, the most popular technique for recording eye movements is video-based eye tracking (Holmqvist et al., 2011). Researchers in both the School of Optometry and Vision Sciences and the School of Psychology have extensive experience in using video-based eye trackers, in particular the EyeLink 1000 (SR Research Ltd, Ontario, Canada) (Dunn et al., 2014; Dunn et al., 2015; Harrison et al., 2015; O'Connor et al., 2010). For this reason, the EyeLink 1000 was chosen to record the eye movements in this thesis.

The EyeLink 1000 is a 1000Hz eye tracker that is available in a two different mounting options. For the experiments carried out in this thesis, the ‘tower mount’ was chosen over the ‘desktop mount’ because of its larger tracking area. According to the EyeLink 1000 technical specifications (SR-Research, 2009), the desktop mount provides a trackable area of 32° H x 25° V corresponding to 800 degrees^2, whereas the tower provides a trackable area of 60° H x 40° V corresponding to 2400 degress^2, a three-fold increase. The tower mount also provides an unobstructed inferior visual field unlike the desktop mount which must be located at a distance of 40-70 cm in front of the participant (SR-Research, 2009), occluding the lower portion of any visual display. The infrared LED array of the desktop mount is also visible to participants in dark viewing conditions, but this is not the case for the tower mount. This becomes especially important when wanting to prevent referenced motion judgements, as demanded by the experiments on the Filehne illusion described in Chapter 7.

There are some well recognised factors that will influence eye movement data quality: spectacle wear that causes IR reflections, and eye make-up that interferes with pupil detection. For these reasons, participants were advised not to eye wear makeup on the day of the experiments and, if possible, to wear contact lenses rather than spectacles.

2.4 Projection screen

A flat projection screen, measuring 200cm horizontally and 155cm vertically, was chosen as the visual display to utilise as much of the trackable area of the EyeLink 1000 tower mount as possible.

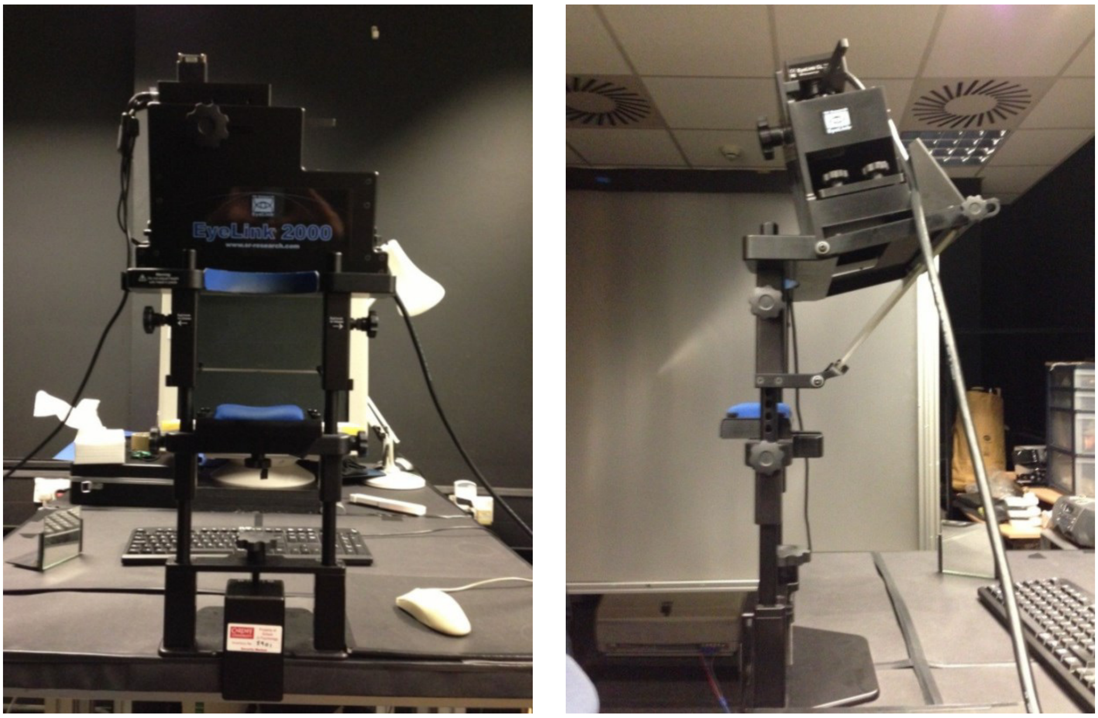

Figure 2.1 The EyeLink 1000 tower mounted eye tracker.

A disadvantage of projecting light onto a flat screen is that the incident light becomes more divergent with the distance from the centre of the screen. This can create a luminance 'hotspot' at the centre of the display, such that stimuli displayed centrally are brighter than those placed peripherally. In an attempt to minimise this effect, the rear projection screen contained an embedded Fresnel lens that collimated the projected light as it passed through the screen.

2.5 Viewing distance

Inducing convergence with base out prisms has been reported to dampen the IN oscillation in some individuals (Dell'Osso et al., 1972). One way to avoid significant convergence is to have a suitably long viewing distance. Many viewing distances have been used in previous studies of IN: 1m (Cesarelli et al., 2000; Bifulco et al., 2003), 1.12m (Dell'Osso, 1973a; Dell'Osso, 1973b), 1.14m (Dell'Osso et al., 1974; Abadi and Whittle, 1991; Dell'Osso and Flynn, 1979; Abadi and Bjerre, 2002), 1.53m (Dell'Osso, 1985; Dell'Osso et al., 1997; Wang and Dell'Osso, 2009), 1.60m (Abel and Malesic, 2007), 2m (Abel et al., 1991). In this thesis, the experimenter chose a viewing distance of 1.4m. At this distance with a typical adult inter-pupillary distance of 64mm (Thompson, 2002), each eye would converge 1.31°. However, as it was not known whether this viewing distance would be sufficient to prevent convergence dampening, the original case report of convergence dampening was reviewed (Dell'Osso et al., 1972). When the base is oriented 'out' (i.e. temporally), ophthalmic prisms displace images towards the prism apex (i.e. nasally). Consequently, such 'base out' prisms induce convergence. They reported that a total of 7^{Δ} base out was required in front of each eye to induce convergence dampening. This resulted in a convergence of 4° per eye, considerably greater than the 1.31° produced here, indicating that a viewing distance of 1.4m would be highly unlikely to induce convergence dampening.

2.6 Projector

A CRT projector (Multiscan VPH 1272QM; Sony, Tokyo, Japan) was chosen to display the visual stimuli (Figure 2.2). The 3 cathode ray tubes of the projector are arranged horizontally. To ensure that the cone of light leaving the projector was symmetric, only the central green cathode ray tube was used. This was achieved by generating all stimuli in green in the display software, with an occluder over the red and blue cathode ray tubes used to eliminate any ambient light from these additional tubes. The projector was further modified by placing a neutral density (ND) filter (Kodak Wratten 2 Neutral Density Filters; Kodak, UK) over the green cathode ray tube. Optical density is the $\log_{10}$ of the reciprocal of the transmitted fraction of light, and the magnitude of the ND filter used in this case was 0.9, reducing the projector output by 87.5%. This modification reduced the projector output in order to:

1. Ensure that projected black backgrounds were not visible when the laboratory illumination was turned off.
2. Ensure that, when multiple visual stimuli were displayed at once, the laboratory was not 'flooded' with light, such that participants could make judgements about motion relative to objects in the room.
3. Reduce any smearing of the stimuli caused by persistence of the phosphor used within the CRT projector.

Figure 2.2 The display screen and the CRT projector .

2.7 Programming environment and stimulus rendering

All visual stimuli were generated using the OpenGL graphics library driven by the Delphi programming environment (Version 7, Borland Software Company; Cupertino, California, USA). Stimuli were rendered using a GeForce 7300 LE graphics card (NVIDIA; Santa Clara, California, USA) and displayed using the CRT projector at a frame rate of 72Hz and a resolution of 1024-by-768 pixels.

2.8 Eye Movement data calibration

Prior to use by each participant, the EyeLink 1000 must be calibrated. Control participants were required to sequentially fixate nine calibration points (0.4° diameter) arranged in a 3-by-3 grid with a separation of 16° between each calibration point. Calibration points were manually accepted by the experimenter, and calibration accuracy was confirmed by using the EyeLink 1000 calibration validation procedure. The EyeLink 1000 grades the calibration validation as either ‘good’, ‘fair’, or ‘poor’. Calibration validations that were deemed ‘fair’ or ‘poor’ were repeated. Calibration is more difficult for IN participants because their slow phases continuously move the eyes off-target. For this reason, differing custom eye-movement calibration techniques have been developed for IN, using either linear regression techniques where eye position is linearly regressed against target position (Jones et al., 2013) or analyses that take advantage of the stereotyped relationship of saccade duration and saccade amplitude (Theodorou et al., 2015). More recently, a custom calibration procedure for use with the EyeLink 1000 has been developed (Dunn, 2014), which can be applied to data retrospectively.

In this thesis, eye movement data for individuals with IN were calibrated retrospectively, using calibration stimuli and stimulus separation as used for the per typical control participants, but with a 12 second recording of eye movements at each calibration location. The MATLAB® code to compute the retrospective calibration of IN eye movement data was generously provided by Dr Matt Dunn, Cardiff University. This calibration first splits IN eye movement data into individual waveform cycles. Next, saccades are identified, with the remainder representing slow phases. A velocity threshold is automatically adjusted until foveations are found in 50% of IN cycles. The median coordinates of this 'foveation data' are calculated so that there is an x and y coordinate pair for each calibration point. A transformation matrix is then applied to the horizontal and vertical components of the data separately.

2.9 Eye movement data processing

EyeLink 1000 data were imported into MATLAB® using an open source function called 'EDFMEX' (Kovach, 2007), and the display gaze samples were extracted using custom functions.

2.9.1 Smoothing and temporal differentiation of eye position data

There is a wide variety of filters used in the literature. In this thesis, raw eye position data were low-pass filtered with a 4th order Butterworth filter with a 60Hz cut-off frequency. This filter was chosen because its effect on eye movement data has been well documented (Juhola, 1986), and unlike other filters, this one does not truncate the number of samples after filtering. First, second and third derivatives of the filtered eye positive waveform were then taken to yield eye velocity, acceleration, and 'jerk', respectively.

2.9.2 Artefact detection and removal

Blinks and other artefacts (e.g. extraneous reflections being mistaken for corneal reflections, poor identification of the pupil from eye makeup etc.) present in the eye movement data (see 2.3 Eye movement recording) mimic saccades and needed to be removed. While many artefacts manifested as large changes in eye position, typically on the order of magnitude of x10^6 ° (Figure 2.3), others had smaller changes in eye position that were within the plausible range of saccades (Figure 2.4), although their durations were too brief (e.g. 15 ms) and their frequencies too high (e.g. 20 Hz) to make them saccades. Although a simple position threshold could be used to remove larger amplitude artefacts, it cannot be used for smaller amplitude artefacts because it would potentially remove actual saccades as well. One solution would have been to use a saccade detecting algorithm that would identify both saccades and artefacts, and to isolate artefacts as those eye movements that were outliers on the saccadic main sequence. However, since the saccade detecting algorithm devised for this thesis relied on the mean and standard deviation of absolute velocity (Chapter 2.9.3 Saccade detection and removal), the presence of artefacts with large position changes would have inflated the mean and standard deviation of absolute velocity making them too large to ensure accurate saccade detection. A jerk thresholding algorithm was therefore designed, taking advantage of the extremely short duration of artefacts; a rapid position change would manifest as large change in jerk (Figure 2.5).

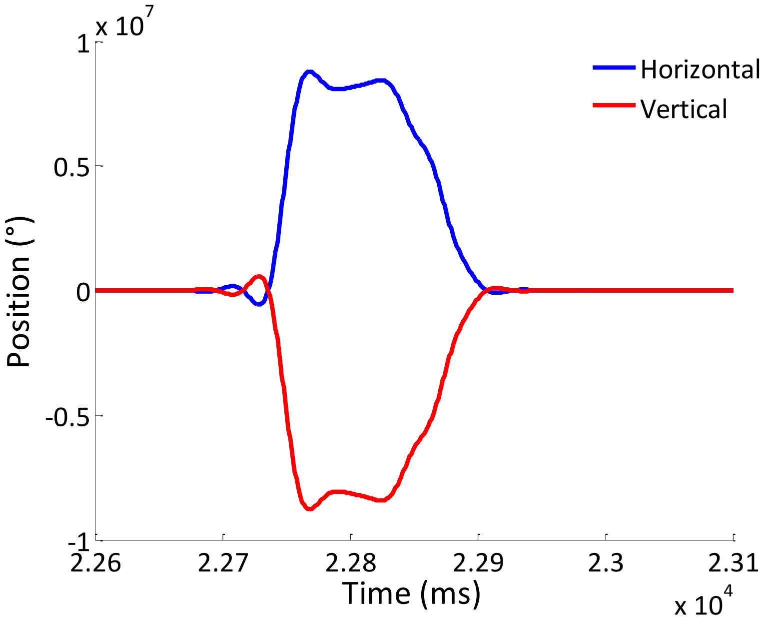

Figure 2.3 Artefacts were those abrupt and large changes in eye position introduced by blinks and other eye tracking. In this example, the artefact can be seen in both the horizontal (blue) and vertical (red) eye position data.

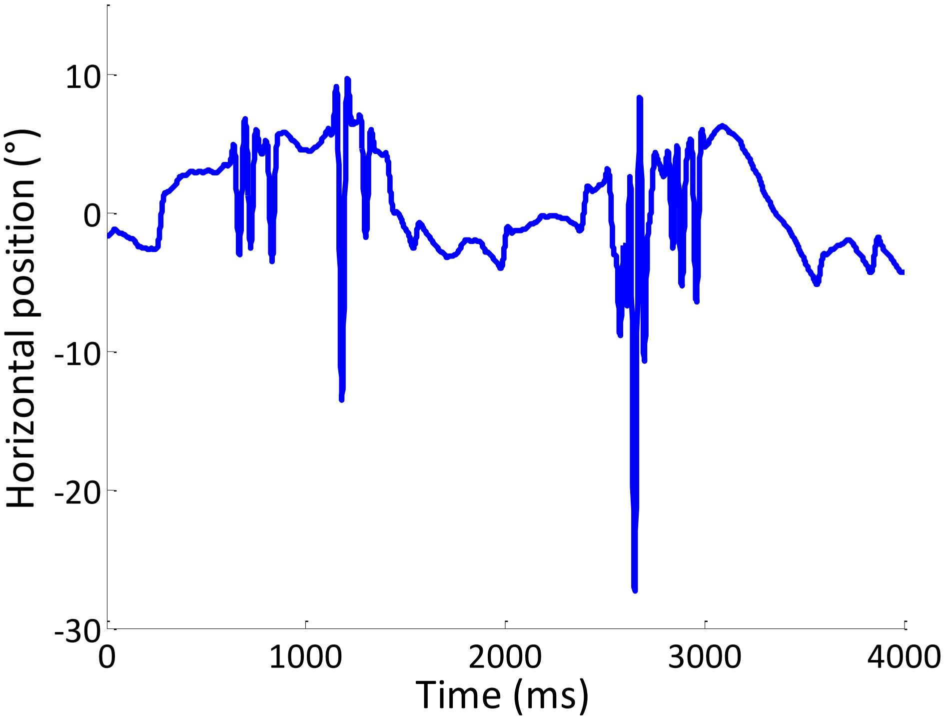

Figure 2.4 Artefacts do not always result in large changes in eye position. In this example, aberrant eye tracking has produced abrupt changes in eye position that are within the range plausible for a saccade.

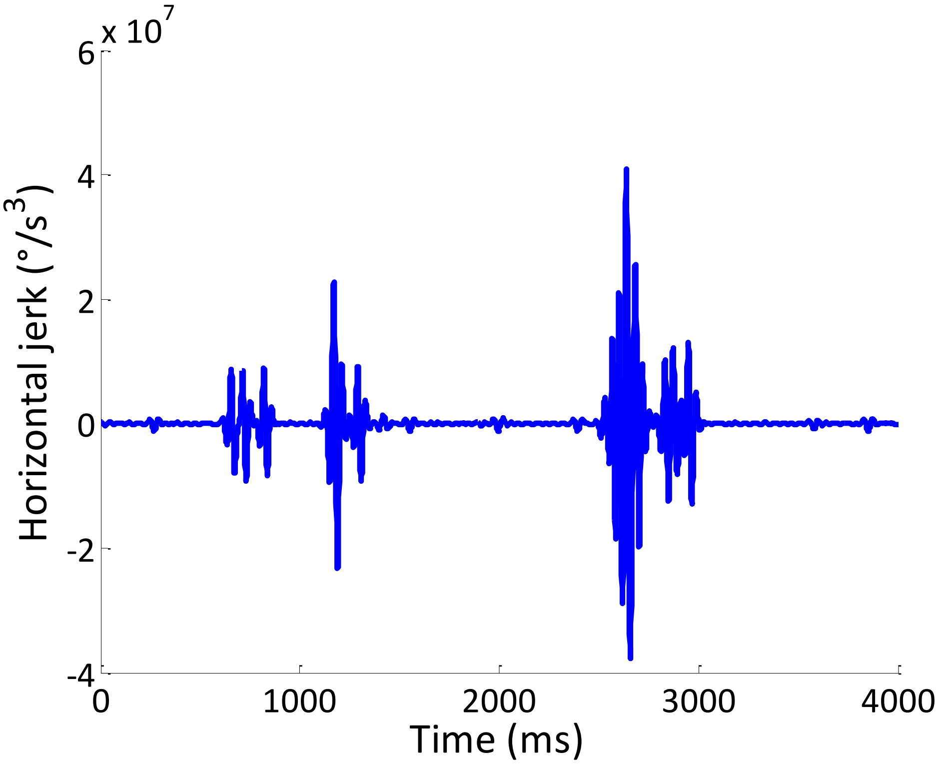

Figure 2.5. Jerk values help distinguish artefacts from genuine saccades. Corresponding jerk values for the data in Figure 2.4

The procedure was based on detecting artefacts as outliers in the jerk distribution in each trial. An example is shown in Figure 2.6, which plots the cumulative distribution function of jerk values, binned in steps of $1x10^5$ °/s^3, for a single trial. Since artefacts were not common in the data, the function rapidly asymptotes. The point of inflection of the asymptote can therefore be used as the threshold for eliminating the artefacts. The point of inflection was based on the gradient of the cumulative function and defined as the point where the gradient equalled 0.027, based on repeated visual inspection of the jerk outputs by the experimenter.

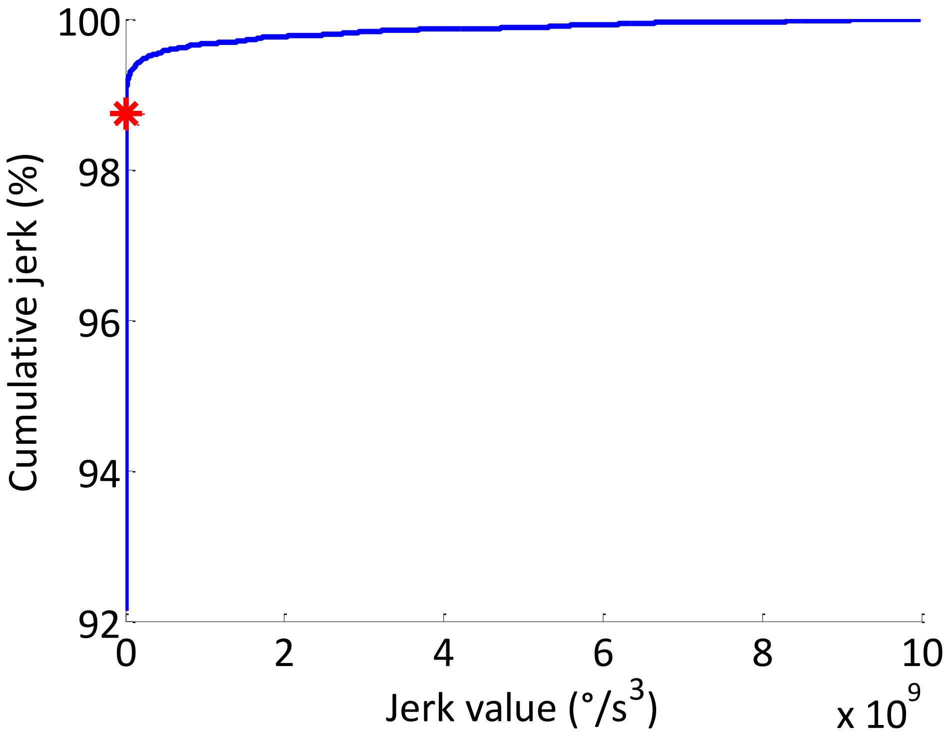

Figure 2.6 A plot of cumulative jerk for horizontal eye movement data for the trial shown in Figure 2.3, with the experimenter defined point of inflection also shown (red asterisk).

The threshold value was then used to screen out the artefacts. Continuous regions that exceeded the threshold were treated as a single artefact, with an additional 200ms being removed either side of the artefact. The start and end points of the artefact were extended until the end of velocity monotonicity in the velocity domain to ensure that no artefact contaminated regions remained. Finally, this entire region was replaced with 'NaN's, a standard computing method for representing an undefined value, in both the horizontal and vertical components for eye position, velocity, acceleration and jerk. Using NaNs avoids the need for data interpolation, sparing the experimenter from having to make potentially inappropriate assumptions about the underlying eye movements (e.g. accelerating, decelerating or constant velocity).

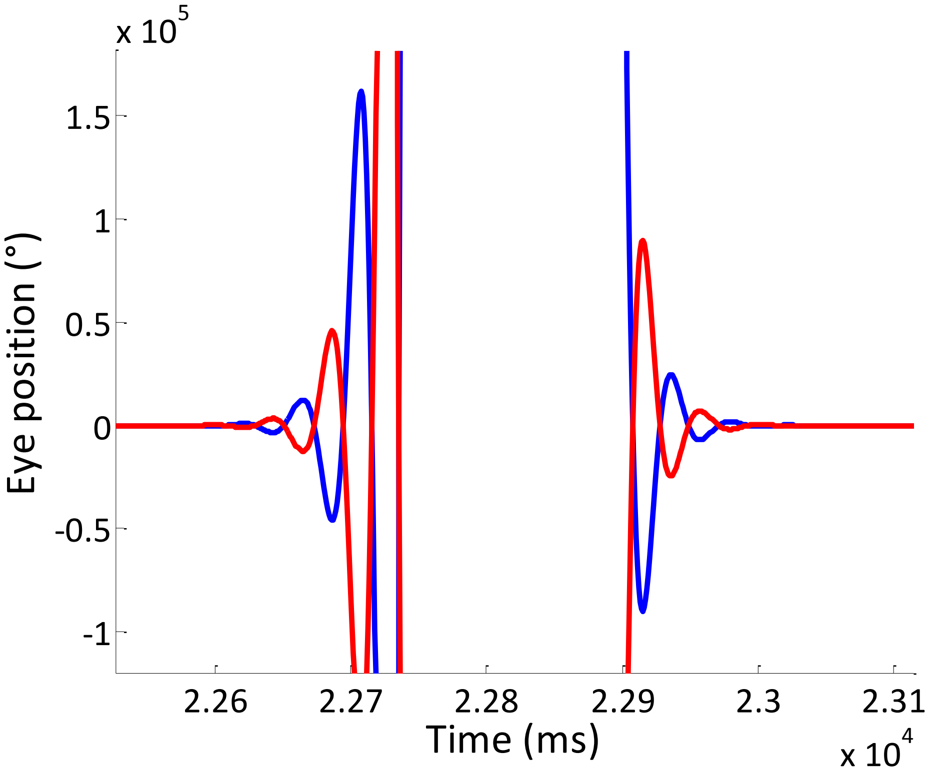

Figure 2.7 Artefacts were time-locked in the horizontal (blue) and vertical (red) components of eye movement data (in this case, eye position).

Artefacts are time-locked in the horizontal and vertical components of eye movement data (Figure 2.7). Therefore, artefacts only needed to be detected in the horizontal component (Figure 2.8 and Figure 2.9) before being removed from both horizontal and vertical components (Figure 2.10).

2.9.3 Saccade detection and removal

Saccades, or more correctly, the horizontal and vertical components of saccades, needed to be detected and removed before slow-phase eye movements could be quantified. The saccade detection algorithm was based on a single absolute velocity criterion, the value of which was set to the mean of absolute velocity, plus a multiple of its standard deviation. The multiple was varied by the experimenter for each participant, on each trial, based on visual inspection of the trial data with the output of the saccade algorithm superimposed.

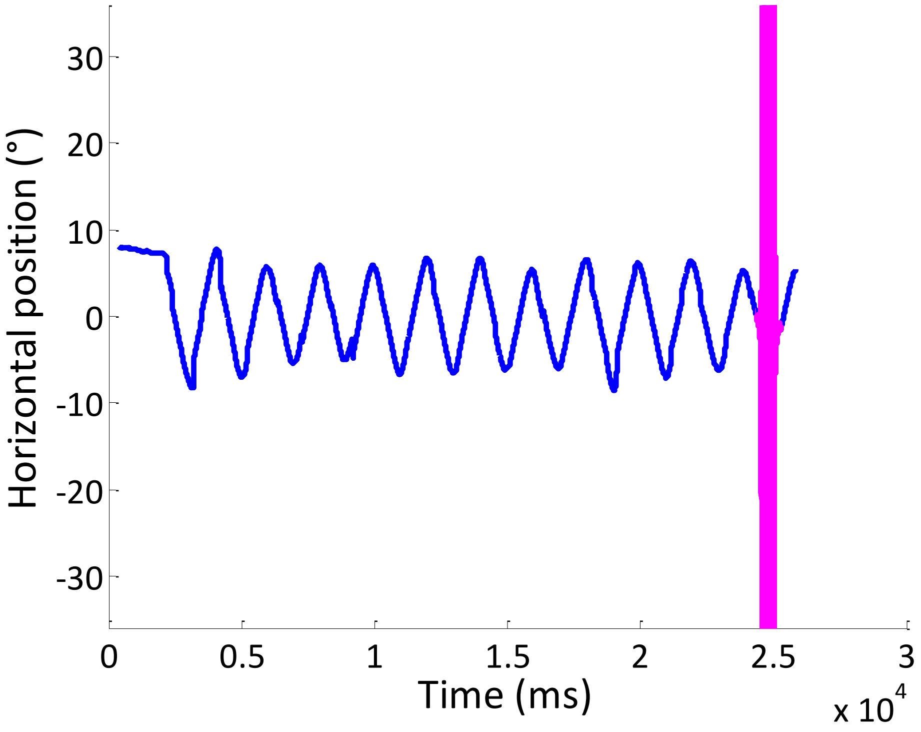

Figure 2.8 Artefact (magenta) detected in horizontal eye position data (blue), using jerk thresholding described in the text.

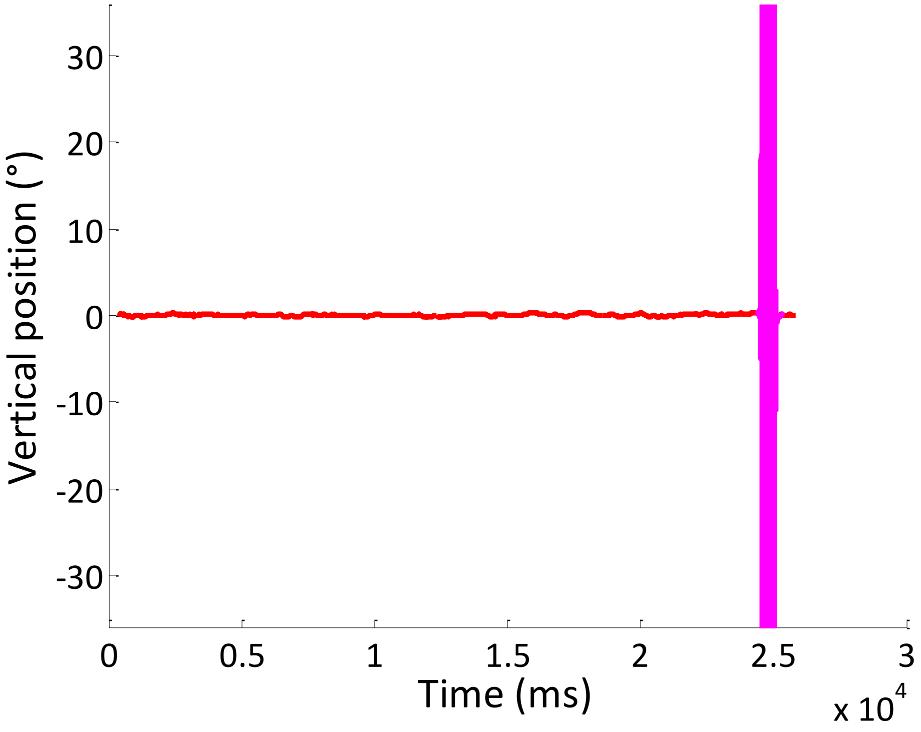

Figure 2.9 Artefact (magenta) detected in vertical eye position data (red), using cumulative jerk thresholding of horizontal jerk.

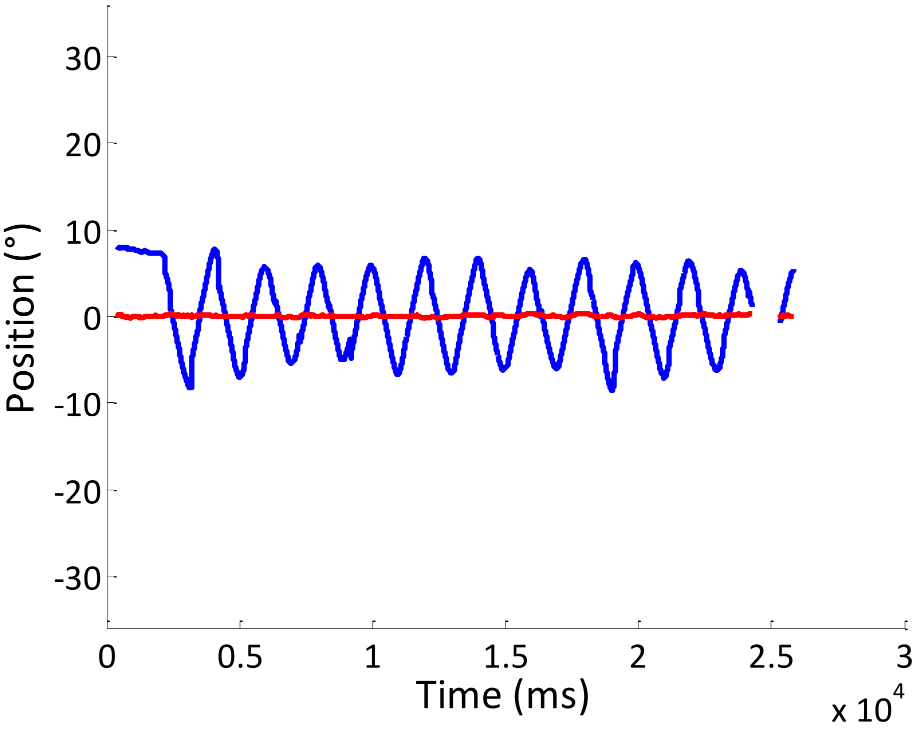

Figure 2.10 Removal of artefacts from horizontal (blue) and vertical (red) eye position data.

The method for detecting saccades proceeded as follows. Local maxima and minima within the velocity data were detected using an open source function for MATLAB® called 'peakdet' (Billauer, 2012). All local maxima that exceeded the absolute velocity criterion were identified and became the centre of candidate saccades (Figure 2.11). For each candidate, the onset and offset corresponded to the preceding and ensuing local minimum, respectively. If any 'NaN's were present in the absolute velocity data of a candidate saccade, the entire velocity data for the candidate saccade were replaced by 'NaN's, rejecting it as either a saccade or slow-phase eye movement.

Saccades were first detected in the horizontal component of eye movement data and removed from both the horizontal and vertical eye movement data before the entire saccade detection process was repeated on the remaining vertical component of eye movement data.

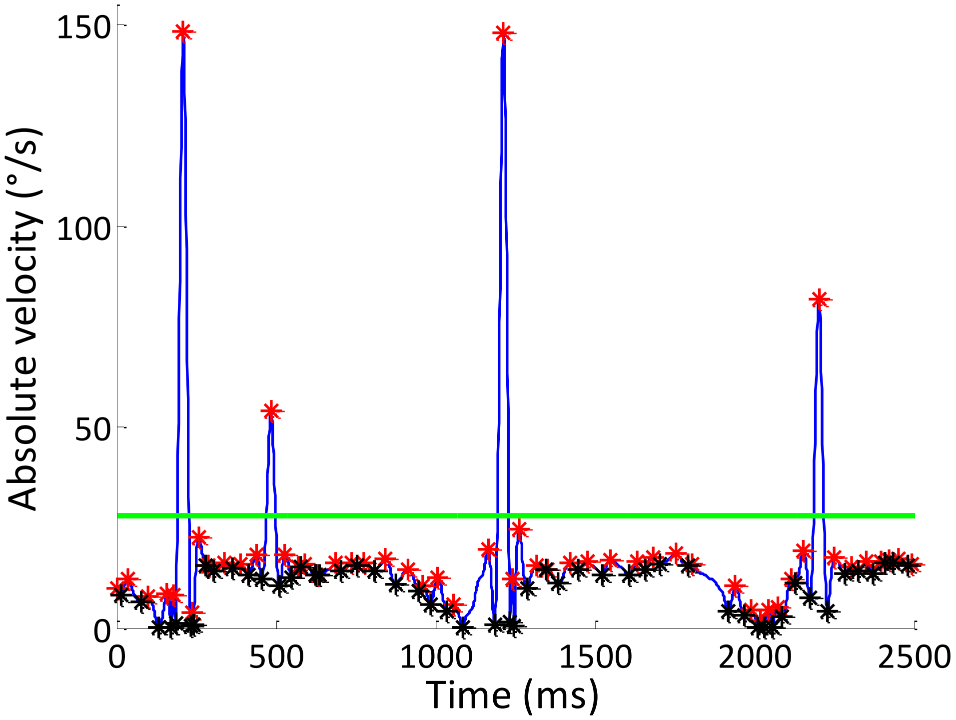

Figure 2.11 Detecting saccades in absolute horizontal eye velocity data (blue) was achieved by first finding all local maxima (red asterisk) and minima (black asterisk). Those local maxima exceeding the velocity criterion (green) were then identified and were treated as the centre of the candidate saccade. The preceding local minimum and ensuing local maximum for each candidate saccade was then determined, which became the saccade onset and offset, respectively. In this example, the velocity criterion was 28.08°/s, which yielded 4 saccades in this segment.

When saccade peak velocity is multiplied by saccade duration and plotted against saccade amplitude, a linear relationship should result. The slope of the least-squares regression line, constrained through zero, is known as the Q-ratio (Harwood et al., 1999; Gitchel et al., 2013) (Figure 2.12). The saccade detecting algorithm was experimentally verified by determining the Q-ratio of 677 centrifugal horizontal saccades made by the experimenter. The eye movements were processed using the method described above. The Q-ratio in this example was 1.82, in close agreement with published data that found Q-ratios for typical individuals to be 1.81 ± 0.39 (Gitchel et al., 2013).

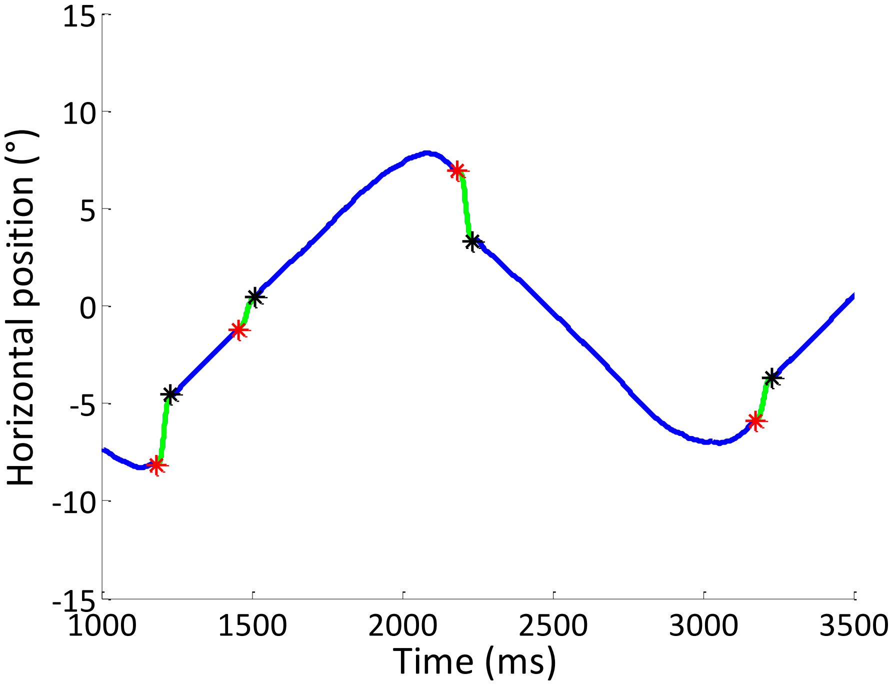

Figure 2.12 Saccades (green) detected in Figure 2.11 are shown on this corresponding eye position trace. Saccade onset (red asterisk) and saccade offset (black asterisk) are also shown.

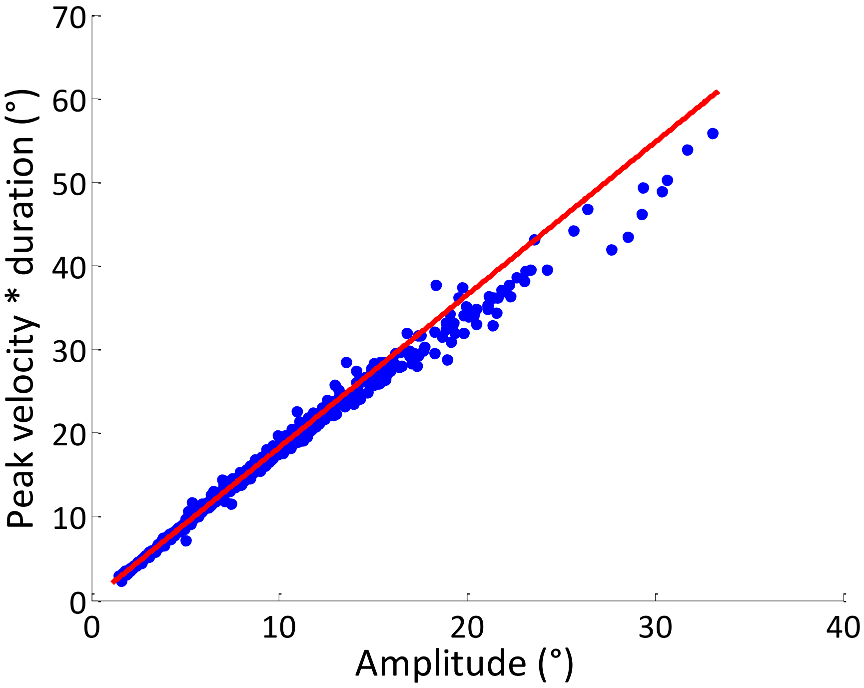

Figure 2.13 Verification of the saccade detecting algorithm by plotting the saccadic Q-ratio for 677 saccades made by the experimenter. A least-squares linear fitting procedure was applied in MATLAB®, with the fit constrained through the origin. This yielded a Q-ratio of 1.82.

2.10 Summary

Slow-phases move the eyes away from the intended target, where-as fast-phases redirect the eye onto the target. These two phases have very different functions in the IN oscillation, and more than likely governed by distinct neural pathways. Separating artefacts from real eye movement data is a necessary preliminary step. Following this, the two types of eye movement, slow- and fast-phases can be segmented so that individual characteristics of either phase may be studied and quantified. The algorithms developed in this chapter provide a convenient method for distinguishing eye tracking artefacts from fast phases and fast-phases from slow-phases. The majority of this thesis concerns the slow-phase eye movements and the perceptual consequences of a continuously moving retinal image. Having now demonstrated that slow-phases can reliably be isolated, they can then be subjected to quantitative analysis using novel methods described in later chapters.

3 The bivariate probability density function: a unifying measure of eye movement performance

3.1 Introduction

In Chapter 1, it was discussed that previous studies of IN eye movements concentrated on analysing the horizontal component of the eye movements, and quantified oculomotor performance either directly or indirectly through retinal slip. Fixation and smooth pursuit share a functionally equivalent goal: the continuous foveation of a target. Yarbus has been attributed with first drawing this parallel between the functions of these two types of eye movement (Dell'Osso, 1986). However, the target is never perfectly imaged on the fovea at all times during fixation (Nachmias, 1959; Skavenski and Steinman, 1970; Kosnik et al., 1986; Kosnik et al., 1987; Cherici et al., 2012) or smooth pursuit (Kowler and McKee, 1987; Kolarik et al., 2010). For this reason, velocity errors occur between the eye and the target and these errors vary over time. Retinal slip is therefore an intuitive method of quantifying performance of both types of eye movement. In smooth pursuit, eye velocity can be expressed as a ratio of target velocity (average eye velocity divided by target velocity) to derive a measure of retinal slip. However, the same cannot be performed for fixation, since the target is not moving, (average eye velocity divided by zero). It is this conundrum has probably lead to the development of so many metrics for fixation in IN, whereas gain has been the mainstay for smooth pursuit in IN. However, this problem can be solved by expressing eye velocities relative to the target. The resulting distributions therefore yield a unifying measure whether quantifying the performance of fixation and pursuit. By calculating the two-dimensional distribution of eye velocities relative to the target, and by implementing measures of accuracy and precision, the disadvantages of other methods (e.g. average smooth gain), can be overcome.

3.2 The bivariate PDF of retinal slip

Raw eye movement data are always expressed relative to a frame of reference. For velocity data the frame of reference is typical taken to be stationarity (0°/s). To calculate retinal slip, eye velocity data must be expressed relative to a specific target, rather than to 0°/s. This global change in the frame of reference requires a simple coordinate shift in the distribution of raw eye velocities:

$$relative\ velocity_{(x_i,y_i)} = \ raw\ velocity\ _{(x_i,y_i)} - \ target\ velocity\ _{(x_i,y_i)}$$

Having performed the coordinate shift, all eye velocities will then be expressed relative to the target. In other words, the origin of the scatter plot represents the target. To visualise the new 'target-relative' eye movement data, one can plot a scatter diagram of horizontal and vertical variables, as in Figure 3.1.

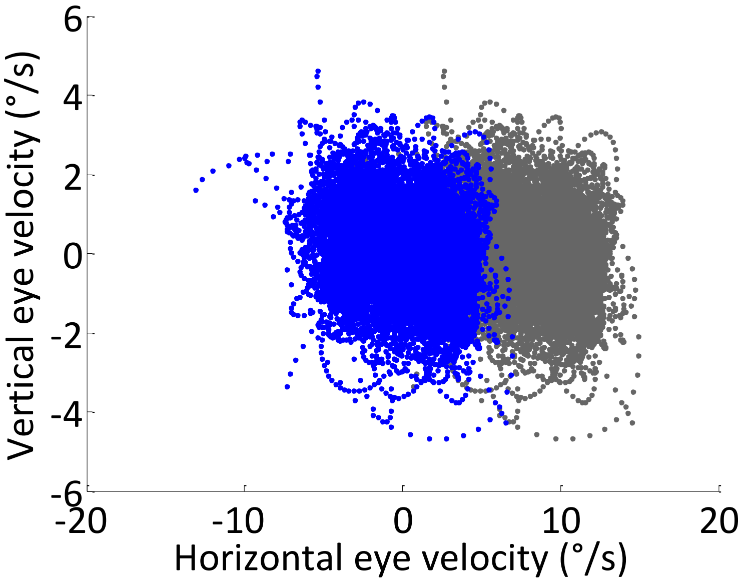

Figure 3.1 Performing a coordinate shift to eye velocity data.The participant was pursuing a target of constant velocity 8°/s rightwards, which is subtracted from each of the actual horizontal eye velocities (grey markers) to yield relative eye velocities (blue markers).

However, since all of the data samples appear as a homogenous blue colour, it is difficult to determine how the data are actually distributed. In other words, we cannot discern the number of data points at a given location on the scatter diagram, so the distribution is misrepresented. This problem has been referred to as 'overstriking' (Huang et al., 1997). A more useful method of visualising this data would be to use a bivariate histogram, where the z-axis, or elevation, indicates the frequency of a particular combination of variables (Figure 3.2).

Bivariate histograms have been used previously to study the variability of eye position in typical individuals (Whittaker et al., 1988). Rather than using a histogram, the observed data can be used to determine the probability that the two variables will take particular values: a bivariate probability density function (PDF). Bivariate PDFs, like histograms, have also been used to study the variability of eye position in typical individuals (Cherici et al., 2012). The bivariate PDF of the target-relative eye velocities in Figure 3.1 can be plotted as a 2D surface (Figure 3.3). However, for this thesis, it is more convenient to consider the bivariate PDF output as a series of isocontours, again visualised in two dimensions (Figure 3.4).

It is routine when quantifying eye movement to select only the most frequent 68% of the observed data (Whittaker et al., 1988) or the highest 68% of its corresponding probability distribution (Bellmann et al., 2004; Crossland et al., 2004a; Crossland and Rubin, 2002; Nachmias, 1959; Cherici et al., 2012). Presumably, the value of 68% was chosen as it is equivalent to the mean ±1 standard deviation of the univariate normal distribution, and served as a method of excluding extreme values preventing them from biasing the results.

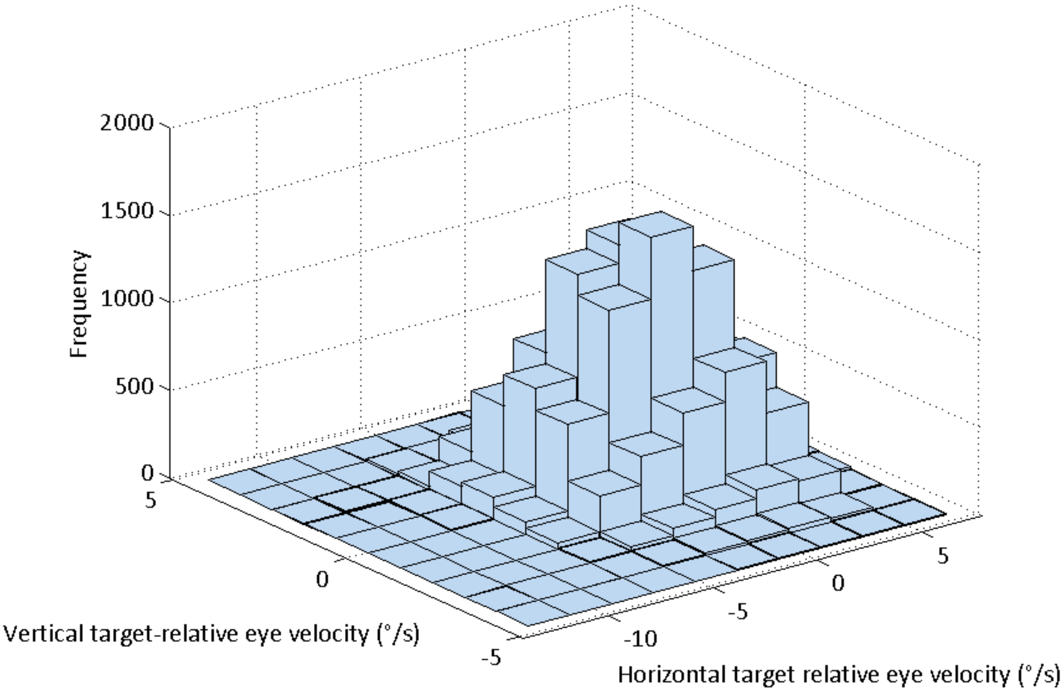

Figure 3.2 A bivariate histogram of the relative eye velocity data presented in Figure 3.1.

The perimeter that encompasses the 68% most probable data is then taken, forming an isocontour than can be subject to further analysis. The 68% isocontour of that target-relative PDF of Figure 3.3 is presented in Figure 3.5.

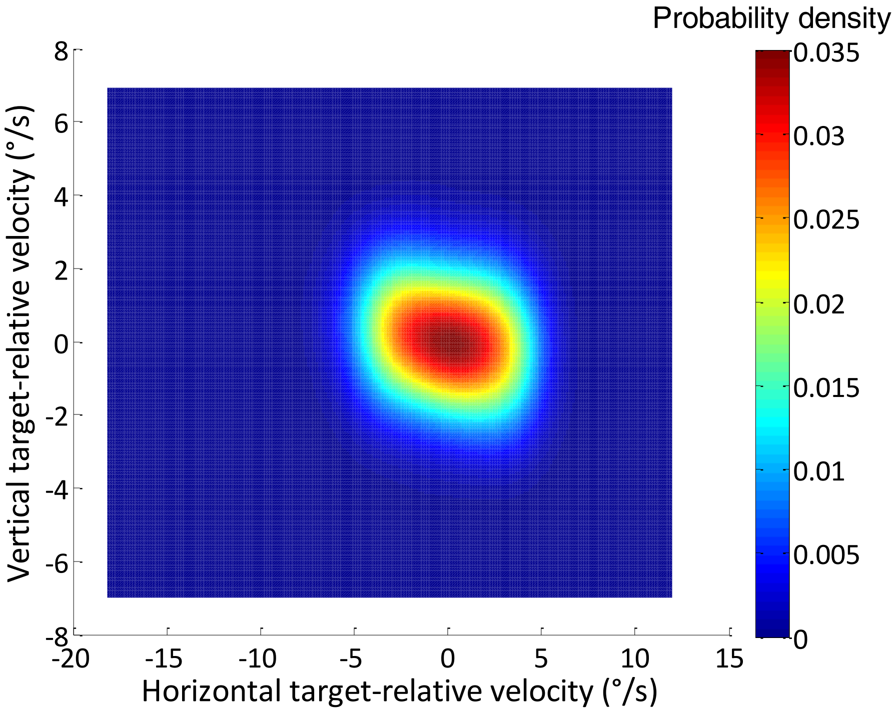

Figure 3.3 The bivariate PDF visualised as a 2-dimensional surface.

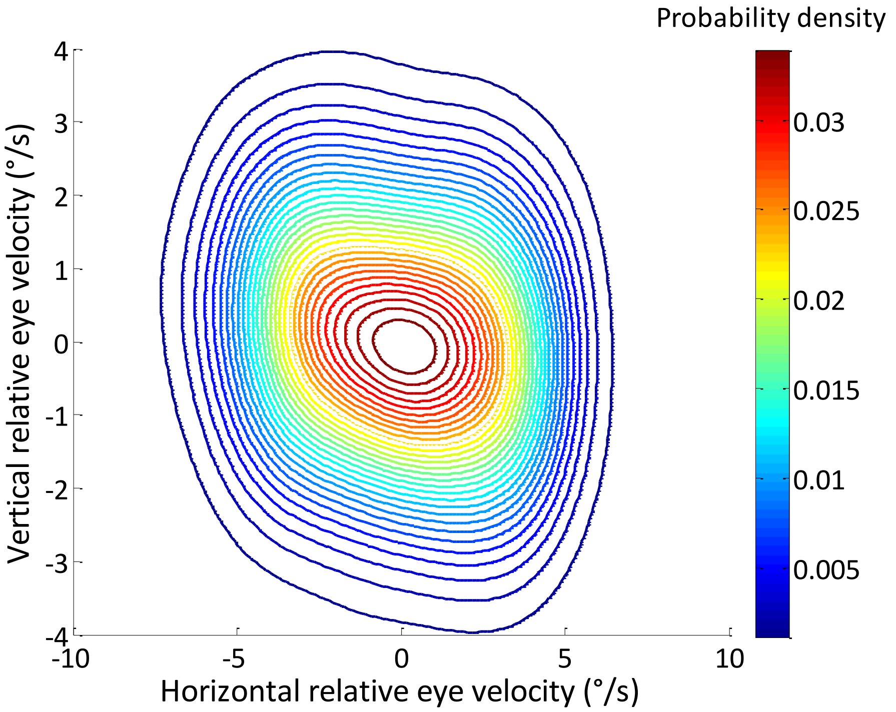

Figure 3.4 The 2D probability surface visualised as a series of probability isocontours. Cooler colours represent lower probability densities, whereas warmer colours represent higher probability densities.

The different metrics that can be computed from the 68% isocontour are summarised as a schematic in Figure 3.6. As mentioned previously, the *origin* of the 2D surface of the PDF and of the 68% isocontour corresponds to the target. The accuracy of the eye movement can be expressed by the *vector* extending from the origin to the centre of mass of the 68% isocontour.

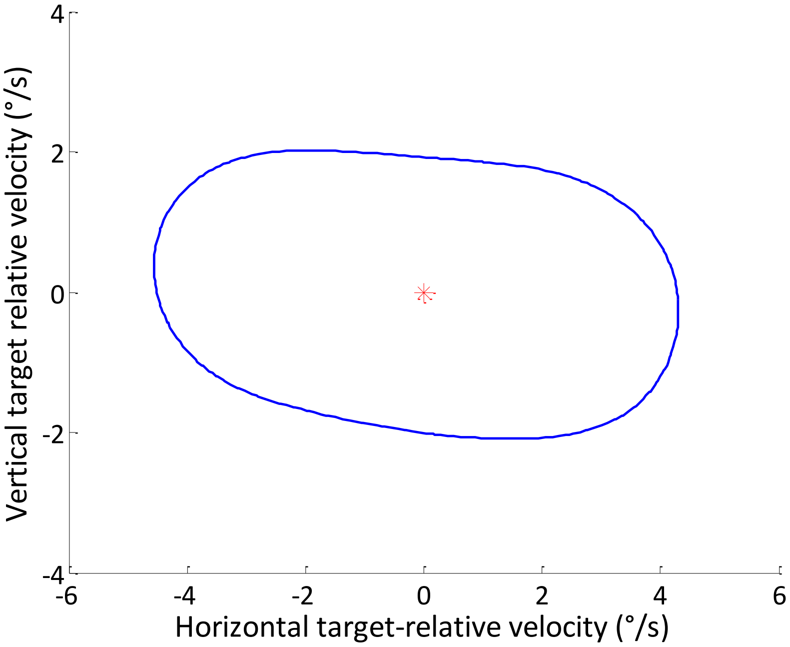

Figure 3.5 The 68% isocontour of the PDF depicted in Figure 3.4. The target (i.e. the origin) is indicated by a red asterisk.

Note that, since accuracy is a vector, it has both magnitude and angle. The *magnitude (rho)* of the vector informs on the proximity of the eye velocities to the target (e.g. a larger magnitude would indicate lower accuracy), whereas the *angle (theta)* informs in which direction the inaccuracy lay (e.g. whether the eye was lagging or leading a moving the target). The precision of eye velocities can be expressed by the *total area* of the isocontour (e.g. a larger area would indicate lower precision). The isocontour can take any shape, but every shape will have a major (longer) and minor (shorter) axis, that are orthogonal to one another. The *orientation* of the major axis informs on the direction along which the lowest precision occurs. The *ratio* of the minor axis to the major axis informs on how symmetrically the precision is distributed in along the major and minor axes (e.g. a ratio of 1 would indicate precision is equally distributed along both axes, whereas a 0 would indicate all the precision is distributed along the major axis).

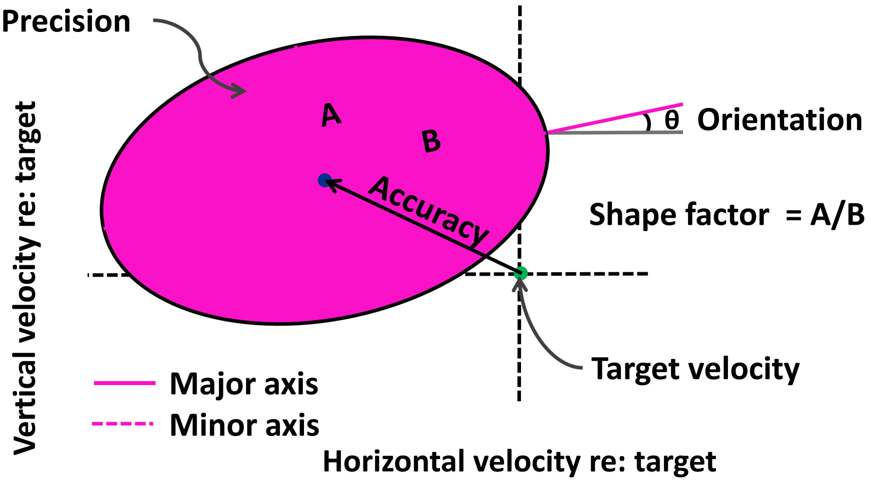

Figure 3.6 A schematic diagram of those performance metrics that can be calculated from the 68% isocontour.

3.3 Implementing the bivariate PDF

Probability density functions in this thesis were generated by an open-source 2D kernel density estimation for MATLAB® called 'kde2d' (Botev, 2007; Botev, 2009). Although the complete process of implementing the bivariate PDF will be discussed in detail, the following is an outline of the steps involved:

1. Specify the area and the resolution with which the PDF is calculated
2. Specify the smoothing parameter to be applied
3. Select and extract the 68% isocontours
4. Convert contours to a binary image and to correct for the presence of more than one contour
5. Calculate the performance metrics from a binary image of contours

The bivariate PDF can only be calculated over a finite area (the '*bounding box*'). The area of the bounding box was specified using the maximum and minimum horizontal and vertical target-relative eye movement data, with margins equivalent to one quarter of the horizontal or vertical range, respectively:

$$(x_{lower}, y_{lower}) = \left(\left(x_{min} - \frac{x_{range}}{4}\right), \left(y_{min} - \frac{y_{range}}{4}\right)\right)$$

$$\left(x_{upper}, y_{upper}\right) = \left(\left(x_{max} - \frac{x_{range}}{4}\right), \left(y_{max} - \frac{y_{range}}{4}\right)\right)$$

The margins act to ensure that there is sufficient ‘space’ surrounding the eye movement data to construct the bivariate PDF. Without margins, the contours corresponding to the least probable data (i.e. the largest contours) are continuous with the bounding box and so they fail to make a complete, closed contour. The PDF is calculated using a specified resolution (the *‘mesh resolution*’). This mesh resolution is analogous to the bin size of a bivariate histogram. The mesh resolution was set to the software default of a 256-by-256 grid equally spaced over the bounding box.

Because the distribution of eye position data is likely to vary across individuals, unlike a fixed PDF bounding box and mesh resolution, this method of varying the bounding box and mesh resolution prevented under- and over-sampling of the observed data that would arise from a ‘one-size-fits-all’ approach. A smoothing parameter is applied to the bivariate PDF (the ‘*kernel bandwidth*’). For oculomotor data, the kernel bandwidth should not be less than the accuracy of the eye tracker, and a 1° kernel bandwidth for position data has been recommended (Castet and Crossland, 2012). Since all eye velocity data in this thesis were derived from raw eye position, the ‘kde2d’ function was modified so that the kernel bandwidth was equal to 1°/s in both meridians (i.e. a circular kernel).

To select the 68% isocontour, the volume under the PDF was utilised. The maximum and minimum probability densities were first determined. Next, the range of probability densities that lay between this maximum and minimum were subdivided into 10,000 intervals. Stepping through each interval, one at a time, the volume of the PDF above was calculated. The volumes under the PDF were calculated using a Riemann sum, a method that numerically approximates the double integral (Weisstein, 2015). In brief, a 256-by-256 mesh was placed at the bottom of the PDF and each mesh element was multiplied by the probability density (i.e. the height of the PDF surface), giving the volume. This process stopped when the volume above equalled 0.68, since the area under the PDF summed to 1. The isocontour that enveloped these data was then extracted using the ‘contour’ function in MATLAB®.

In order to obtain the desired performance metrics, image processing techniques must be used to convert the 68% isocontour to a binary image. A binary image is so called because the pixels can take only one of two possible numerical values, either 1 or 0. In MATLAB®, pixel values of 1 (one) are represented by white, while values of 0 (zero) are black.

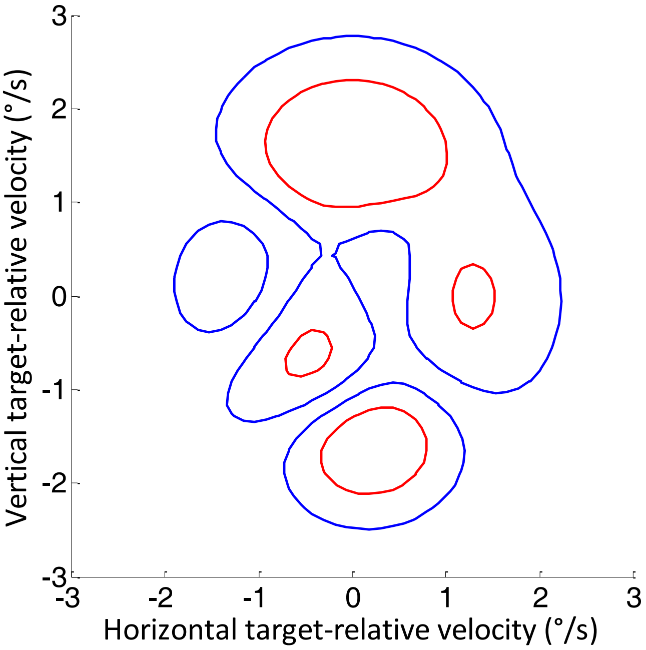

Figure 3.7 Hypothetical data generated using the 'peaks' function in MATLAB to illustrate the relationships between parent contours (blue) and child contours (red).

For the purposes of the performance metric analysis, the area enclosed by a contour will be represented as 'white' (i.e. the pixel values will be 1) whereas areas outside of the contours will be represented as 'black' (i.e. the pixel values will be 0). Complicating this process is that occasionally multiple contours that contribute to the overall 68% isocontour, although infrequent, can occur. These multiple contours can either occur outside of ('parent' contours representing 'islands' of data) or inside of ('child' contours representing 'holes' in the data) other contours. For example, this is shown in Figure 3.7. If correct performance metrics are to be calculated from the binary image, the parent-child relationship must be taken into consideration. On the binary image, the area within the parent contours will be represented as white, while the area within the child contours will be represented as black. The parent-child relationships of all contours were established using the open-source function 'contour2area' (Sundqvist,

2010) (Figure 3.7). To construct an appropriate binary image, a blank 'canvas' matrix of zeros was produced (i.e. a black image). Superimposed on this were the parent contours (i.e. white regions). Finally, the child contours (i.e. black regions) were then superimposed on the corresponding parent contours. The following method outlines each step in more detail:

1. Create a 'canvas' matrix

- The difference between the maximum and minimum limits of each axis when the all of the 68% isocontours were plotted was determined.
- A matrix containing zeros that was 20 times the axis dimensions was produced.
- This zero matrix served as a background 'canvas' with which to create binary image.
- Since the zero matrix contained all zeros, it would be displayed as black.

2. Perform a co-ordinate shift on the contour coordinates

- Images can only have positive pixel coordinates. Therefore, to facilitate the mapping of contour coordinates onto the 'canvas' matrix, a sufficient offset was added to the contour coordinates to make the entire horizontal and vertical axis positive.
- The contour coordinates were then also scaled by a factor of 20 to match the 'canvas' matrix

3. Convert parent contour coordinates to a binary 'white' mask.

- The coordinates of each of the scaled parent contours were treated as vertices of a polygon, which were then converted to binary masks using the 'poly2mask' function in MATLAB®. Pixels within each polygon were designated 1 ('white') while pixels outside were set to a value of 0 ('black').
- Pixel coordinates with a value of 1 ('white') were then directly mapped onto the 'canvas' matrix as 1s ('white').

4. Convert the child contour coordinates to a 'black' binary mask.

- The conversion of contours to a binary mask was repeated for child contours, except in this case, when directly mapped on to the 'canvas' matrix, they took the value of 0s ('black').

The composite binary image (Figure 3.8) ensures that the parent-child relationship of the contours (Figure 3.7) was preserved by removing regions identified as child contours.

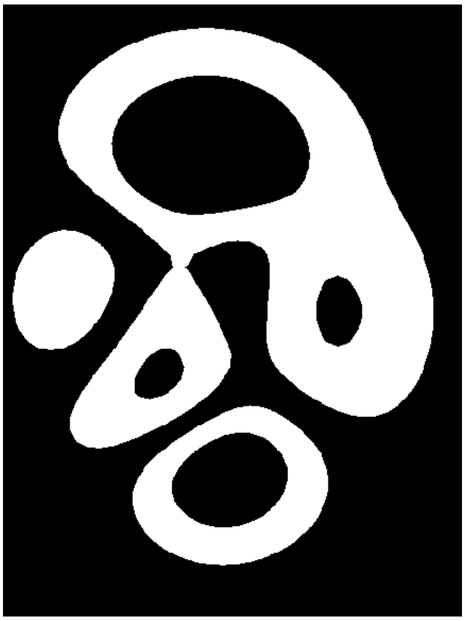

Figure 3.8 Conversion of those parent and child contours in Figure 3.7 to a composite binary image. The original relationship between 'parent' (filled white representing 'islands') and child contours (filled black representing 'holes') have been maintained.

All performance metrics were calculated from the composite binary image (Figure 3.9). To do so, all 'white' pixels of the binary image must be treated as contiguous (i.e. as part of the same object) rather than dis-contiguous (i.e. as separate objects). The centroid (i.e. the x and of the y coordinates of the centre of mass) of the contiguous data is calculated as the mean of the x coordinates and the mean of the y coordinated of those 'white' pixels. The total area of the contiguous data is the sum of those 'white' pixels. The original data were offset and then scaled by a factor of 20, so a reverse scaling and reverse offset was then applied to yield the actual values for the centroid and total area.

Principal component analysis (PCA) was performed on the contiguous binary image to determine both the orientation and ratio of the major and minor axes. In brief, the covariance matrix of the x and y coordinate of 'white' pixel values were computed as well as the Eigenvalues and Eigenvectors of the covariance matrix. The square root of the ratio of the smallest Eigenvector to the largest Eigenvector was taken as a measure of the shape factor (the ratio of the major and minor axes). The four-quadrant inversetangent was taken of the largest Eigenvector, providing the angle between the major axis and the horizontal axis. An alternative method to self-calculating the centroid, total area, orientation and ratio of the major and minor axes, is to use the ‘regionprops’ function of the image processing toolbox for MATLAB®. Subsequent to implementing the analysis, the image processing toolbox was made available through a site-licence to Cardiff University. The self-calculated values were verified against those of the ‘regionprops’ function, with identical results being obtained.

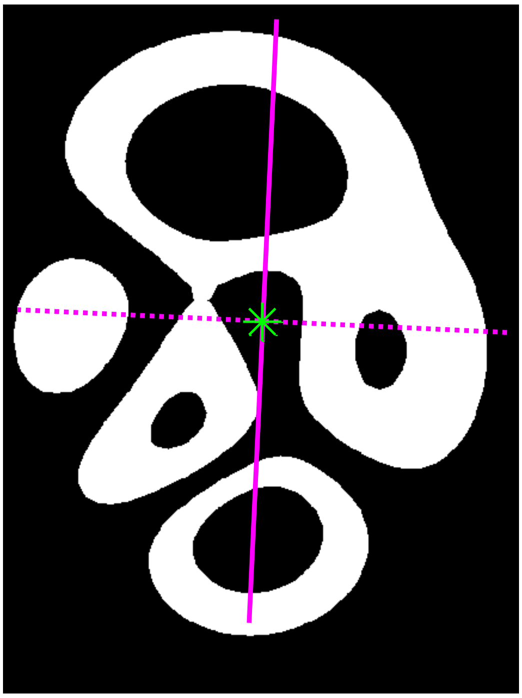

Figure 3.9 Determining the centre-of-mass (green asterisk) and the major (solid magenta) and minor (dashed magenta) for the hypothetical contours shown in Figure 3.8.

3.4 Summary

In this chapter, I have resolved existing difficulties in obtaining a single method that quantifies retinal slip whether or not a target is stationary or moving. This has been achieved by describing eye velocity relative to the intended target. In doing so, I have been able to extend an existing methodology that has been successfully used to quantifies fixation performance, to quantifying performance during smooth pursuit. This work will therefore permit performance on either task to be directly compared. Further, the proposed method tackles known shortcomings of existing methods used to quantify smooth pursuit: it will quantify both accuracy and precision of retinal slip, and it will quantify retinal slip in two dimensions. The retinal slip distributions, when subjected to commonly used image processing techniques, can provide the appropriate performance metrics. The performance metrics obtained by self-calculation have been successfully verified against commercially available image processing packages. The method described in this chapter will be used subsequent chapters to investigate retinal slip in individuals with IN and to make appropriate interpretations of psychophysical responses in the presence of ongoing retinal slip.

4 IN fixation as a function of gaze angle: null zones

4.1 Introduction

As discussed in the general introduction, when attempting to fixate static targets, the degree of IN is reported to vary as a function of horizontal gaze angle (Dell'Osso, 1973a; Dell'Osso, 1973b; Kurzan and Buttner, 1989; Abadi and Whittle, 1991). Given that pursuit requires the fixation of a target that moves continuously over a range of positions, the degree of IN as the target is followed may also vary and so potentially needs to be taken into account. To explore this issue, I first investigate the IN null zone for attempted fixation of stationary targets using the traditional measure of intensity. Later, I then compared intensity to the various measures derived from the bivariate PDF.

4.2 Pilot testing to determine the null zone location

In light of the lack of sufficient detail in the literature, I undertook pilot testing to determine the null zone of one participant, JS, who has been a volunteer at the Research Unit for Nystagmus for a number of years and has participated in many eye movement studies of IN (Wiggins et al., 2007, Jones et al., 2013, Dunn et al., 2014, Dunn et al., 2015, Wiggins, 2007, Jones, 2011, Dunn, 2014). Additionally, the null zone for this participant has been well characterised, being located between +10° (Wiggins et al., 2007, Wiggins, 2007) and +12° (Jones et al., 2013, Jones, 2011). In this section, the location of JS's null zone was determined to verify the methodology, equipment and analyses.

4.2.1 Methods

The single participant (male; 57 years) viewed a single 0.4° diameter dot target that was presented against a black background. Targets were presented over a horizontal range of ±16° at 4° intervals. The participant was instructed to look at each target as best they could. Targets were presented in a random order. Each presentation of the targets was self-paced and controlled by a wireless keyboard. Each target was presented for a total of 14s: 2 seconds for the participant to acquire the target, and the remaining 12s for eye movement analysis. Assuming a typical IN frequency of approximately 3-4Hz, this would yield 36-48 cycles of nystagmus per recording, sufficient for the purposes of this experiment.

4.2.2 Analysis

Intensity was calculated on a cycle-by-cycle basis at each location for each individual, as the amplitude of the slow phase divided by the duration of the slow phase (i.e. mathematically analogous to slow phase amplitude multiplied by its frequency). Amplitude was defined as the difference between the absolute maximum and the absolute minimum eye position during the slow phase. The duration of the slow phase was calculated as the time difference between the end of one fast phase and the start of the next.

It has previously been shown that there can be large variation in the amplitude of the IN oscillation at a given location (Abadi and Whittle, 1991). For each gaze location, the mean and standard deviation of the slow phases was calculated. Outliers were designated as those intensity values that exceeded 2 standard deviations above and below the mean and were excluded from the analysis. The mean and standard deviation of the remaining slow phases was then recalculated.

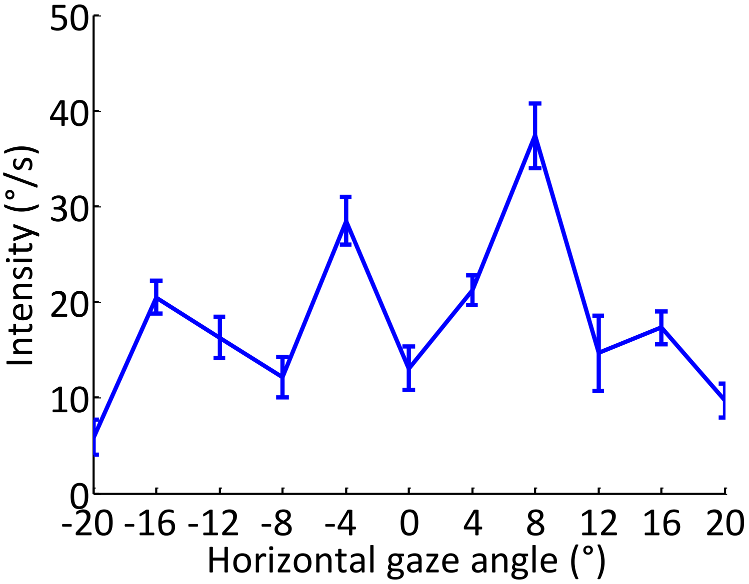

Figure 4.1 Mean intensity a as a function of gaze angle for participant JS, with minimum intensity at -20°. Error bars indicate ±95% confidence intervals.

4.3 Pilot testing of null zone locations

During pilot testing of the experiments the null zone for JS was found to be -20° with the greatest inaccuracy at +8° (Figure 4.1). The findings of the pilot study were therefore extremely inconsistent with historical data for JS. The error bars indicate the 95% confidence intervals and so indicate that for most gaze locations, the intensity was within a narrow range. This study used a chin rest to fix the participants head so that only the eye position could be varied. The head was restrained such that an approximate head turn of 30° and moving the null from +10° to -20° would not have been possible. Previous studies of JS null zone had been determined by allowing JS to adopt his preferred head posture to place his eyes in the null position (Jones, 2011; Wiggins, 2007). While the eyes will have the same position in the orbit, the two methods cannot be assumed to be identical, and could be a source of the differences. Despite the methodological differences, other psychological factors, for example arousal level (Jones et al., 2013; Abadi and Dickinson, 1986) could have been yet another reason for the difference. The literature indicates that a *sequential* presentation of targets is used to characterise the intensity-gaze angle relationship (Dell'Osso, 1973a; Dell'Osso and Flynn, 1979; Kurzan and Buttner, 1989; Abadi and Bjerre, 2002; Bifulco et al., 2003; Cesarelli et al., 2000; Dell'Osso, 1973b; Abadi and Worfolk, 1989; Abel et al., 1991; Abadi and Whittle, 1991), although the sequence may not necessarily be at *random*. The task of finding a target presented at an unknown location could have been a potential stressor sufficient enough to distort the regular pattern of intensity observed for JS. For this reason, participant JS was retested following a 2 weeks interval to investigate left-to-right and right-to-left presentation orders and the resulting intensity gaze angle distributions.

4.4 Effect of presentation sequence

The hypothesis under test is that random target presentations, because their target location cannot be predicted, will result in a different intensity-gaze angle relationship to left-to-right and right-to left presentations that can be predicted. Pilot testing was then repeated on subject JS (male; 57 years) for left-to-right and right-to-left presentations.

4.4.1 Results

No consistent relationship was found between intensity and gaze angle across different presentation types (Figure 4.2). The results do not represent a change of head position during eye tracking, as that would manifest as a lateral shift in the intensity-gaze angle distribution, rather than an entirely different distribution, with different intensity values.

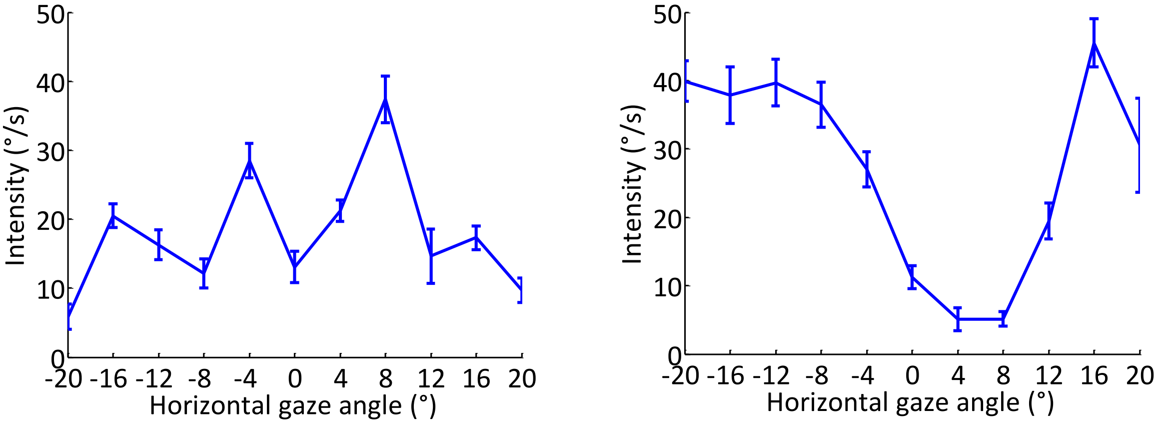

(a) Random presentation (minimum -20°) **(b)** Left-to-right presentation (minimum +4°)

(c) Right-to-left presentation (minimum -4°)

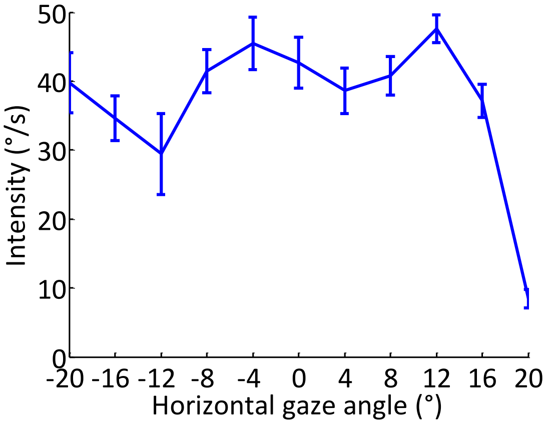

Figure 4.2 Relationship between horizontal gaze angle and PDF accuracy for (a) random, (b) left-to-right and (c) right-to-left presentations.

It is possible that the pattern of eye movements is dependent upon the target presentation order (i.e. predictable vs unpredictable locations). From the data presented in Figure 4.2, it can be appreciated that the intensity values are considerably different for all three presentation types, despite the small 95% confidence intervals. However, an alternative explanation for the different distributions is just a chance trial-by-trial fluctuation in intensity. To determine the most likely explanation for the observed data, I sought to determine the null zones under each of the target presentation conditions (random, left-to-right, and right-to-left).

4.4.2 Methods

Fourteen participants with IN (8 male, 6 female; mean 47.5 ± 14.44 years) viewed a single 0.4° diameter dot target that was presented against a black background. Targets were presented over a horizontal range of ±16° at 4° intervals. Participants were instructed to look at each target to the best of their ability. The three presentation types (random, left-to-right, and right-to-left) were run as separate blocks during the same session, and the order of the blocks randomised. In each block, the presentation of the targets was self-paced and controlled by a wireless keyboard. Each target was presented for a total of 14s: 2 seconds for the participant to acquire the target, and the remaining 12s for eye movement analysis. Assuming a typical IN frequency of approximately 3-4Hz, this would yield 36-48 cycles of nystagmus per recording, sufficient for the purposes of this experiment.

4.4.3 Analysis

Intensity differences between the presentation types was investigated using the mean intensity for the IN group at each location, since the results of a study by Abadi and Bjerre (2002) found that of 143 participants with IN, approximately 73% had a null zone within 10° of the straight ahead position. If the intensity data were averaged across the IN group, a reduction in intensity should be noted at or in close proximity to the straight ahead position (i.e. 0°) for each group. Intensity was calculated on a cycle-by-cycle basis as before. The IN group had large differences in intensity at each gaze angle. Consequently, averaging high intensity IN (e.g. 30-40°/s) with low intensity IN (e.g. 0-10°/s) could make it difficult to detect any discernible trends with gaze angle. Therefore, the intensity data for each participant was normalised (i.e. rescaled to between 0 and 1) by subtracting the minimum intensity value from all values and then dividing by the range. The mean normalised intensity values were then plotted as a function of eccentricity.

4.4.4 Results

The plots of group mean intensity as a function of gaze angle for each target presentation type are presented in Figure 4.3. Data for each individual is presented in

Appendix 2. In general, the group intensity results indicate that, despite averaging across 14 participants with IN, a lower intensity IN oscillation occurs in the region close to the straight ahead position for each presentation type, consistent with published data. However, there are subtle differences in the 3 different distributions. For example the minimum intensities occurred at -4°, 0° and +4° for random, right-to-left and left-to-right presentations, respectively. A 9 (location) x 3 (presentation condition) repeated measures linear mixed model analysis was performed on the normalised intensity which indicated no significant effect for presentation type [$F(2,312.73)= 1.04$, $p= .343$] or a significant interaction between presentation type and location [$F(8,311.267)= .710$, $p= .783$]. To more closely examine the differences between the three presentation types, the null zone locations for each presentation type were correlated with one another (random vs right-to-left, random vs left-to-right, and left-to-right vs right-to-left). A scatter plot of each of the comparisons is presented in Figure 4.4. To aid comparison, a diagonal parity line was plotted. If data points lay on this line, then the null zone location was identical under the two presentation types being correlated, while the farther from this line, the more inconsistent the null zone became.

The correlations data (i.e. the correlation coefficient r and the significance of the correlation) are presented alongside the respective scatter plots in Figure 4.4. The effect sizes for the correlations can be gauged from the correlation coefficient r, where 0.1 is small, 0.3 is medium and 0.5 is large (Cohen, 1992). Since three correlations were being made, the Bonferroni corrected alpha value is 0.0167 (i.e. 0.05 divided by 3). Using this adjusted alpha value, only one of the comparisons was statistically significant: left-to-right vs right-to-left. It is important to state that despite a significant correlation, it must be emphasised that the significant correlation for the predictable target presentations do not mean that the null zone locations are in any way more repeatable than under unpredictable target presentations. But, what the correlations would indicate are that the null zones are located on a consistent side, either left or right.

(a) Random presentation

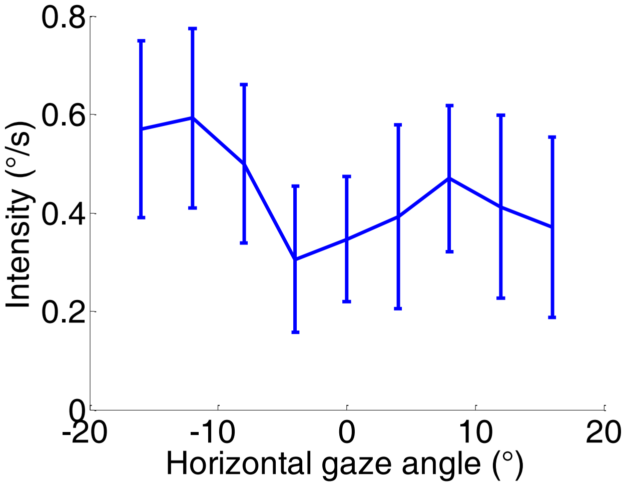

(b) Right-to-left presentation

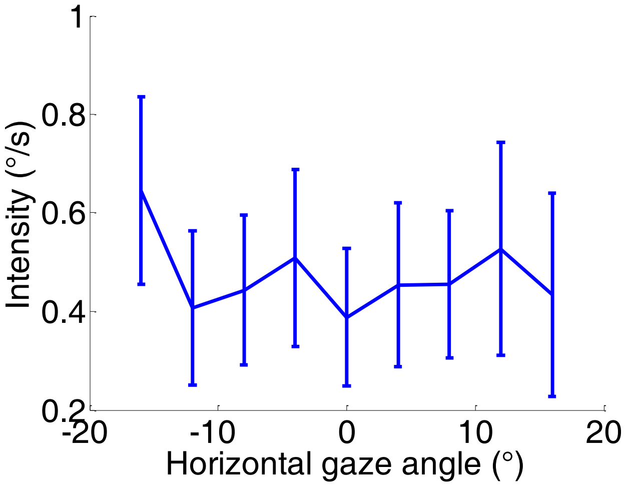

(c) Left-to-right presentation

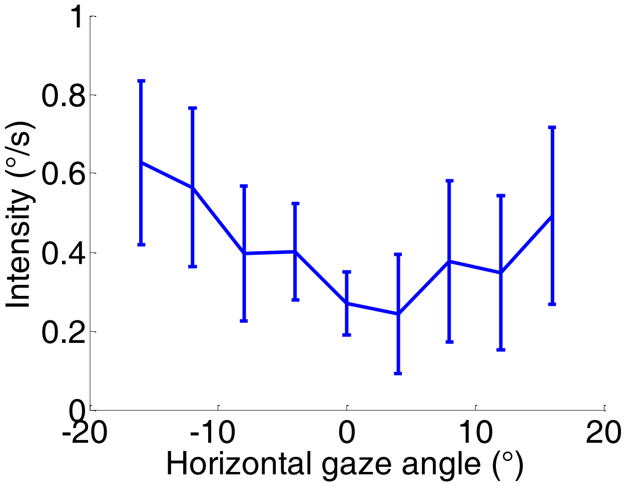

Figure 4.3 Mean intensity as a function of gaze angle for each presentation type for (a) random, (b) right-to-left, and (c) left-to-right presentation intervals. Error bars indicate the 95% confidence intervals.

(a) Random vs L-R (r = 0.25, p = 0.39)

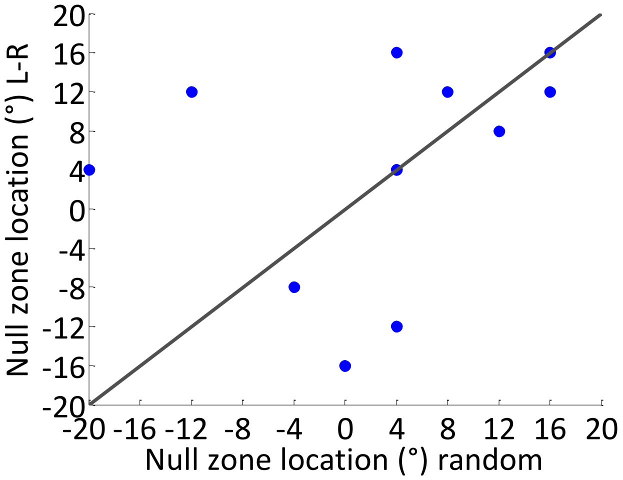

(b) Random vs R-L (r = 0.52, p = 0.06)

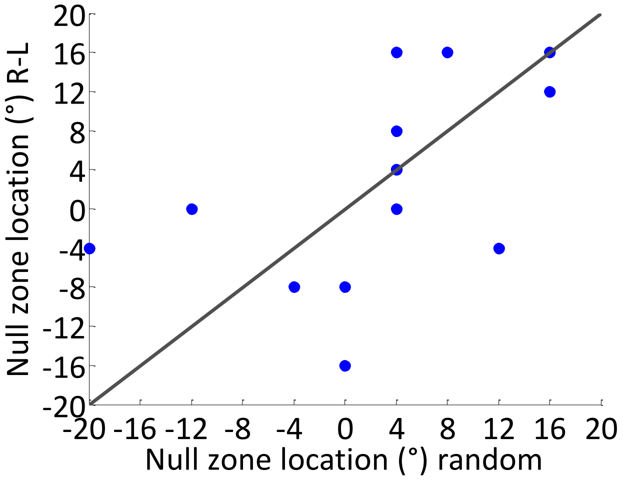

(c) L-R vs R-L (r = 0.75, p = 0.002)

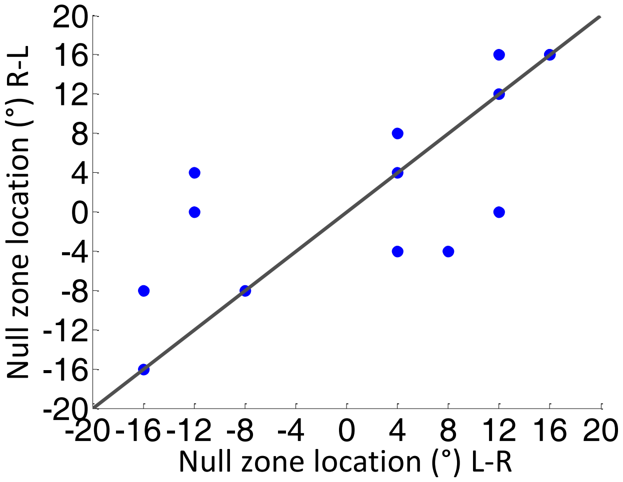

Figure 4.4 Scatter plot comparing null zones located by (a) random and left-to-right presentation, (b) random and right-to-left presentation, and (c) left-to-right and right-to-left presentations.

For example in Figure 4.4 (c) comparing predictable target presentations, a null zone identified at +8° under left-to-right target presentation corresponds to a null zone at -4° under right-to-left target presentation. However, the number of participants in this experiment, and therefore the analysis, was small being perhaps the borderline minimum for generating a meaningful correlation.

As previously discussed, there is no established protocol for determining the null position, with each investigator using their preferred, but unreported, technique. It is possible that different methodologies (e.g. duration of experiment, choice of target etc.) could produce less repeatable data. To the best of my knowledge, there are no documented reports on the minimum duration for eye movement recordings, or more formally the number of recorded IN cycles necessary per gaze angle, for adequately determining the null zone. This is an important aspect of measuring the intensity-gaze angle distribution for two reasons: it has been reported that when fixating a target, the IN waveform varies over a duration of 5 minutes (Dunn, 2014). It has also been reported that inattention can modulate the intensity of the IN oscillation (Abadi and Dickinson, 1986). However, in my experiments each experimental block was of reasonably short duration, with 14 seconds of eye movement recording at 9 locations totalling approximately 3 minutes. The experiment was also self-paced. The participant had to voluntarily press a button to begin each trial in an experimental block. Between individual trials, participants were free to blink and relax, but unable to remove their head from the chin rest. As such, both fatigue and inattention would likely not have led to differences in intensity.

At least one study alludes to an inherent variability in establishing the relationship between intensity and gaze angle:

"The choice of non-accommodative targets at 1.14 m was deliberate. Our experience has shown that, to avoid the variables associated with anxiety, one must minimize the effort to see, which is responsible for the intensification of [IN]. At this distance the damping effects of convergence on [IN] are not great; in fact, damping usually becomes noticeable at reading distance or nearer. By depriving the subject of an identifiable (accommodative) target, we remove the anxieties associated with the identification

process. In this way, we can make an accurate, uncontaminated measure of the variation of [IN] with gaze angle as different target lights are activated." (Dell'Osso and Flynn, 1979)

In my study, non-accommodative targets (i.e. dots of light as opposed to detailed targets such as letters) were also used and the viewing distance (1.40m) was greater than that recommended to avoid convergence dampening. Further, my experiment was performed under complete darkness, removing any feature other than the target itself. Even under these ideal conditions when "effort-to-see" has been minimised as far as possible, no repeatable intensity-gaze angle distribution was determined. "Shifting" null zones have also been reported in those IN participants with periodic alternating nystagmus (PAN) (Abadi and Dickinson, 1986). However, all of our participants have been previously screened for PAN using at least 6 minutes of eye movement recordings. Methodologies aside, to the best of my knowledge, repeated measurements have not been used in any study of the null zone (Abadi and Bjerre, 2002; Dell'Osso et al., 1974; Dell'Osso, 1973a).

It is clearly more difficult for me to determine the null zone location in those with IN than first anticipated. The natural environment contains many accommodative stimuli, some of which will be at or beyond the threshold visual acuity of those with IN. It is certain that these visual stimuli would exert "effort to see". Further, such natural visual stimuli may be found in familiar (i.e. predictable) or unfamiliar (i.e. unpredictable) locations. If the null zone is so sensitive that its measurement is influenced by "effort-to-see", in addition to the predictability of visual targets such that it can only be measured under a highly restricted set of experimental conditions, the significance placed upon null zones in those with IN should be scrutinised.

4.5 Comparison of intensity with PDF accuracy and precision

Each cycle of IN begins and ends with the eye being directed at the target. During the interval between, the eye is carried to one side of the target by the slow phase, before the fast phase redirects they eye back on to the target. The direction of the IN oscillation is referred to by the direction of the fast phase. It is often reported in the literature that IN oscillation is left-beating to the left of the null (i.e. the slow phase move rightwards), and vice versa (Kurzan and Buttner, 1989). Therefore, if such statements were correct, at all gaze positions other than the null zone, the beat direction should be in a consistent direction. However, in my experience this is not the case. In Figure 4.5, it can be seen that the slow phase direction can reverse during attempted fixation. Intensity is based on scalar quantities because neither amplitude nor frequency has sign. Intensity is therefore insensitive to changes in the direction of the slow phase. The schematic in Figure 4.6 depicts two identical slow phases, but which have opposing directions. Because their amplitude and frequency are identical, they have identical intensities.

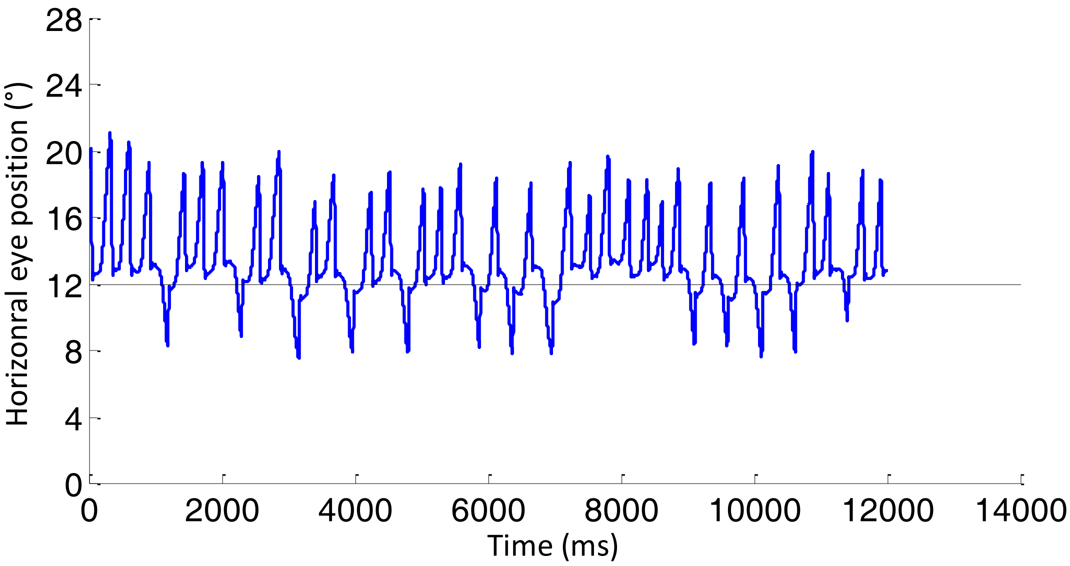

Figure 4.5 Example of frequent slow phase reversals as the participant (LB) attempts to fixate on a target presented at 12° to the right.

Knowing that the beat direction may change as a participant views a target makes intensity is a particularly useful measure when attempting to find that gaze position giving the minimum oscillation.

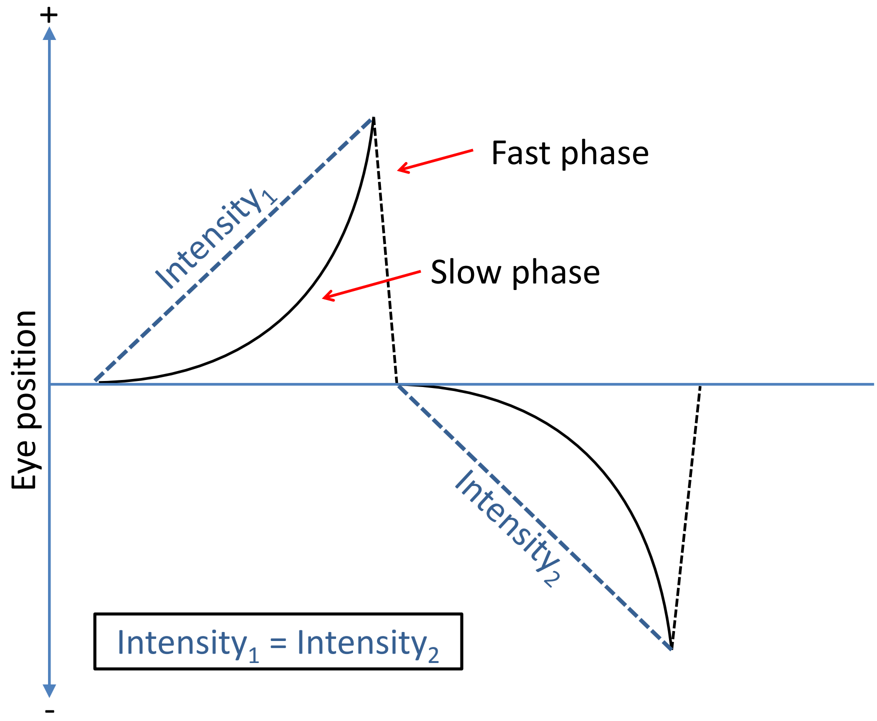

Figure 4.6 Schematic showing two identical slow phases, each in a different direction. Because amplitude and frequency are sign less, the intensity of the two slow phases is equal.

However, it is of interest how the PDF metrics compare to intensity when determining null zone locations. Slow phases moving to the left will have a negative velocity, whereas slow phases moving to the right will have a positive velocity. The bivariate PDF is a vector quantity, meaning that it is sensitive to changes in the beat direction. For example, consider the two slow cycles of nystagmus presented in Figure 4.7. Each slow phase is identical, but only the direction of the slow phase has changed. In the first cycle, the slow phase is moving rightwards and so will have a positive velocity distribution. In the second cycle, the slow phase is moving leftwards and will have a negative velocity distribution. The intensities of each slow phase are equal, but the change in the beat direction will affect the corresponding bivariate PDF metrics.

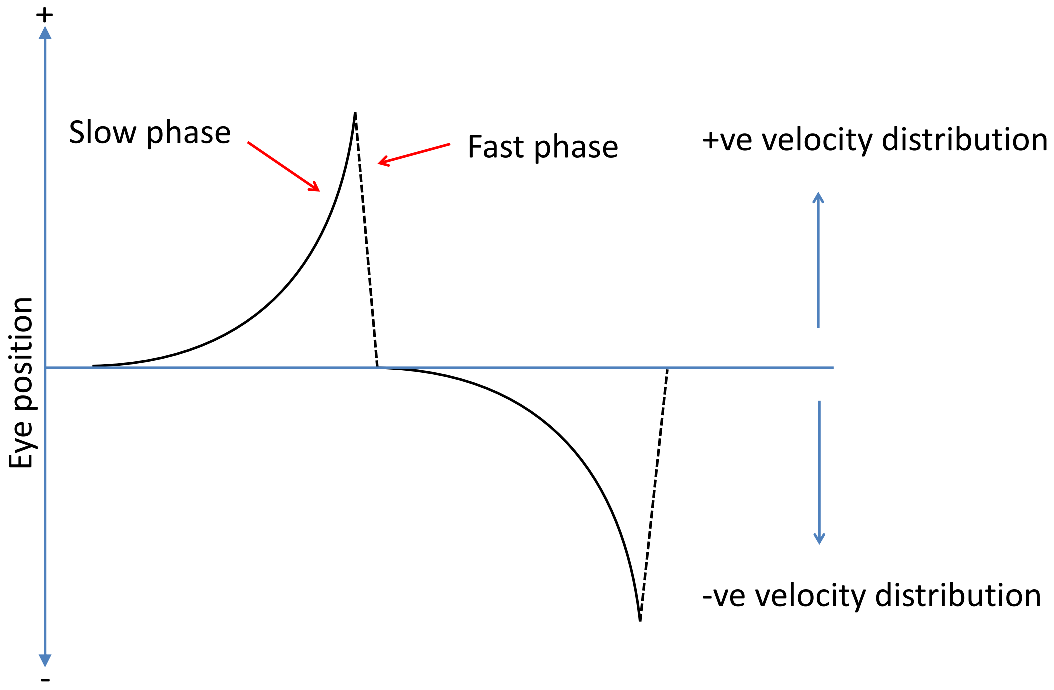

Figure 4.7 A schematic representation of the effects of slow phase direction reversal. Slow phase reversal will increase measures derived from vector quantities (i.e. PDF precision) but not scalar quantities (intensity).

The first IN cycle yields a positive velocity distribution, while the second produces a negative velocity distribution. Since the PDF precision is based on the entire velocity distribution from all slow phases (i.e. it is based on a vector quantities), changes in slow phase direction will decrease PDF precision (i.e. larger velocity distribution resulting in a larger isocontour area). The PDF accuracy is the centre of mass of the PDF precision isocontour. As this will be symmetric about the origin, PDF accuracy will correspond exactly to the origin (i.e. PDF accuracy has increased due to changes in slow phase direction).

The IN literature is most unusual in that it uses absolute values when quantifying the stability of fixation. Studies of fixation for typical controls, and those with pathology of the fovea, always take the direction of the eye movement into consideration (Cherici et al., 2012; Crossland et al., 2005; Crossland et al., 2004a; Crossland et al., 2009; Crossland and Rubin, 2002; Crossland et al., 2004b; Gonzalez et al., 2011; Kosnik et al., 1986; Kosnik et al., 1987; Schuchard, 1992; Whittaker et al., 1988). Indeed, changes in slow phase direction provides useful information.

a) Random presentation (intensity)

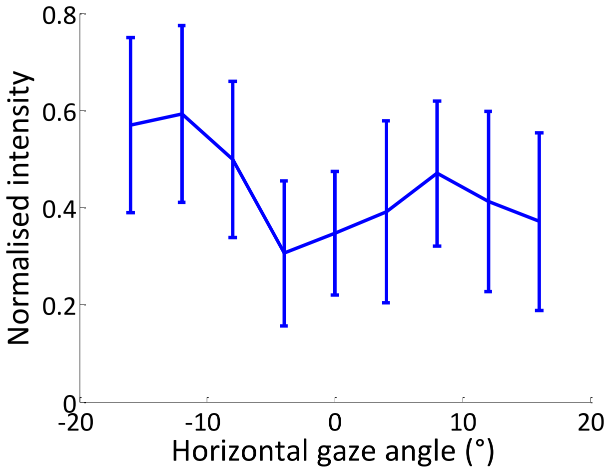

b) Random target presentation (accuracy)

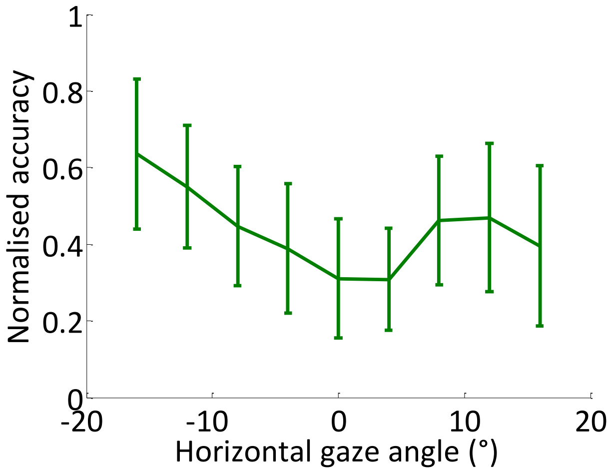

c) Random target presentation (precision)

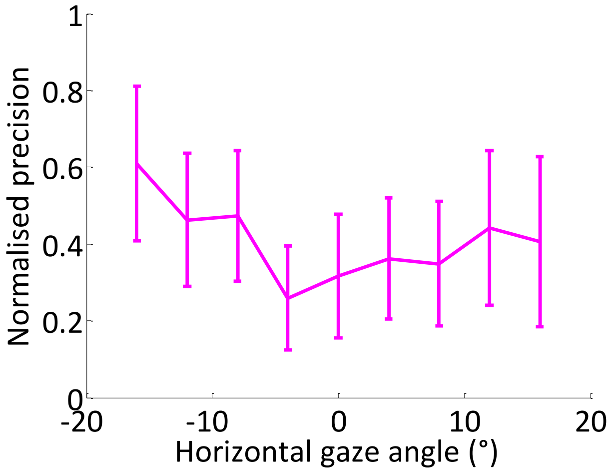

Figure 4.8 Gaze angle as a function of (a) mean normalised intensity, (b) mean normalised accuracy, and (c) mean normalised precision for random target presentation. Error bars indicate the 95% confidence intervals.

a) Right-to-left target presentation (intensity)

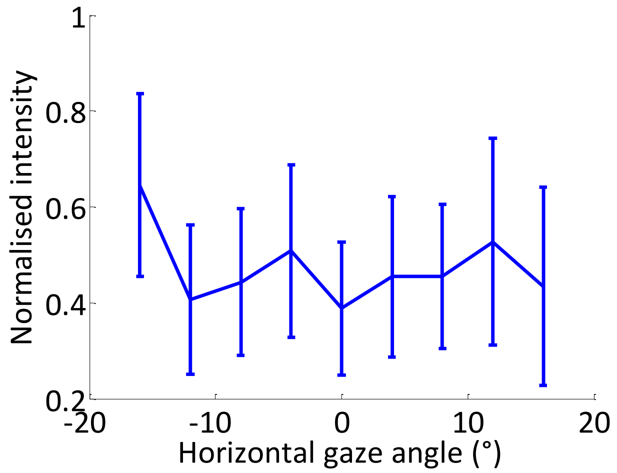

b) Right-to-left target presentation (accuracy)

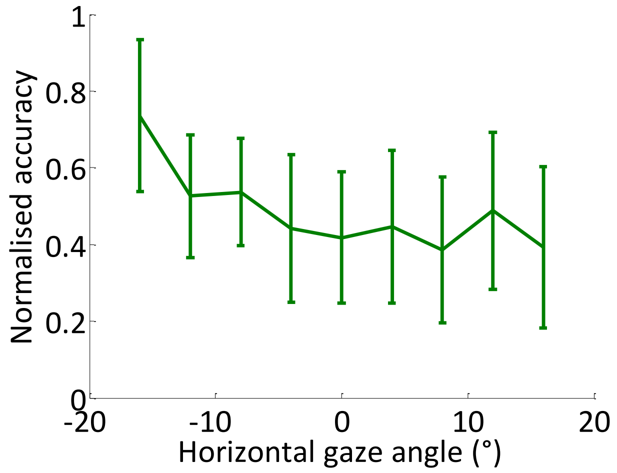

c) Right-to-left target presentation (precision)

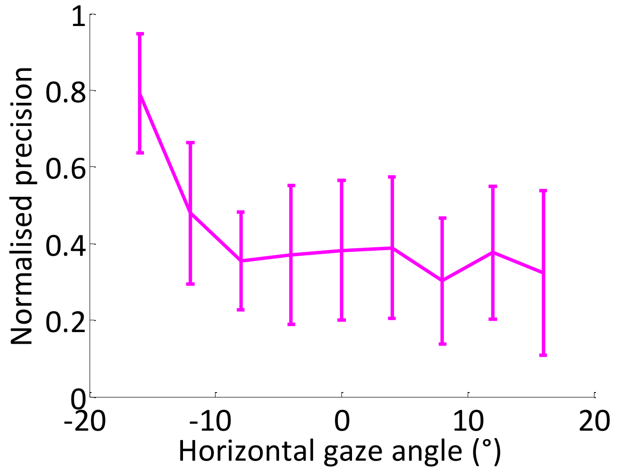

Figure 4.9 Gaze angle as a function of (a) mean normalised intensity, (b) mean normalised accuracy, and (c) mean normalised precision for right-to-left target presentation. Error bars indicate the 95% confidence intervals.

a) Left-to-right target presentation (intensity)

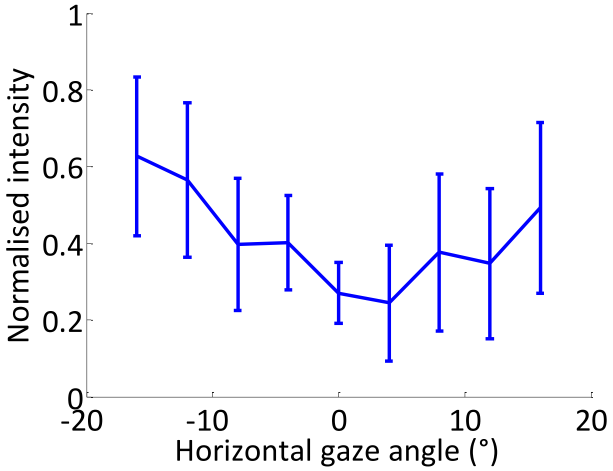

b) Left-to-right target presentation (accuracy)

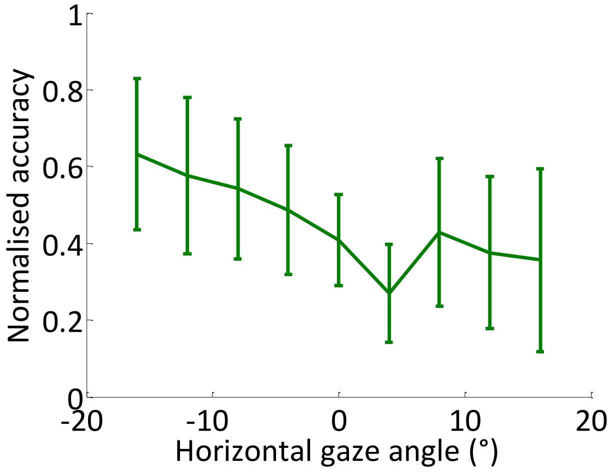

c) Left-to-right target presentation (precision)

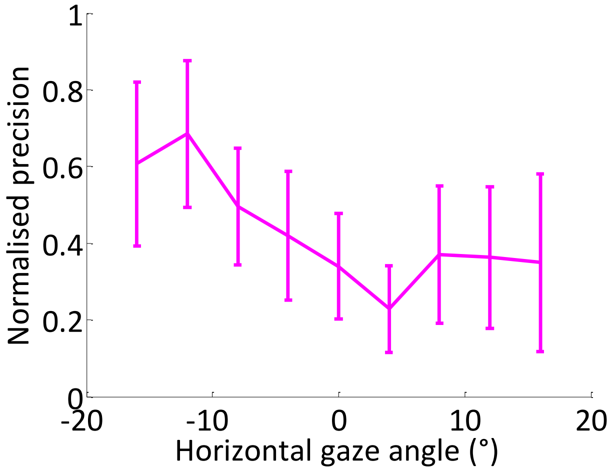

Figure 4.10 Gaze angle as a function of (a) mean normalised intensity, (b) mean normalised accuracy, and (c) mean normalised precision for left-to-right target presentation. Error bars indicate the 95% confidence intervals.

Nonetheless, so that intensity can be compared with various PDF metrics, the absolute velocity distributions were *temporarily* used. From these data, the mean results for each metric for each presentation type will be obtained.

4.5.1 Analysis

The data for 14 participants were analysed and bivariate PDFs calculated for the *absolute* velocity distributions. As before, the data for each metric (intensity, PDF accuracy or PDF precision) was first normalised (i.e. rescaled to between 0 and 1) by subtracting the minimum intensity value from all values and then dividing by the range. The mean normalised intensity, PDF accuracy and PDF precision values were then plotted as a function of eccentricity.

4.5.2 Results

It can be readily appreciated from the group intensity, PDF accuracy and PDF precision plots for random (Figure 4.8), right-to-left (Figure 4.9), and left-to-right (Figure 4.10) presentation, that differing relationships are obtained for each target presentation types. The data suggest that accuracy or precision quantifies the slow phase in a similar manner for each target presentation type (random, left-to-right, or right to left).

To more formally characterise this similarity intensity was plotted against PDF accuracy and against PDF precision for *random* target presentations for 18 participants (10 male, 8 female; mean 46.0 ± 15.3 years). A best fit line for each plot was then determined. For all but one participant (SP), the slopes of the best fit lines for accuracy and for precision were all positive (Table 4.1). This result indicates that, as intensity increased, there was a reduction in precision (i.e. an increased PDF area) and a reduction in accuracy (i.e. the centre of the PDF was further away from the target).

Accuracy vs intensity **Precision vs Intensity**

(a) Participant JS (slope = 1.23, R^2 = 0.97) **(b)** Participant LB (slope = 18.22, R^2 = 0.95)

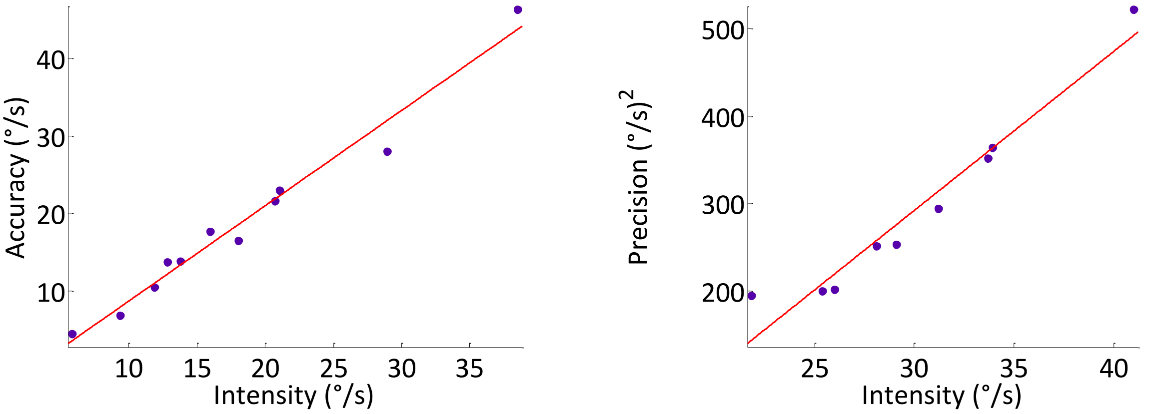

(c) Participant JT (slope = 0.14, R^2 = 0.07) **(d)** Participant DT (slope = 2.78, R^2 = 0.03)

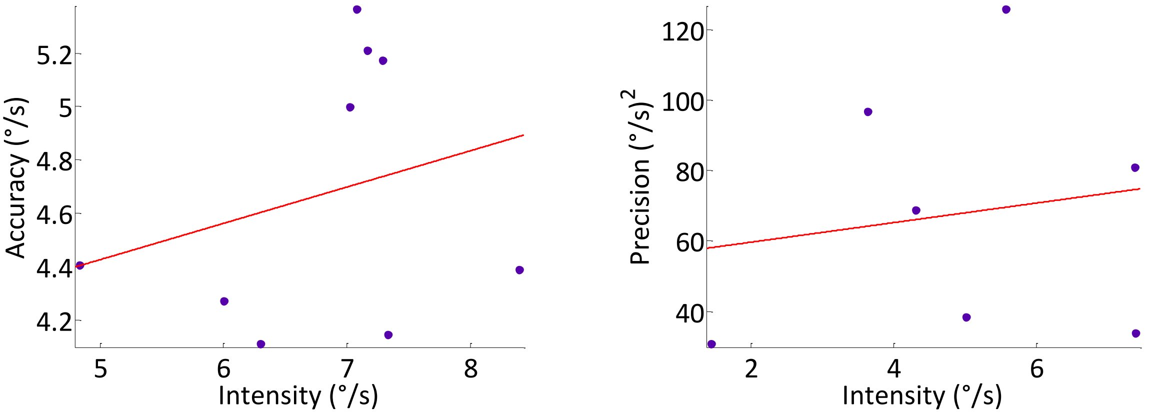

Figure 4.11 Example scatter plots showing the lines of best fit for (a) and (b) the participants with the best R^2 for PDF accuracy and PDF precision, and (c) and (d) the participants with the worst R^2 for PDF accuracy and PDF precision.

Participant	Absolute PDF accuracy		Absolute PDF precision	
	Slope (± 95% CI)	R^2	Slope (± 95% CI)	R^2
MT	1.73 (± 0.75)	0.81	11.95 (± 8.56)	0.81
JC	0.23 (± 0.38)	0.22	5.42 (± 7.49)	0.30
LB	1.10 (± 0.47)	0.79	18.22 (± 3.89)	0.95
VW	1.03 (± 0.53)	0.69	13.31 (± 6.84)	0.68
RW	0.57 (± 0.32)	0.71	7.03 (± 24.41)	0.06
CT	1.06 (± 0.16)	0.96	49.16 (± 9.11)	0.94
SM	1.10 (± 0.30)	0.92	17.00 (± 9.28)	0.22
SP	0.10 (± 0.35)	0.08	-3.49 (± 5.97)	0.25
DB	0.70 (± 0.30)	0.82	10.62 (± 8.30)	0.57
DC	0.78 (± 0.25)	0.93	8.10 (± 0.30)	0.91
DP	2.17 (± 3.29)	0.26	22.7 (± 64.00)	0.09
DT	0.21 (± 0.97)	0.06	2.78 (± 19.34)	0.03
GT	0.86 (± 0.26)	0.92	2.47 (± 7.08)	0.11
GT2	0.56 (± 0.33)	0.74	14.87 (± 50.49)	0.08
JT	0.14 (± 0.43)	0.07	3.72 (± 8.40)	0.14
JS	1.23 (± 0.15)	0.97	52.18 (± 18.09)	0.83
MB	0.85 (± 0.37)	0.84	10.27 (± 5.78)	0.76
JM	0.95 (± 0.19)	0.96	11.64 (± 1.86)	0.82

Table 4.1 Data for the line of best fit for accuracy and precision as a function of intensity.

On the whole, the R^2 values for both PDF accuracy (0.65 ±0.34) and PDF precision (0.48 ±0.37) were reasonably high, suggesting that either absolute PDF accuracy or absolute PDF precision could be used instead of intensity to determine the null zone. However, the merits and pitfalls of using of absolute values when determining fixation performance have already been discussed. The participants with the best and worst R^2 values for PDF accuracy and PDF precision are presented in Figure 4.11. One reason why precision may have been associated with lower R^2 values may have been because intensity is inherently a one dimensional measure and fails to encompass the imprecision introduced by vertical eye movements during the slow phase. Another possible reason is that intensity is that constant velocity that generates the *same* eye excursion as the slow phase, in the *same* duration. Because a defining characteristic of IN slow phases are that they are accelerating (CEMAS, 2001), the slow phase velocity is *increasing.* Of course, there are many possible increasing slow phases having the same intensity but different velocity distributions. Each of these different velocity distributions will have a different spread of velocities, and so a different two-dimensional 'area' for the precision of the PDFs. This may have contributed to a lower R^2 for precision (Figure 4.12).

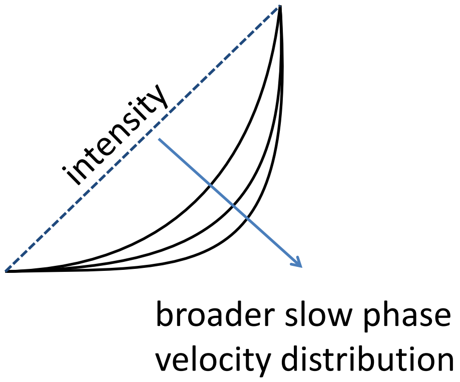

Figure 4.12 Schematic representation depicting different slow phases with increasing departure from an entirely linear slow phase. With increasing departure from the line representing intensity there is an increase in the expected slow phase velocity distribution which would correspond to larger PDF isocontours and lower precision. However, all three depicted slow phases will have the same intensity.

4.6 Vertical null zones

Null zones are thought of as existing along an infinitely thin, mid vertical line. However, those with IN are capable of moving their eyes above and below this imaginary line. Therefore, in this section, intensity for eye movements along the mid vertical axis was investigated to determine whether or not a null zone existed above or below the horizontal midline. The experiment conducted in an identical manner as for along the horizontal except on this occasion the axis was vertical. The vertical fixation targets were presented at random locations, each for 14s. Eighteen participants with IN (10 male, 8 female; mean 46.0 ± 15.3 years) took part in this experiment, with the group mean normalised intensity plotted as a function of vertical gaze angle (Figure 4.13). A repeated measures analysis of the mean normalised intensity data indicated no significant difference in the mean normalised intensity with vertical gaze angle [F(8,117.58)=.742, p=.654].

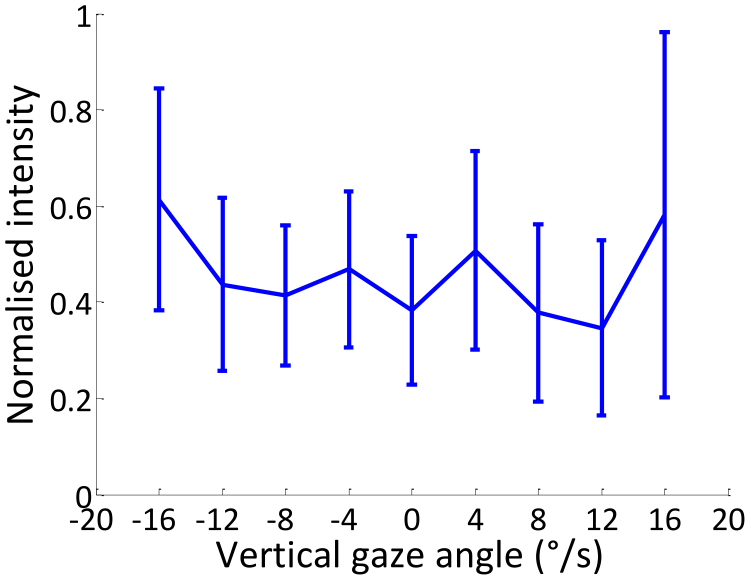

Figure 4.13 Mean normalised intensity as a function of vertical gaze angle for each presentation type for presentation. Error bars indicate the 95% confidence intervals.

This result would suggest that no variation in the intensity of the IN oscillation occurs on vertical gaze.

4.7 Conclusions

In this chapter, experimental work attempted to characterise the change in the magnitude of the IN oscillation with horizontal gaze angle using intensity as the eye movement measure. There are no accepted standardised methods for evoking a change in gaze angle (e.g. head fixed and vary eye position, or vary head position with eyes fixed). Additionally, there is a complete lack of information in the literature concerning how intensity should be calculated and the corresponding null zone located. Attempts to determine the null zones were motivated by future pursuit experiments, where individuals will need to follow targets that move through a range of horizontal gaze positions. The presence and location of a null zone would be expected to impact on overall pursuit performance, for example by introducing potential pursuit asymmetry. That said, while this chapter did determine that as a group, those with IN have minimum intensity at or in close proximity to the straight ahead position. However, this minimum was slightly different for different presentation conditions. Predictable target presentation conditions yielded more similar null zone locations than did unpredictable target locations. Yet, even for predictable target locations, the results were by no means replicable. It would seem that the null zone can only be determined under a stringent set of experimental conditions, which questions the significance of the null zone in the real-world. Given these findings, the effect of any change in the magnitude of the IN during a sweep of a pursuit target will be ignored, however asymmetries between different pursuit directions will be considered possible.

5 Pursuit performance in those with and without IN

5.1 Introduction

In Chapter 1, it was discussed that it is unclear whether or not those with IN have normal smooth pursuit eye movements. Whatever the mechanism, previous studies have showed that those with IN are capable of following a moving target. In this chapter, pursuit along different directions, i.e. horizontal (right-left) and vertical (up-down), will be investigated using the generalised eye movement analysis developed in Chapter 3. Additionally, two claims that have been made in the IN literature with respect to pursuit will be investigated. The first claim is that those with IN may be better at following rapidly oscillating targets than typical individuals, while the second claim is that the slow phase is always opposite to the direction of pursuit target motion.

5.2 Accuracy and precision as a function of pursuit target direction

The Filehne illusion is a pursuit-based illusion in which stationary objects are perceived to move in a direction opposite to the direction of the pursuit. This illusion is hypothesised to result from the magnitude of retinal signals exceeding the magnitude of extra-retinal signals. As the Filehne illusion is measured during horizontal pursuit (Freeman and Banks, 1998; Dash et al., 2009; Freeman et al., 2010), the oculomotor performance of horizontal pursuit in those with IN will be characterised.

Few studies have investigated the ability those with IN to follow a target vertically. Of those that did, normal OKN gains (Abadi and Dickinson, 1985) or normal pursuit eye movements (Collewijn et al., 1985) were reported. In Chapter 1, it was discussed that, current measures of smooth pursuit quantification are inadequate for characterising vertical smooth pursuit in those with IN, since only eye velocity along the direction of the target motion can used in the calculation. However, the IN oscillation is reported to be predominantly horizontal. Therefore, when determining how well someone can follow a target, the ability to continuously image the target should be assessed along the direction of motion, but also orthogonal to it. Failing to do so may result in a substantial deficit in target following being overlooked. In addition to characterising pursuit of a horizontally moving target for the Filehne illusion, this chapter will also investigate pursuit of a vertically moving target.

For those with IN, the gaze angle of the null zone when the eye serially fixates stationary horizontal targets is reported to differ to the gaze angle of the null zone when the eye smoothly rotates through a range of gaze angles (i.e. the gaze angle of the null zone undergoes a lateral shift). The magnitude of this null zone shift during pursuit is reported to depend not only on the speed of attempted pursuit by shifting *farther* for faster pursuit targets, but also on the pursuit direction by shifting in the *opposite* direction to attempted pursuit (Dell'Osso, 1986; Kurzan and Buttner, 1989). For example, in Figure 5.1 the null zone is located at the straight ahead position when pursuing leftwards. However, on pursuing rightwards the null zone will shift leftwards. Reports on the gaze angle shift of the null zone in the literature, although few in number, suggest that the shift can be by as much as 25° for a velocity of 15°/s (Kurzan and Buttner, 1989). Because the null zone that gaze angle where the IN oscillation is least, any potential shift in the null zone is likely to impact of smooth pursuit performance by introducing a directional asymmetry. For example, in Figure 5.1 rightward pursuit will cause the null zone to be shifted leftwards. Because the intensity of the nystagmus increases away from the null, the larger eye IN oscillation on rightwards pursuit may result in less accurate and less precise pursuit

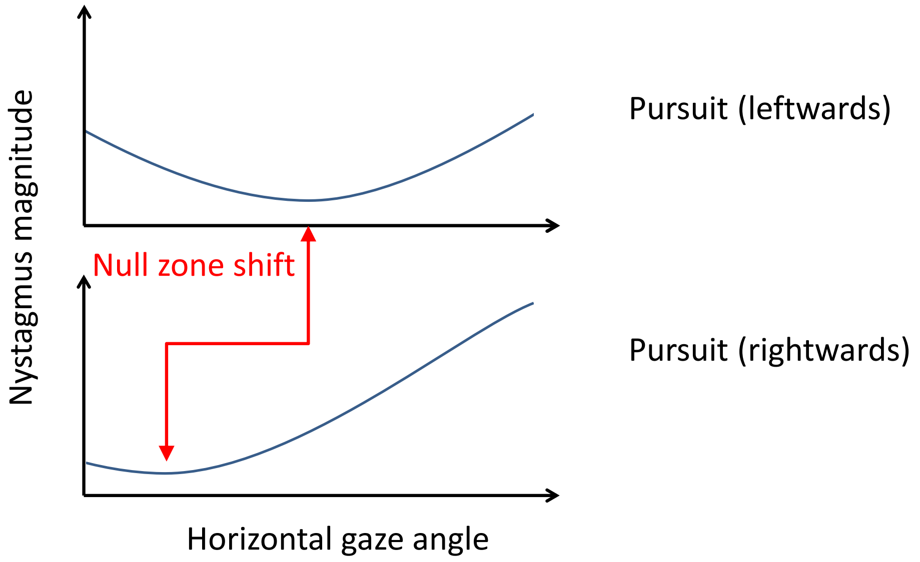

Figure 5.1 A shift in the location of a null zone may result in asymmetric pursuit performance.

For this reason, pursuit will be studied in both directions along a given axis (i.e. leftwards and rightwards).

5.2.1 Methods

Fifteen participants with IN (8 male, 7 female; mean 44.2 ± 14.3 years) and fifteen normally sighted participants (9 males, 6 female; mean 29.5 ± 8 years) as a control group, completed a monocular pursuit task in exchange for payment.

5.2.2 Procedures

It was explained to participants that it was their task to follow a moving target as carefully as possible. The target moved with a constant velocity of 8°/s or 16°/s through peak-to-peak amplitudes of 4°, 8°, 16° or 32°. Each experimental trial commenced with participants fixating a green central dot subtending 0.4° in the centre of an otherwise uniform black background. To initiate a trial, the subject pressed either mouse button on a wireless keyboard which caused the uniform background and fixation target to be immediately replaced with another 0.4° target, stepped either to the left or right of the straight ahead position. After 2 seconds, the time interval allotted for participants to acquire the target, it began to move for 24 seconds. Finally, the participant returned their fixation to the central fixation dot ready to begin the next trial. Horizontal target motion was run as a separate block to vertical target motion.

5.2.3 Analysis

Constant velocity targets that oscillate to-and-fro are known to be highly predictable. Consequently, participants will quickly anticipate the target motion and so fail to pursue the target until reversal of direction (Figure 5.2). Additionally, when a reversal does occur, participants often will make catch-up saccades (Figure 5.3). In summary, target prediction will generate unreliable eye movement data close to reversals. For this reason, only the central 70% of each target sweep will be retained, with 15% at either end being set to 'NaN'. Removing a fixed *proportion* of each slope rather than a fixed *duration* ensured the number of potential data points used to construct the bivariate PDF was constant across all experimental trials. Otherwise, for targets with greater frequency (e.g. 4Hz), there would be a greater proportion of data removed than for targets with a lower frequency (e.g. 0.5Hz).

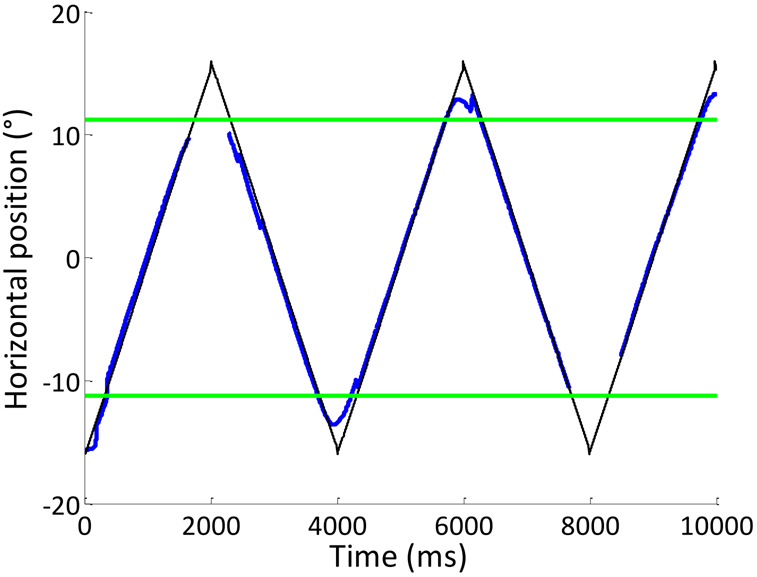

Figure 5.2 Participants fail to adequately pursue (blue) the target (black) to the reversal. Only eye movement data that was within the central 70% of each slope (i.e. between the two green lines) was used for further analysis.

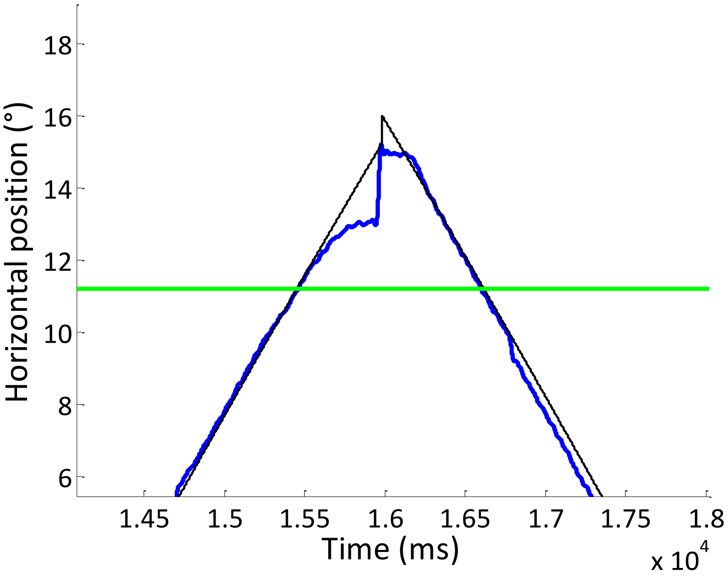

Figure 5.3 Participants make catch-up saccades when the target reverses direction. Again, the green line demarcates that portion of the slope to be removed.

Each combination of velocity and amplitude was repeated once, and the eye movement data for repeats concatenated before parsing the data into respective target directions. Target-relative eye velocity PDFs were then computed as described in Chapter 3. As more than one independent variable was manipulated, a repeated measures 4 (direction) x 2 (velocity) x 4 (peak-to-peak amplitude) analysis was performed in SPSS (Version 23, IBM corporation). All significant main effects were followed up with a pairwise comparison with Bonferroni adjustment for multiple comparisons. On those occasions when sphericity was violated, Greenhouse-Geisser correction was applied. When analysing directional data (i.e. accuracy theta), linear statistics are inappropriate (Figure 5.4). Instead, directional data were analysed using the circular statistics toolbox for MATLAB® (Berens, 2012; Berens and Valesco, 2009).

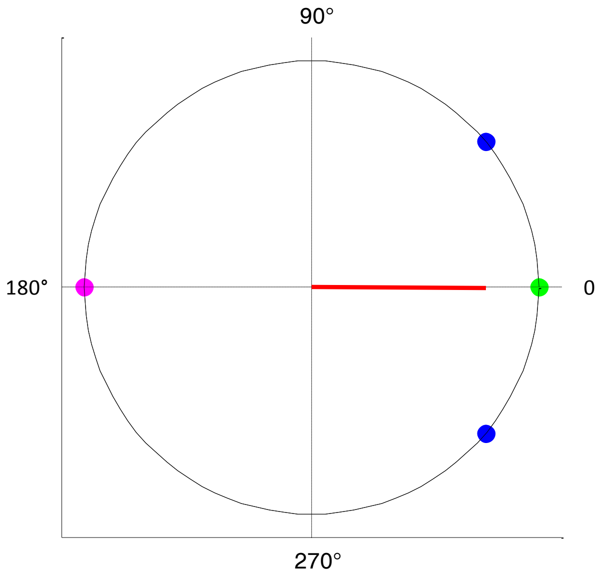

Figure 5.4 An example of inadequacy of linear statistics when analysing directional data. For angles of 40° and 320° (blue), the arithmetic mean direction is 180° (magenta), even though both angles are centred on the circular mean direction, ϴr, 0° (green) with a resultant vector, r, of 0.766 (red line).

In brief, mean directions (*ϴr*) were reported together with the resultant vector (*r*). The resultant vector can take a value between 0 and 1, with 0 indicating uniform distribution of data, and 1 indicating all data lie along a single direction. The Rayleigh z test was used to determine whether the directional data were uniformly distributed around a circle, with a significant result indicating that the directional data have a mean direction. Axial data (i.e. the major axis orientation) can have values within the limited range of $-\pi/2$ to $+\pi/2$, such that major axis orientation will ‘flip’ to an angle of $-\pi/2$ when it exceeds $+\pi/2$. This characteristic of axial data produces a diametrically bimodal distribution, with data lying at opposite locations on a circle (Figure 5.5, left). Consequently Θr and r of axial data will lie along a direction approximately orthogonal to the axis data. To calculate the actual Θr and r of axial data, all axial data must be first transformed by doubling the angular data. Next the mean direction and resultant vector are calculated for the transformed data. Finally, the angular data are reverse-transformed by dividing the mean direction by two, giving the corrected Θr for the axial data. No transformation is applied to the r when reverse-transforming the data (Fisher, 1993) (Figure 5.5 (b)).

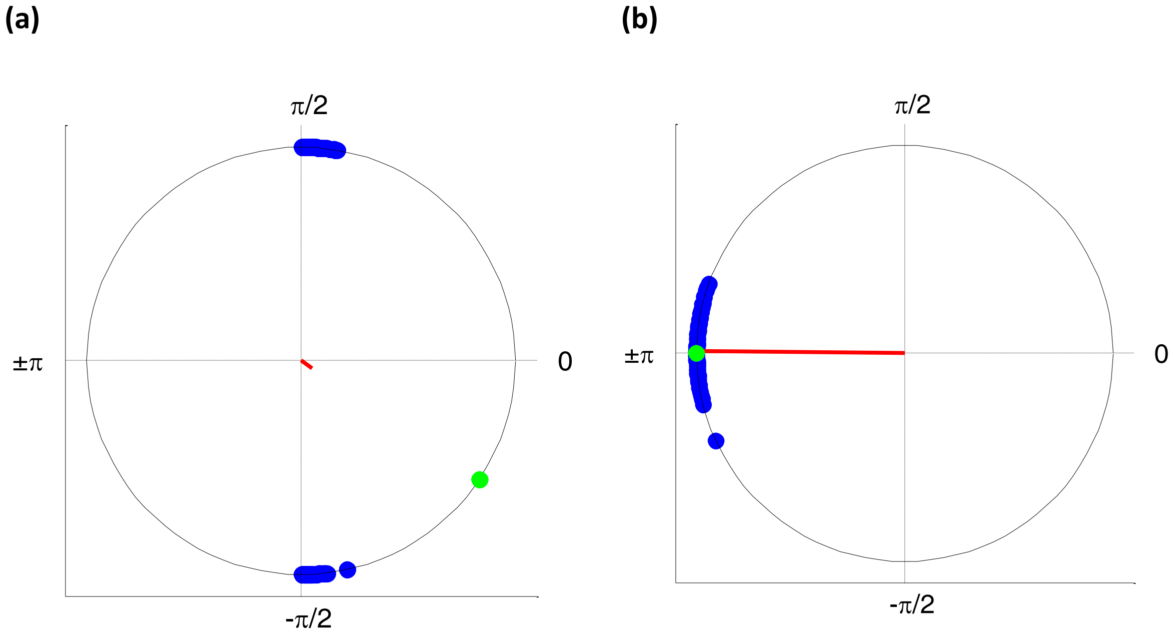

Figure 5.5 Left: Because values for the major axis orientation (blue) took the range of $-\pi/2$ to $+\pi/2$, it resulted in a diametrically bimodal distribution. The mean direction, Θr, of this diametrically bimodal distribution was -33.8° (green) and the resultant vector, r (red), was 0.0607. Right: To correct for diametric bimodal distributions, angle doubling was used. The double angle mean direction (green), $2\Theta r$, and resultant vector (red), r, were 179.35° ± 1.32 and 0.992, respectively. The single angle mean direction (magenta), Θr, of the original data set was therefore 89.67° ± 0.662.

To compare the uniformity of angular data, all the angular data were transformed so that it lay along 0°. A Kuiper’s V test for uniformity of data around the circle was then performed with a mean direction of 0°. In this test, if the result is significant, data have a mean direction of 0°. Finally, a one sample test for mean angle was performed on the transformed data to determine if *Θr* was significantly different from 0°. To aid interpretation of the results, all angles herein are reported in degrees of arc (°), rather than radians.

5.2.4 Results: target-relative PDFs

Typical target relative PDFs for typical individuals and those with IN are shown in Figure 5.8 and Figure 5.9. So that a visual comparison can be made, the results for control participants are presented on the same scale as the PDFs for typical control participants.

5.2.5 Results: between control participants and INs

A repeated measures analysis with group as the between subjects factor indicated a significant difference between typical individuals and those with IN for accuracy [$F(1,28)= 30.64$ $p< .001$)] and for precision [$F(1,28)= 20.95$ $p< .001$)].

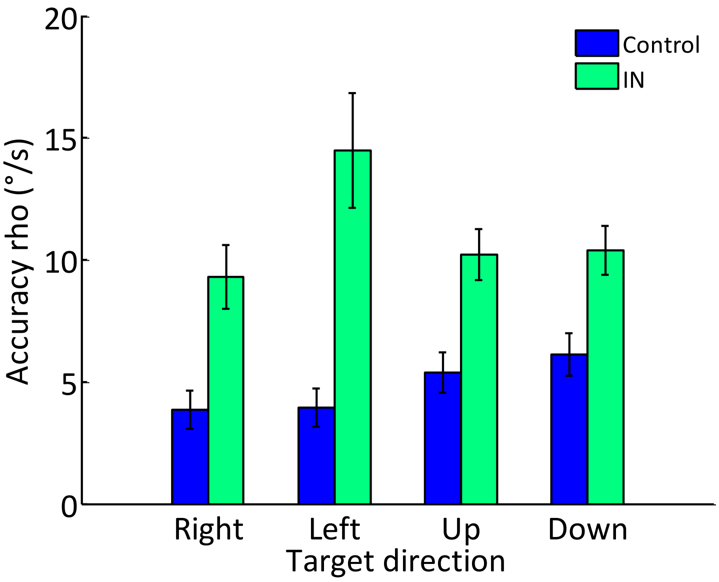

Figure 5.6 Mean accuracy rho for control participants and INs as a function of target direction. Error bars indicate 95% confidence intervals.

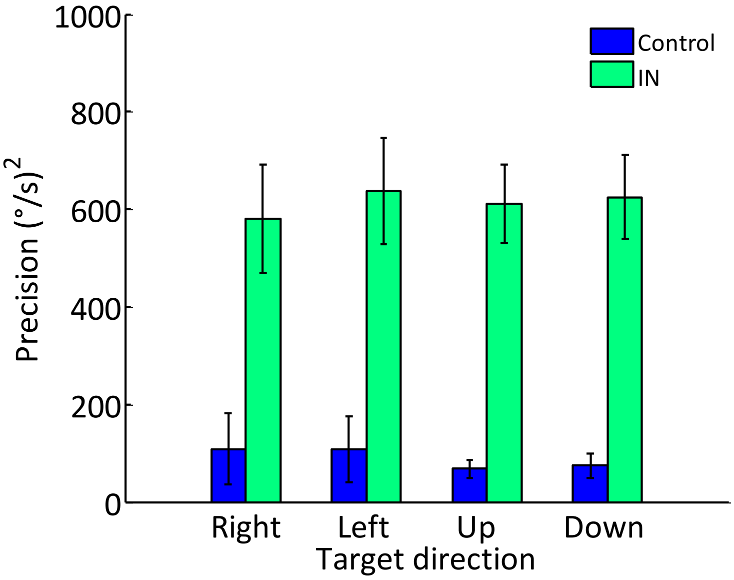

Figure 5.7 Mean precision for control participants and INs as a function of target direction. Error bars indicate 95% confidence intervals.

The results of this between-subjects analysis indicate that, when results are pooled across the directions, those with IN have significantly less accurate and less precise pursuit than typical individuals. In the following sections, the effect of pursuit direction will be considered within-subjects.

5.2.6 Results: control participants

5.2.6.1 Accuracy theta

All target directions had a significant mean direction and resultant vectors (rightwards, Θr = 181.40°, 95% CI ± 7.74, r = 0.784, Rayleigh $z_{73.828}$, $p < .001$; leftwards, Θr = 344.73°, 95% CI ± 6.70, r = 0.862, Rayleigh $z_{89.221}$, $p < .001$; upwards, Θr = 274.76°, 95% CI ± 6.36, r = 0.890, Rayleigh $z_{95.115}$, $p < .001$; downward Θr = 93.20°, 95% CI ± 4.68, r = 0.911, Rayleigh $z_{99.592}$, $p < .001$) (Figure 5.10). On normalising the transformed angular data to 0°, a Kuiper's test for uniformity of data around the circle indicated that all target directions were significantly non-uniform with a Θr of 0° (rightward, $V_{94.096}$, $p < .001$; leftward, $V_{99.821}$, $p < .001$; upwards $V_{106.467}$, $p < .001$; downwards $V_{109.151}$, $p < .001$).

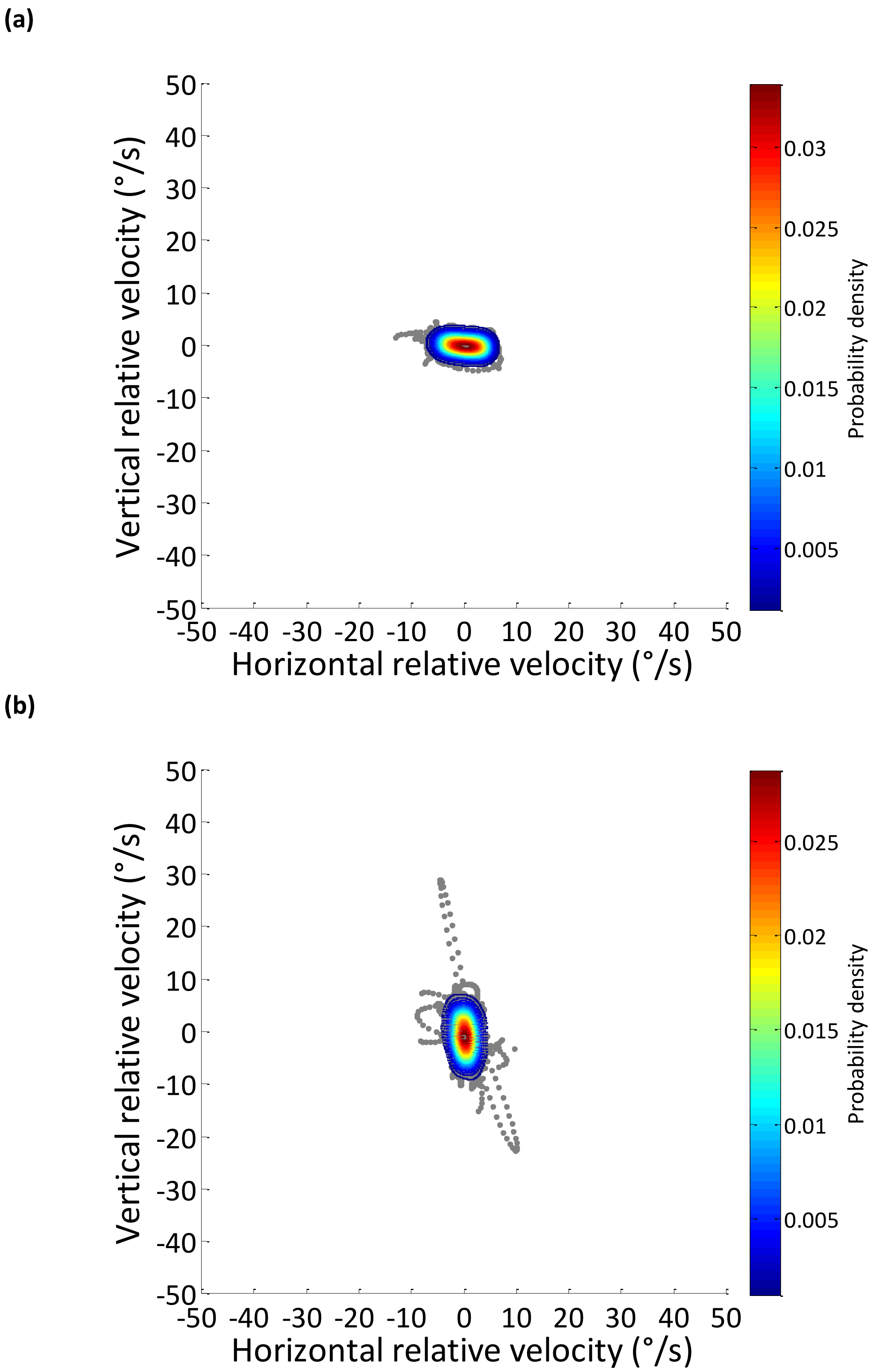

Figure 5.8 Representative probability density functions superimposed on the relative velocity data for pursuit during (a) horizontal rightward motion (accuracy 0.08°/s, precision 29.78 (°/s)^2) and (b) vertical upward motion (accuracy 0.88°/s, precision 37.52 (°/s)^2) for a typical individual (SLL).

(a)

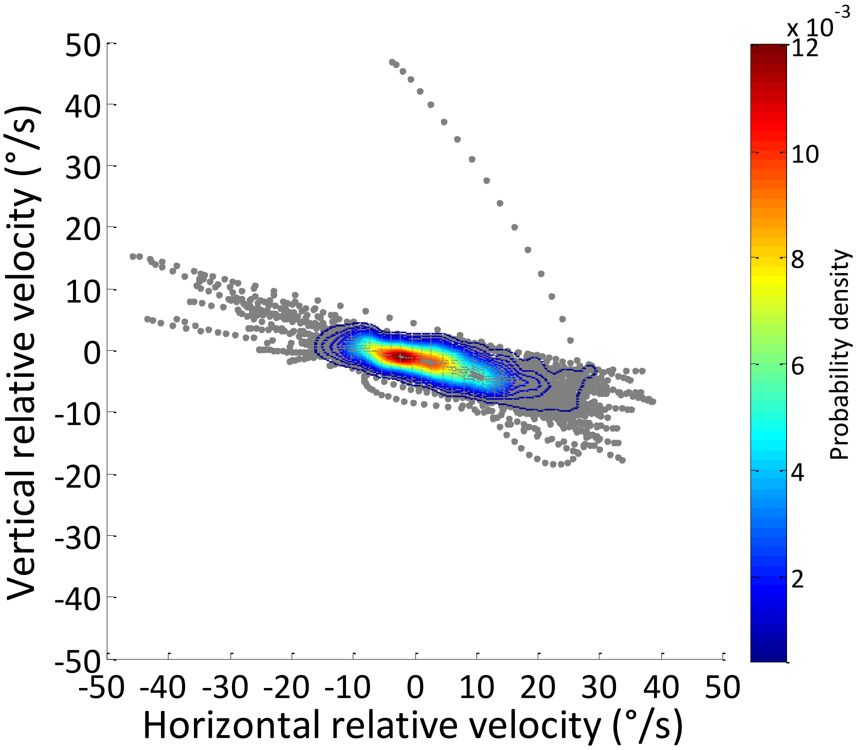

(b)

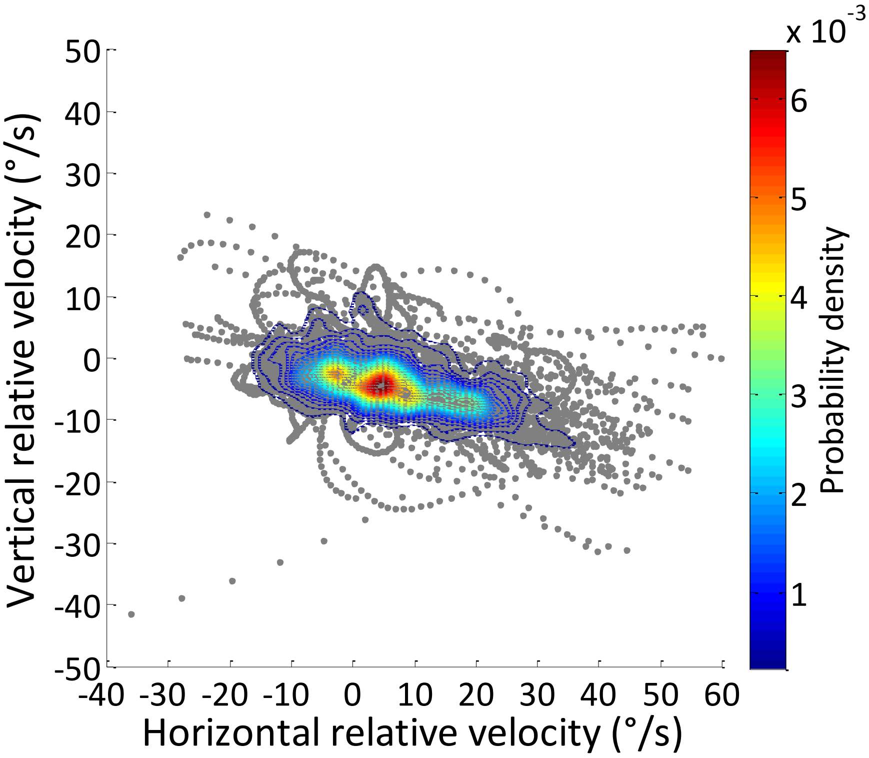

Figure 5.9 Representative probability density functions superimposed on the relative velocity data for pursuit during (a) horizontal rightward motion (accuracy 2.59°/s, precision 112.18 $(°/s)^2$) and (b) vertical upward motion (accuracy 7.39°/s, precision 239.02 $(°/s)^2$) for an individual with IN (MT).

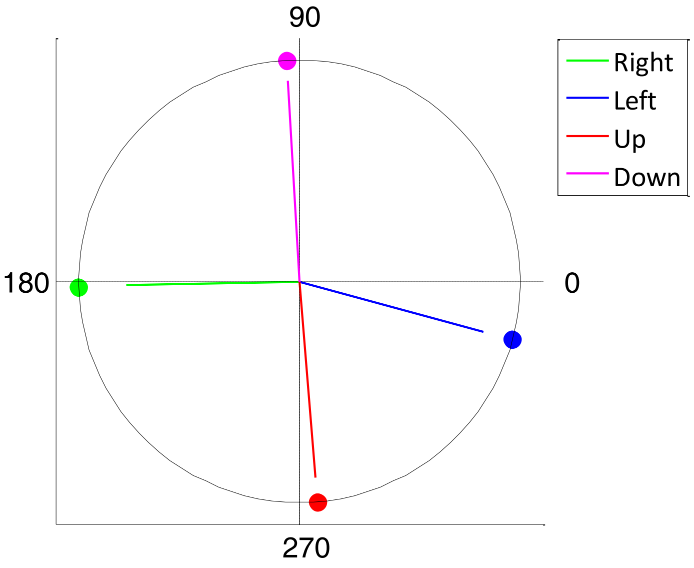

Figure 5.10 Accuracy theta data for control participants, with mean angle and resultant vector colour-coded for direction.

Finally, a one sample test for a mean direction of 0° indicated that only a leftward target direction was significantly different from 0° (*Ɵr* = 344.734°, h=1), with all other target directions having no significant difference from 0° (rightward, *Ɵr* = 1.397°, h = 0; upward *Ɵr* = 4.758°, h=0; downward *Ɵr* = 3.1991°, h=0).

These results indicate that the isocontour centre was:

1. Parallel to the direction of target motion
2. Located behind the target with respect to its direction of motion.

These results indicate that the most probable eye velocities used by control participants were less than that of the target. This result confirms previous reports that the eye velocities of typical participants are less than the target (i.e. that smooth pursuit gain was less than 1.0) for horizontal (Murphy, 1978; Rottach et al., 1996) and vertical targets (Ke et al., 2013; Rottach et al., 1996). Even though velocity data were pooled across different velocities and peak-to-peak amplitudes, the accuracy theta was highly significant with small 95% confidence intervals. For this reason, no further analysis of accuracy theta (e.g. by velocity) was considered. For the isocontour centre to be located immediately behind the target with respect to its direction of motion, the axis with the lowest accuracy is the axis along which the target moves, rather than the orthogonal axis.

5.2.6.2 Accuracy rho

The direction of target motion had a significant effect on accuracy [$F(2.033, 28.46) = 25.01$, $\eta^2 = .642$, $p < .001$]. There was no significant right-left asymmetry ($p = 1.00$) or up-down asymmetry ($p = .246$) in accuracy. However, both upward and downward target directions differed significantly from rightward ($p = .004$ and $p < .001$, respectively) and leftward motion ($p < .001$ and $p < .001$, respectively).

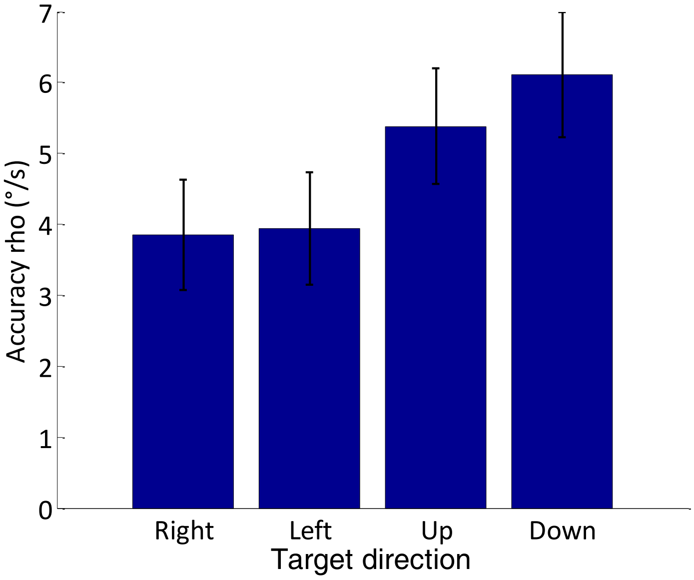

Figure 5.11 Mean accuracy rho for control participants as a function of target direction. Error bars indicate 95% confidence intervals.

These results, taken together with the results of the accuracy theta, indicate that eye velocities for horizontally moving targets better matched that of the target than for vertically moving targets (i.e. a higher gain would be expected for horizontal target motions than for vertical). Indeed, this finding is in agreement with previous studies (Collewijn and Tamminga, 1984; Ke et al., 2013; Rottach et al., 1996). Horizontal gain asymmetries have been reported previously (Ke et al., 2013; Sharpe and Sylvester, 1978). The lack of asymmetry in this study may have been attributed to restricting the data to only the most probable 68% of eye velocities.

5.2.6.3 *Precision and shape factor*

The direction of target motion had no significant effect on overall precision [*F*(1.03, 14.36) =1.691, η^2 = .108, *p* = .214], but had a significant effect on shape factor [*F*(1.053, 14.743) = 11.99, η^2 = .461, *p* = .003], suggesting that precision differed along the major and minor axes. There was no significant right-left asymmetry in shape factor (*p* = 1.00), but an up-down asymmetry existed that was only just significant (*p* = .042). Shape factors for horizontal targets were larger (i.e. more symmetric axes) than for vertical targets (upwards target motion, *p* = .033 and *p* = .035 versus rightwards and leftwards, respectively; downwards target motion, *p* = .015 and *p* = .015 versus rightward and leftward target motion, respectively).

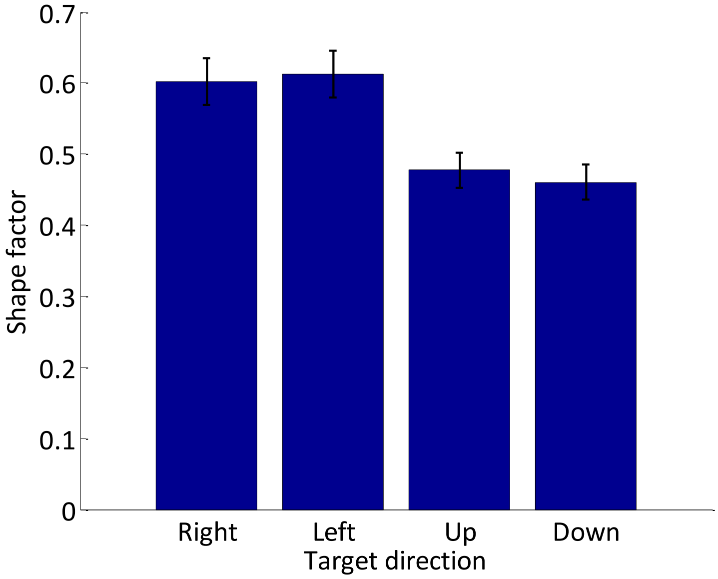

Figure 5.12 Mean shape factors for control participants as a function of target direction. Error bars indicate 95% confidence intervals.

Despite no significant change in precision, vertical target motion produced greater asymmetry between major and minor axes. There were two possible explanations that could account for such an asymmetry:

1. A reduction in precision along the major axis (i.e. more spread of velocities along this axis)
2. An increase in precision along the minor axis (i.e. less spread of velocities along this axis).

To determine which of these two possibilities was responsible for the change in shape factor, the major and minor axes for horizontal and vertical target motion were compared.

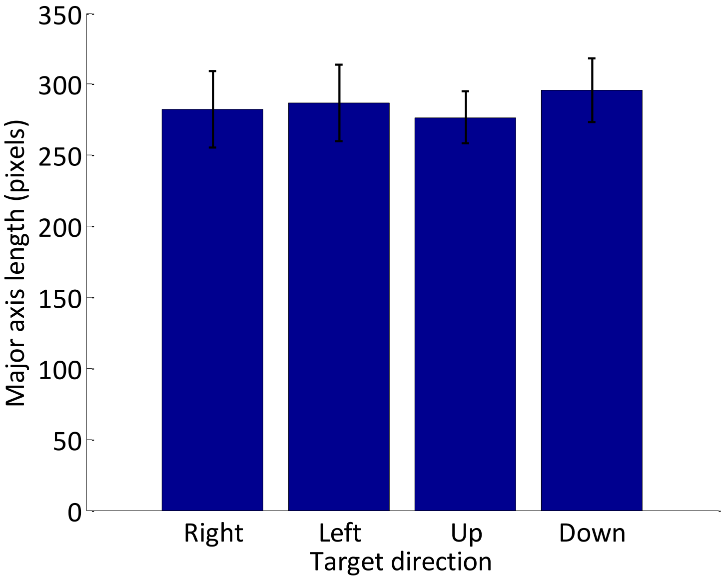

Figure 5.13 Mean major axis lengths of the 68% isocontours for each target direction. Error bars indicate 95% confidence intervals.

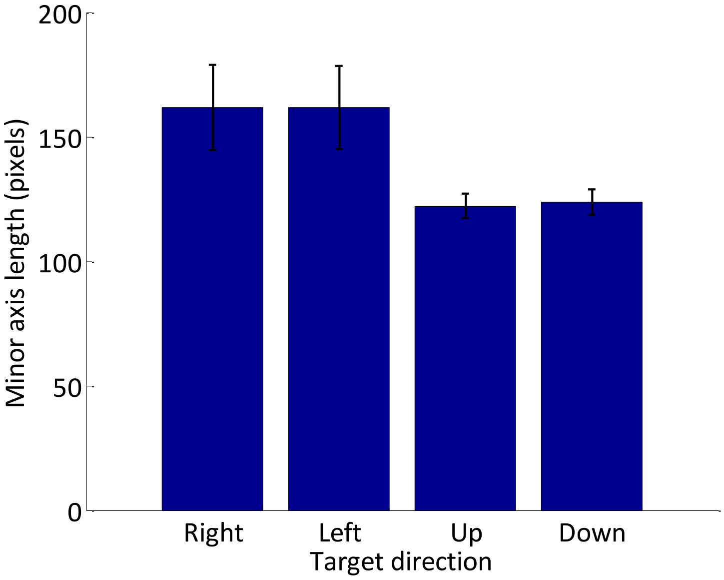

Figure 5.14 Mean minor axis lengths of the 68% isocontours for each target direction. Error bars indicate 95% confidence intervals.

This indicated relatively little difference in the magnitude of the major axes for different target directions (Figure 5.13), but the magnitude of the minor axis was substantially reduced for vertical target directions than for horizontal target directions (Figure 5.14).

5.2.6.4 Orientation of isocontour major axis

To fully interpret the asymmetry noted in the minor axis lengths, it was necessary to determine the orientation of the major axes. The major axes had a significant mean direction for all target directions (rightwards, Θr = 1.64°, 95% CI ± 4.39, r = 0.718, Rayleigh $z_{61.80}$, $p < .001$; leftwards , Θr = 1.13°, 95% CI ± 4.26, r = 0.733, Rayleigh $z_{64.42}$, $p < .001$; upwards, Θr = 89.67°, 95% CI ± 0.662, r = 0.992, Rayleigh $z_{118.06}$, $p < .001$; downwards, Θr = 89.8°, 95% CI ± 0.703, r = 0.991, Rayleigh $z_{117.82}$, $p < .001$) (Figure 5.15).

On normalising the transformed angular data to 0°, a Kuiper's test for uniformity of data around the circle indicated that all target directions were significantly non-uniform with a $2\Theta r$ of 0° (rightward, $V_{85.974}$, $p < .001$; leftward, $V_{87.853}$, $p < .001$; upwards $V_{119.020}$, $p < .001$; downwards $V_{118.902}$, $p < .001$). Finally, a one sample circular t-test was performed on the transformed data to determine if $2\Theta r$ was significantly different from 0°, which found that for all target directions $2\Theta r$ was statistically equal to 0° (rightward, $2\Theta r$ = 3.279°, h = 0; leftward, $2\Theta r$ = 2.263°, h=0; upward $2\Theta r$ = 359.347°, h=0; downward $2\Theta r$ = 359.664°, h=0).

These results indicate that the major axis was always parallel to the direction of motion, and the minor axis was always orthogonal. These data indicates that the control of eye velocity is always more variable along the direction of target motion. The precision along the direction of target motion appears to be similar for horizontal and vertical target motions since there was little difference between the magnitudes of the major axes. Precision along the axis orthogonal to the target motion is less for horizontal targets than vertical. This suggests greater variability of vertical eye velocity on following horizontal targets than of horizontal eye velocity when following vertical targets. This precision anisotropy during pursuit is a finding that, to the best of my knowledge, has not been previously reported.

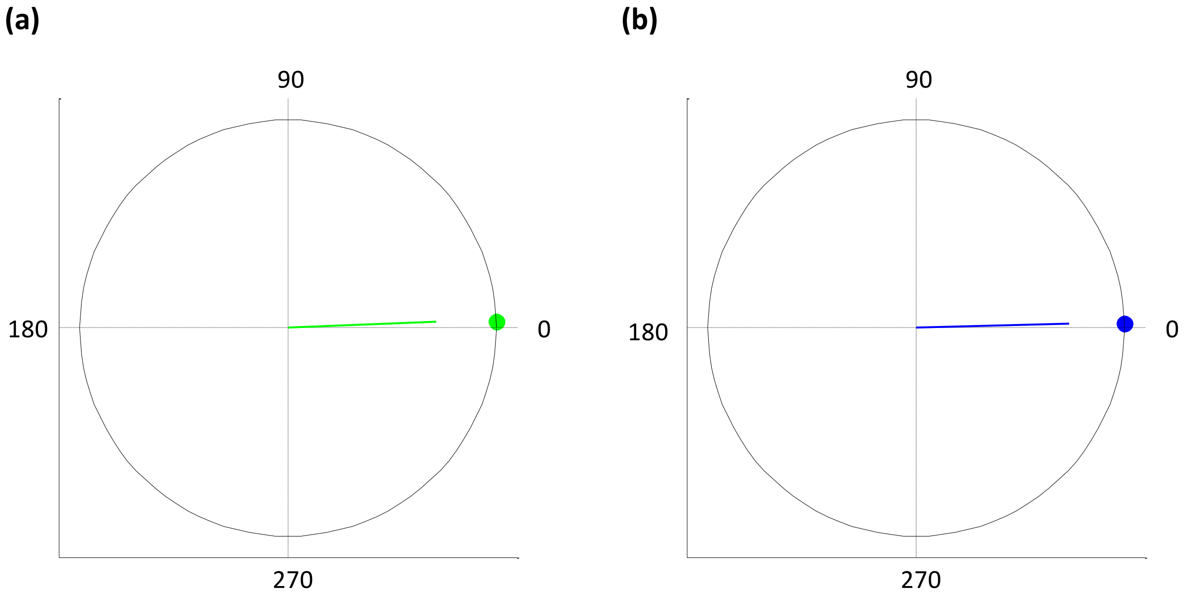

Rightward

Leftward

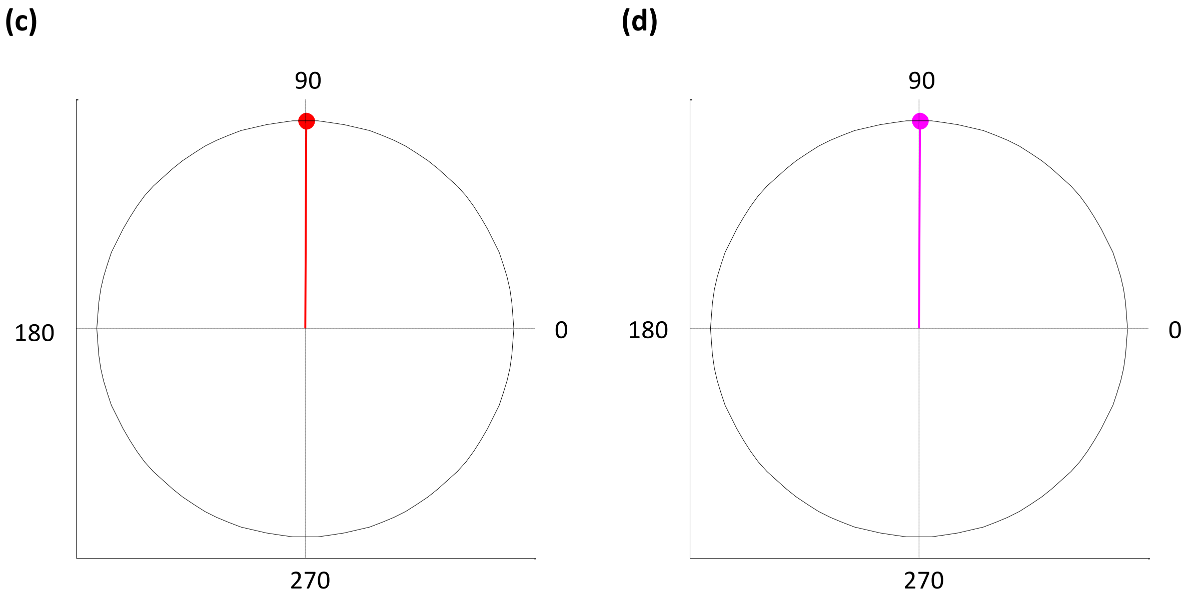

Upward

Downward

Figure 5.15 The orientation of the major axis of the 68% isocontour colour-coded for direction.

It has been suggested that early investigators assumed the variability of eye velocity along the direction of pursuit to be on a par with the variability during fixation, and so its importance had been neglected (Kowler and McKee, 1987). Subsequent studies have characterised the precision of eye movements during smooth pursuit (Kowler and

McKee, 1987; Kolarik et al., 2010), but only in the direction of the target motion. This study has demonstrated that the precision of eye movements in the axis orthogonal to the target motion is imprecise, particularly for horizontal pursuit.

5.2.6.5 *Summary of findings*

In this section, the main findings for control participants were:

1. Eye speed is inaccurate along the direction of target motion, but accurate along the orthogonal axis, irrespective of the target direction.
2. Eye speed is lower when following vertically moving targets than for horizontally moving targets
3. Eye speed is always more variable along the direction of target motion than the orthogonal axis.
4. Eye speed is less variable in the orthogonal axis for horizontally moving targets than for vertically moving targets.

5.2.7 Results: IN participants

5.2.7.1 *Accuracy theta*

All target directions had a significant mean direction and resultant vectors (rightwards, Θr = 184.34°, 95% CI ± 15.406, $r = 0.453$, Rayleigh $z_{24.62}$, $p < .001$; leftwards , Θr = 356.57°, 95% CI ± 8.918, $r = 0.709$, Rayleigh $z_{60.32}$, $p < .001$; upwards, Θr = 272.97°, 95% CI ± 7.822, $r = 0.779$, Rayleigh $z_{72.81}$, $p < .001$; downwards, Θr = 79.541°, 95% CI ± 7.798, $r = 0.781$, Rayleigh $z_{73.13}$, $p < .001$) (Figure 5.16).

On normalising the transformed angular data to 0°, a Kuiper's test for uniformity of data around the circle indicated that all target directions were significantly non-uniform with a Θr of 0° (rightward, $V_{54.20}$, $p < .001$; leftward, $V_{84.93}$, $p < .001$; upwards $V_{93.35}$, $p < .001$; downwards $V_{92.12}$, $p < .001$). Finally, a one sample circular t-test was performed on the transformed data to determine if Θr was significantly different from 0°, which found all target directions other than downwards (Θr 349.54°, h=1), the mean direction was statistically equal to 0° (rightward, Θr = 4.34°, h = 0; leftward, Θr = 356.57°, h=0; upward Θr = 2.97°, h=0).

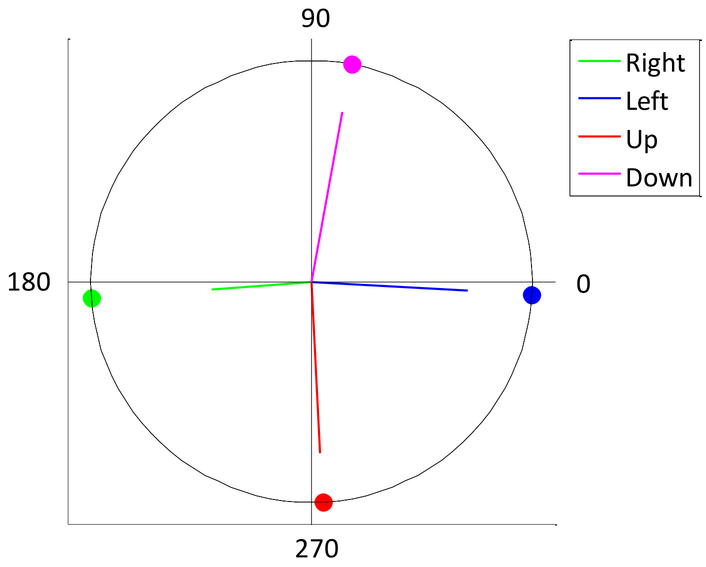

Figure 5.16 Accuracy theta data for IN participants, with mean angle and resultant vector colour-coded for target direction.

These results indicate that the centre of the isocontour was:

1. Parallel to the direction of the direction of motion.
2. Located behind the target with respect to its direction of motion

IN is frequently described a predominantly horizontal oscillation (Averbuch-Heller et al., 2002), however, few have simultaneously characterised the horizontal and vertical eye velocities (Collewijn et al., 1985). Because it is predominantly horizontal, the centre of the isocontour lay along the horizontal axis for horizontally moving targets. However, because the oscillation is predominantly horizontal, when combined with voluntary vertical pursuit, it was expected that the centre of the isocontour would lie oblique for vertically moving targets rather than parallel to the direction of motion. Interestingly this was not the case. This finding may be explained by the waveforms of the participants, which were all jerk. Following the fast-phase, the eye has been redirected back at the presumed target location and is at rest. Therefore the major contribution to the retinal slip at this point is the target, which continues to travel vertically with constant velocity. The eye is now lagging behind the target and accelerates laterally. However, because of acceleration, the most probable eye velocities are low eye velocities. Consequently, it can be readily appreciated that, even for vertical target motion, the isocontour is parallel to the direction of target motion and behind the target with respect to its direction of motion. Of course, this argument assumes that the slow phase is always in the direction of the target, whether horizontal or vertical, but even if the slow phase were to move in the opposite direction to the target motion, the same argument would apply. Even though data were pooled across different velocities and peak-to-peak amplitudes, the accuracy theta was highly significant with small 95% confidence intervals. For this reason, no further analysis of accuracy theta was considered (i.e. for target speed and for peak-to-peak amplitude).

5.2.7.2 Accuracy rho

Target direction has no significant effect on accuracy (Figure 5.17). This indicates that, irrespective of the target direction, those with IN were just as inaccurate. This result can be accounted for again by jerk waveforms. Following the end of the fast-phase, the eye is at the presumed target location and at rest. At this point, the major contribution to retinal slip is the target, which continues to move with constant velocity. Irrespective of the target motion, this will generate substantial retinal slip, hence similar accuracy. Figure 5.17 does show a horizontal asymmetry in accuracy.

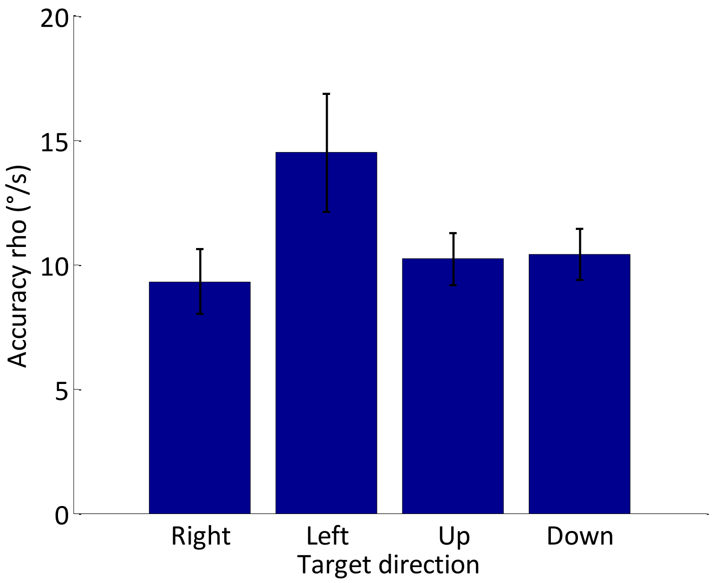

Figure 5.17 Mean accuracy rho of IN participants as a function of target direction. Error bars indicate 95% confidence intervals.

It was surprising that, given this obvious asymmetry, the results were not significant. Nonetheless, the horizontal differences can be attributed to the slow-phase direction. If trials were dominated by slow-phases that were in the same direction as the pursuit target, the accuracy would be expected to be lower than if the slow-phases were in the opposite direction. This result has exposed a substantial deficit in those with IN as they attempt to foveate a vertically moving target. While previous research has suggested that those with IN can accurately follow a vertically moving OKN target (Abadi and Dickinson, 1985), these studies mask any potential deficit in the ability to foveate vertically moving targets by assuming the fovea is continuously aligned with the target horizontally and no retinal slip. Tracking an OKN stimulus is different to tracking a typical smooth pursuit stimulus. For individuals with IN, the large OKN target is continuously imaged on the fovea whereas typical smooth pursuit dot target will not. Outside of the foveation period, those with IN will be tracking the target extra-foveally. Extra-foveal smooth pursuit in those with foveal pathology has been shown to have a gain considerably less than 1.0, with a median of 0.74 versus 0.91 for controls (Shanidze et al., 2016). The result of extra-foveal pursuit of those with foveal pathology indicate that the eye velocity is less than the target (i.e. it is inaccurate). In a different study, a qualitative investigation was performed on vertical ‘smooth pursuit’ in IN (Collewijn et al., 1985). Since the gross trajectory of the eye movements of those with IN matched that of the target, it was concluded that vertical smooth pursuit was normal. However, without quantifying the results, it is not possible to determine how robust this conclusion was. In either case, this study has highlighted the misleading conclusions that may be reached if only one component of eye velocity is examined in isolation.

5.2.7.3 Precision

Target direction had no significant effect on precision [$F(1.06, 14.85) = .098$, $\eta^2 = .007$, $p = .744$] (Figure 5.18). This result indicates that, irrespective of the target direction, the control of eye velocity in those with IN was just as imprecise.

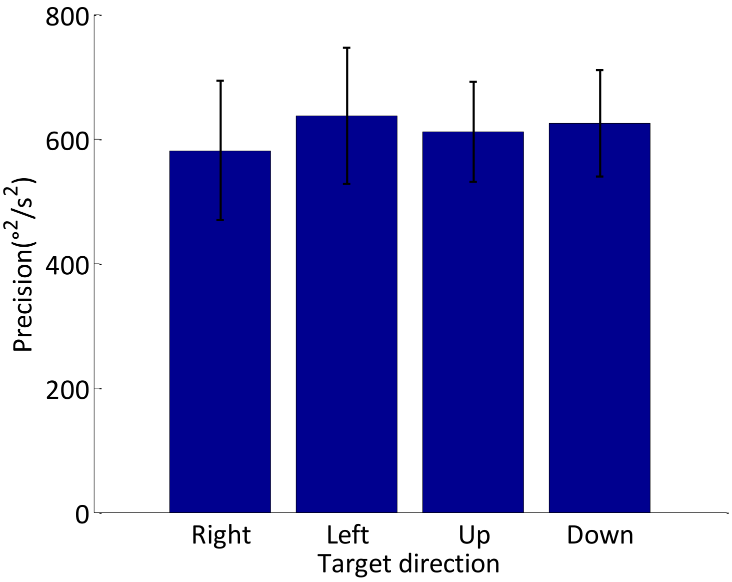

Figure 5.18 Mean precision for IN participants as a function of target direction. Error bars indicate 95% confidence intervals.

This result is not particularly surprising. In those with IN, precision in the horizontal direction will be dominated by the slow-phase. Irrespective of the target direction, the major contribution to imprecision will come from the slow-phase. The PDF analysis selects only the most probable eye velocities. So, for horizontal pursuit, although the slow phase parameters (e.g. amplitude) varied, these extreme fluctuations were unlikely to contribute to the bivariate PDF, given their low probability of occurring. This method therefore acted as a means to exclude outlier data. On this basis, it would be expected that two dimensional precision should not differ between horizontally and vertically moving targets.

Few studies have reported the precision of those with IN when tracking horizontally moving stimuli. Because of the importance of placed on the foveation period for high resolution vision (Dell'Osso et al., 1992a), studies of ‘pursuit’ restrict their analyses and hence measures of precision to only just the foveation period (Dell'Osso et al., 1992b). It is therefore those studies that examine horizontal OKN in those with IN where whole slow-phase precision is likely to be reported. One study investigating horizontal OKN found that horizontal precision, as measured by the standard deviation of gain. was approximately 2-3 greater than typical controls (Yee et al., 1980). The results of this study reported that, although no results were provided, leftward OKN results were similar to rightward. This agrees with the findings of this study that no horizontal asymmetry was found. Previous studies have reported normal vertical ‘smooth pursuit’ (Collewijn et al., 1985) and normal vertical OKN (Abadi and Dickinson, 1985). Of these studies, one was mostly qualitative (Abadi and Dickinson, 1985), and simply reported mean OKN gain, a measure of accuracy. The other study presented eye movement traces of vertical ‘pursuit’ in IN (Collewijn et al., 1985), but while the eye movements appear to track the target sufficiently (i.e. implied accuracy), the precision of the eye movements cannot be easily gauged. Consequently, there is a lack of knowledge surrounding the precision as those with IN foveate a vertically moving target.

5.2.7.4 *Shape factor*

While the target direction had no significant effect on precision, target direction had a significant effect on shape factor [$F(1.139, 15.948) = 8.279$, $\eta^2 = .372$, $p = .009$], with the shape factor for downward target direction differing significantly from leftward ($p = .044$).

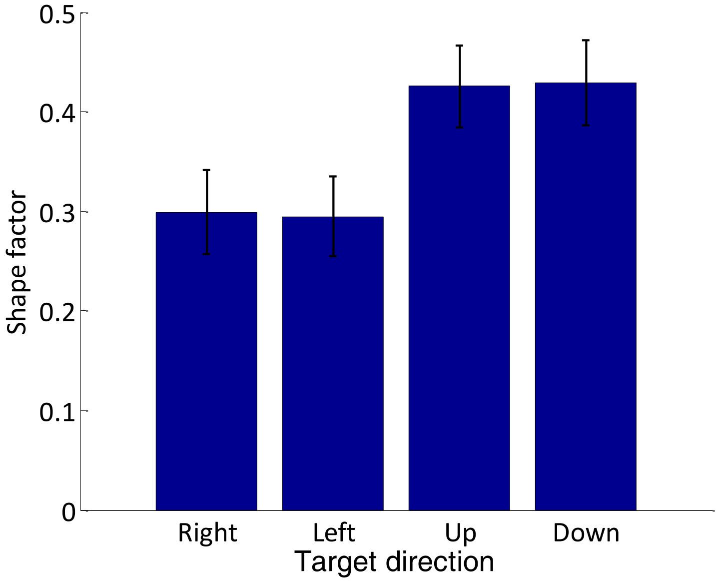

Figure 5.19 Shape factor as a function of target direction. Error bars indicate 95% confidence intervals.

Despite no significant overall change in precision, horizontal target motion produced greater asymmetry between major and minor axes. There were two possible explanations that could account for such an asymmetry:

2. A reduction in precision along the major axis (i.e. more spread of velocities along this axis)
3. An increase in precision along the minor axis (i.e. less spread of velocities along this axis).

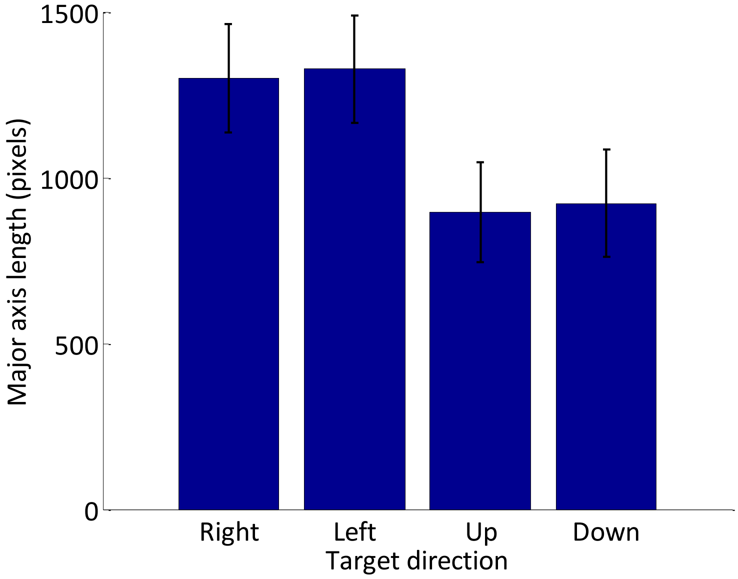

Figure 5.20 Mean major axis lengths for IN participants as a function of target direction. Error bars indicate 95% confidence intervals.

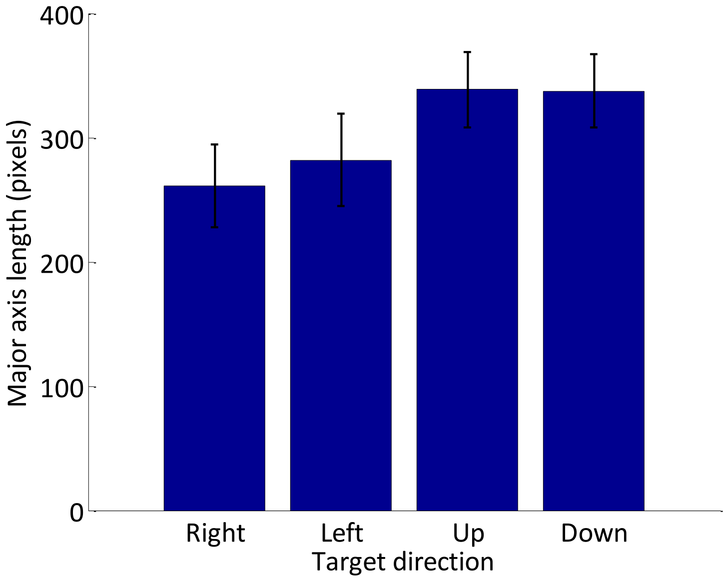

Figure 5.21 Mean minor axis lengths for IN participants as a function of target direction. Error bars indicate 95% confidence intervals.

To determine which of these two possibilities was responsible, the major and minor axes for horizontal and vertical target motion were compared. The asymmetry in major and minor axes for horizontal target motion can be attributed to a substantial reduction in precision along the major axis (i.e. more spread of velocities along this axis) (Figure 5.20), and to a lesser extent, an increase in precision along the minor axis (i.e. less spread of velocities along this axis) (Figure 5.21).

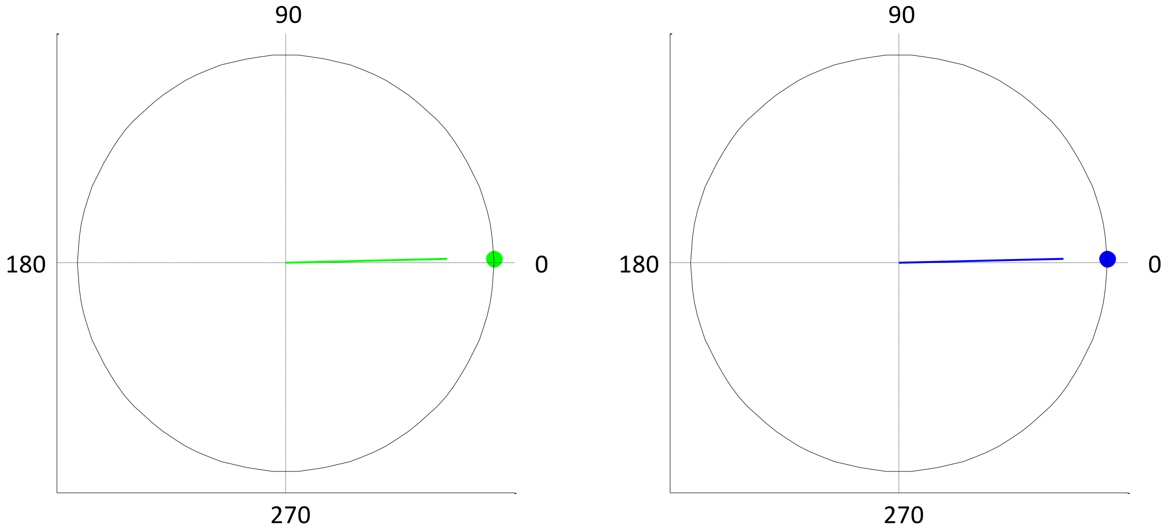

Rightward

Leftward

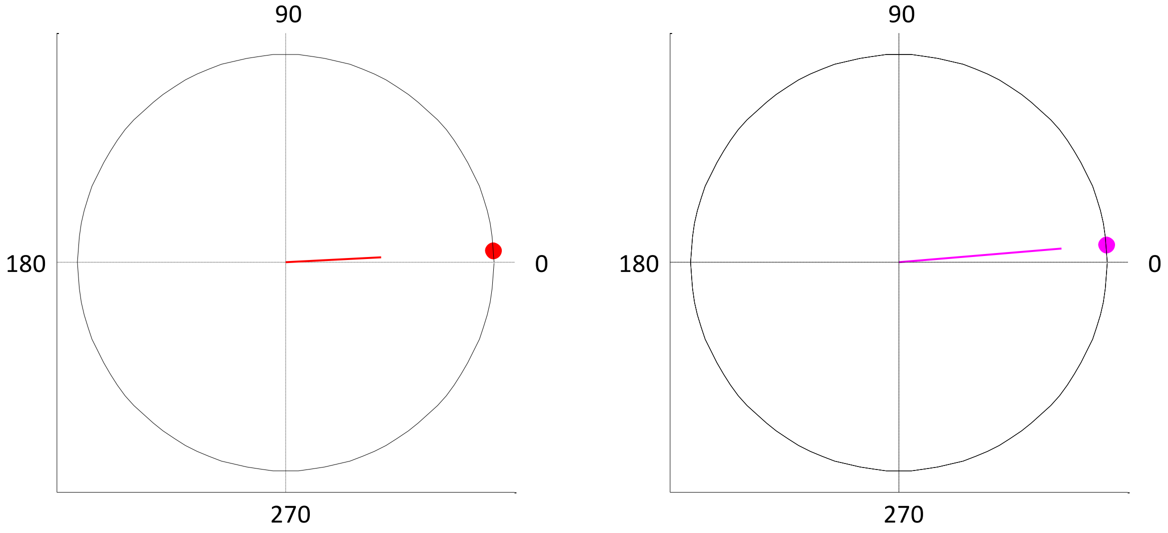

Upward

Downward

Figure 5.22 The mean angle and resultant vector of the 68% isocontour major axis for each direction of target motion.

5.2.7.5 Orientation of major axis

The major axis of the 68% isocontour had a significant mean direction for all target directions (rightwards, Θr = 1.263°, 95% CI ± 3.924, r = 0.777, Rayleigh $z_{72.484}$, $p < .001$; leftwards , Θr = 1.339°, 95% CI ± 3.807, r = 0.793, Rayleigh $z_{75.552}$, $p < .001$; upwards, Θr = 3.476°, 95% CI ± 7.542, r = 0.461, Rayleigh $z_{25.548}$, $p < .001$; downwards, Θr = 4.054°, 95% CI ± 7.556, r = 0.461, Rayleigh $z_{25.463}$, $p < .001$) (Figure 5.22).

On normalising the transformed angular data to 0°, a Kuiper's test for uniformity of data around the circle indicated that all target directions were significantly non-uniform with a $2\Theta r$ of 0° (rightward, $V_{93.172}$, $p < .001$; leftward, $V_{95.113}$, $p < .001$; upwards $V_{54.963}$, $p < .001$; downwards $V_{54.724}$, $p < .001$). Finally, a one sample circular t-test was performed on the transformed data to determine if $2\Theta r$ was significantly different from 0°, which found for all directions $2\Theta r$ was statistically equal to 0° (rightward, $2\Theta r$ = 2.525°, $h = 0$; leftward, $2\Theta r$ = 2.678°, $h = 0$; upward $2\Theta r$ = 6.952°, $h = 0$; downward $2\Theta r$ = 8.109°, $h = 0$).

While IN is described as a predominantly horizontal oscillation (Averbuch-Heller et al., 2002), this presumably relates to the IN waveform when stationary targets are foveated. Whether or not this statement would apply to moving targets, and in all directions of target motion, was unclear. The results show that, unlike typical controls, the major axis for those with IN was always aligned horizontally, irrespective of the direction of target motion. This indicates that, even for moving stimuli, the IN oscillation is predominantly horizontal, with the axis of lowest precision (i.e. greatest spread of velocities) always horizontal.

The major axis lengths are shorter when following vertically moving targets than for horizontally moving targets. This finding reflects the well-documented change in horizontal gaze angle and the intensity of the nystagmus. As eye traverses a number of gaze angles, the distribution of velocities that compose each slow-phase will vary, leading to a corresponding change in precision over time. In addition, any changes in the slow-phase direction occurring during trials will contribute to lower precision because the distribution of eye velocities will have increased because the direction of eye travel will have abruptly changed. When following vertically moving targets, there is no change in horizontal eye-in-orbit position other than that due to the slow-phase. Consequently, the major axis length would be expected to be less when following a vertically moving target than horizontal. Further, the static null zone has been reported to be in the straight ahead position for the majority of individuals with IN (Abadi and Bjerre, 2002). As the target moved through a vertical axis along the straight ahead position, most IN individuals would have been close to their null position and so the horizontal velocity distribution would be either at or close to a minimum.

5.2.7.6 Summary of findings

In this section, the main findings for IN participants were:

1. Eye speed is inaccurate along the direction of target motion, but more accurate in the orthogonal axis, irrespective of target direction
2. Eye speeds are just as low when following vertically moving targets as horizontal targets
3. Eye speed is always more variable along the horizontal direction than the vertical direction, irrespective of the direction of target motion.

5.3 Accuracy and precision as a function of target frequency

Target frequency is not a unique stimulus parameter but the product of both target speed and peak-to-peak amplitude. As a result, it is possible to generate the same target frequency through an almost limitless combination of target speed and peak-to-peak amplitude. For example, a target moving at 16°/s across 16° and 8°/s across 8° both have a target frequency, i.e.1Hz. In typical individuals, it is well documented that the gain of pursuit decreases as a function of target frequency (St-Cyr and Fender, 1969; Fender and Nye, 1961; Bahill et al., 1980; Pola and Wyatt, 1985). However, for individuals with IN, only a single study has investigated the effect of target frequency and concluded that individuals with IN can follow rapidly oscillating targets with better accuracy than typical control participants (Dell'Osso et al., 1972). However, this study was small (n=1), and relied on a qualitative comparison of the phase of the eye movements in those with and without IN. Importantly, the target motion was triangular, and the IN waveform of the single participant was pendular. The cited study, however, did use the entire pendular slow-phase in order to reach their conclusion, rather than restricting the analysis to only the foveation periods. Such a result, if generalizable, would necessitate that the IN pursuit of moving targets be more accurate than typical controls.

This image has been removed by the author for copyright reasons

Figure 5.23 Pendular waveform of an IN subject when viewing a static target (green), and when viewing a target with a triangular waveform target (black). Both waveforms are shown overlaid (black on green), having the same time scale (in seconds) but different amplitude scales. Figure adapted from Dell'Osso et al. (1972).

In contrast, the results presented in the previous section would suggest that those with IN are inaccurate and imprecise when compared to controls. Nonetheless, in this section, I will formally investigate the effect of target frequency on the ability to follow a moving target.

5.3.1 Methods and analysis

Eye movement data for all participants were re-analysed in terms of target frequency, calculated as target speed divided by peak-to-peak amplitude. This analysis was performed on three target frequencies that were common to each target speed: 0.5, 1.0 and 2.0 Hz. A repeated measures, 4 (direction) x 2 (velocity) x 3 (peak-to-peak amplitude), analysis was performed in SPSS. All significant main effects were followed up with a pairwise comparison with Bonferroni adjustment for multiple comparisons. On those occasions where the assumption of sphericity was violated, Greenhouse-Geisser correction was applied.

5.3.2 Results: between control participants and INs

For both accuracy and precision as a function of target frequency, a between-groups comparison of control and INs indicated a significant effect for group [accuracy $F(1,28)= 29.55$, $p< .001$, precision [$F(1,28)= 22.06$, $p< .001$].

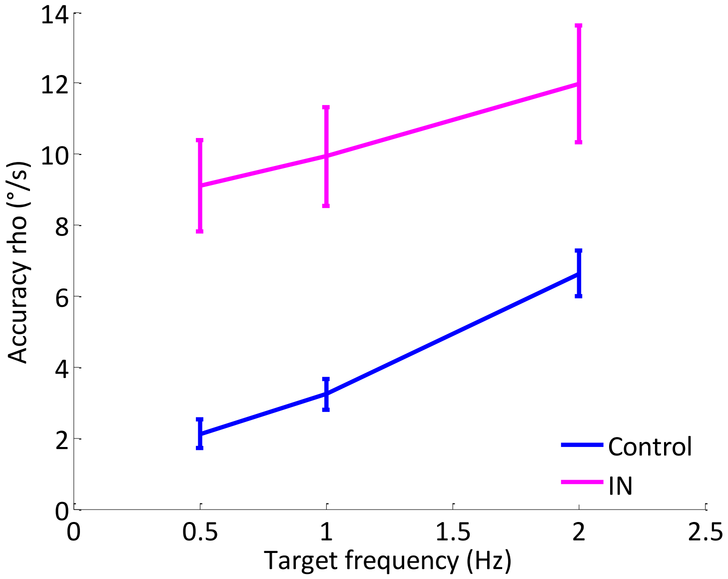

Figure 5.24 Between-subjects comparison of accuracy rho as a function of target frequency. Error bars indicate 95% confidence intervals.

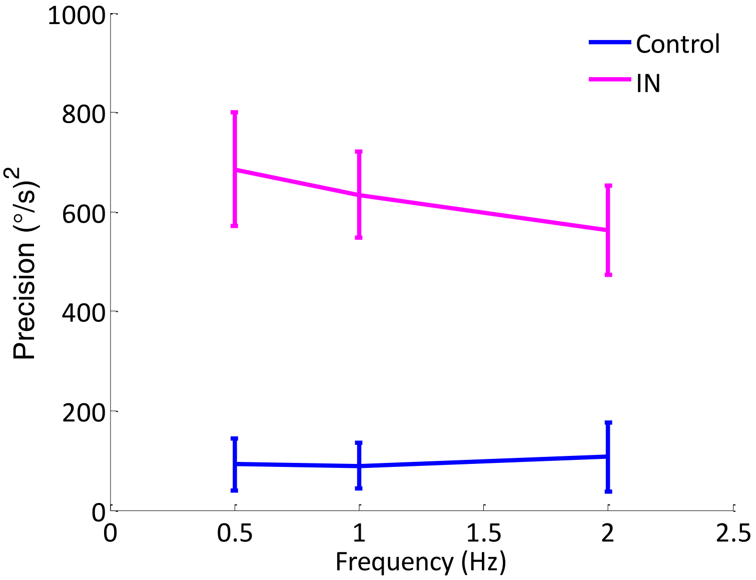

Figure 5.25 Between-subjects comparison of precision as a function of target frequency. Error bars indicate 95% confidence intervals.

The results of this analysis indicate that pooling across the different frequencies, those with IN are always of lower accuracy and precision than typical controls. It can be concluded that those with IN are less able to accuracy foveate more rapidly oscillating targets than typical controls, so disagreeing with the suggestion of previous research (Dell'Osso et al., 1972). A more likely alternative would be that, since the sole participant in the study had pendular waveform IN, rather than actually attempting to pursue the oscillating target, the phase of the pendular slow-phase simply equalled that of the target. Indeed, the frequency of the pendular 'smooth pursuit' was equal to the frequency of the pendular IN 'fixation' (Figure 5.23), suggesting that the participant may have been passively viewing the oscillating stimulus rather than actively following it. In the following sections, the effect of target frequency will be considered within groups.

5.3.3 Results: within control participants

Target frequency had a significant effect on accuracy [$F(1.412,19.771) = 196.337$, $\eta^2 = .933$, $p < .001$], with the accuracy decreasing as target frequency increased (Figure 5.26).

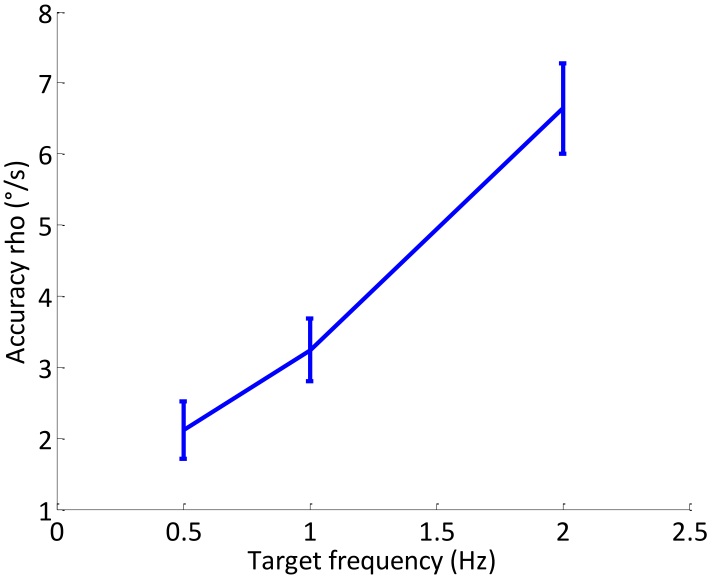

Figure 5.26 Effect of target frequency on accuracy rho. Error bars indicate 95% confidence intervals.

Follow-up pairwise comparisons found that all three frequencies differed significantly from each other (p < .001, respectively). This result confirms the previous reports that the accuracy decreases as target frequency increases (Fender and Nye, 1961; Pola and Wyatt, 1985; St-Cyr and Fender, 1969). Additionally, there was a significant speed and frequency interaction [$F(1.878,26.29) = 57.93$, $\eta^2 = .805$, $p < .001$], indicating that the accuracy across different target frequencies was significantly different for each target speed, with higher speeds having lower accuracy at any given frequency (Figure 5.27).

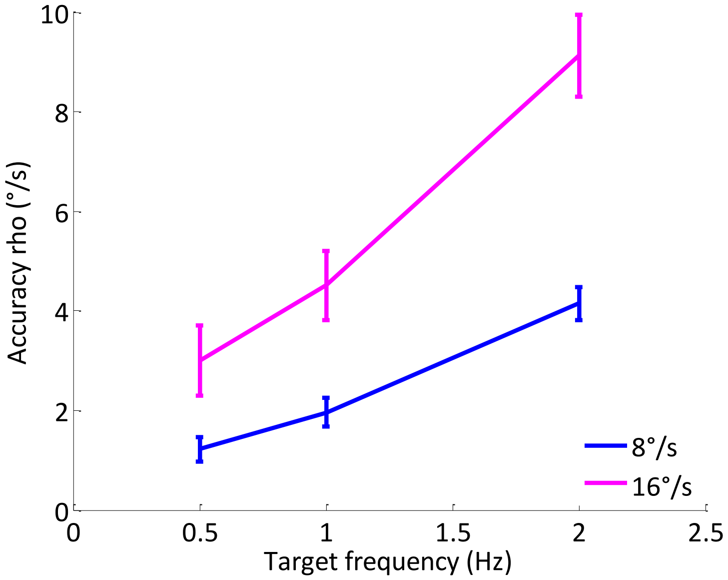

Figure 5.27 Effect of target frequency on accuracy rho with separated plots based on target speed. Error bars indicate 95% confidence intervals.

Comparing the target speeds, the performance gap widens with an increase in target frequency. As was mentioned previously, target frequency depends on both the target peak-to-peak amplitude as well as target speed. To the best of my knowledge, no previous study has investigated how manipulating the variables that give rise to a particular frequency influence smooth pursuit performance in typical controls. The interaction between target frequency and target speed was further explored by examining the decline in accuracy for each target speed, relative to 0.5Hz (Figure 5.28). Despite an increase in target speed, there appears to be a robust and consistent relationship between frequency and accuracy. However, this study only tested a limited number of target speeds to determine whether or not this relationship holds for target speeds that were faster or slower than those tested.

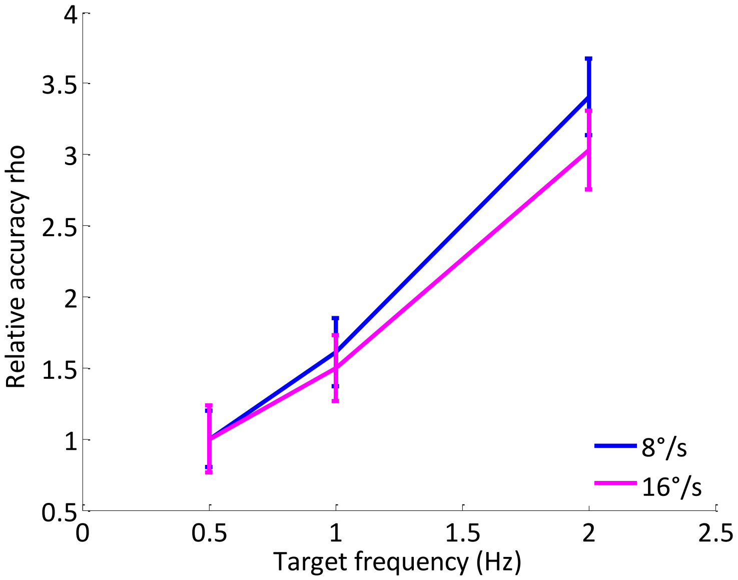

Figure 5.28 The relationship between target frequency and relative accuracy rho. Error bars indicate 95% confidence intervals.

There was no significant interaction of direction and frequency with accuracy [*F*(3.703,51.84) = 1.37, η^2 = .089, *p* =.236]. No significant effect was found for precision as a function of frequency [*F*(1.387,19.413) = 1.677, η^2 = .107, *p* =.205].

5.3.3.1 Summary of findings

In this section, the main findings for control participants were:

1. Accuracy decreases as a function of target frequency.
2. For any given frequency, greater target speed resulted in lower accuracy.
3. Normalising the results for each target velocity to 0.5Hz revealed a consistent relationship between frequency and accuracy, albeit for a limited number of target speeds.
4. Target frequency had no effect on precision.

5.3.4 Results: within IN participants

Target frequency had a significant effect on accuracy [*F*(1.245,17.433) = 6.742, η^2 = .325, *p* = .014], with accuracy decreasing with higher frequency target motion (Figure 5.29). Follow-up pairwise comparisons showed that a frequency of 2Hz was significantly different from 1Hz (*p* = .037) and 0.5Hz (*p* < .001). As mentioned previously, these results are in disagreement the suggestions presented in previous research (Dell'Osso et al., 1972). The most probable explanation for the differences between previous results and mine, as discussed, is due to the participants of this study having jerk waveforms rather than pendular waveforms. The slow phase is involuntary and can only be interrupted by a fast-phase. However, the fast phase must be programmed before being executed. Being saccades, fast-phases will have a latency period. During this period, if the intended target changes course, presumably the fast phase will be made to the predicted target position rather than being modified to compensate for the targets new position. Therefore the eye will not be directed toward the target as planned, but away from the target. The more rapid the oscillation becomes, the more likely that there will be a target reversal during the slow phase. In this manner, we would expect the accuracy to diminish as target frequency increases. Since the typical IN frequency is 3-4Hz, this will place a limit on the number of corrective fast-phases that can be made. Consequently performance is expected to decrease considerably as the frequency of the target oscillation increases beyond the frequency of the IN.

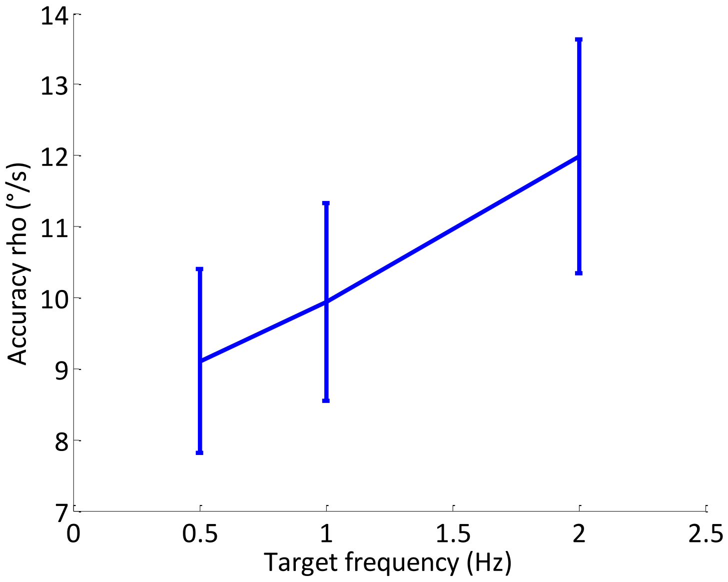

Figure 5.29 Effect of target frequency on accuracy rho. Error bars indicate 95% confidence intervals.

Additionally, there was a significant speed x frequency interaction for accuracy [*F*(1.604, 22.459) = 8.50, η^2 = .378, *p* = .001] (Figure 5.30).

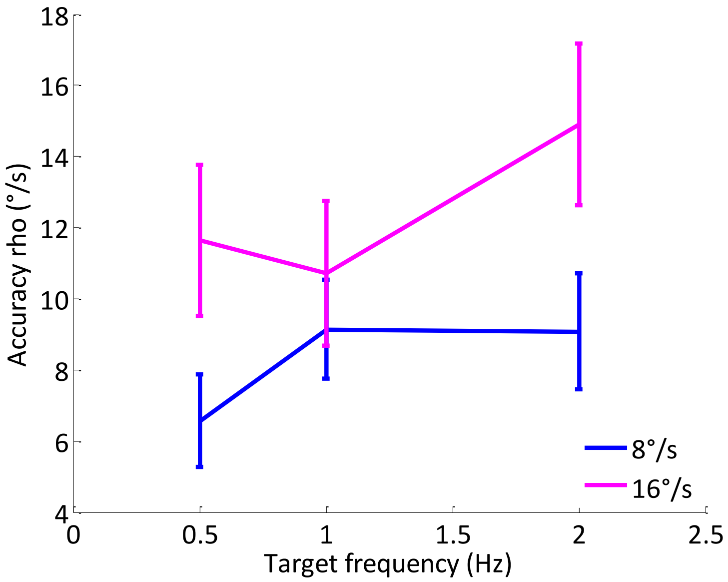

Figure 5.30 The relationship between target frequency and normalised accuracy rho. Error bars indicate 95% confidence intervals.

For the 8°/s target, as frequency is increasing, the peak-to-peak amplitude of the pursuit target decreases from 16° to 4°. With the reduction in peak-to-peak amplitude, accuracy begins to decrease until 8°. Thereafter, there is no reduction in accuracy. This may be perhaps because a peak-to-peak amplitude of 4° was smaller than the IN oscillation itself and so accuracy could not decrease any further. For the 16°/s target, as frequency increases, those with IN maintain the same level of accuracy until a peak-to peak-amplitude of 8° where accuracy decreases. However, it is difficult to account for why accuracy has decreased at this particular frequency. For each individual, the accuracy for each velocity was normalised to 0.5Hz (Figure 5.31), however, unlike typical individuals, no consistent relationship was found between target frequency and accuracy with target speed. There was no significant interaction between direction and frequency with accuracy [$F(2.70,37.81) = .869$, $\eta^2 = .058$, $p = .521$]. There was a significant effect for precision as a function of frequency [$F(1.77,24.80) = 4.30$, $\eta^2 = .235$, $p = .029$], with the highest frequency differing significantly from the lowest frequency ($p = 0.29$) (Figure 5.32).

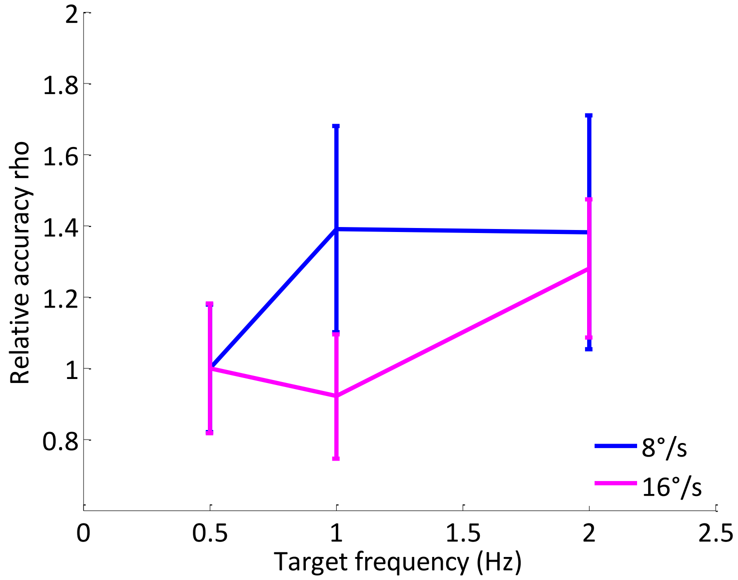

Figure 5.31 The relationship between target frequency and normalised accuracy rho. Error bars indicate 95% confidence intervals.

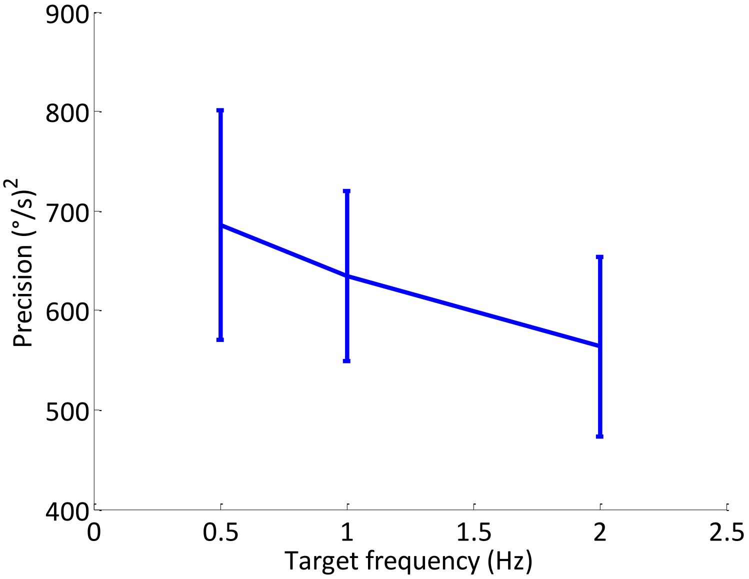

Figure 5.32 The effect of target frequency on precision. Error bars indicate 95% confidence intervals.

This relationship is particularly interesting because it is an inverse relationship, suggesting that, as the target frequency increases, individuals with IN are more precise. However, these results in the context of accuracy would suggest that, because those with IN were inaccurate at higher target frequencies, they were less able to follow the target. If they were less able to follow the target, they would not have moved their eyes through as many horizontal eye-in-orbit positions when following horizontally oscillating targets. Therefore the reduction in accuracy is associated with a reduction in precision. No significant interaction was found for speed and frequency with precision [$F(1.38,19.35) = 2.124$, $\eta^2 = .132$, $p = .138$], or for direction and frequency with precision [$F(1.57,22.01) = 1.20$, $\eta^2 = .079$, $p = .309$].

5.3.4.1 Summary of findings

In this section, the main findings for IN participants were:

1. Accuracy decreases as a function of target frequency
2. For any given frequency, greater target speed resulted in lower accuracy
3. Normalising the relationship revealed a complex relationship between target speed, target frequency and accuracy.
4. Precision improved for higher target frequencies, but this improvement is associated with lower accuracy, suggesting that it was due to the target was poorly followed.

5.4 Slow-phase direction when foveating a moving target

A recent review of IN suggested that the slow phases of IN are opposite to the direction of target motion:

"[IN] also shows an apparent reversed optokinetic nystagmus (OKN) response and inverted pursuit; that is, the fast phases of OKN beat in the same direction as the OKN stimulus, and smooth pursuit movements appear to be initiated in a direction opposite to the actual target movement" (Richards and Wong, 2015) (see Figure 5.33).

This image has been removed by the author for copyright reasons

Figure 5.33 Recent IN literature suggests that the slow-phase is always opposite to the direction of target motion. Figure taken from Richards and Wong (2015).

In this section, eye movement recordings were re-analysed to determine the proportion of slow-phases in the same or opposite direction with respect to target motion.

5.4.1 Method

Only the horizontal component of eye velocity was used in this analysis. By taking the sign of each velocity sample of a given slow-phase, the direction of the slow-phase could be determined. If more than 50% of the slow phase was had a positive velocity with respect to the target motion, it was designated as moving in the ‘same’ direction as the target, otherwise it was designated as moving ‘opposite’ to the target. This analysis was only performed on the combinations of peak-to-peak amplitude and velocity that gave the lowest target frequency (i.e. 32° and 8°/s) so that there would be an adequate number of whole slow phases per sweep for analysis.

5.4.2 Results

The percentage of slow-phases moving in the same and opposite directions with respect to the direction of target motion are summarized and presented in Table 5.1. The results of this experiment strongly disagree with the statement that the slow-phase is always opposite to the direction of target motion. Additional qualitative evidence for this conclusion is presented in Figure 5.34.

	Rightward target motion		Leftward target motion	
Participant	**Same (%)**	**Opposite (%)**	**Same (%)**	**Opposite (%)**
JS	100	0	0	100
MT	94	6	73	27
JC	51	49	19	81
LB	66	34	21	79
VW	50	50	76	24
RW	45	55	85	15
CT	100	0	60	40
SM	93	7	36	64
DB	53	47	94	6
DC	63	37	15	85
DP	100	0	69	31
JT2	82	18	92	8
NB	55	45	66	34
MB	33	67	55	45
JM	57	43	69	31

Table 5.1 Slow-phase direction with respect to the direction of target motion. From this table it is apparent that the slow-phase does not always move opposite with respect to the direction of target motion.

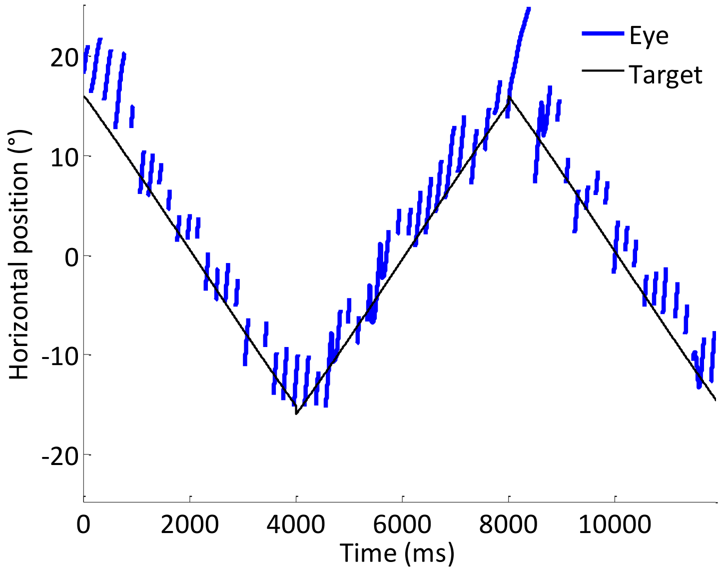

Figure 5.34 Position-time plot of IN eye movements (participant JS) on following a target moving with 8°/s and a peak-to-peak amplitude of 32°. The slow phase direction is opposite for leftward target motion, but the same for rightward target motion.

In Figure 5.34, as the target moves leftward (i.e. downwards on the position-time plot), the slow-phase direction is rightwards (i.e. upwards on the position-time plot), which would agree with the cited literature (i.e. slow phase is in the opposite direction). However, as the target moves rightwards, the slow-phase direction is also rightwards, which would disagree with the cited literature (i.e. slow phase is in the same direction). In other words, while it is possible for the slow-phase to move opposite with respect to the direction of target motion, this is not a universal finding. Previous reports on the 'clinical characteristics' of IN have suggested that those with IN *can* have inverted pursuit (i.e. the slow-phase is opposite to the direction of the target motion) (Gresty et al., 1984). However, at some point since this statement has presumably been misinterpreted as those with IN *must* have inverted pursuit. Perhaps, such confusion concerning IN eye movements has arisen from the use of only secondary sources (i.e. clinical texts) as evidence for the inversion of 'pursuit' (Richards and Wong, 2015).

Studies have reported that the gaze angle of the null zone identified during fixation does not correspond to that observed during pursuit (see Section 5.2). The direction of the slow phase is reported to depend on the null zone location, with the slow phase being leftward at gaze angles to the right of the null zone and vice versa. In other words, the slow-phase direction does not depend on the target direction per se but gaze angle of the shifted null zone. Unfortunately, due to the limited horizontal range of recorded eye movements in this study (0±16° horizontally), the null zones during pursuit were not discernible in the eye movement data (for example, see Figure 5.34).

5.5 Conclusions

In this chapter, pursuit accuracy and precision was investigated along different directions for those with and without IN. The reasons for this were three-fold. First, previous studies had limited their analyses to the same direction as the target motion. Consequently, pursuit in those with IN had not been adequately characterised, particularly for targets moving vertically. Second, the results of one study suggested that those with IN can follow rapidly oscillating targets better than typical individuals.

Third, the Filehne illusion is a pursuit based illusion, and so pursuit performance may offer insights on the results of perceptual judgements made during this task. Each of these reasons will be considered in turn.

In characterising pursuit along different directions, results indicate that, for those with and without IN, the most probable eye velocities were always lower than that of the target irrespective of the pursuit direction. In addition, contrary to previous research, the results suggest that that those with IN are inaccurate when tracking vertically moving targets. Eye speed of those with IN is always more variable along the horizontal axis than the vertical axis, irrespective of the direction of target motion reflecting the underlying horizontal oscillation.

Target velocities and peak-to-peak amplitudes can be combined to describe targets by their frequency of oscillation. In characterising the pursuit targets of different frequencies, results have dismissed claims that those with IN are able to follow more rapidly oscillating targets with a higher accuracy than typical individuals. Indeed, the opposite was found, that accuracy for those with IN diminished as frequency increased.

With respect to the Filehne illusion, one of the main findings of this study was that those with IN have lower precision pursuit compared to typical individuals. A number of studies have suggested that lower pursuit precision is associated with poorer motion discrimination thresholds (Rasche and Gegenfurtner, 2009; Kowler and McKee, 1987). However, this association is concerned with the early portion of smooth pursuit, i.e. when the eye is accelerating to reach the target velocity but before steady-state pursuit is reached. In the study by Rasche and Gegenfurtner (2009), the results suggested that, beyond 450ms of the onset of pursuit, psychophysical variability exceeds pursuit variability. However, the Filehne illusion experiment was designed so as to take place during steady-state smooth pursuit. It could be speculated that the lower precision of IN pursuit might impact on the Filehne illusion, although to what extent is uncertain. The linear transducer model proposed by Freeman and Banks (1998) suggests that, as eye speed increases, so too does the extra-retinal signal. However, such variability in the magnitude of the extra-retinal signal may cause motion judgements to be less precise in those with IN rather than in typical individuals. This is because experimental work in this chapter indicated that typical controls tended to under pursue the target. Therefore, any increase or decrease in eye speed (i.e. extra-retinal signal) will be offset by a corresponding reduction or increase in retinal image motion (i.e. retinal signal). When two signals are combined, the net effect of any imprecision is likely to be cancelled and perceived head-centric speed relatively unaffected.

However, for those with IN, even though the most probable eye velocity was less than the target, the precision was drastically less than for typical individuals. Therefore it is likely that the eye velocity would exceed the target. Under this circumstance, increases or decreases in eye velocity (i.e. extra retinal signal) will increase or decrease retinal image motion (i.e. retinal signal). Consequently, when the two signals are combined, the net effect of any imprecision is unlikely to be cancelled but may make those with IN less precise at estimating perceived head centric speed (i.e. both extra-retinal and retinal signals are noisier). An alternative view could be that the internal noise associated with each of the signals differs, with the noise associated with the extra-retinal signals being greater than the retinal. If the level of noise associated with extra-retinal signal varies with its magnitude, then when the two signals are combined, and perceived head centric speeds would then be less precise. However, these mechanisms are purely speculative, and although the Filehne illusion will be measured in a following chapter, the results will still be unable to determine which of the mechanisms are responsible if indeed perceived head-centric speed judgements are less precise in those with IN when compared to typical controls.

6 Comparison of the oculomotor performance of fixation and pursuit in those with and without IN

6.1 Introduction

It has been discussed in Chapter 3 that fixation and pursuit share the same functional goal of imaging intended targets either continuously on, or suitably close to, the fovea. For either type of eye movement, the velocity of the eye must match, as much as possible, the velocity of the target. However, the difference between the two eye movement conditions is that during fixation the target is stationary, whereas during pursuit the target is moving.

It is because of the functional similarity (gaze-holding), but the contrasting kinematics (i.e. eye velocity), that many studies investigating perceived head-centric speed perception in typical individuals have compared visual perception under the two conditions (Freeman et al., 2010; O'Connor et al., 2010; Freeman et al., 2003; Freeman et al., 2002). When typical individuals fixate, there is a lack of any large deliberate eye movement. Consequently, extra-retinal signals can be assumed to be negligible, and the major component of perceived head-centric speed is the retinal signal. In contrast, during pursuit the extra-retinal signals cannot be assumed to be negligible and so both retinal and extra-retinal signals will be required to estimate head-centric speed.

Despite the assumption that the eye is stationary during fixation, there are known fixational eye movements (e.g. drift, tremor and microsaccades) that, although small in amplitude, occur spontaneously and continuously (Martinez-Conde et al., 2004; Yarbus, 1967; Rucci et al., 2007; Pritchard, 1961). Such fixational eye movements ensure the eyes are never truly stationary, but in incessant motion. The data presented in Chapter 5 indicated that pursuit is neither perfectly accurate nor precise. Therefore, it would be of interest to similarly quantify fixation and compare the oculomotor performance of these two eye movements. Presumably, the lack of a common method of quantifying these two eye movements has prevented their direct comparison. A generalised oculomotor performance measure for both kinds of gaze holding eye movements (i.e. fixation and pursuit) was developed in Chapter 3. In this chapter, the oculomotor performance of fixation and pursuit along horizontal and vertical directions will be compared in those with IN and in typical control participants.

6.2 Methods

Experimental work relating to fixation (Chapter 4) and pursuit (Chapter 5) were re-analysed for this chapter. Only those participants that took part in *both* experiments were included in this analysis, giving 15 individuals with IN (8 male, 7 female; mean 44.2 ± 14.3 years) and 15 typical individuals (8 male, 7 female; mean 29.3 ± 8.1 years) as a control group. The fixation target was a randomly presented 0.4° dot presented between -16° and +16°, along either the horizontal or vertical direction, with each fixation direction run as a separate experiment. In order that a comparison could be made with pursuit data, pursuit trials through the same gaze angles (i.e. -16° to +16°) were used. A pursuit target of 8°/s was chosen on the basis of those results for typical individuals presented in Chapter 5, where results demonstrated 8°/s targets were more accurately and more precisely followed than a 16°/s target through the same range of gaze angles. It was decided that this lower velocity would enable fixation to be compared against high performance pursuit, yielding a conservative estimate of any differences between the two types of eye movement. Since the data in Chapter 5 indicated no horizontal (i.e. left-right) or vertical (i.e.) up-down asymmetries, horizontal fixation data were arbitrarily compared against rightwards pursuit and vertical fixation data against upwards pursuit.

The gaze angle shift of the null zone during pursuit has already been discussed in Chapter 5. However, as a reminder, its importance for this chapter will be reviewed. It has been reported that the gaze angle of the null zone during pursuit does not correspond to the gaze angle of the null during fixation. The null gaze angle of the null zone undergoes a shift during pursuit. The direction of the shift has been reported to depend not only on the on the speed of the attempted pursuit, i.e. a shifting further on faster pursuit, but also on the pursuit direction by shifting in the opposite direction to attempted pursuit (Kurzan and Buttner, 1989). While the reports of the shift in the location of the null zone have been limited, a potential shift in the gaze angle of the null zone location would be expected to impact on a comparison of the accuracy and precision of fixation and pursuit in those with IN. For example, because the null shifts in the opposite direction to the attempted pursuit, a null zone located in the straight ahead position during *fixation* may be shifted to an eccentric left gaze angle during rightwards *pursuit* and vice versa. It has been reported that the shift can be as much as 25° for a target of 15°/s (Kurzan and Buttner, 1989). Indeed, a shift of 25° would place the null zone at a gaze angle (i.e. -25°) beyond those examined in experiment (i.e. -16°) and so will be unlikely to be detected on eye movement recordings. Since the null zone corresponds to the minimum IN oscillation, such a shift in the null zone may give a false impression that the IN oscillation is of smaller magnitude during fixation (i.e. more accurate, more precise) than for pursuit (i.e. less accurate, less precise).

However, contrary to previous studies investigating the null zone during fixation (Abadi and Whittle, 1991; Dell'Osso and Flynn, 1979; Dell'Osso et al., 1974), the data from Chapter 4 indicated that null zones during fixation are not consistent either within an individual or on average within a group. For this reason, the data relating to fixation at different gaze angles along a given direction was collapsed so that a single representative PDF for fixation could be generated for each individual. Separate PDFs were generated for the horizontal and vertical directions. For each group, the mean PDF accuracy and precision of fixation and pursuit was calculated for each direction. To compare oculomotor performance between fixation and pursuit within individuals, paired sample t-tests were used, however repeated measures analyses were used to compare between individuals.

6.3 Results: control participants

Representative PDF results for typical individuals for fixation are presented in Figure 6.1, and for pursuit in Figure 6.2. So that PDFs of typical individuals can be visually compared with those of INs (Figure 6.5 and Figure 6.6), the same scale has been used on all plots. The mean PDF accuracy and precision for fixation and pursuit in control participants along horizontal and vertical directions are shown in Figure 6.3 (a) and (b).

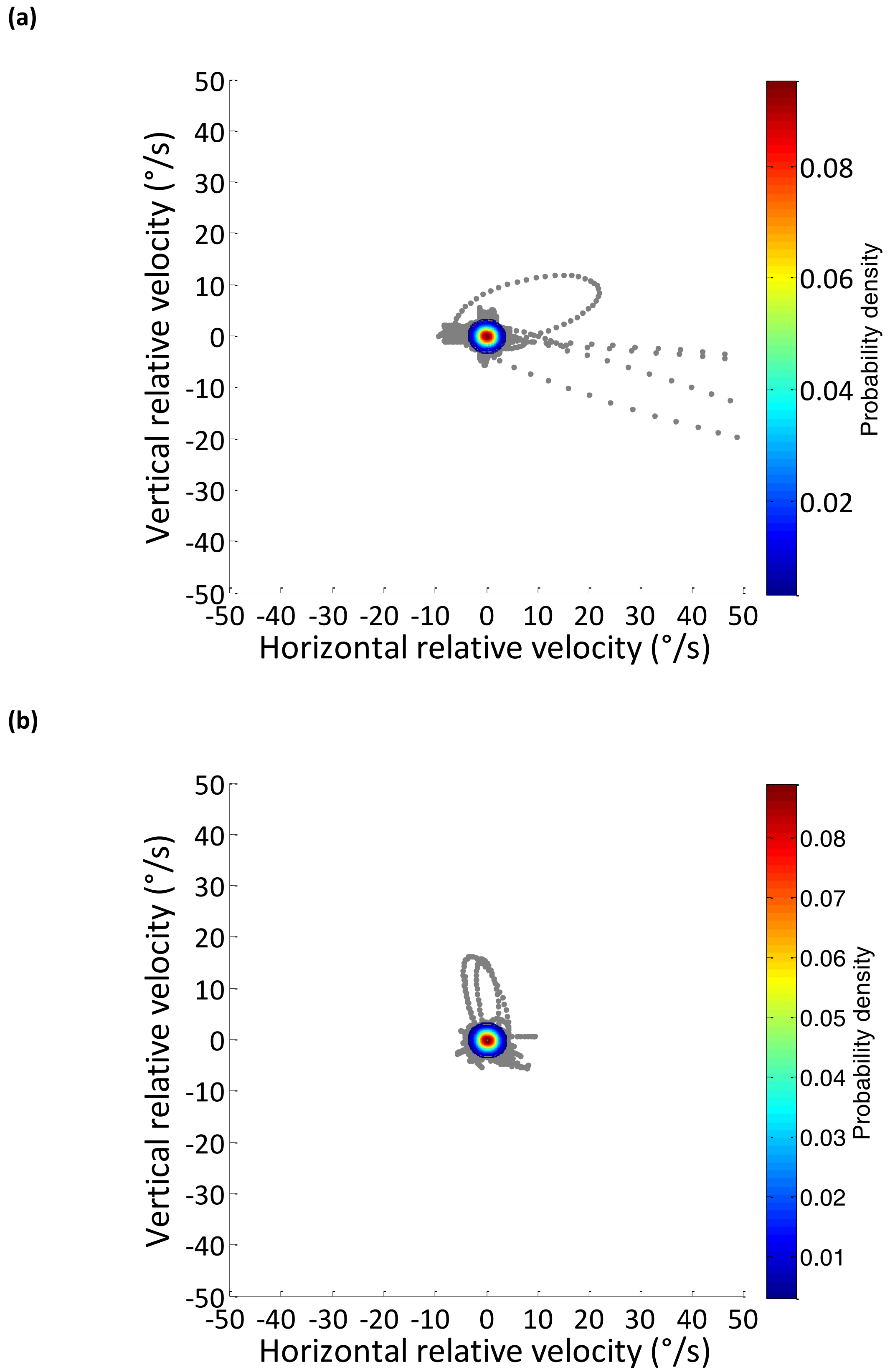

Figure 6.1 Representative probability density functions for fixation along (a) horizontal (accuracy 0.11°/s, precision 11.67 $(°/s)^2$) and (b) vertical (accuracy 0.10°/s, precision 29.70 $(°/s)^2$) direction for a typical individual (LM).

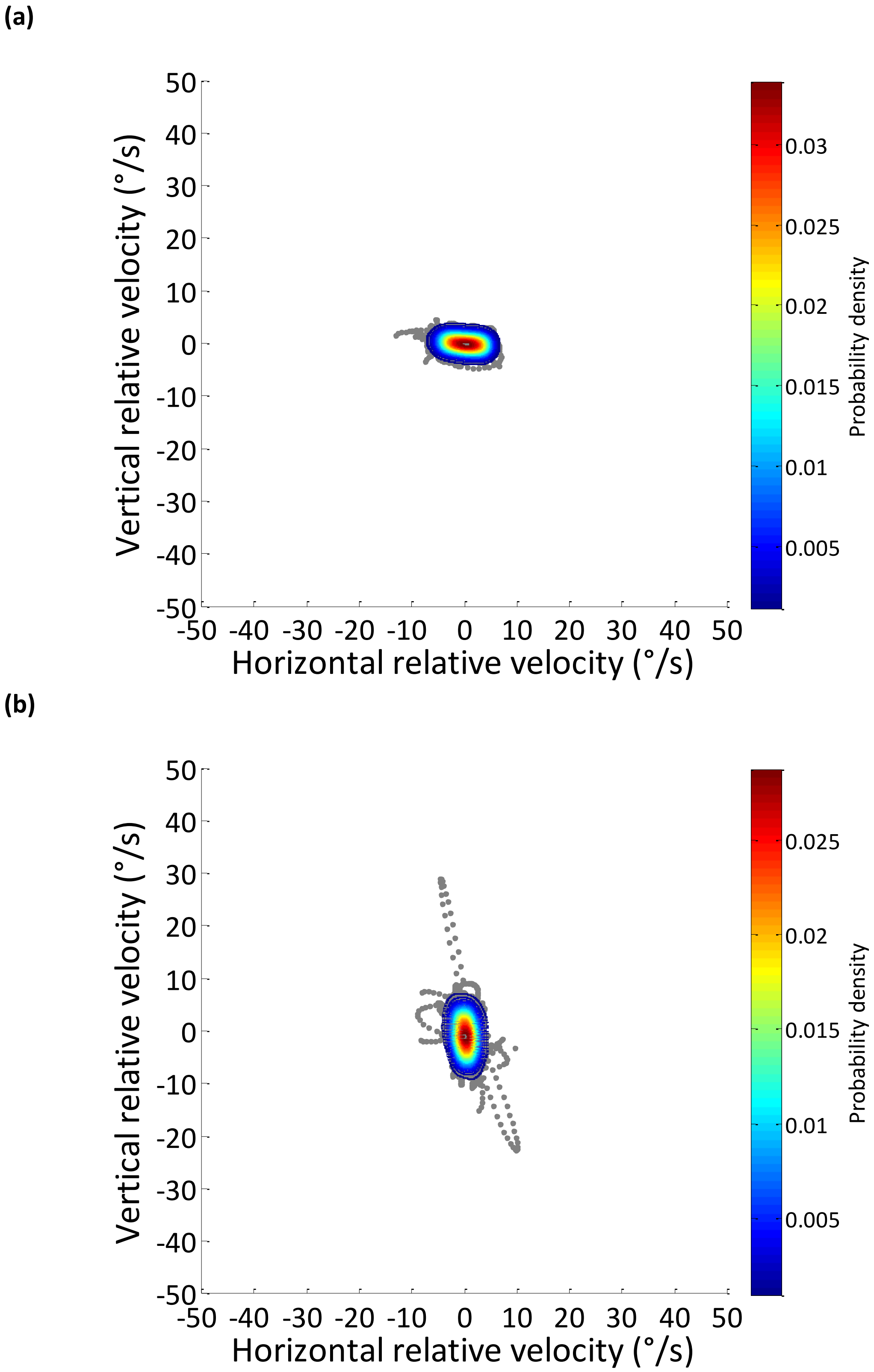

Figure 6.2 Representative probability density functions for pursuit during (a) horizontal rightward motion (accuracy 0.08°/s, precision 29.78 (°/s)^2) and (b) vertical upward motion (accuracy 0.88°/s, precision 37.52 (°/s)^2) for a typical individual (SLL).

There was a significant difference in PDF accuracy between fixation and pursuit along the horizontal [*t*(14)= -5.65, *p*< .001] and vertical [*t*(14)= -7.11, *p*< .001] direction, with pursuit being always less accurate than fixation.

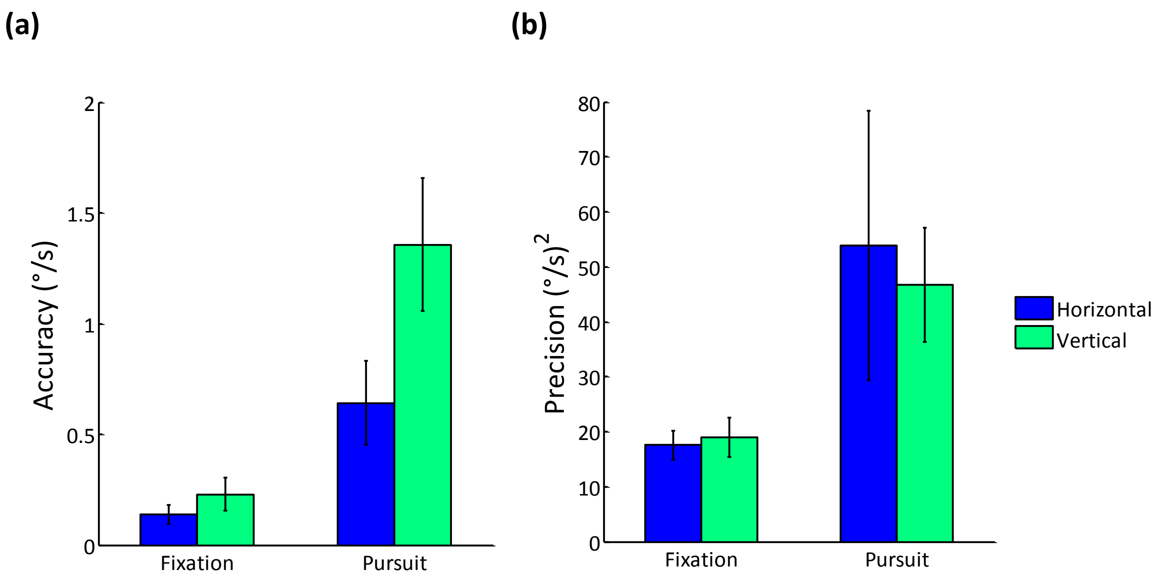

Figure 6.3 Comparisons of (a) mean PDF accuracy and (b) mean PDF precision during conditions of fixation and pursuit for typical control participants. Error bars indicate the 95% confidence intervals.

Similarly, there was a statistical difference in the PDF precision between fixation and pursuit along the horizontal [*t*(14)= -3.14, *p*= .007], and the vertical [*t*(14)= -7.05, *p*< .001] direction, again with pursuit always being less precise than fixation.

The accuracy of fixation along the horizontal direction was compared with the vertical, indicating a significant difference [*t*(14)= -3.28, *p*= .006], with fixation along the horizontal being more accurate than along the vertical, indicating an anisotropy. No significant difference was found for precision, with the precision of fixation along the horizontal direction being just as precise as fixation along the vertical.

Similarly, the accuracy of pursuit along the horizontal direction was compared with the vertical, indicating a significant difference [*t*(14)= -4.49, *p*< .001], with pursuit along the horizontal being more accurate than along the vertical, indicating an anisotropy. No significant difference was found for precision, with the precision of pursuit along the horizontal being just as precise as fixation along the vertical.

An accuracy of zero would indicate that the most probable eye velocity matched that of the target, whether or not the target was stationary (i.e. fixation) or moving (i.e. pursuit). Therefore, to investigate gaze holding, a t-test was performed to determine whether the accuracy values were significantly different from zero. The accuracy of fixation was significantly different from zero along the horizontal [$t(14)= 6.33$, $p< .001$] and vertical [$t(14)= 6.18$, $p< .001$], suggesting that gaze holding is not perfect during fixation. Similarly, the accuracy of pursuit was significantly different from zero along the horizontal [$t(14)= 6.67$, $p< .001$] and vertical [$t(14)= 8.83$, $p< .001$], suggesting that gaze holding is not perfect during pursuit.

6.4 Results: IN participants

The mean PDF accuracy and precision for fixation (Figure 6.5) and pursuit (Figure 6.6) in those with IN participants along horizontal and vertical directions are shown. There were no significant differences in PDF accuracy or precision when fixation and pursuit were compared along the horizontal or vertical directions. This suggests that fixation is just as accurate and precise as pursuit, irrespective of the direction considered. Further comparisons indicate no significant differences in the accuracy or precision of fixation when fixation along the horizontal is compared with fixation along the vertical.

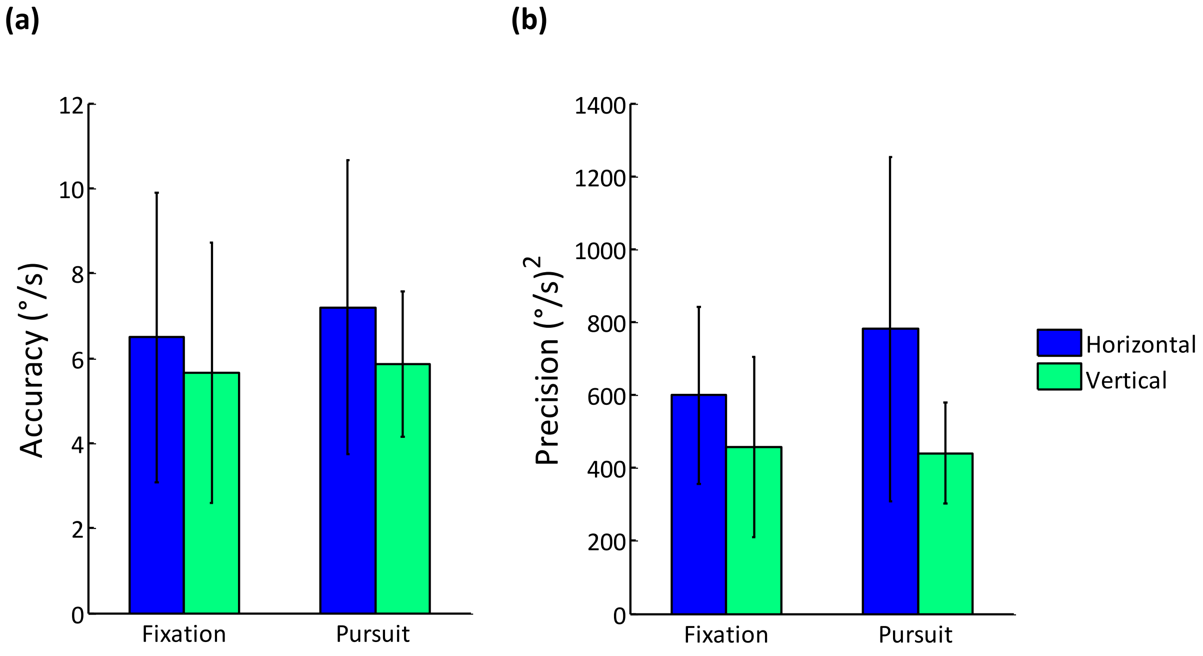

Figure 6.4 Comparisons of (a) mean PDF accuracy and (b) mean PDF precision during conditions of fixation and pursuit for participants with IN. Error bars indicate the 95% confidence intervals.

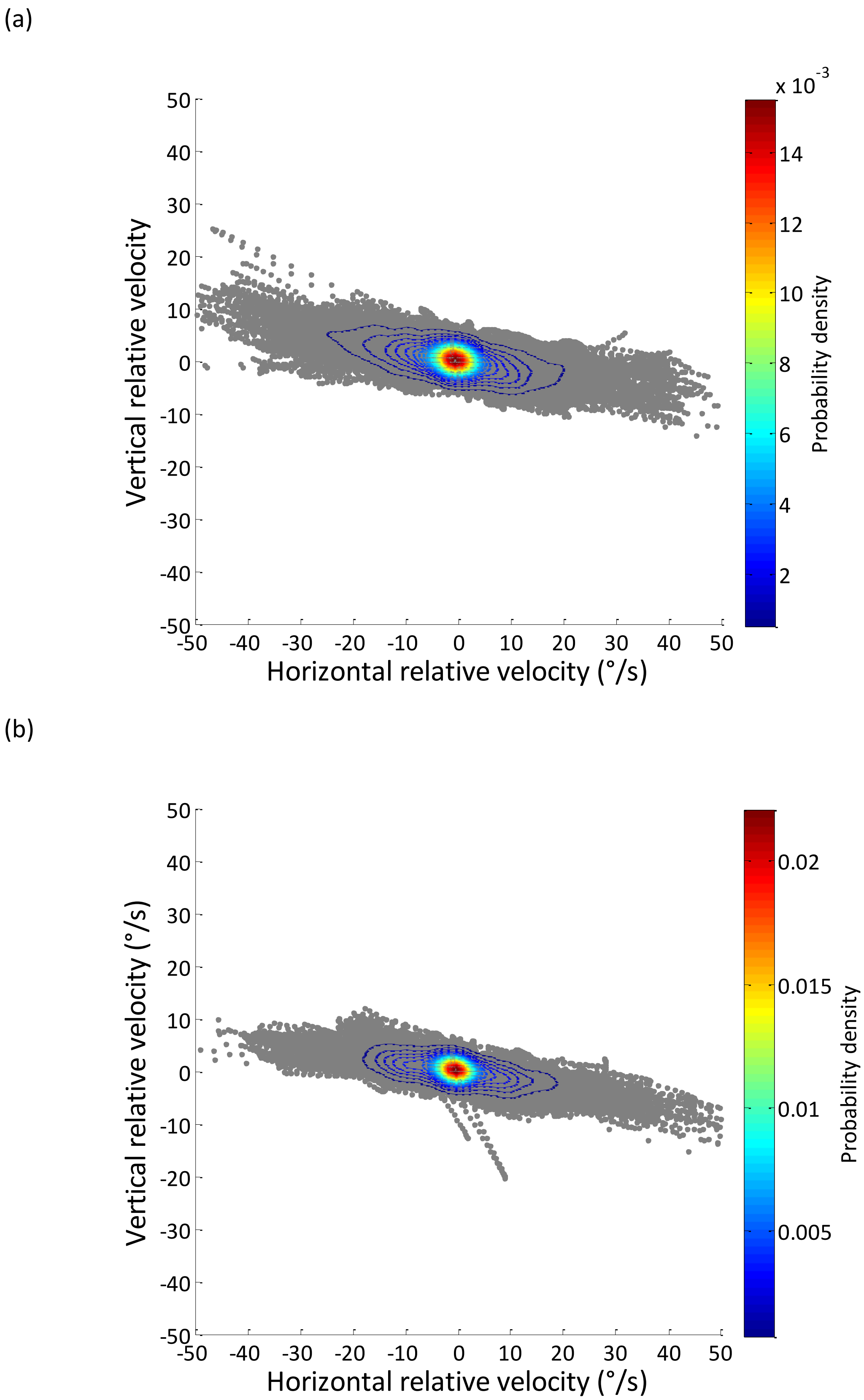

Figure 6.5 Representative probability density functions for fixation along (a) horizontal (accuracy 1.15°/s, precision 134.80 $(°/s)^2$) and (b) vertical (accuracy 1.28°/s, precision 96.43 $(°/s)^2$) directions for an individual with IN (JC).

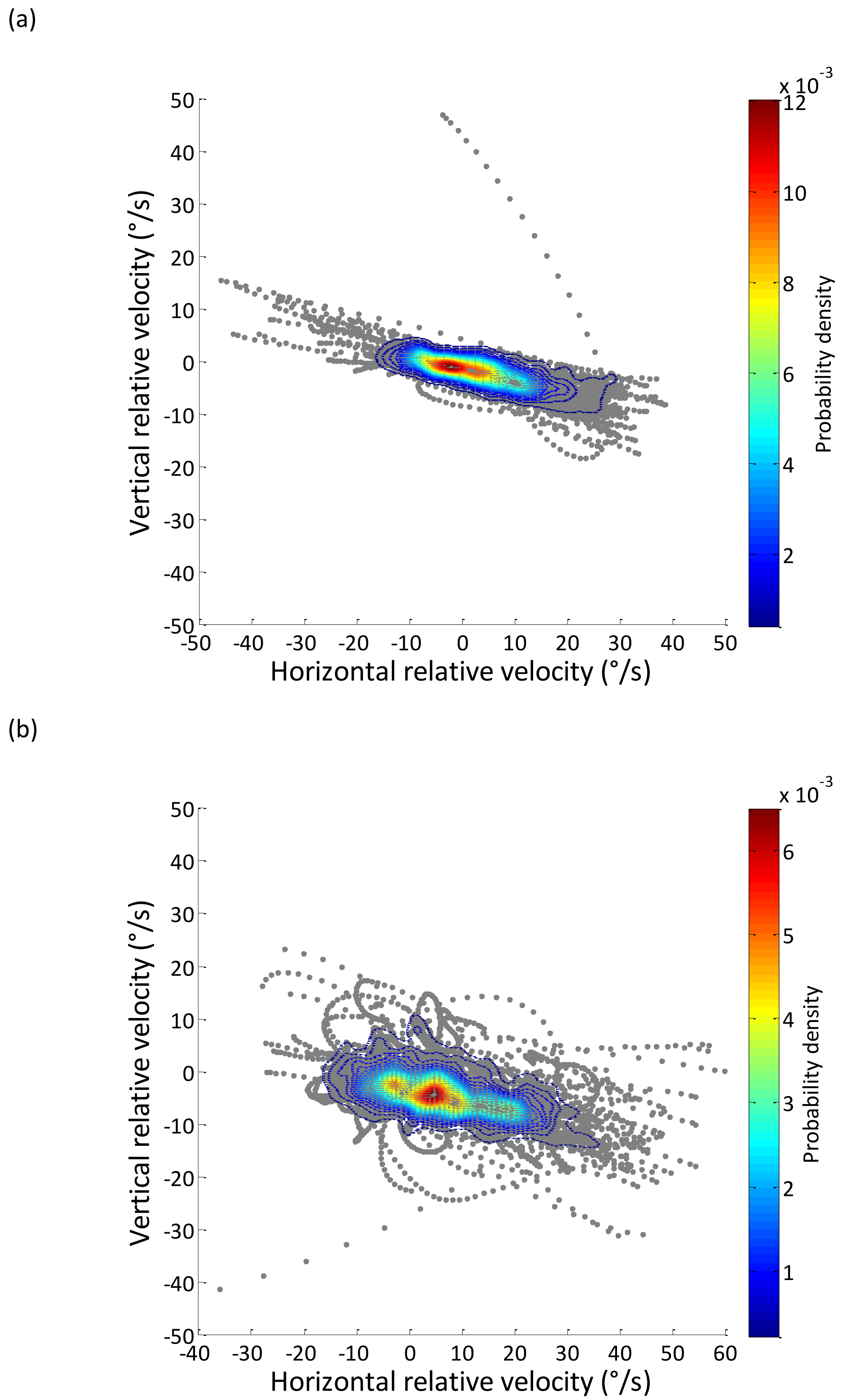

Figure 6.6 Representative probability density functions for precision during (a) horizontal rightward motion (accuracy 2.59°/s, precision 112.18 $(°/s)^2$) and (b) vertical upward motion (accuracy 7.39°/s, precision 239.02 $(°/s)^2$) for an individual with IN (MT).

Similarly, there were no significant differences in accuracy or precision when pursuit along the horizontal direction was compared with pursuit along the vertical direction. The gaze holding of fixation and pursuit were also investigated in those with IN by using a t-test to compare accuracy of fixation and pursuit from zero. The accuracy of fixation was significantly different from zero along the horizontal [$t(14)= 3.715$, $p= .002$] and vertical [$t(14)= 3.59$, $p= .001$]. Similarly, the accuracy of pursuit was significantly different from zero along the horizontal [$t(14)= 4.07$, $p= .001$] and vertical [$t(14)= 6.70$, $p< .001$]. These data suggest that the gaze holding of fixation and pursuit in those with IN is not perfect.

6.5 Results: between control participants and INs

Fixation and pursuit were compared between typical individuals and those with IN using a 2 (groups) x 2 (eye-movement) x 2 (directions) repeated measures analysis. There was a significant effect group for in terms of accuracy [$F(1,28)= 33.61$, $\eta^2= .546$, $p< .001$] and precision [$F(1,28)= 26.34$, $\eta^2= .485$, $p< .001$]. This result suggests that, when data are pooled across the two groups, those with IN are less accurate and less precise. However, there was no significant effect for accuracy or precision for eye movement type or direction. In a repeated measures analysis, effects are determined by pooling the data across conditions and across groups (i.e. typical individuals and those with IN). Therefore, it was likely that the lack of effect for eye movement and direction were due to pooling of the IN data with typical controls. For example, there were no statistical differences determined within the IN group in section 6.4, suggesting that fixation and pursuit data were similar, and horizontal and vertical data were similar. However, the IN values for the accuracy and precision of fixation and pursuit were considerably larger than for typical individuals (compare Figure 6.3 and Figure 6.4). Consequently, when the values were pooled, the means based on type of eye movement and direction would reflect the trends of the IN group for type of eye movement and direction. For this reason, separate independent samples t-tests were performed. IN fixation was significantly less accurate [horizontal $t(14.004)= -3.63$, $p= .003$, vertical $t(14.016)= -3.45$, $p= .004$] and less precise [horizontal $t(14.003)= -4.65$, $p< .001$, vertical $t(14.016)= -3.47$, $p= .004$] along both horizontal and vertical directions when compared to controls. Similarly, IN pursuit was significantly less accurate [horizontal *t*(14.08)= -3.70, *p*= .002, vertical *t*(14.86)= -5.069, *p*< .001] and less precise [horizontal *t*(14.075)= -3.01, *p*< .009, vertical *t*(14.15)= -5.51, *p*< .001] along both horizontal and vertical directions when compared to controls.

6.6 Summary of findings

During fixation, it is known that the eye is never stationary as a result of numerous fixational eye movements. However, the accuracy and precision of these eye movements, relative to pursuit, has never been compared directly. Between groups comparisons in Chapter 5 indicated that those with IN were less accurate and less precise at pursuit than typical controls. The experimental work in this chapter has found that fixation is also more accurate and more precise in typical individuals than those with IN.

Experimental work presented in Chapter 5 indicated that for typical controls, there was a significant difference in accuracy but not precision when horizontal and vertical pursuit are compared, with vertical pursuit being less accurate than horizontal. The experimental work in this chapter found a similar pattern of results for fixation, indicating a significant difference in accuracy but not precision when horizontal and vertical fixation were compared, with horizontal fixation more accurate than vertical. When fixation was compared to pursuit, typical controls were always more accurate and more precise during fixation than pursuit when respective directions were compared.

Experimental work indicated that, for those with IN, pursuit was just as accurate and just as precise along the horizontal as vertical. In this chapter, the experimental work found a similar pattern of results for fixation, indicating no significant difference in accuracy or precision when horizontal and vertical fixation was compared. When fixation was compared to pursuit, those with IN were just as accurate and precise during fixation as pursuit when respective directions were compared.

In Chapter 5, the summary discussed that lower precision during pursuit may lower the precision of retinal and extra-retinal signals in those with IN. However, when the signals are combined, perceived head speed may be less precise. Under conditions of fixation, the eye velocity (i.e. extra-retinal signal) of typical individuals is approximately zero, which results in the magnitude of the extra-retinal signal being negligible. For typical individuals, it is the magnitude of the retinal signal that is likely to dominate motion judgements during fixation.

In contrast, in those with IN, eye velocity (i.e. extra-retinal signal) is not zero and the precision of fixation is drastically less than for typical individuals. During fixation, as with pursuit, both retinal and extra-retinal signals will be expected for motion judgements in those with IN. However, since the magnitude of the extra-retinal signal during fixation is likely to be less than during pursuit (i.e. a target is not being deliberately followed), motion judgements during fixation are likely to be more precise than those made during pursuit.

7 Perceptual compensation for pursuit eye movements: the Filehne illusion in those with and without IN

7.1 Introduction

In Chapter 1, a transducer model for perceptually compensating for the retinal motion image induced by eye movements was discussed. This model requires that both retinal image velocity and eye velocity are estimated, by means of signals, which are then summed to recover perceived head-centric motion. During smooth pursuit, the magnitude of the retinal signal exceeds that of the extra-retinal signal, giving rise to a plethora of pursuit-based illusions of motion. In this chapter, the experimental work will investigate this perceptual compensation during pursuit eye movements in those with IN, a topic that has not previously been investigated.

7.2 The Filehne illusion in IN

In order to measure the Filehne illusion, an individual must make a pursuit eye movement. For those with IN, it was discussed that the actual mechanism by which a target is followed has not been resolved, however in this experiment it is assumed that, whatever the exact mechanism may be, pursuit is analogous to that of typical individuals, but simply less accurate and less precise. However, as part of that lack of precision, null zones during pursuit will be again discussed. If an individual with IN sequentially fixates a series of horizontally displaced targets, it is widely reported that there will be a particular gaze angle at which the IN oscillation is minimum (i.e. the null zone) (Dell'Osso and Flynn, 1979; Dell'Osso et al., 1974). It has also been reported that, if the eyes follow a pursuit target through a range of gaze angles, then the gaze angle of the minimum oscillation will not correspond to the gaze angle of minimum oscillation as found by serially fixating a series of horizontal targets (Dell'Osso, 1986; Kurzan and Buttner, 1989). The null zone location identified during fixation undergoes a lateral “shift” in gaze angle during pursuit. However, the gaze angle shift is reported to depend not only on the speed of attempted pursuit, i.e. shifting further on faster pursuit targets, but also on the pursuit direction by shifting in the *opposite* direction to attempted pursuit (Dell'Osso, 1986; Kurzan and Buttner, 1989). For example, if on pursuing rightwards the minimum oscillation is located at the straight ahead position, then when pursuing leftwards the null will be expected to have shifted rightwards.

At the time of devising the battery of experiments for this thesis, the literature was heavily relied upon to inform the development of the experimental methodology. Therefore, it was felt that if the gaze angle shift of the null zone in response in pursuit eye movements was a general finding in those with IN, rather than being confined to the few select cases discussed and presented in the literature (Dell'Osso, 1986; Kurzan and Buttner, 1989), then an asymmetry in the magnitude of the IN on different gaze angles may be expected to influence the psychophysical responses in the respective directions. For this reason, when quantifying the Filehne illusion, the experiment was planned to be performed for pursuit along the left and right directions independently.

The results of Chapter 4 suggest that, while the null zone when measured under fixation is not consistent, the extent to which this may reflect any shift in the gaze angle during pursuit is uncertain. The results from the experimental work in Chapter 5 would suggest that there is no asymmetry in pursuit performance, since both accuracy and precision were not significantly different for left and rightward target directions. However, it is possible that, if horizontal pursuit was asymmetric, and if the direction of the asymmetry was idiosyncratic across individuals, by averaging across the IN group, the effect would not have been immediately obvious. Furthermore, eye velocity was collapsed across a range of gaze angles (e.g. -16° through to +16°) for each pursuit trial so that a bivariate PDF could be produced. This collapsing of data points may have obscured subtle shifts in gaze angle of the null zone. For these reasons, the potential effects of a shifted null zone on pursuit and the psychophysical responses of those with IN should not be immediately excluded. When the Filehne illusion is measured on typical individuals, pursuit is along both the left and rightward directions. Interestingly, however, the results are not reported by the direction of the motion (Turano and Massof, 2001; Freeman et al., 2002; Freeman et al., 2000b), but instead are presumably treated as individual trial repeats when calculating the point of subjective equality (PSE) of the psychometric functions. Therefore, the results of typical individuals should additionally be explored for any asymmetry. Having discussed the preliminary issues in attempting to measure the Filehne Illusion, the experimental details and results will now be presented.

7.2.1 Methods

Twelve participants with IN (4 male, 8 female; mean 46.3 ± 17.1 years) and 12 typical individuals (8 male, 4 female; mean 29.3 ± 7.0 years) as a control group participated in this experiment. To ensure that perceptual judgements of motion were unreferenced, the experiment took place in a completely dark lab with a modified projector system was modified (see section 2.6). A single green dot (diameter 0.6°) was used as a pursuit target that moved with a velocity of 8°/s over a 16° extent against a black background. A black annular test window (outer annulus diameter 10°, inner annulus diameter 2°) surrounded the pursuit target. The annulus containing the test pattern was superimposed on, and moved coherently with, the target. The test stimulus consisted of green dots (diameter 0.4°, density 0.7 dots/°) randomly positioned within the annular window. The test stimulus was only presented within the annular window for 500ms, randomly perturbed by ± 50ms to prevent prediction, with the onset and offset of the test stimulus symmetric about the midpoint of the pursuit aspect of the trial (i.e. it was presented as the target crossed the straight ahead position).

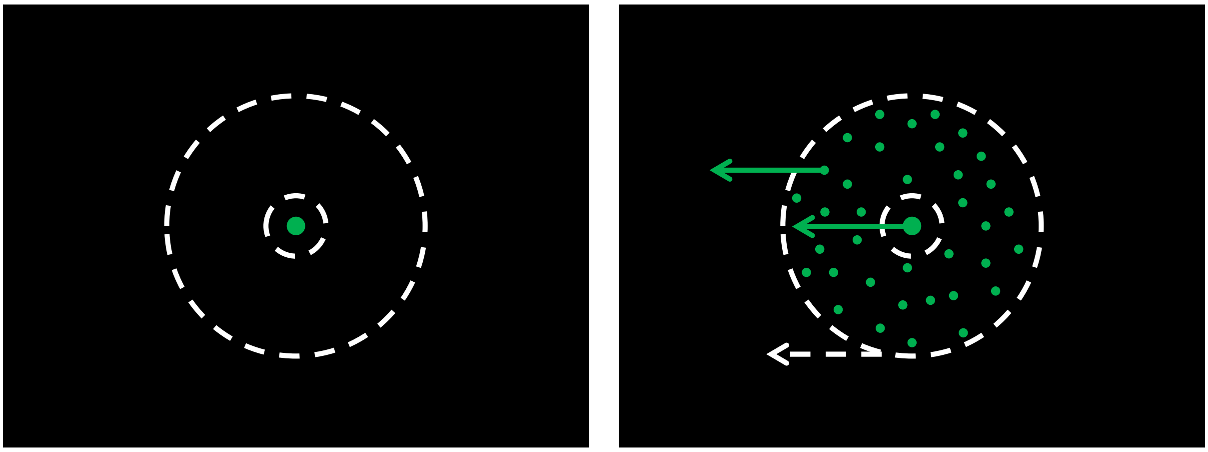

Figure 7.1 Schematic of stimuli that were presented during the Filehne illusion (white dashed lines are for illustrative purposes to outline the test annulus). A 0.6° diameter green dot was presented as a fixation target, surrounded by a test annulus (outer diameter 10°, inner diameter 2°). Both the target and the annulus moved coherently with a speed of 8°/s, either leftward or rightwards with a peak-to-peak amplitude of 16°. The test stimulus was presented within the annulus for 500 ± 50ms.

The relative velocity, with respect to the pursuit target, of the test stimulus within the annulus was linearly adjusted using a 1-up 1-down staircase procedure. Two independent staircases were randomly interleaved, one assigned to rightward pursuit and one assigned to leftward pursuit. The starting velocity for each staircase was selected on the basis of the mean PSE of the psychometric function that yielded a percept of stationarity for typical individuals using a similar experimental setup (Freeman et al., 2002). This mean PSE is typically around 70% of the relative motion between the target and the test stimulus. So that participants would presumably start the experiment close to perceived stationarity, the starting velocity was set to either 50% or 90% relative velocity. Each staircase was randomly assigned to one of these two starting velocities, such that the probability of each staircase starting high (i.e. 90% relative velocity) or low (i.e. 50% relative velocity) on each run was equal.

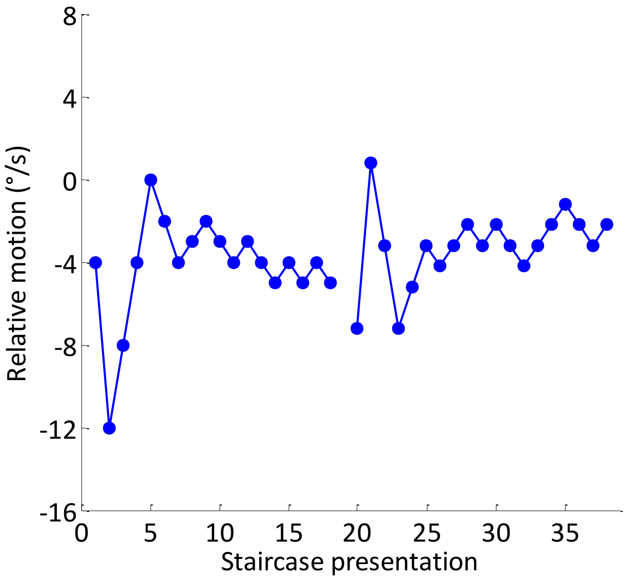

Figure 7.2 The sequence of stimuli presented to a typical individual during 2 runs of a single staircase. Large spikes in the test stimulus indicate the beginning of a new staircase run.

To present an appropriate number of relative test velocities in an appropriate amount of time, one of two possible 'fine' staircase steps was derived for each participant, either 0.5°/s or 1.0°/s. In Figure 7.2, the minimum relative velocity step was 1.0°/s. The step size was based on the results of a practice run, where the sequence of relative test velocities presented for each staircase was then plotted (Figure 7.2). The magnitude of the 'fine' relative velocity step was selected based upon an ideal of 2 to 3 relative velocity presentations before a reversal occurred. To reduce the time required to estimate the point of subjective equality, 3 reversals using a 'coarse' step (e.g. the first 3 presentations of each staircase in Figure 7.2) placed the relative test velocity (presumably) close to the point of subjective equality (PSE), followed by 8 reversals using a 'fine' 0.5°/s velocity step to more accurately define the PSE (e.g. the remaining presentations for each staircase in Figure 7.2). The magnitude of the 'coarse' relative velocity step was initially set at 8 times that of the 'fine' relative velocity step, and halved after each reversal so that it would equal the 'fine' relative velocity step after the third reversal (see Table 7.1). Each staircase terminated after 11 reversals (3 coarse, 8 fine) or 100 trials, whichever occurred first. When one staircase had terminated, the other was still active. However, to avoid repeated presentations in the same pursuit direction (i.e. non-random presentation), thereby indicating to the participant that only one staircase was operating, "dummy trials" were inserted but not recorded for the staircase that had terminated, using random relative velocities drawn from the final relative test velocity ±10%.

	0.5°/s 'fine' relative velocity step size (°/s)	**1.0°/s 'fine' relative velocity step size (°/s)**
Until 1st reversal	4.0	8.0
Until 2nd reversal	2.0	4.0
Until 3rd reversal	1.0	2.0
Thereafter	0.5	1.0

Table 7.1 Details of the staircase procedure used in the experiment.

7.2.2 Procedures

Each participant was told that their task was to follow the pursuit target as carefully as possible and to indicate the direction of perceived motion of the test stimulus with respect to their head. Hence, they judged the motion of the test stimulus relative to head-centric stationary. To check participant understanding of the task and that they were not mistakenly reporting the relative motion of the stimulus with respect to the pursuit dot (a retino-centric judgement), participants were asked to verbally explain the nature of the motion judgement task to the experimenter before the main experiment took place. Participants were then given one practice run to familiarise themselves with the test stimulus, button controls and task before completing a minimum of four runs of trials in succession, with each run lasting approximately 4-5 minutes. To eliminate any extraneous fixed references in the lab that might be revealed by the light produced during the presentation of the relative motion test stimulus once participants had begun to dark adapt, participants were given a 3 minute rest between runs with the room lights on. As a reminder, Chapter 2 described that the CRT projector was fitted with a neutral density filter that reduced the output of the projector by 87.5%, the purpose of which was to ensure that projected black backgrounds were not visible when the laboratory illumination was turned off as well as ensuring that, when multiple visual stimuli were displayed at once, the laboratory was not 'flooded' with light, such that participants could make judgements about motion relative to objects in the room.

Each experimental trial commenced with participants fixating a green central dot subtending 0.6° in the centre of an otherwise uniform black background. To initiate a trial, the subject pressed either mouse button (i.e. left or right) on a wireless keyboard which caused the uniform background and fixation target to be immediately replaced with the pursuit target, which appeared at 8°, either to the left or right of the straight ahead position, depending which of the randomly selected staircases was operating. After a 1 second delay that allowed participants to acquire the pursuit target, it began to move at 8°/s. Participants indicated their responses using a mouse button press. To discourage participants from terminating pursuit eye movements early, responses were only accepted by the computer after the pursuit trial had ended.

7.2.3 Results

Psychophysical data were analysed offline using MATLAB® with a Probit analysis (Finney, 1971). The point of subjective equality (PSE) was taken as target velocity corresponding to the 50% of the psychometric function. Typical psychometric functions for control participants and IN participants are presented in Figure 7.3 and Figure 7.4, respectively. In each psychometric function, the x-axis indicates relative motion between the pursuit target and the test stimulus, and the y axis indicates the percentage of correct responses that the relative motion was judged as moving in the direction of the pursuit target. Since the pursuit target was moving with 8°/s, a relative motion of -8°/s between the pursuit target and the test stimulus would correspond to the test stimulus being stationary with respect to the screen, whereas a relative motion of 0°/s indicates that the test stimulus moved with the same velocity as the pursuit target.

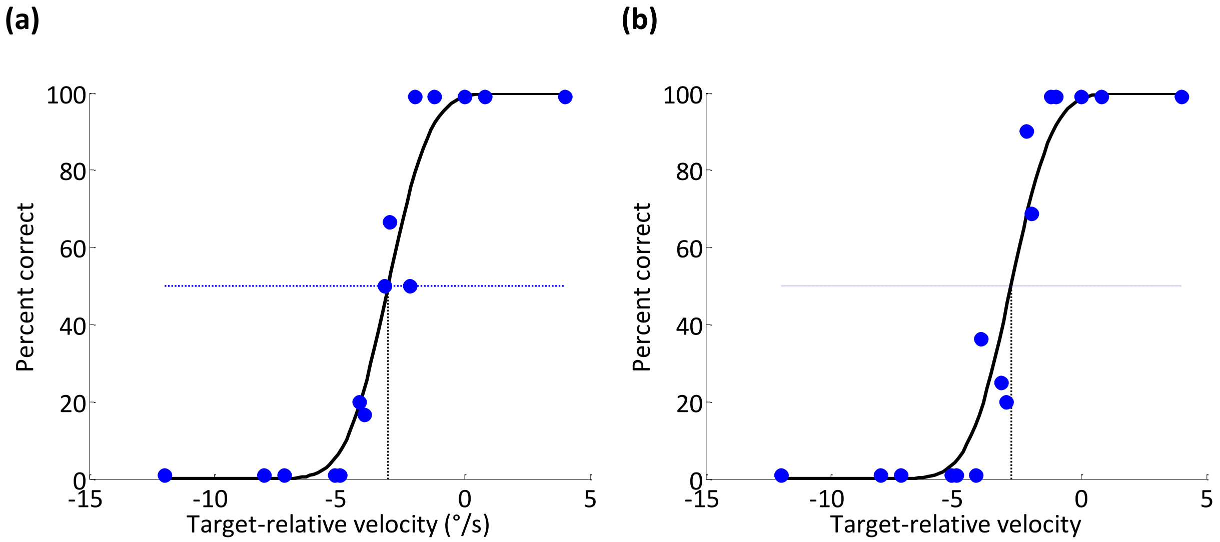

Figure 7.3 Typical psychometric functions for a control participant (TR) showing (a) the leftward PSE (3.92°/s) and (b) the rightwards PSE (-3.06/s).

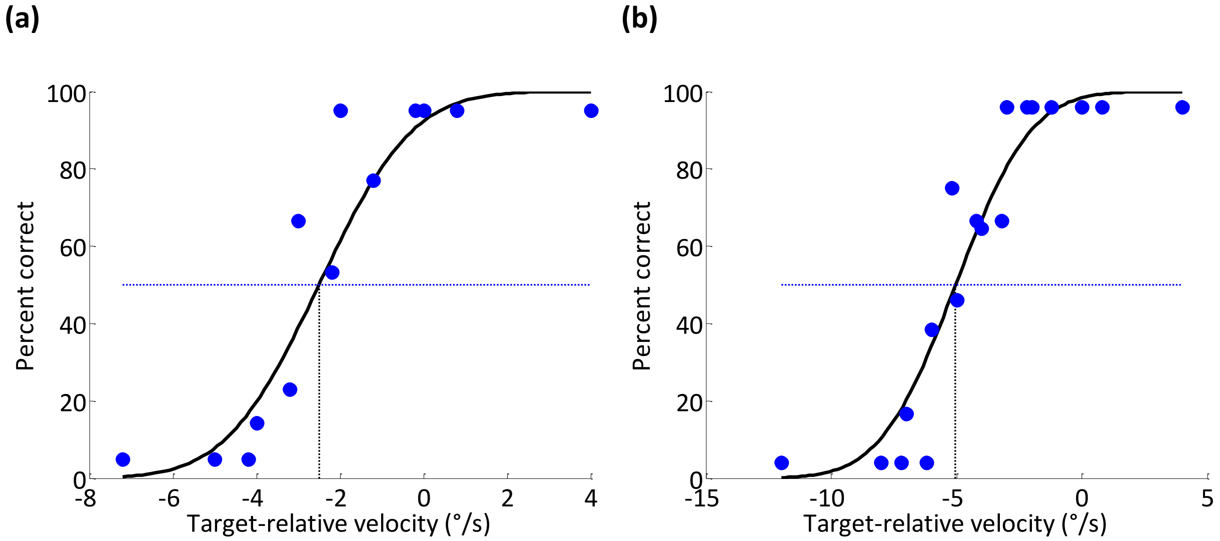

Figure 7.4 Typical psychometric functions for an IN participant (JT) showing (a) the leftward p50 (-2.50°/s) and (b) the rightward p50 (-5.03°/s).

The psychophysical data presented in Figure 7.5 would suggest that a *non-veridical* percept of stationarity was experienced by both those with and without IN as they followed the pursuit target. Individual one-sample t-tests were performed to determine whether the results of each group were significantly different from a veridical perception of stationary (i.e. -8°/s). The PSEs for both those with IN (rightward [$t(11)= 6.67$, $p< .001$], leftward [$t(11)= 9.91$, $p< .001$]) and controls (rightwards [$t(11)= 12.36$, $p< .001$], leftwards [$t(11)= 11.61$, $p< .001$]) indicate that perception of stationarity was significantly non-veridical.

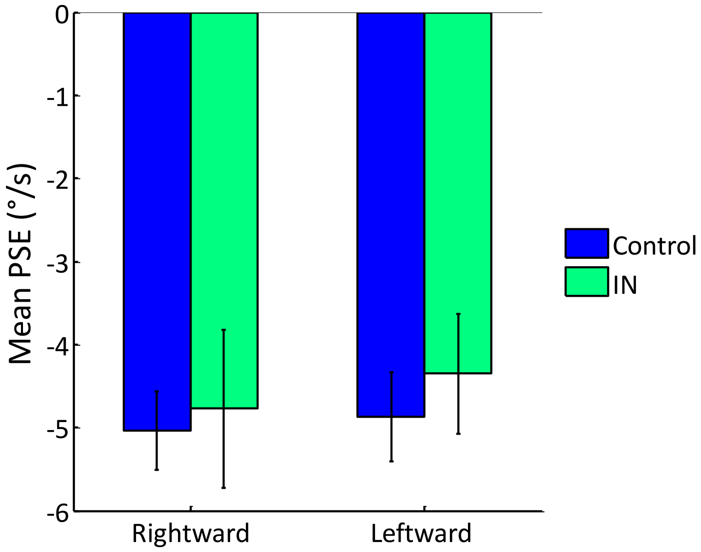

Figure 7.5 Psychophysical results of the Filehne illusion for IN and control participants. Data are the mean PSE values for each group and direction, while error bars indicate 95% confidence intervals.

A repeated measures analysis of the PSEs, with group as a between-subjects measure, indicated no significant effect for group [$F(1,22) = .853$, $\eta^2 = .037$, $p = 0.366$], suggesting the results for typical individuals were no different to those with IN.

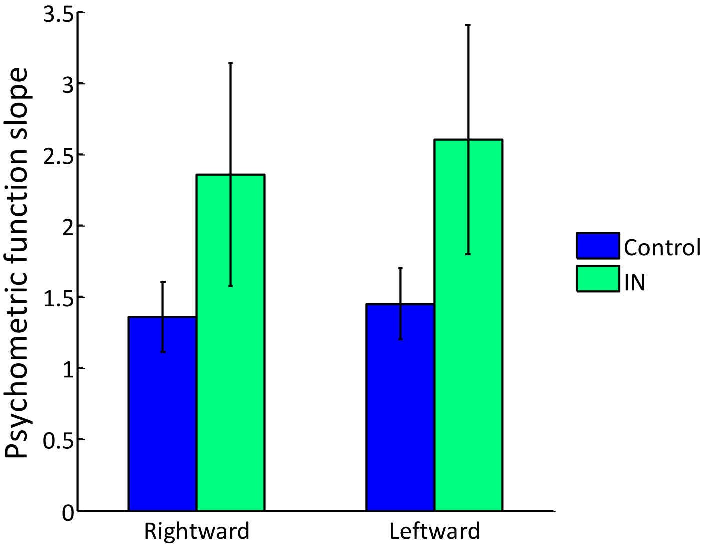

Figure 7.6 Comparison of the slopes of the psychometric functions between typical individuals and those with IN.

The slope of the psychometric function (i.e. precision) can be calculated from the psychometric function as the difference between the 84% correct value of the psychometric function minus the 50% correct value.

While the means of the PSEs were not significantly different, the slopes of the respective psychometric functions were compared (Figure 7.6). A repeated measures analysis of the pursuit direction, with group as a between-subjects measure indicate no significant effect for direction [$F(1,22)= 9.75$, $\eta^2= .042$, $p= .330$], but a significant effect for group [$F(1,22)= 7.67$, $\eta^2 = .259$, $p = .011$]. This result suggests that the precision of the perceived head centric speed is lower in those with IN than typical individuals.

In the transducer model, perceived velocity (*H'*) of an object is the result of summing estimates of retinal image velocity (carried by a retinal signal, *R'*) and eye velocity (carried by an extra-retinal signal, *P'*). Note that the sign of *R'* is *negative* since the retinal image motion moves in the direction opposite to the eye movement. The transducer model can be stated as the following equation:

$$H' = R' + P'$$

Because the magnitude of the retinal signal exceeds that of the extra-retinal signal during pursuit, the retinal signal is varied by manipulating the relative motion of the test stimulus with respect to the pursuit target until the perceived speed, H', is zero:

$$0 = R' + P'$$

Rearranging gives:

$$R' = -P'$$

However, both *R'* and *P'* are estimates of *R* and *P* with respective gains of *r* and *p*:

$$rR = pP$$

Rearranging for R, the retinal image motion that achieves a percept of stationarity can be expressed as:

$$R = P\frac{p}{r}$$

This equation demonstrates that the Filehne illusion does not measure the individual gains of the extra-retinal signal, p, and the retinal signal, r, but rather their *ratio*. If these gains were equal, the ratio, $\frac{p}{r}$, would be 1, and so P would equal R (i.e. the eye movements would be completely compensated for by the eye movements).

For those with IN, there was no difference in the mean PSEs when compared to typical individuals (i.e. no difference in the gain ratio of the retinal and extra-retinal signals). This would indicate that the ratio of the signals was similar to typical controls. The slopes of the psychometric functions for those with IN were shallower than those for typical individuals, despite there being no difference in the mean PSEs between the two groups. This may suggest that those with IN are less precise at estimating retinal image motion, but this low precision is offset by a less precise estimate of eye velocity (i.e. their gain ratios are the same). Note that the gain ratio does not reveal the accuracy with which either signal is encoded, only simply that their ratios were constant.

7.3 Velocity discrimination in IN

In the previous section, it was discussed that it is not possible to determine individual gains for either the retinal or extra-retinal signal using the Filehne illusion. One method of attempting to separate the two signals is to examine motion processing in the absence of eye movement (i.e. no extra-retinal signal). For this reason, a velocity discrimination task was performed on both groups during fixation and will serve as the basis for exploring motion judgements during fixation.

When typical individuals fixate a target, there are tiny fixational eye movements (i.e. drift, tremor and microsaccades) that continuously keep the eye in motion (Martinez-Conde et al., 2004; Rucci et al., 2007; Yarbus, 1967; Pritchard, 1961). Indeed, the data in Chapter 6 demonstrated that, even for typical individuals, there is some measurable inaccuracy and imprecision in velocity control during fixation. This would inevitably be added to any motion of the environment. Consequently, even during fixation the extra-retinal and retinal signals must be compared so that the head-centric speed of objects can be estimated. Indeed, if this were not the case, the perception of oscillopsia would ensue.

The transduction of retinal and extra-retinal signals is assumed to be linear. Therefore, as eye speed increases so too does the magnitude of the extra-retinal signal. In Chapter 6, it was demonstrated that eye speed is close to zero for typical individuals. Therefore it is the magnitude of the retinal signal that will contribute most to motion judgments during fixation in typical individuals.

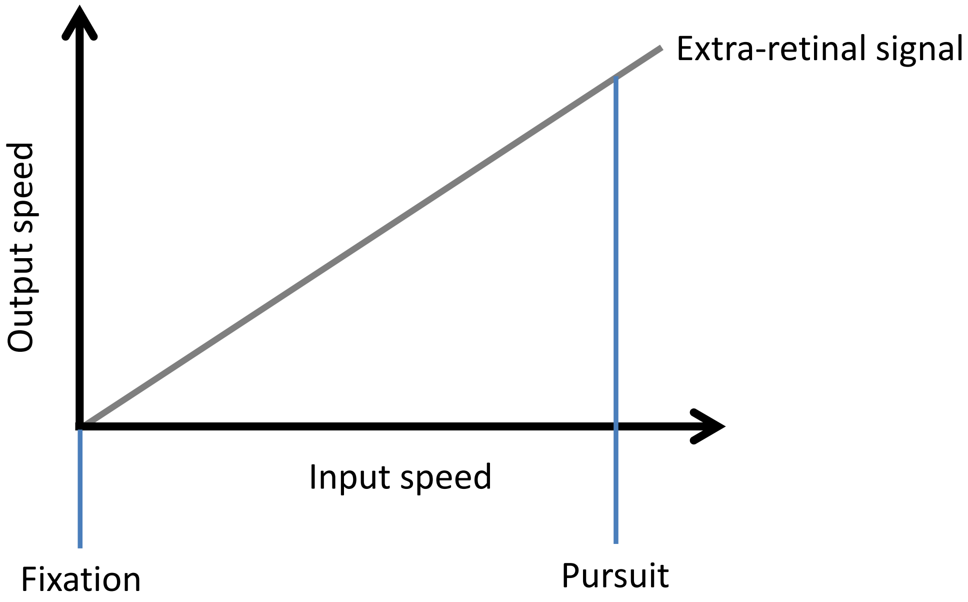

Figure 7.7 A schematic depicting the linear transduction of the extra-retinal signal during fixation and pursuit for typical individuals.

In contrast, those with IN do have considerable eye movements during fixation (i.e. slow phases), and the experimental data in Chapter 6 indicated that eye velocity during fixation was considerably greater than zero. However, the same assumption for typical individuals about the extra-retinal signal being zero cannot be applied to those with IN. As with IN pursuit, it is the magnitude of both the extra-retinal and retinal signals that will determine the motion judgements during fixation. Despite no significant difference in the precision of fixation and pursuit in those with IN, the magnitude of the extra-retinal signal during fixation may not be as large as during pursuit. Consequently, assuming the same gain of the retinal and extra-retinal signals, a lower magnitude extra-retinal signal may suggest that the precision of velocity discrimination is more precise than that for perceived head-centric speed during the Filehne illusion.

To reiterate, velocity discrimination judgements during fixation in either group of participants will not yield a *pure* estimate of the retinal signal. In typical individuals, such judgements of retinal signal are relative judgements made between the test stimulus and an implicitly stationary fixation target, whereas for those with IN there are still retinal and extra-retinal signals being combined with a similar relative motion judgement being performed. Nonetheless, such an experiment will serve as a basis for exploring the nature of motion perception in both groups during fixation.

7.3.1 Methods

Eleven participants with IN (6 male, 5 female; mean 46.9 ± 14.6 years), and 7 typical individuals (4 male, 3 female; mean 30.1 ± 9.1 years) as a control group, took part in the velocity discrimination task. The stimuli were identical to those used in the previous experiment. However, instead of a pursuit target, a single green dot (diameter 0.6°) was used as a fixation target, with the black annular test window containing the test stimulus centred on the fixation target. All other experiment parameters (e.g. lab setup, staircases, starting relative velocity, etc.) were the same as for the previous experiment.

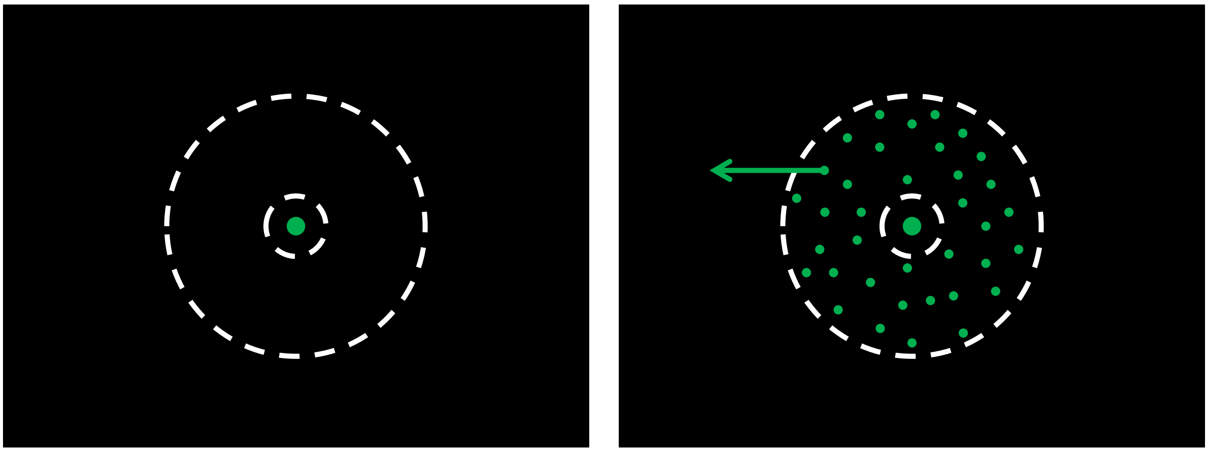

Figure 7.8 Schematic of stimuli presented (white dashed lines indicating the outline of the test annulus are for illustrative purposes and were not present during the experiment). A 0.6° diameter green dot was presented as a fixation target, surrounded by a test annulus (outer diameter 10°, inner diameter 2°).

7.3.2 Psychometric results

Typical psychometric functions for IN participants for this task are presented in Figure 7.9, with the x and y axes of the psychometric functions reporting the same information as the previous experiment. The mean PSEs for those with IN are presented in Figure 7.10. A paired samples t-test indicated no significant difference in the PSEs for leftward and rightward motion [*t*(10)= .337, *p*= .743]. Individual one-sample t-tests indicated that the PSEs for both rightward [*t*(10)= .426, *p*= .679] and leftward [*t*(10)= -.297, *p*= .773] directions were not significantly different from 0°/s.

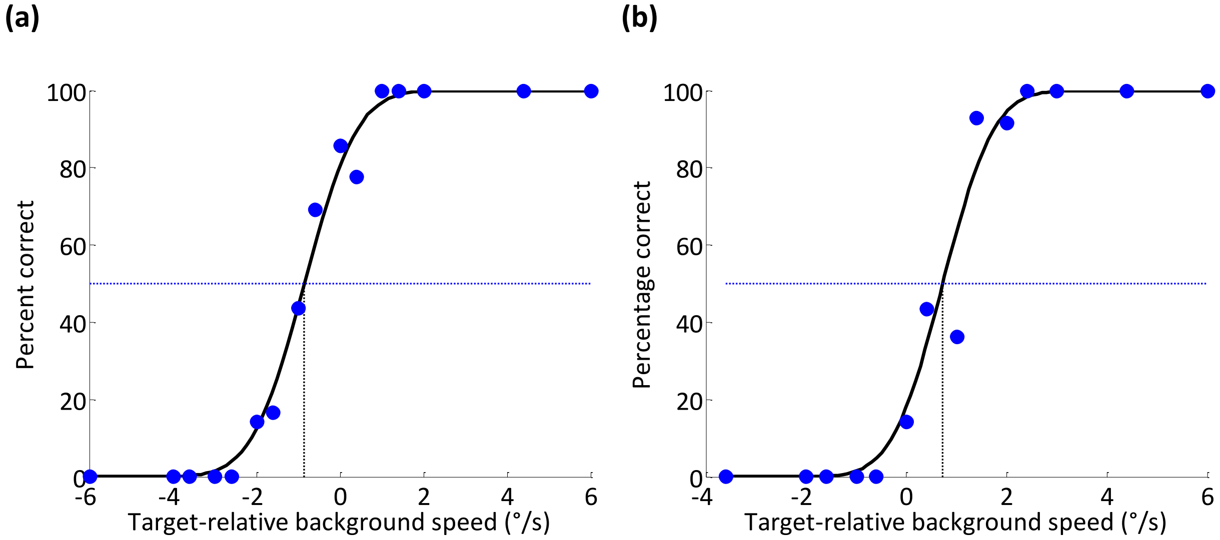

Figure 7.9 Typical psychometric functions for an IN participant (DT) showing (a) the leftward PSE (-0.86°/s) and (b) the rightward PSE (0.73°/s).

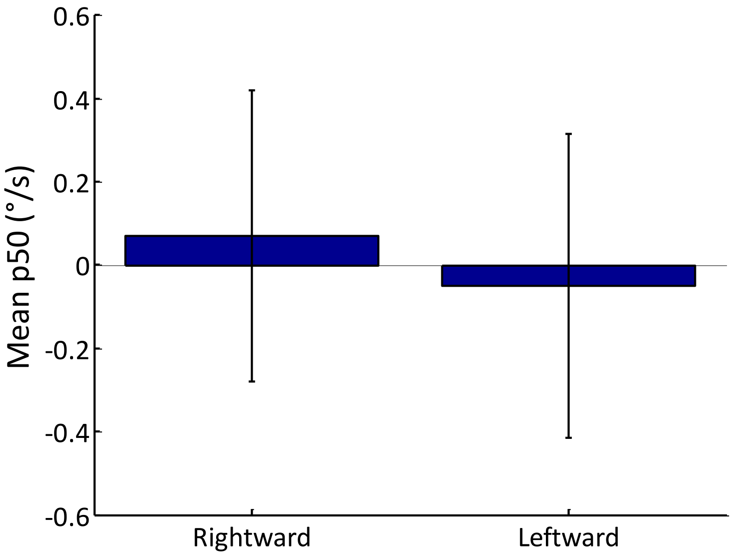

Figure 7.10 Psychophysical results of the velocity discrimination experiment for those with IN. Data are the mean PSE values for each initial test stimulus direction, while error bars indicate 95% confidence intervals.

Unfortunately this experiment was only performed on a small cohort of 7 typical individuals early in pilot testing to confirm that the experimental parameters (e.g. dot density, stimulus duration, etc.) of the experiment were sufficient. However, although the number of participants is not quite as large as for the group with IN (n=11), these data are also presented for comparison. Mean PSEs for the typical individuals are presented in Figure 7.11.

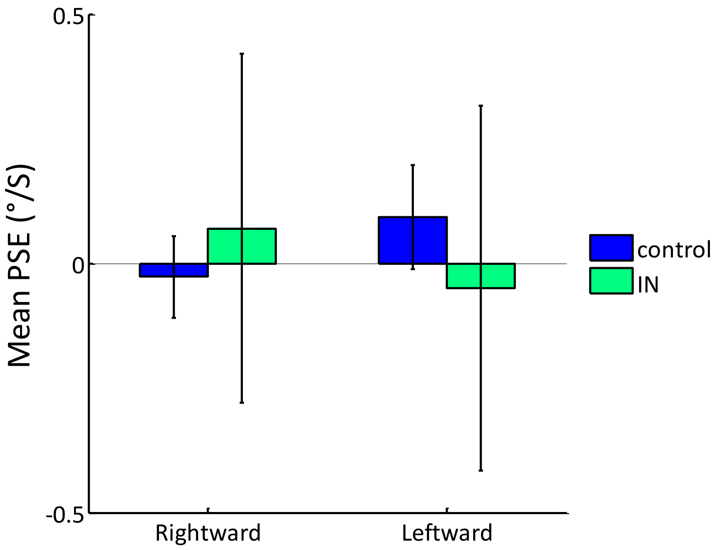

Figure 7.11 A comparison of the mean PSEs of velocity discrimination for typical individuals and those with IN.

A paired samples t-test indicated no significant difference in the PSEs for leftward and rightward motion [*t*(6)= -.1.09, *p*= .317], while individual one-sample t-tests indicated that the PSEs for both rightward [*t*(6)= -.502, *p*= .634] and leftward [*t*(6)= 1.321, *p*= .235] directions were again not significantly different from 0°/s.

Because of the unequal group numbers, a linear mixed model analysis for repeated measures was performed. There was no effect for group [*F*(1,18)= .160, *p*= .693]. As in the Filehne illusion experiment, the slopes of the respective psychometric functions for both groups were investigated (Figure 7.12). Again, to compare the two groups, a linear mixed model analysis for repeated measures performed. There was a significant effect for group [*F*(1,18)= 21.14, *p*<.001].

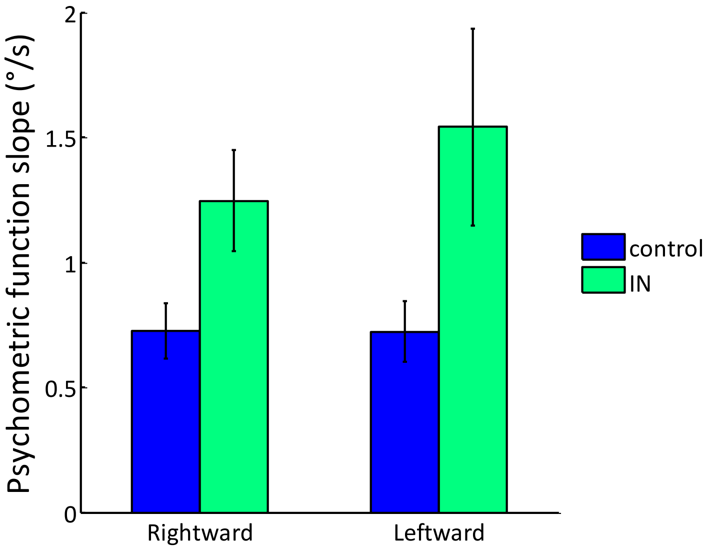

Figure 7.12 The mean slopes of the psychometric functions for those with IN and typical individuals

Although there appears to be an asymmetry in the slope values of those with IN, a follow up t-test indicated that this was not significant [*t*(10)=-1.30, *p*=.224]. The results indicate that, for those with IN, while the PSEs are similar typical individuals, there is a significant difference in the slopes of the PSEs. As described earlier, such a result would seem consistent with motion judgements for typical individuals being dominated by the retinal signal, whereas for those with IN the signal is dominated by low precision retinal and extra-retinal signals.

7.4 Summary

During pursuit eye movements in typical individuals, a number of illusions of motion can occur. One such illusion, the Filehne illusion, gives the head-centric percept that stationary objects are moving in a direction opposite to the direction of the pursuit target. The Filehne illusion can be predicted using the simple linear transducer model proposed by Freeman and Banks (1998), whereby retinal and extra-retinal signals, encoded with differing gains, result in the magnitude of the retinal signal exceeding that of the extra-retinal signal. Those with IN are hypothesised to use retinal and extra-retinal signals in the same manner as typical individuals. Yet, despite this hypothesis, there has been no previous investigation as to whether or not those with IN experience a similar mismatch in the magnitude of these two signals during pursuit eye movements.

In this chapter, the Filehne illusion was investigated in those with and without IN. The psychophysical results indicate that the percept of stationarity experienced by both those with IN and typical individuals was non-veridical, with both groups perceiving stationary objects as moving in a direction opposite to attempted pursuit, i.e. both groups were experiencing a Filehne illusion. The outcome of this study suggests that the retinal image motion induced by pursuit eye movements in those with IN is compensated for in a manner consistent with typical individuals.

While the mean PSEs for both groups were similar, the slopes of the respective psychometric functions did differ significantly. Given that the Filehne illusion measures the ratio of the extra-retinal and retinal signals, this suggests that those with IN have similar gains ratios (i.e. no statistical difference in the PSEs between INs and typical individuals) but that the signals contributing to these signals are of lower precision.

To further investigate the retinal and extra-retinal signals in motion judgements, a velocity discrimination task during fixation was performed. For typical individuals, if the eye is assumed to be stationary during fixation then there is assumed to be no extra-retinal signal such that motion judgements are based solely on the retinal signal. For those with IN, the considerable eye velocities that are occurring even during fixation would suggest that motion judgements are based on *both* extra-retinal and retinal signals during fixation. Although the number of typical individuals tested for comparison was slightly lower than in the IN group, the results nonetheless suggest that the ratio gains of the extra-retinal and retinal signals in those with IN were similar to the assumed retinal signal of typical individuals. However, the motion discrimination of those with IN was less precise than typical individuals, presumably because of the lower precision of eye velocity during the slow phase, as demonstrated in Chapter 6.

8 General discussion and future work

8.1 Introduction

The overarching aim of this thesis was to investigate, using the Filehne illusion, the perceived head-centric speed of objects in those with IN. However, before conducting this experiment, a number of other related topics were explored. As the Filehne illusion is a pursuit-induced illusion, the ability of those to follow a target was characterised. In addition, when undertaking pursuit, the magnitude of the IN is reported to vary, and therefore the relationship between IN and gaze angle was investigated. The main findings of each of these experiments together with those relating to the Filehne illusion will be reviewed and discussed here more generally before considering this work in the context of understanding oscillopsia.

8.2 Eye movement analysis

In Chapter 3, I developed a novel approach to eye movement analysis by extending existing techniques that are used to quantify the positional stability of fixation in two dimensions. By utilising the retinal slip of the intended target, this eye movement measure is now generalised such that it can be applied to either fixation or pursuit. However, it is not restricted to only these two eye movements. Indeed, other potential applications of this analysis would be to quantify oculomotor performance during optokinetic nystagmus. It is hoped that these analyses could be utilised by others for *any* eye movement that attempts to stabilise an image with respect to the fovea. Importantly, because the *same* analysis can be used on all types of gaze holding eye movements, rather than simply just being used for *measurement*, such eye movements can be directly *compared*, whether it be in typical individuals or those with oculomotor disorders.

8.3 Studies of fixation

In chapter 4, I attempted to characterise the null zones of those with IN, so that the oculomotor performance of pursuit as a function of null zone location could then be derived. This is because the magnitude of the IN oscillation increases as gaze angles move away from the null zone. Therefore it was hypothesised that those pursuing *through* their null zone would have more accurate, more precise pursuit (i.e. a smaller magnitude IN oscillation) than those pursuing *away* from their null zone (i.e. a larger magnitude IN oscillation). However, a critical review of the literature revealed an absence of important experimental details in the studies involved, such as the:

- presentation order of the fixation targets
- minimum number of IN cycles recorded per gaze angle
- calculation of intensity from eye movements
- method by which the null zone is determined from intensities

In pilot work that attempted to address these concerns, the location of the null zone was determined for a small number of participants. However, the results for one well-studied participant did not appear to agree with previous data that had been collected over a number of years. The location of the null zone identified in the current study was nearly 30° left of all previous accounts. The random order of target presentation was considered likely to be responsible for producing a difference in the intensity of the resulting eye movements, and therefore the gaze angle at which intensity was at a minimum (i.e. the resulting null zone). More specifically, it was hypothesised that anticipation relating to the uncertainty of the location of impending target presentations altered the pattern of eye movements. Therefore, two additional experimental conditions were added to test this hypothesis: sequential presentation from left-to-right and from right-to-left. Because the location of subsequent target presentations in each of these conditions could be predicted, consistent results were expected for IN intensity at each gaze angle. While *more similar* results were obtained for predictable target presentations, i.e. left-to-right and right-to-left, *identical* null zone locations were not necessarily obtained in a given participant. Nonetheless, the results indicate that the predictability of target location would appear to influence the resulting pattern of eye movements. In the current study, even under seemingly 'ideal' conditions by the standards of the literature (Dell'Osso and Flynn, 1979) (i.e. no other visible features, lack of resolution stimuli, etc.), the gaze angle of the null zone was not repeatable for an individual. However, since there are no studies specifically documenting the repeatability of null zone measurements reported anywhere in the literature, the current study would be the first to document this finding.

Surgery is often performed to move null zones from eccentric gaze angles to the straight ahead position. If null zones are determined in the manner of the current experiments prior to any surgical intervention as the literature would seem to suggest (Dell'Osso and Flynn, 1979), then this raises a serious concern. Such surgical interventions may be relying on potentially uninformative information about a given individual’s null zone. A number of studies discuss “effort to see” and the effect this can have on the intensity of the IN oscillation (Dell'Osso and Flynn, 1979). Although no clear description for “effort-to-see” is provided in the literature, it will be assumed that it refers to the viewing of stimuli that contain spatial information close to the resolution threshold of the individual. This study did not use detailed stimuli, but easily visible 0.4° spots of light. In contrast, the natural environment contains many stimuli of various spatial frequencies, some of which will be at or beyond the threshold resolution of those with IN. Therefore, it would be safe to assume that the environment will contain visual stimuli that could be classed as requiring “effort to see” on the part of those with IN. Further, stimuli that require “effort to see” may be found in locations that are either familiar (i.e. predictable) or unfamiliar (i.e. unpredictable) to individuals with IN. This would suggest that, under real world conditions, the gaze angle of the null zone would be inconsistent. However, if simultaneous recording of both head and eye position as individuals navigate the environment were performed, the results of such an experiment could help us better understand the real-world importance of the null zones and the interplay between the magnitude of the IN oscillation with gaze angle under natural viewing conditions.

In this thesis, the null zone has been considered to be that horizontal gaze angle resulting in the minimum intensity eye oscillation as the eye shifts gaze along an infinitely thin, imaginary horizontal line that passes through the line of sight when the eyes are in the straight ahead position. However, those with IN are capable of moving their eyes vertically, either above or below this imaginary horizontal line. The relative state of vergence (i.e. the extent to which the visual axes intersect for different focal distances) is known to vary as a function of vertical gaze, giving rise to “pattern” deviations (Von Noorden and Campos, 2002). For example, a “V-pattern” deviation describes the eyes being relatively more convergent in down-gaze than up-gaze, and vice versa for an “A-pattern” deviation. Therefore, comparing up-gaze with down-gaze, each eye may have a different gaze angle. It has been reported that, in some - but not all - individuals with IN, the IN oscillation is dampened by convergence (Abadi and Bjerre, 2002). Therefore, it was hypothesised that the magnitude of the IN oscillation could vary as a function of *vertical gaze angle* as well as *horizontal gaze angle*. Indeed, there are reports of head tilts (i.e. a change in the vertical positioning of the eyes in the orbit) as well as head turns (i.e. a change in the horizontal positioning of the eyes in the orbit) in those with IN (Abadi and Whittle, 1991). At the time the experiments in this thesis were planned, pilot work was undertaken to coarsely sample across visual space in an attempt to determine a two-dimensional null zone. Twenty-five dot stimuli, identical to those used in Chapter 4, were presented in a 5-by-5 grid with the central dot straight ahead and an inter-dot spacing of 4°. Eye movements were, as before, sampled for 14s at each location. However, although data collection continued, progress on analysing this preliminary experiment was halted on the realisation that the gaze angle of the horizontal null zone was not consistent.

However, data presented in Chapter 4 did not fully explore the possibility of a vertical null zone. All vertical gaze angles had the *same* horizontal gaze angle. In addition, the data in Chapter 4 indicated that the intensity at the *same* horizontal gaze angle can vary (i.e. leading to an inconsistent horizontal null zone). Therefore, it is possible that the variability in the intensity at the same horizontal gaze angle was obscuring any trend for a reduction in intensity with gaze angle. Alternatively, it is possible that IN intensity is determined by the horizontal angle which remains largely unchanged with vertical elevation of gaze. Nonetheless, the possibility of a vertical null zone is a topic for future exploration.

8.4 Studies of pursuit

In Chapter 5, experimental work characterised the ability of those with IN to follow a moving target. Since the Filehne illusion is a pursuit-based illusion, and because previous studies of IN did not fully characterise IN vertical pursuit, it was necessary to understand how those with IN follow moving targets along both horizontal and vertical directions. Experimental work replicated the findings of previous studies that have investigated pursuit along the horizontal direction by finding that pursuit is inaccurate and imprecise. However, previous studies on vertical pursuit have considered only the vertical component of eye movements, not the vertical *and* horizontal components together. Consequently, previous studies have failed to characterise the inaccuracy and imprecision during vertical pursuit that was documented in the current study. Irrespective of the direction of the pursuit, the least precision was always found along the horizontal axis due to the underlying oscillation. One caveat of the current study is that the pursuit target motion is at a constant velocity and periodic. Such stimuli are known to be highly predictable (Bahill et al., 1980; Bahill and McDonald, 1983). Indeed, in the current study, typical individuals were observed to anticipate target reversals after a single sweep (see Figure 5.2 and Figure 5.3). The extent to which the current study was influenced by predictive eye movement behaviour is unclear. Nonetheless, predictive eye movement behaviour would likely overestimate human pursuit performance, and so the results might be regarded as the upper limits of performance. Future experiments, using less predictable target motions, such as random walk sine waves (Lisberger et al., 1981), could further investigate pursuit performance in those with IN.

The presence of an ongoing horizontal eye oscillation during vertical pursuit introduces an interesting possibility for the misperception of the trajectory of vertically moving targets. For example, in typical individuals, vertically moving targets appear to move obliquely during horizontal smooth pursuit eye movements (Souman et al., 2006). For example in Figure 8.1, a pursuit target (green), moving rightward will cause a vertically moving target (blue) to be perceived as though it is moving upwards and to the left.

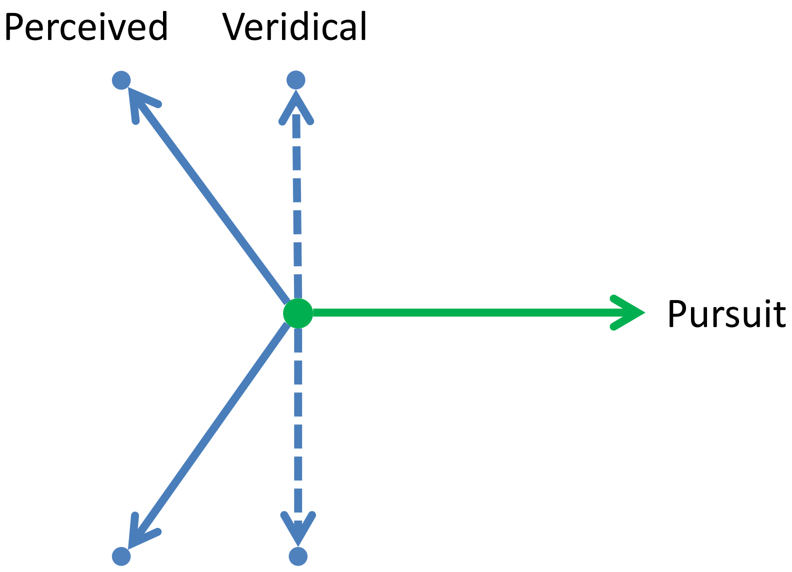

Figure 8.1 Trajectory misperception occurs during a smooth pursuit eye movements . On pursing a horizontally moving target (green), vertically moving targets (blue dashed line) are misperceived as moving obliquely in their in their trajectory (solid line). Similar trajectory misperception may occur during the slow phase of IN.

This illusion of motion arises because, as with other pursuit-based illusions, the magnitude of the retinal signal exceeds that of the extra-retinal signal. Consequently, targets with zero horizontal velocity (although moving vertically) are perceived to move in a direction opposite to the pursuit eye movement. In this thesis, the untested assumption is that those with IN have complete compensation for the oscillation during fixation. However, if the horizontal slow phase during fixation is treated as a brief epoch of, albeit accelerating, smooth pursuit, then any errors in the compensation of the slow phase may be evident as a misperception of the trajectory of a vertically moving target. During fixation in IN, such an experiment might be able to confirm whether or not the magnitudes of the retinal and extra-retinal signals are equal (i.e. oscillopsia is truly absent). The fast-phases of IN are goal directed (i.e. they redirect gaze on to the target). However, the extent to which the fast phases would compensate for any potential error in the perceived trajectory of vertically moving targets is also unclear. Future work could therefore explore the role of the influence of the slow phase on visuo-motor action (i.e. how does the velocity of the slow phase impact upon the targeting accuracy of the fast-phase).

8.5 Studies on the comparison of fixation and pursuit

In Chapter 6, the oculomotor performance of two different gaze-holding eye movements was compared. The results of this experimental work demonstrated that, for typical individuals, the accuracy and precision of fixation eye movements is superior to pursuit eye movements. However, for those with IN, there was no significant difference in the either the accuracy or the precision of between fixation and pursuit.

The generalised eye movement analysis developed in Chapter 3 may have potential for investigating fixation and visual function in IN. For example, there is clinical interest in the highest spatial frequency that can be resolved at maximum contrast (i.e. visual acuity), as this determines how much “detail” an individual can see. However, visual acuity represents only a single datum on the contrast sensitivity function (CSF). While much focus has been on determining the upper limits of spatial vision during the foveation period, visual functioning during the reminder of the slow phase has largely been overlooked. Spatiotemporal CSFs that define the visibility of spatial stimuli (i.e. spatial frequency and contrast) moving with particular speeds have been published for typical individuals (Kelly, 1979). It may be possible to use the bivariate PDF of velocity to model the spatiotemporal CSFs to explore visual potential during the entire slow phase of those with IN.

8.6 Filehne illusion

In Chapter 7, the psychophysical data showed that both typical individuals and those with IN perceived stationary objects to move in a direction opposite to the direction of the pursuit target motion. Therefore these results indicate that those with and without IN were experiencing the Filehne illusion. Indeed, the magnitude of the Filehne illusion was not statistically different between those with IN and typical individuals, suggesting that the mechanisms for estimating head-centric motion are similar in the two groups.

In this thesis, I have only considered the simple linear model proposed by Freeman and Banks (1998). In general, this model provides a robust account for a number of other pursuit-based illusions of motion (Freeman and Banks, 1998; Freeman, 1999; Freeman, 2001). For example, in addition to the Filehne illusion, the model also accounts for the Aubert-Fleischl phenomenon, in which pursued stimuli are perceived as moving more slowly, and trajectory misperception, in which, as previously mentioned, the perception of the trajectory of moving targets is distorted. Having demonstrated the presence of the Filehne illusion in those with IN, I envision further experiments aimed at quantifying these illusions to provide a more complete picture of the use of retinal and extra-retinal signals during pursuit. For example, the current results predict that those with IN should perceive the same magnitude of illusion as typical individuals. It is worth noting that, in this thesis, it was assumed that the transduction of the retinal image motion and eye velocity to obtain their respective signals was *linear*. However, Freeman (2001) has reported evidence to suggest that, at least for some typical individuals, transduction can be *non-linear*. In that study, the linear model fitted data for both the Filehne illusion and the Aubert-Fleischl phenomenon, but not for other velocity-matching data from some participants. To what extent non-linearity is present in those with IN is unclear, but this is unlikely to be revealed by only measuring the Filehne illusion or Aubert-Fleischl phenomenon alone. Nonetheless, with further experiments (i.e. similar experimental paradigms), it should be possible to model potential non-linear transduction in those with IN.

Using the simple linear transducer model proposed by Freeman and Banks (1998), both the retinal and extra-retinal signals can be subject to error, hence both have separate gains. For pursuit-based illusions of motion, including the Filehne illusion, the accepted explanation is that the magnitude of the retinal signal exceeds that of the extra-retinal signal. Although neither signal necessarily needs to be accurate, it is their ratio that determines the magnitude of the illusion. Freeman and Banks (1998) demonstrated in typical individuals that the magnitude of the retinal signal can be modulated by spatial frequency, which in turn modulates the magnitude of the Filehne illusion. In this thesis, having established that the Filehne illusion is experienced by those with IN, future work is expected to investigate the contribution of the spatial properties of the retinal image to perceived head-centric motion in those with IN. Many individuals with IN will also have an associated ocular condition (e.g. retinal dystrophies) (Abadi and Bjerre, 2002). Therefore, it may be reasonable to assume that the gain of the retinal signal in typical individuals does not equal the gain of the retinal signal in those with IN and an associated retinal condition. In this thesis, the overwhelming majority of participants had idiopathic IN with no known retinal defects. Nonetheless, differences in the retinal gain may well exist between typical individuals and idiopathic IN and between IN with and without an associated condition. Unfortunately, the measurement of retinal gain requires an absence of eye movements, so it is not immediately clear whether this hypothesis can be tested in those with an involuntary eye oscillation. Freeman et al. (2000a) have expanded the simple transducer model to account for non-constant eye velocity, a factor that was not considered previously in this thesis. If the eye is pursuing a target with constant speed, then any timing differences in the retinal and extra-retinal signal become irrelevant. However, during sinusoidal pursuit, Freeman et al. demonstrated that the phase of the two signals differs, albeit very little. However, with larger eye velocities during the slow phase and the possibility of pendular IN waveforms, it is unclear to what extent timing errors play a role in perceived head-centric motion judgements.

Typical individuals, following the onset of certain pathology (e.g. Multiple Sclerosis), will frequently develop nystagmus and oscillopsia (Bandini et al., 2001; Brickner, 1936). Consequently, these *formally* typical individuals now experience a failure of those mechanisms for determining perceived head-centric motion (i.e. oscillopsia). Indeed, this condition would provide an opportunity for an obvious and informative comparison with those with IN, as relative differences in the ratio of the retinal and extra-retinal gains measured during the Filehne illusion may offer insights as to the perceptual origins of oscillopsia.

8.7 Closing remarks

The perception of head-centric motion is not always perfect. The Filehne illusion demonstrates that errors in the use of retinal and extra-retinal signals can occur in typical individuals as well as for those with IN. Oscillopsia and the Filehne illusion are hypothesised to share a common theoretical underpinning, a mismatch in the magnitude of these retinal and extra-retinal signals. It is anticipated that the study of normal errors in these signals during pursuit will inform our understanding of oscillopsia. For example, manipulating the retinal input can modulate the magnitude of the Filehne illusion, suggesting that the same may be true of oscillopsia. This work forms the foundation for further study of perceived head-centric motion in those with IN. However, it was clearly highlighted in this chapter that our understanding of how those with IN may use retinal and extra-retinal signals, and to what extent the simple linear transducer model can be generalised to those with a pathological eye oscillation, is currently unclear. Consequently, this work has inspired a series of additional lines of enquiry that may serve to further our understanding of IN and the perceptual consequences of involuntary eye movements.

9 References

Abadi, R. V. & Bjerre, A. 2002. Motor and sensory characteristics of infantile nystagmus. *British Journal of Ophthalmology,* 86**,** 1152-60.

Abadi, R. V. & Dickinson, C. M. 1985. The influence of preexisting oscillations on the binocular optokinetic response. *Annals of Neurology,* 17**,** 578-86.

Abadi, R. V. & Dickinson, C. M. 1986. Waveform characteristics in congenital nystagmus. *Documenta Ophthalmologica,* 64**,** 153-67.

Abadi, R. V., Pascal, E., Whittle, J. & Worfolk, R. 1989. Retinal fixation behavior in human albinos. *Optometry and Vision Science,* 66**,** 276-80.

Abadi, R. V. & Whittle, J. 1991. The nature of head postures in congenital nystagmus. *Archives of Ophthalmology,* 109**,** 216-20.

Abadi, R. V., Whittle, J. P. & Worfolk, R. 1999. Oscillopsia and tolerance to retinal image movement in congenital nystagmus. *Investigative Ophthalmology and Visual Science,* 40**,** 339-45.

Abadi, R. V. & Worfolk, R. 1989. Retinal slip velocities in congenital nystagmus. *Vision Research,* 29**,** 195-205.

Abel, L. A. & Malesic, L. A. 2007. Oscillopsia in "inverse latent" infantile nystagmus syndrome. *Optometry and Vision Science,* 84**,** 1017-23.

Abel, L. A., Williams, I. M. & Levi, L. 1991. Intermittent oscillopsia in a case of congenital nystagmus. Dependence upon waveform. *Investigative Ophthalmology and Visual Science,* 32**,** 3104-8.

Averbuch-Heller, L., Dell'osso, L. F., Leigh, R. J., Jacobs, J. B. & Stahl, J. S. 2002. The torsional component of "horizontal" congenital nystagmus. *Journal of Neuro-Ophthalmology,* 22**,** 22-32.

Bahill, A. T., Iandolo, M. J. & Troost, B. T. 1980. Smooth pursuit eye movements in response to unpredictable target waveforms. *Vision Research,* 20**,** 923-31.

Bahill, A. T. & Mcdonald, J. D. 1983. Smooth pursuit eye movements in response to predictable target motions. *Vision Research,* 23**,** 1573-83.

Bandini, F., Castello, E., Mazzella, L., Mancardi, G. L. & Solaro, C. 2001. Gabapentin but not vigabatrin is effective in the treatment of acquired nystagmus in multiple sclerosis: How valid is the GABAergic hypothesis? *Journal of neurology, neurosurgery, and psychiatry,* 71**,** 107-10.

Bedell, H. E. 2000. Perception of a clear and stable visual world with congenital nystagmus. *Optometry and Vision Science,* 77**,** 573-81.

Bedell, H. E., Abplanalp, P. L. & Mcguire, C. A. 1987. Oculomotor responses to target displacements by patients with congenital idiopathic nystagmus and nystagmus associated with albinism. *Clinical Vision Sciences,* 2**,** 21-31.

Bedell, H. E. & Currie, D. C. 1993. Extraretinal signals for congenital nystagmus. *Investigative Ophthalmology and Visual Science,* 34**,** 2325-32.

Bedell, H. E., White, J. M. & Abplanalp, P. L. 1989. Variability of Foveations in Congenital Nystagmus. *Clinical Vision Sciences,* 4**,** 247-252.

Bellmann, C., Feely, M., Crossland, M. D., Kabanarou, S. A. & Rubin, G. S. 2004. Fixation stability using central and pericentral fixation targets in patients with age-related macular degeneration. *Ophthalmology,* 111**,** 2265-70.

Berens, P. 2012. *Circular Statistics Toolbox for MATLAB* [Online]. Available: http://de.mathworks.com/matlabcentral/fileexchange/10676-circular-statistics-toolbox--directional-statistics- [Accessed October 2015].

Berens, P. & Valesco, M. J. 2009. The Circular Statistics Toolbox for MATLAB. Max Planck Institute for Biological Cybernetics.

Bifulco, P., Cesarelli, M., Loffredo, L., Sansone, M. & Bracale, M. 2003. Eye movement baseline oscillation and variability of eye position during foveation in congenital nystagmus. *Documenta Ophthalmologica,* 107**,** 131-6.

Billauer, E. 2012. *peakdet: Peak detection using MATLAB* [Online]. Available: http://www.billauer.co.il/peakdet.html [Accessed May 2013].

Botev, Z. 2007. *kde2d: a fast and accurate state-of-the-art bivariate kernel density estimator* [Online]. Available: http://uk.mathworks.com/matlabcentral/fileexchange/17204-kde2d-data-n-min-xy-max-xy- [Accessed January 2015].

Botev, Z. 2009. *kde2d* [Online]. MATLAB Central. Available: http://uk.mathworks.com/matlabcentral/fileexchange/17204-kernel-density-estimation [Accessed December 2014 2014].

Brickner, R. M. 1936. Oscillopsia: a new symptom commonly occuring in multiple sclerosis *Archives of Neurology & Psychiatry,* 36**,** 586-589.

Brodsky, M. C. & Dell'osso, L. F. 2014. A unifying neurologic mechanism for infantile nystagmus. *JAMA Ophthalmology,* 132**,** 761-8.

Buchele, W., Brandt, T. & Degner, D. 1983. Ataxia and oscillopsia in downbeat-nystagmus vertigo syndrome. *Advances in Oto-Rhino-Laryngology,* 30**,** 291-7.

Buncic, J. R. 2004. A Clinician's Approach to Infantile Nystagmus. *American Orthoptic Journal,* 54**,** 88-94.

Carpenter, R. 1988. *Movements of the Eyes*.

Castet, E. & Crossland, M. 2012. Quantifying eye stability during a fixation task: a review of definitions and methods. *Seeing and Perceiving,* 25**,** 449-69.

Cemas 2001. Classification of Eye Movement Abnormalities and Strabismus (CEMAS): Report of an NEI Sponsored Workshop. Bethesda, MD.

Cesarelli, M., Bifulco, P., Loffredo, L. & Bracale, M. 2000. Relationship between visual acuity and eye position variability during foveations in congenital nystagmus. *Documenta Ophthalmologica,* 101**,** 59-72.

Cham, K. M., Anderson, A. J. & Abel, L. A. 2008. Factors influencing the experience of oscillopsia in infantile nystagmus syndrome. *Investigative Ophthalmology and Visual Science,* 49**,** 3424-31.

Cherici, C., Kuang, X., Poletti, M. & Rucci, M. 2012. Precision of sustained fixation in trained and untrained observers. *Journal of Vision,* 12.

Chung, S. T. & Bedell, H. E. 1996. Velocity criteria for "foveation periods" determined from image motions simulating congenital nystagmus. *Optometry and Vision Science,* 73**,** 92-103.

Cogan, D. G. 1967. Congenital nystagmus. *Canadian Journal of Ophthalmology,* 2**,** 4-10.

Cohen, J. 1992. A power primer. *Psychological Bulletin,* 112**,** 155-9.

Collewijn, H., Apkarian, P. & Spekreijse, H. 1985. The oculomotor behaviour of human albinos. *Brain,* 108 (Pt 1)**,** 1-28.

Collewijn, H. & Tamminga, E. P. 1984. Human smooth and saccadic eye movements during voluntary pursuit of different target motions on different backgrounds. *The Journal of Physiology,* 351**,** 217-50.

Crossland, M. D., Culham, L. E., Kabanarou, S. A. & Rubin, G. S. 2005. Preferred retinal locus development in patients with macular disease. *Ophthalmology,* 112**,** 1579-85.

Crossland, M. D., Culham, L. E. & Rubin, G. S. 2004a. Fixation stability and reading speed in patients with newly developed macular disease. *Ophthalmic and Physiological Optics,* 24**,** 327-33.

Crossland, M. D., Dunbar, H. M. & Rubin, G. S. 2009. Fixation stability measurement using the MP1 microperimeter. *Retina,* 29**,** 651-6.

Crossland, M. D. & Rubin, G. S. 2002. The use of an infrared eyetracker to measure fixation stability. *Optometry and Vision Science,* 79**,** 735-9.

Crossland, M. D., Sims, M., Galbraith, R. F. & Rubin, G. S. 2004b. Evaluation of a new quantitative technique to assess the number and extent of preferred retinal loci in macular disease. *Vision Research,* 44**,** 1537-46.

Dash, S., Dicke, P. W., Chakraborty, S., Haarmeier, T. & Thier, P. 2009. Demonstration of an eye-movement-induced visual motion illusion (Filehne illusion) in Rhesus monkeys. *Journal of Vision,* 9**,** 5 1-13.

Dell'osso, L. F. 1973a. Fixation characteristics in hereditary congenital nystagmus. *American Journal of Optometry and Archives of American Academy of Optometry,* 50**,** 85-90.

Dell'osso, L. F. 1973b. Improving visual acuity in congenital nystagmus. *In:* Smith, J. L. G., J. S. (ed.) *Neuro-Ophthalmology Symposium of the University of Miami and the Bascom Palmer Eye Institute.* Saint Louis: C. V. Mosby Company.

Dell'osso, L. F. 1985. Congenital, latent and manifest latent nystagmus--similarities, differences and relation to strabismus. *Japanese Journal of Ophthalmology,* 29**,** 351-68.

Dell'osso, L. F. 1986. Evaluation of smooth pursuit in the presence of congenital nystagmus. *Neuro-Ophthalmology,* 6**,** 383-406.

Dell'osso, L. F., Averbuch-Heller, L. & Leigh, R. J. 1997. Oscillopsia suppression and foveation-period variation in congenital, latent, and acquired nystagmus. *Neuro-Ophthalmology,* 18**,** 163-183.

Dell'osso, L. F., Ellenberger, C., Jr., Abel, L. A. & Flynn, J. T. 1983. The nystagmus blockage syndrome. Congenital nystagmus, manifest latent nystagmus, or both? *Investigative Ophthalmology and Visual Science,* 24**,** 1580-7.

Dell'osso, L. F. & Flynn, J. T. 1979. Congenital nystagmus surgery. A quantitative evaluation of the effects. *Archives of Ophthalmology,* 97**,** 462-9.

Dell'osso, L. F., Flynn, J. T. & Daroff, R. B. 1974. Hereditary congenital nystagmus. An intrafamilial study. *Archives of Ophthalmology,* 92**,** 366-74.

Dell'osso, L. F., Gauthier, G., Liberman, G. & Stark, L. 1972. Eye movement recordings as a diagnostic tool in a case of congenital nystagmus. *American Journal of Optometry and Archives of American Academy of Optometry,* 49**,** 3-13.

Dell'osso, L. F., Van Der Steen, J., Steinman, R. M. & Collewijn, H. 1992a. Foveation dynamics in congenital nystagmus. I: Fixation. *Documenta Ophthalmologica,* 79**,** 1-23.

Dell'osso, L. F., Van Der Steen, J., Steinman, R. M. & Collewijn, H. 1992b. Foveation dynamics in congenital nystagmus. II: Smooth pursuit. *Documenta Ophthalmologica,* 79**,** 25-49.

Dicke, P. W., Chakraborty, S. & Thier, P. 2008. Neuronal correlates of perceptual stability during eye movements. *The European Journal of Neuroscience,* 27**,** 991-1002.

Donaldson, I. M. 2000. The functions of the proprioceptors of the eye muscles. *Philosophical Transactions of the Royal Society of London. Series B, Biological Sciences,* 355**,** 1685-754.

Dunn, M. J. 2014. *Quantifying perception and oculomotor instability in infantile nystagmus* Doctor of Philosophy, Cardiff University

Dunn, M. J., Margrain, T. H., Woodhouse, J. M., Ennis, F. A., Harris, C. M. & Erichsen, J. T. 2014. Grating visual acuity in infantile nystagmus in the absence of image motion. *Investigative Ophthalmology and Visual Science,* 55**,** 2682-6.

Dunn, M. J., Margrain, T. H., Woodhouse, J. M. & Erichsen, J. T. 2015. Visual Processing in Infantile Nystagmus Is Not Slow. *Investigative Ophthalmology and Visual Science,* 56**,** 5094-101.

Ehrt, O. 2012. Infantile and acquired nystagmus in childhood. *European Journal of Paediatric Neurology*.

Felius, J., Fu, V. L., Birch, E. E., Hertle, R. W., Jost, R. M. & Subramanian, V. 2011. Quantifying nystagmus in infants and young children: relation between foveation and visual acuity deficit. *Investigative Ophthalmology and Visual Science,* 52**,** 8724-31.

Fender, D. H. & Nye, P. W. 1961. An investigation of the mechanisms of eye movement control. *Kybernetik,* 1**,** 81-8.

Filehne, W. 1922. Uber das optische Wahrnehmen von Bewegungen. *Zeitschrift fu¨r Sinnephysiologie,* 53**,** 134–145.

Finney, D. J. 1971. *Probit analysis,* Cambridge, Cambridge University Press.

Fisher, N. I. 1993. *Statistical analysis of circular data,* Cambridge, Cambridge University Press.

Freeman, T. C. 1999. Path perception and Filehne illusion compared: model and data. *Vision Research,* 39**,** 2659-67.

Freeman, T. C. 2001. Transducer models of head-centred motion perception. *Vision Research,* 41**,** 2741-55.

Freeman, T. C. & Banks, M. S. 1998. Perceived head-centric speed is affected by both extra-retinal and retinal errors. *Vision Research,* 38**,** 941-5.

Freeman, T. C., Banks, M. S. & Crowell, J. A. 2000a. Extraretinal and retinal amplitude and phase errors during Filehne illusion and path perception. *Perception and Psychophysics,* 62**,** 900-9.

Freeman, T. C., Banks, M. S. & Crowell, J. A. 2000b. Extraretinal and retinal amplitude and phase errors during Filehne illusion and path perception. *Perception and Psychophysics,* 62**,** 900-9.

Freeman, T. C., Champion, R. A. & Warren, P. A. 2010. A Bayesian model of perceived head-centered velocity during smooth pursuit eye movement. *Current Biology,* 20**,** 757-62.

Freeman, T. C., Naji, J. J. & Margrain, T. H. 2002. Head-centred motion perception in the ageing visual system. *Spatial Vision,* 15**,** 117-27.

Freeman, T. C., Sumnall, J. H. & Snowden, R. J. 2003. The extra-retinal motion aftereffect. *Journal of Vision,* 3**,** 771-9.

Gitchel, G. T., Wetzel, P. A. & Baron, M. S. 2013. Slowed saccades and increased square wave jerks in essential tremor. *Tremor and Other Hyperkinetic Movements,* 3**,** 1-7.

Goldstein, H. P., Gottlob, I. & Fendick, M. G. 1992. Visual remapping in infantile nystagmus. *Vision Research,* 32**,** 1115-24.

Gonzalez, E. G., Tarita-Nistor, L., Mandelcorn, E. D., Mandelcorn, M. & Steinbach, M. J. 2011. Fixation control before and after treatment for neovascular age-related macular degeneration. *Investigative Ophthalmology and Visual Science,* 52**,** 4208-13.

Gresty, M., Page, N. & Barratt, H. 1984. The differential diagnosis of congenital nystagmus. *Journal of Neurology, Neurosurgery, and Psychiatry,* 47**,** 936-42.

Grunfeld, E. A., Morland, A. B., Bronstein, A. M. & Gresty, M. A. 2000. Adaptation to oscillopsia: a psychophysical and questionnaire investigation. *Brain,* 123 (Pt 2)**,** 277-90.

Haarmeier, T. & Thier, P. 1996. Modification of the Filehne illusion by conditioning visual stimuli. *Vision Research,* 36**,** 741-50.

Harris, C. M. 1997. Nystagmus and eye movement disorders. *In:* Taylor, D. (ed.) *Paediatric Ophthalmology.* 2nd ed. Oxford: Blackwell Science.

Harrison, J. J., Sumner, P., Dunn, M. J., Erichsen, J. T. & Freeman, T. C. 2015. Quick phases of infantile nystagmus show the saccadic inhibition effect. *Investigative Ophthalmology and Visual Science,* 56**,** 1594-600.

Harwood, M. R., Mezey, L. E. & Harris, C. M. 1999. The spectral main sequence of human saccades. *The Journal of neuroscience,* 19**,** 9098-106.

Hertle, R. W. & Dell'osso, L. F. 1999. Clinical and ocular motor analysis of congenital nystagmus in infancy. *Journal of AAPOS,* 3**,** 70-9.

Holmqvist, K., Nyström, M., Andersson, R., Dewhurst, R., Jarodzka, H. & Van De Weijer, J. 2011. Eye-tracker hardware and its properties. *Eye Tracking: A Comprehensive Guide to Methods and Measures.* Oxford: Oxford University Press.

Huang, C., Mcdonald, J. A. & Stuetzle, W. 1997. Variable resolution bivariate plots. *Journal of Computational and Graphical Statistics,* 6**,** 383-396.

Jacobs, J. B. & Dell'osso, L. F. 2004. Congenital nystagmus: hypotheses for its genesis and complex waveforms within a behavioral ocular motor system model. *Journal of Vision,* 4**,** 604-25.

Jones, P. H. 2011. *The Impact of Stress on Visual Function in Nystagmus.* Doctor of Philosophy, Cardiff University.

Jones, P. H., Harris, C. M., Woodhouse, J. M., Margrain, T. H., Ennis, F. A. & Erichsen, J. T. 2013. Stress and visual function in infantile nystagmus syndrome. *Investigative Ophthalmology and Visual Science,* 54**,** 7943-51.

Juhola, M. 1986. The effect of digital lowpass filters on the maximum velocity of saccadic eye movements. *Computers in Biology and Medicine,* 16**,** 361-70.

Ke, S. R., Lam, J., Pai, D. K. & Spering, M. 2013. Directional asymmetries in human smooth pursuit eye movements. *Investigative Ophthalmology and Visual Science,* 54**,** 4409-21.

Kelly, D. H. 1979. Motion and vision. II. Stabilized spatio-temporal threshold surface. *Journal of the Optical Society of America,* 69**,** 1340-9.

Kolarik, A. J., Margrain, T. H. & Freeman, T. C. 2010. Precision and accuracy of ocular following: influence of age and type of eye movement. *Experimental Brain Research,* 201**,** 271-82.

Kommerell, G. 1986. Congenital nystagmus: control of slow tracking movements by target offset from the fovea. *Graefe's Archive for Clinical and Experimental Ophthalmology,* 224**,** 295-8.

Kosnik, W., Fikre, J. & Sekuler, R. 1986. Visual fixation stability in older adults. *Investigative Ophthalmology and Visual Science,* 27**,** 1720-5.

Kosnik, W., Kline, D., Fikre, J. & Sekuler, R. 1987. Ocular fixation control as a function of age and exposure duration. *Psychology and Aging,* 2**,** 302-5.

Kovach, C. 2007. *EDFMEX* [Online]. S.R. Research. Available: https://www.srsupport.com/showthread.php?255-Import-of-EDF-file-into-Matlab&p=6781#post6781 [Accessed June 2012].

Kowler, E. & Mckee, S. P. 1987. Sensitivity of smooth eye movement to small differences in target velocity. *Vision Research,* 27**,** 993-1015.

Kurzan, R. & Buttner, U. 1989. Smooth pursuit mechanisms in congenital nystagmus. *Neuro-Ophthalmology,* 9**,** 313-325.

Leigh, R. J., Dell'osso, L. F., Yaniglos, S. S. & Thurston, S. E. 1988. Oscillopsia, retinal image stabilization and congenital nystagmus. *Investigative Ophthalmology and Visual Science,* 29**,** 279-82.

Leigh, R. J. & Zee, D. S. 1999. Smooth pursuit and visual fixation. *The Neurology of Eye Movements.* 3rd ed. New York: Oxford University Press.

Lisberger, S. G., Evinger, C., Johanson, G. W. & Fuchs, A. F. 1981. Relationship between eye acceleration and retinal image velocity during foveal smooth pursuit in man and monkey. *Journal of Neurophysiology,* 46**,** 229-49.

Lueck, C. J. 2005. Nystagmus. *Practical Neurology,* 5**,** 288-291.

Mack, A. & Herman, E. 1973. Position constancy during pursuit eye movement: an investigation of the Filehne illusion. *Quarterly Journal of Experimental Psychology,* 25**,** 71-84.

Martinez-Conde, S., Macknik, S. L. & Hubel, D. H. 2004. The role of fixational eye movements in visual perception. *Nature Reviews Neuroscience,* 5**,** 229-40.

Mclean, R., Proudlock, F., Thomas, S., Degg, C. & Gottlob, I. 2007. Congenital nystagmus: randomized, controlled, double-masked trial of memantine/gabapentin. *Annals of Neurology,* 61**,** 130-8.

Meyer, C. H., Lasker, A. G. & Robinson, D. A. 1985. The upper limit of human smooth pursuit velocity. *Vision Research,* 25**,** 561-3.

Murphy, B. J. 1978. Pattern thresholds for moving and stationary gratings during smooth eye movement. *Vision Research,* 18**,** 521-30.

Nachmias, J. 1959. Two-dimensional motion of the retinal image during monocular fixation. *Journal of the Optical Society of America,* 49**,** 901-8.

O'connor, E., Margrain, T. H. & Freeman, T. C. 2010. Age, eye movement and motion discrimination. *Vision Research,* 50**,** 2588-99.

Pola, J. & Wyatt, H. J. 1985. Active and passive smooth eye movements: effects of stimulus size and location. *Vision Research,* 25**,** 1063-76.

Pritchard, R. M. 1961. Stabilised images on the retina. *Scientific American,* 204**,** 72-78.

Rasche, C. & Gegenfurtner, K. R. 2009. Precision of speed discrimination and smooth pursuit eye movements. *Vision Research,* 49**,** 514-23.

Rashbass, C. 1961. The relationship between saccadic and smooth tracking eye movements. *Journal of Physiology,* 159**,** 326-38.

Richards, M. D. & Wong, A. 2015. Infantile nystagmus syndrome: clinical characteristics, current theories of pathogenesis, diagnosis, and management. *Canadian Journal of Ophthalmology,* 50**,** 400-8.

Rottach, K. G., Zivotofsky, A. Z., Das, V. E., Averbuch-Heller, L., Discenna, A. O., Poonyathalang, A. & Leigh, R. J. 1996. Comparison of horizontal, vertical and diagonal smooth pursuit eye movements in normal human subjects. *Vision Research,* 36**,** 2189-95.

Rucci, M., Iovin, R., Poletti, M. & Santini, F. 2007. Miniature eye movements enhance fine spatial detail. *Nature,* 447**,** 851-4.

Sarvananthan, N., Surendran, M., Roberts, E. O., Jain, S., Thomas, S., Shah, N., Proudlock, F. A., Thompson, J. R., Mclean, R. J., Degg, C., Woodruff, G. & Gottlob, I. 2009. The prevalence of nystagmus: the Leicestershire nystagmus survey. *Investigative Ophthalmology and Visual Science,* 50**,** 5201-6.

Schuchard, R. a. R., T.W. 1992. Retinal locus for fixation: pericentral fixation targets. *Clinical Vision Sciences,* 7**,** 511-520.

Shanidze, N., Fusco, G., Potapchuk, E., Heinen, S. & Verghese, P. 2016. Smooth pursuit eye movements in patients with macular degeneration. *Journal of Vision,* 16**,** 1.

Sharpe, J. A. & Sylvester, T. O. 1978. Effect of aging on horizontal smooth pursuit. *Investigative Ophthalmology and Visual Science,* 17**,** 465-8.

Skavenski, A. A. & Steinman, R. M. 1970. Control of eye position in the dark. *Vision Research,* 10**,** 193-203.

Souman, J. L., Hooge, I. T. & Wertheim, A. H. 2006. Frame of reference transformations in motion perception during smooth pursuit eye movements. *Journal of Computational Neuroscience,* 20**,** 61-76.

Sr-Research 2009. EyeLink 1000 Technical Specifications. Ontario: SR-Research.

St-Cyr, G. J. & Fender, D. H. 1969. Nonlinearities of the human oculomotor system: time delays. *Vision Research,* 9**,** 1491-503.

Straube, A., Bronstein, A. & Straumann, D. 2012. Nystagmus and oscillopsia. *European Journal of Neurology,* 19**,** 6-14.

Sundqvist, P. 2010. *Contour2Area* [Online]. Available: http://uk.mathworks.com/matlabcentral/fileexchange/26480-contour2area [Accessed December 2014].

Theodorou, M., Clement, R., Taylor, D. & Moore, A. 2015. The development of infantile nystagmus. *British Journal of Ophthalmology,* 99**,** 691-5.

Thomas, M. G., Gottlob, I., Mclean, R. J., Maconachie, G., Kumar, A. & Proudlock, F. A. 2011. Reading strategies in infantile nystagmus syndrome. *Investigative Ophthalmology and Visual Science,* 52**,** 8156-65.

Thompson, P. 2002. Eyes wide apart: overestimating interpupillary distance. *Perception,* 31**,** 651-6.

Tilikete, C. & Vighetto, A. 2011. Oscillopsia: causes and management. *Current Opinion in Neurology,* 24**,** 38-43.

Tkalcevic, L. A. & Abel, L. A. 2003. Effects of stimulus size and luminance on oscillopsia in congenital nystagmus. *Vision Research,* 43**,** 2697-705.

Turano, K. A. & Massof, R. W. 2001. Nonlinear contribution of eye velocity to motion perception. *Vision Research,* 41**,** 385-95.

Ukwade, M. T. & Bedell, H. E. 1992. Variation of congenital nystagmus with viewing distance. *Optometry and Vision Science,* 69**,** 976-85.

Van Vliet, A. G. 1982. Nystagmus. *Documenta Ophthalmologica,* 52**,** 435-46.

Von Noorden, G. K. & Campos, E. C. 2002. *Binocular Vision and Ocular Motility: Theory and Management of Strabismus,* St. Louis, Missouri, Mosby.

Waddington, J. & Harris, C. M. 2015. Human optokinetic nystagmus and spatial frequency. *Journal of Vision,* 15**,** 7.

Wang, Z. I. & Dell'osso, L. F. 2009. Factors influencing pursuit ability in infantile nystagmus syndrome: Target timing and foveation capability. *Vision Research,* 49**,** 182-9.

Wang, Z. I., Dell'osso, L. F., Prakash, S. & Chen, X. 2012. Smooth-pursuit changes after the tenotomy and reattachment procedure for infantile nystagmus syndrome: model predictions and patient data. *Journal of Pediatric Ophthalmology and Strabismus,* 49**,** 295-302.

Weisstein, E. W. 2015. *Riemann Integral* [Online]. MathWorld -- A Wolfram Web Resource. Available: http://mathworld.wolfram.com/RiemannIntegral.html [Accessed January 2015].

Westheimer, G. 1954. Eye movement responses to a horizontally moving visual stimulus. *Archives of Ophthalmology,* 52**,** 932-41.

Whittaker, S. G., Budd, J. & Cummings, R. W. 1988. Eccentric fixation with macular scotoma. *Investigative Ophthalmology and Visual Science,* 29**,** 268-78.

Wiggins, D. 2007. *The impact of orbital eye position, visual demand and stress on infantile nystagmus syndrome.* Doctor of Philosophy, Cardiff University.

Wiggins, D., Woodhouse, J. M., Margrain, T. H., Harris, C. M. & Erichsen, J. T. 2007. Infantile nystagmus adapts to visual demand. *Investigative Ophthalmology and Visual Science,* 48**,** 2089-94.

Wist, E. R., Brandt, T. & Krafczyk, S. 1983. Oscillopsia and retinal slip. Evidence supporting a clinical test. *Brain,* 106 (Pt 1)**,** 153-68.

Wurtz, R. H. 2008. Neuronal mechanisms of visual stability. *Vision Research,* 48**,** 2070-89.

Yamazaki, A. 1978. Abnormalities of smooth pursuit and vestibular eye movements in congenital jerk nystagmus. *In:* Shimizu, K. O., J.A. (ed.) *Ophthalmology: Proceedings of the XXIII International Congress.* Kyoto.

Yarbus, A. L. 1967. Eye movements during fixation on stationary objects. *Eye Movements and Vision.* New York: Plenum Press.

Yee, R. D., Baloh, R. W. & Honrubia, V. 1980. Study of congenital nystagmus: optokinetic nystagmus. *British Journal of Ophthalmology,* 64**,** 926-32.

10 Appendix 1: Participant details

ID	Sex/Age	Associations	Ocular alignment	Spectacle Rx	VA (logMAR)
CT	F/57	Idiopathic	R XOT	R: -5.50 DS L: -5.50 DS	R: 0.30 L: 0.10
GT	M/61	Idiopathic	R SOT	R: -3.00 / -1.00 x 150 L: -3.75 / -1.50 x 160	R: 0.76 L:0.80
JS	M/57	Idiopathic	Ortho	R: -12.00 /-2.00 x 32 L: -10.50 /-1.00 x 90	R:0.30 L: 0.30
RW	M/34	Idiopathic	Ortho	R: Plano L: Plano	R:0.54 L:0.40
SP	F/35	Idiopathic	Ortho	R: Plano L: Plano	R: L:
VW	F/23	Idiopathic	Alt SOT	R: +2.25 /-3.75 x 20 L: +2.50 / -3.75 x 160	R: 0.32 L: 0.36
SW	F/71	Idiopathic	Ortho	R: Plano L: Plano	R:0.36 L:0.42

Table 10.1 Clinical and oculomotor information for IN participants. Ortho = orthotropia, Alt = alternating, SOT = esotropia, XOT = exotropia

ID	Sex/Age	Associations	Ocular alignment	Spectacle Rx	VA (logMAR)
MB	M/18	Idiopathic	Ortho	R: -3.00 DS L: -3.00 DS	R: 0.26 L: 0.38
JT	F/54	Idiopathic	Ortho	R: -4.00 / - 2.25 x 35 L: -2.25 / -5.00 x 60	R: 0.68 L:0.68
NB	M/48	Idiopathic	Ortho	R: +1.50 / -1.00 x 180 L: +2.50 / -0.50 x 180	R: 0.30 L: 0.24
DT	M/54	Achromatopsia	L SOT	L: -11.00 DS L: -12.00 DS	R: 0.54 L: 0.70
DB	M/46	Idiopathic	Ortho	R: -7.00 / -0.75 x 6 L: -9.25 / -1.75 x 176	R: 0.68 L: 0.66
DC	F/36	Idiopathic	Ortho	R: -3.75 / -2.00 x 90 L: -3.50 / - 3.50 x 90	R: 0.30 L: 0.30
DP	M/41	Idiopathic	Ortho	R: -2.00 / -3.00 x 100 L: -5.00 / -1.50 x 80	R: 0.36 L: 0.80
MT	F/69	Idiopathic	Ortho	R: plano L: plano	R: 0.20 L: 0.40

Table 10.2 Clinical and oculomotor information for IN participants. Ortho = orthotropia, Alt = alternating, SOT = esotropia, XOT = exotropia

ID	Sex/Age	Associations	Ocular alignment	Spectacle Rx	VA (logMAR)
SM	M/57	Idiopathic	Ortho	R: plano L: plano	R: 1.02 L: 0.76
JC	F/52	Idiopathic	Ortho	R: -4.25 / -2.00 30 L:-2.50 / -4.75 x 62	R: 0.52 L: 0.13
LB	F/28	Idiopathic	Ortho	R: plano L: plano	R: 0.20 L: 0.30
GT2	M/63	Idiopathic	Ortho	R: -1.25 / -0.50 x 25 L: -0.25 / -0.50 x 120	R: 0.40 L: 0.42
JM	M/43	Ocular Albinism	L SOT	R: +7.75 / -2.75 x 157 L: +7.50 /-2.75 x 60	R: 0.80 L: 0.98

Table 10.3 Clinical and oculomotor information for IN participants. Ortho = orthotropia, Alt = alternating, SOT = esotropia, XOT = exotropia

ID	Sex/Age	Ocular alignment	Spectacle Rx	VA (logMAR)
TF	M/49	Ortho	R: -2.50 / -2.00 x170 L: -1.75 / -2.00 x 170	R: 0.06 L: -0.2
TK	M/31	Ortho	R: plano L: plano	R: 0.00 L: -0.04
LM	M/30	Ortho	R: plano L: plano	R: -0.10 L: -0.10
SLL	F/24	Ortho	R: plano L: plano	R: -0.10 L: -0.08
SP2	M/21	Ortho	R: plano L: plano	R: 0.00 L: 0.00
CJ	M/27	Ortho	R: plano L: plano	R: 0.04 L: 0.00
CD	M/28	Ortho	R: plano L: plano	R:0.00 L:0.02
CR	F/26	Ortho	R: plano L: plano	R: 0.04 L: 0.02

Table 10.4 Clinical and oculomotor information for typical participants. Ortho = orthotropia, Alt = alternating, SOT = esotropia, XOT = exotropia

ID	Sex/Age	Ocular alignment	Spectacle Rx	VA (logMAR)
TR	M/31	Ortho	R: -2.50 / -2.00 x 83 L: -1.75 / -2.25 x 83	R: -0.06 L: -0.06
BF	F/27	Ortho	R: Plano L: Plano	R: -0.02 L: -0.04
MS	M/24	Ortho	R: Plano L: Plano	R: -0.10 L: -0.10
EM	F/21	Ortho	R: Plano L: Plano	R: -0.10 L: -0.08
JB	M/32	Ortho	R: Plano L: Plano	R: 0.00 L: 0.00
JB2	M/24	Ortho	R: Plano L: Plano	R: 0.04 L: 0.00
AN	M/45	Ortho	R: Plano L: Plano	R:0.00 L:0.02
RL	F/26	Ortho	R: Plano L: Plano	R: 0.04 L: 0.02

Table 10.5 Clinical and oculomotor information for typical participants. Ortho = orthotropia, Alt = alternating, SOT = esotropia, XOT = exotropia

ID	Sex/Age	Ocular alignment	Spectacle Rx	VA (logMAR)
LS	F/21	Ortho	R: plano L: plano	R: 0.00 L: 0.00
SB	F/21	Ortho	R: Plano L: Plano	R: 0.00 L: -0.04

Table 10.6 Clinical and oculomotor information for typical participants. Ortho = orthotropia, Alt = alternating, SOT = esotropia, XOT = exotropia

10 Appendix 2: Individual null zone plots for IN participants

Participant MT

(a) random presentation

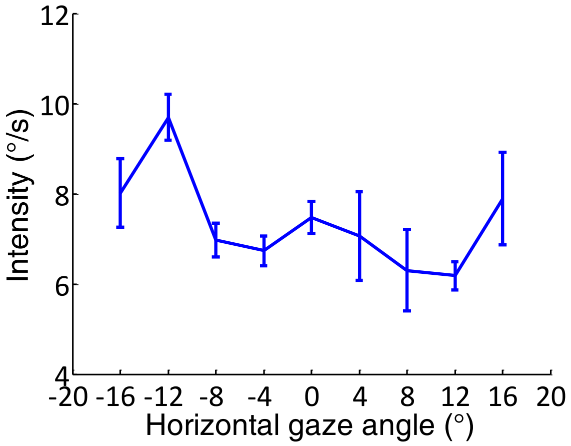

(b) left-to-right presentation

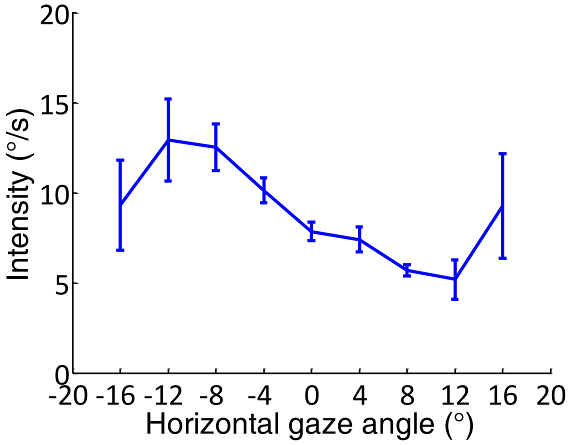

(c) right-to-left presentation

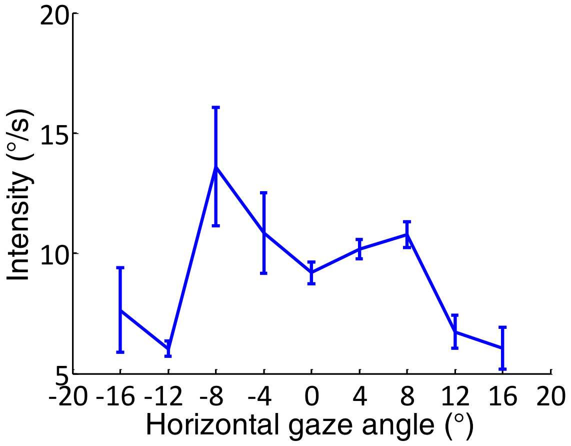

Participant JC

(a) random presentation

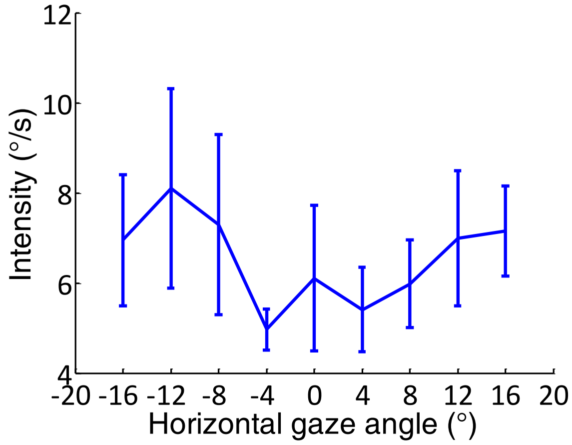

(b) left-to-right presentation

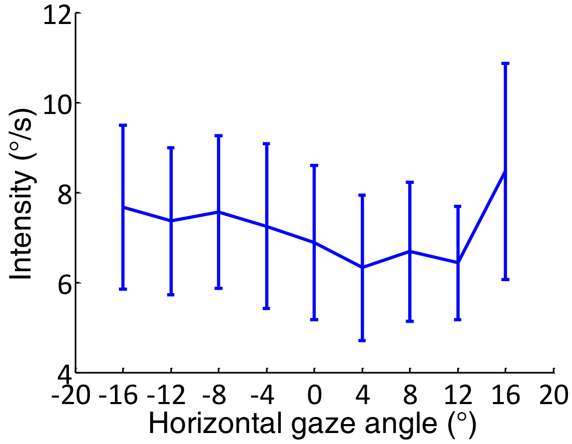

(c) right-to-left presentation

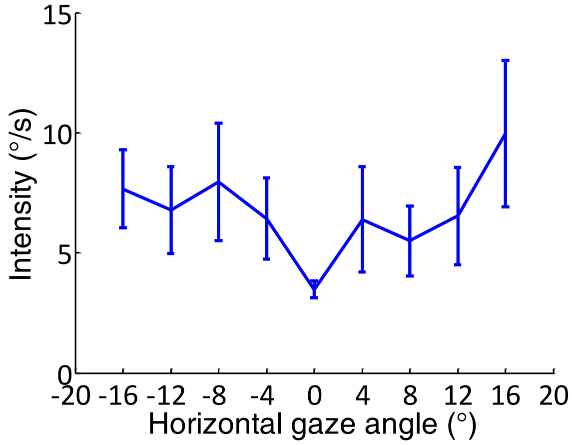

Participant LB

(a) random presentation

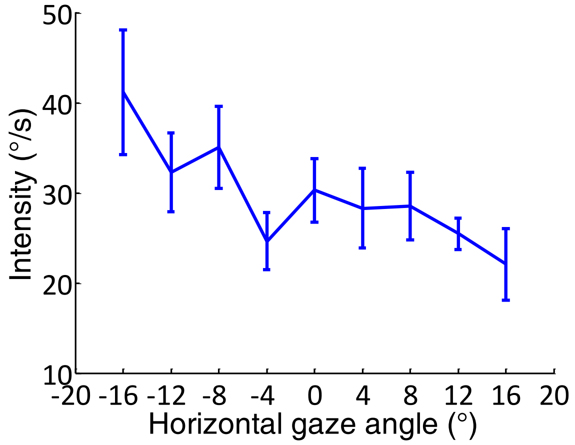

(b) left-to-right presentation

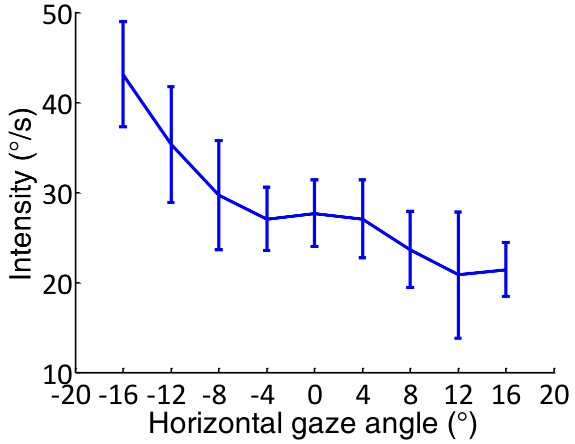

(c) right-to-left presentation

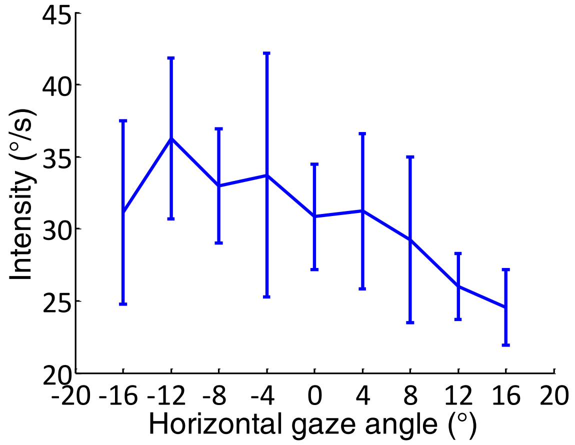

Participant CT

(a) random presentation

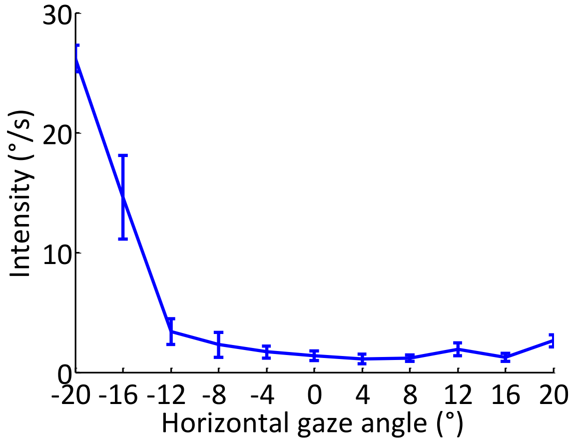

(b) left-to-right presentation

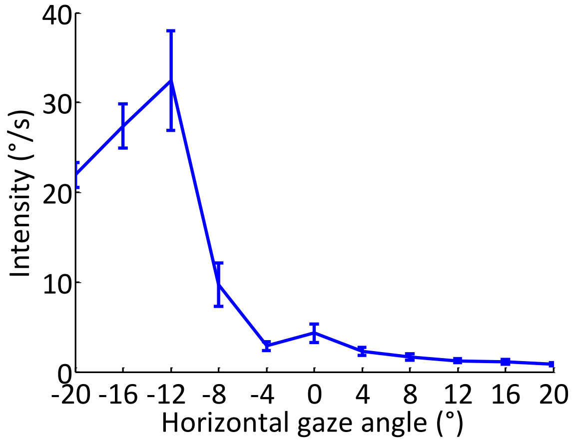

(c) right-to-left presentation

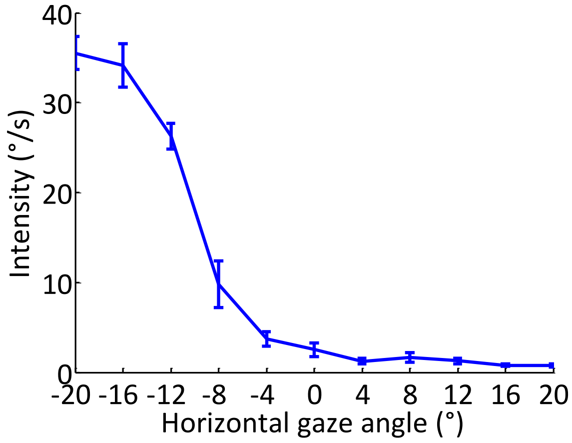

Participant RW

(a) random presentation

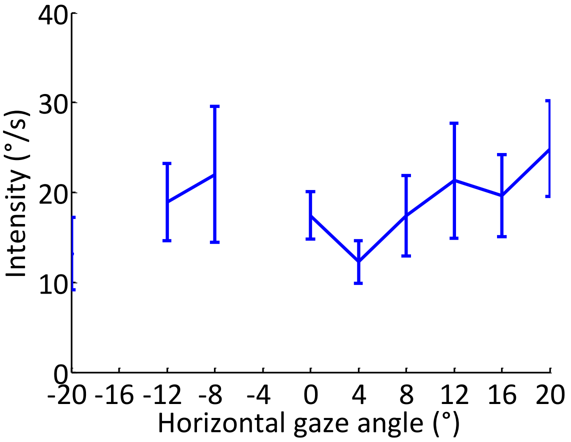

(b) left-to-right presentation

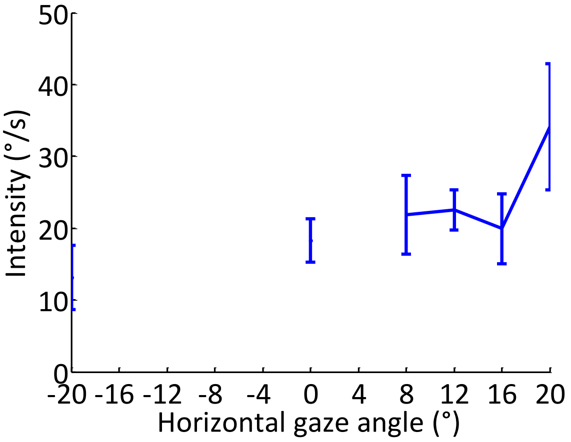

(c) right-to-left presentation

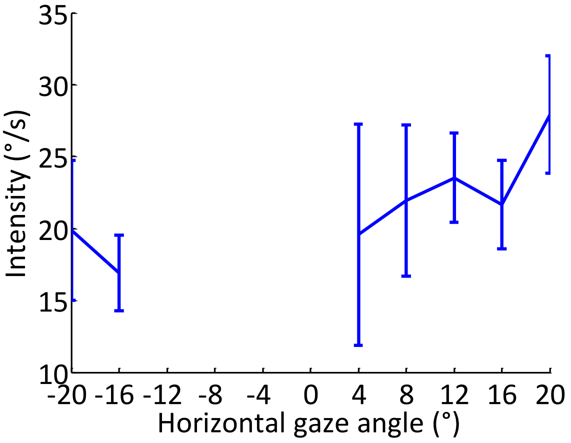

Participant CT

(a) random presentation

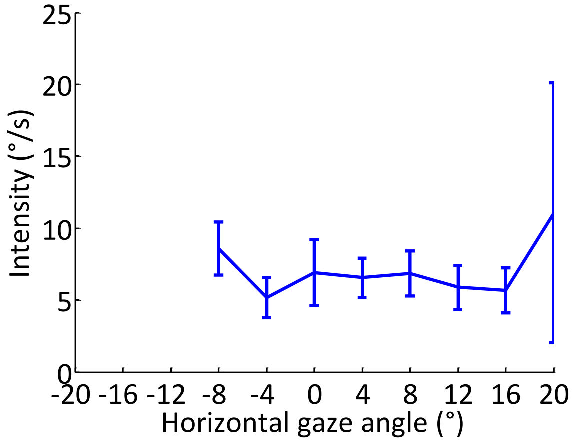

(b) left-to-right presentation

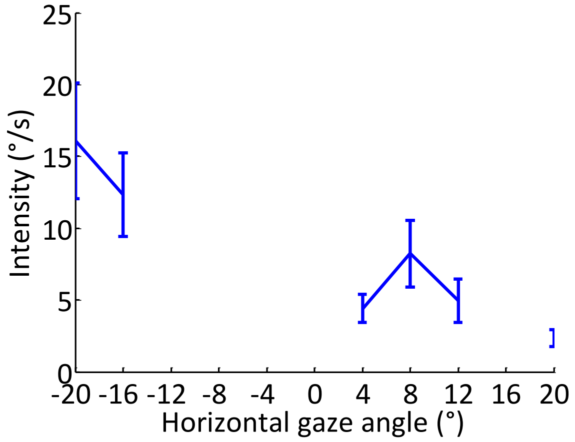

(c) right-to-left presentation

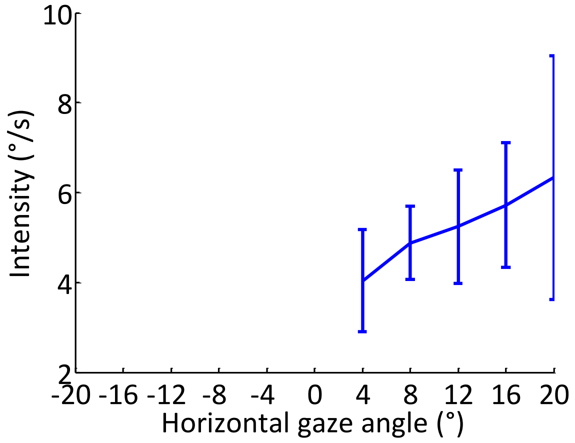

Participant SM

(a) random presentation

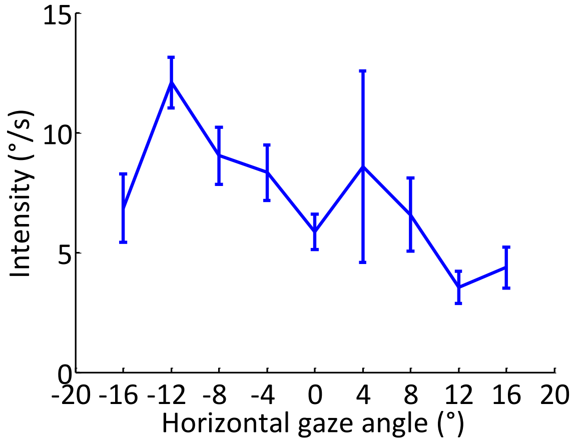

(b) left-to-right presentation

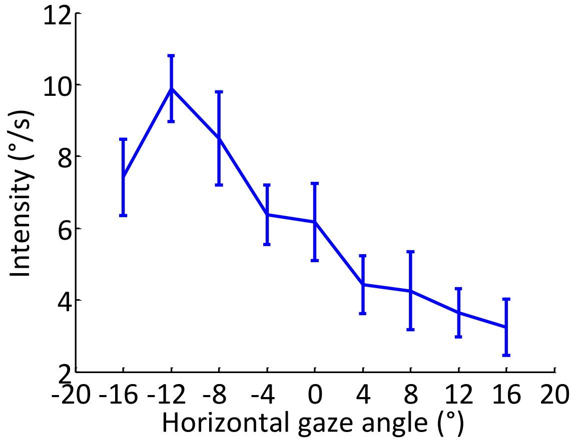

(c) right-to-left presentation

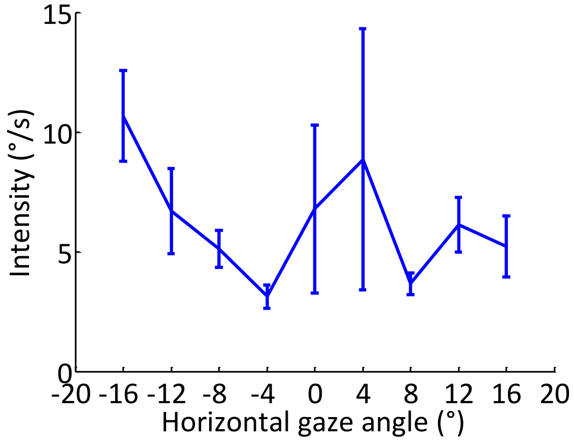

Participant DB

(a) random presentation

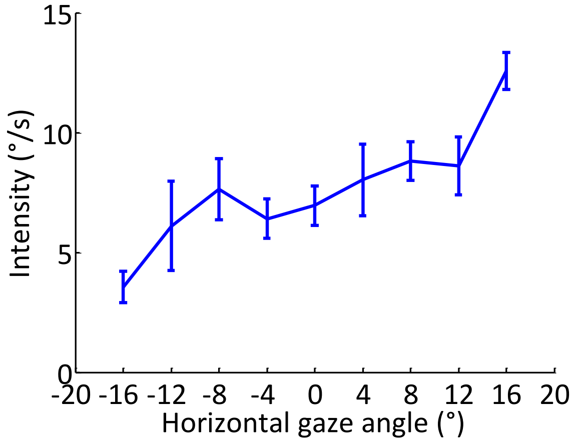

(b) left-to-right presentation

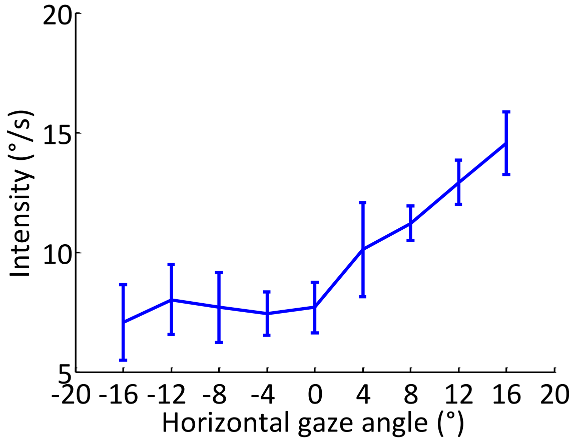

(c) right-to-left presentation

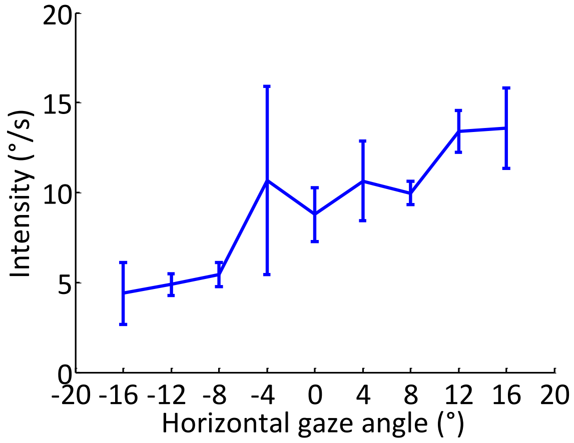

Participant DP

(a) random presentation

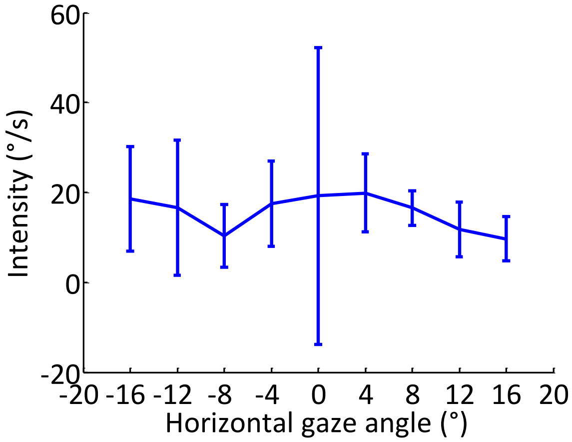

(

b) left-to-right presentation

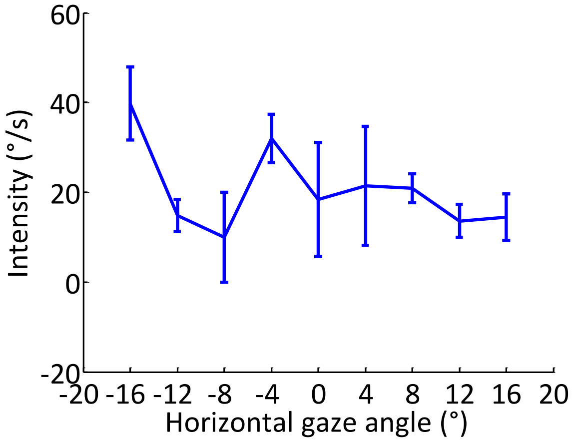

(c) right-to-left presentation

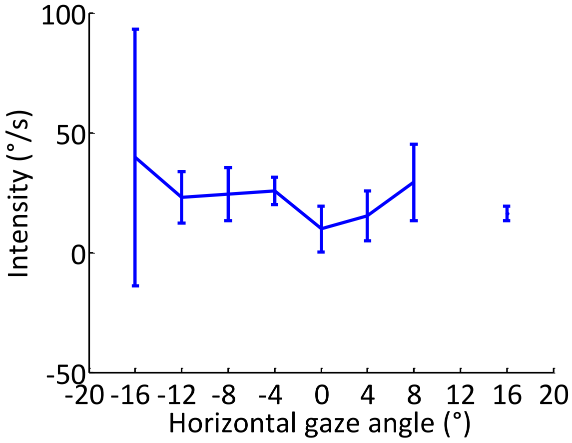

Participant DT

(a) random presentation

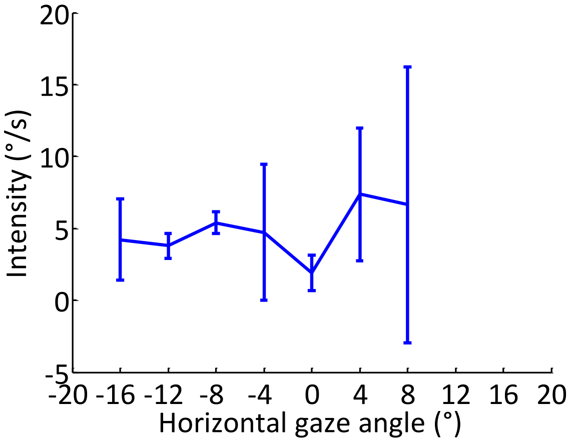

(b) left-to-right presentation

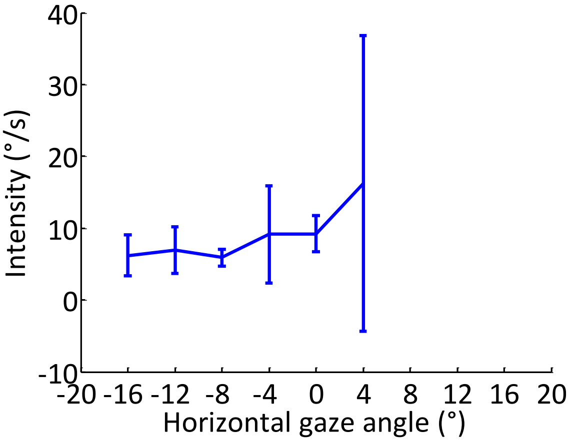

(c) right-to-left presentation

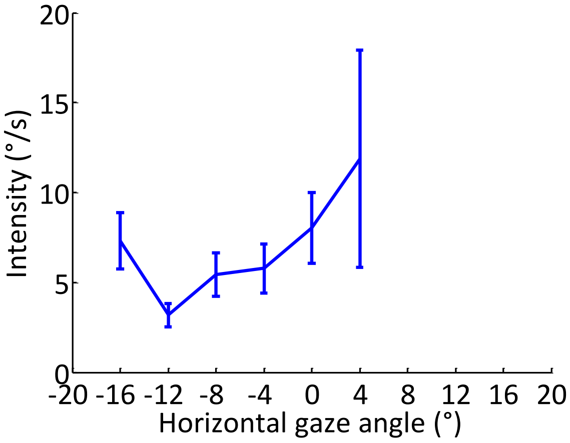

Participant GT2

(a) random presentation

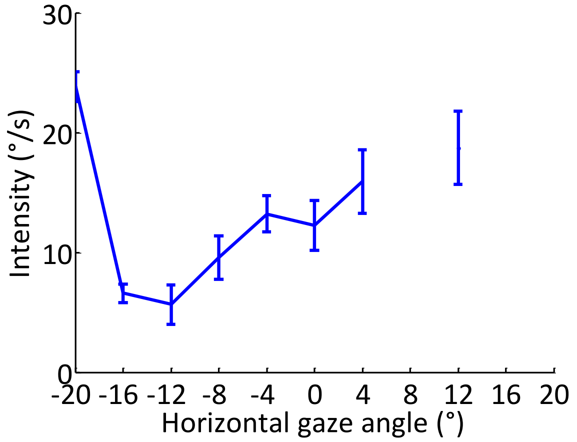

(b) left-to-right presentation

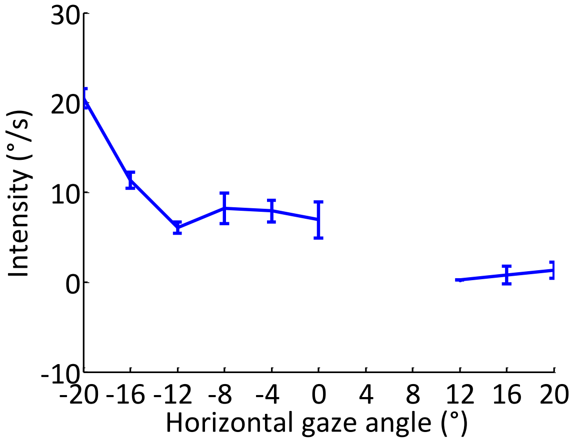

(c) right-to-left presentation

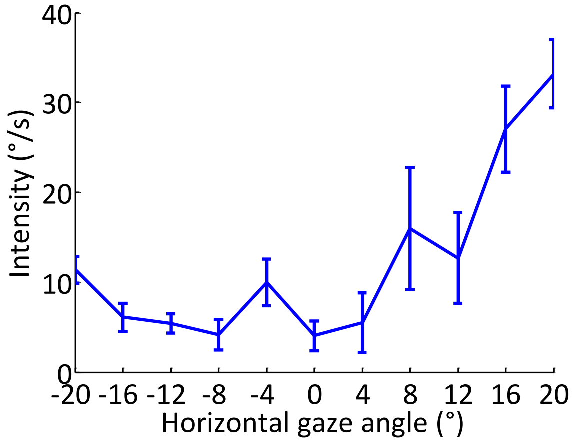

Participant JT

(a) random presentation

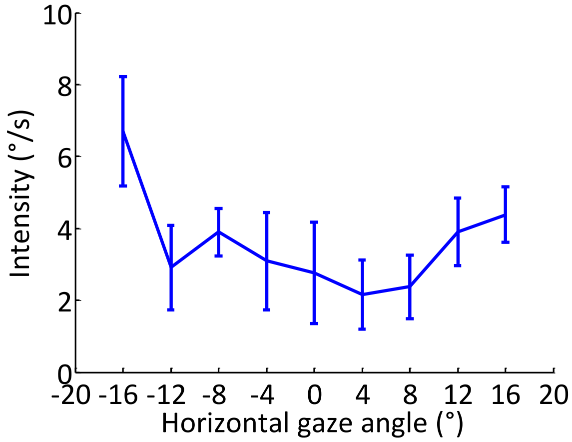

(b) left-to-right presentation

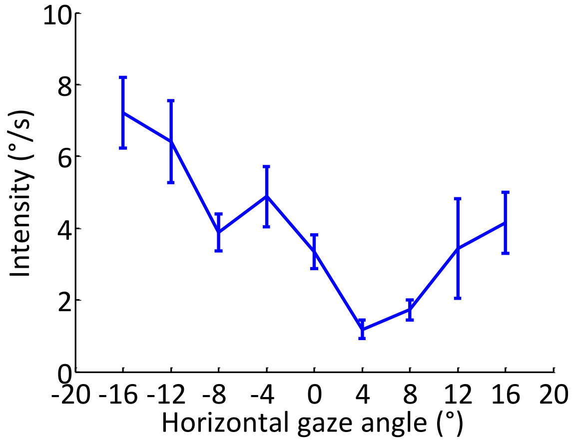

(c) right-to-left presentation

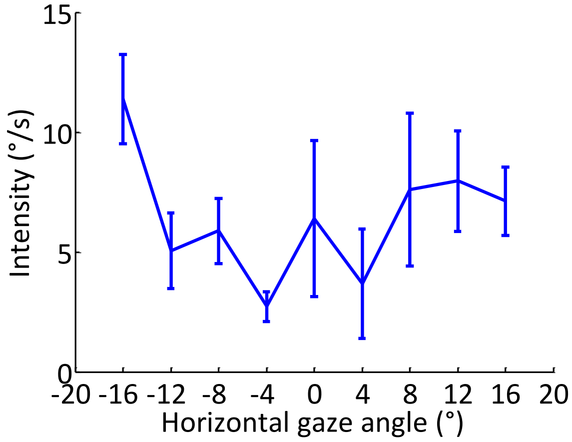

Participant MB

(a) random presentation

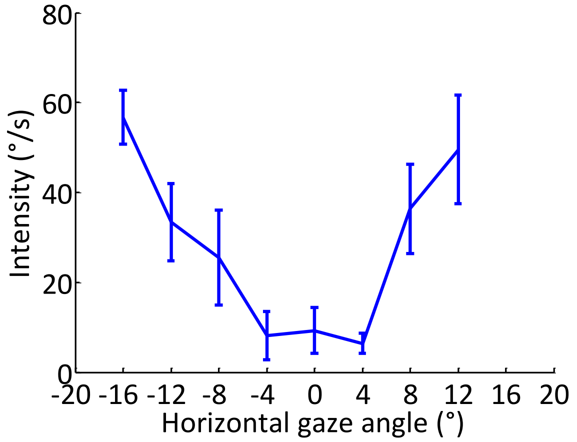

(b) left-to-right presentation

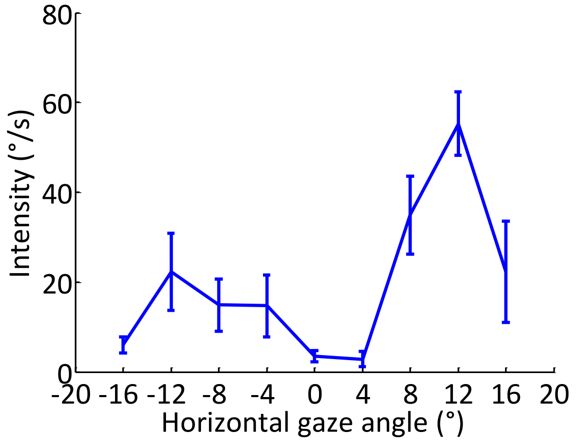

(c) right-to-left presentation